UNIVERSITAT POLITÈCNICA
DE CATALUNYA
BARCELONATECH

ANALYSIS OF FOREARM MUSCLES ACTIVITY BY MEANS OF NEW PROTOCOLS OF MULTICHANNEL EMG SIGNAL RECORDING AND PROCESSING

by

MÓNICA ROJAS MARTÍNEZ

Advisor

MIGUEL ÁNGEL MAÑANAS VILLANUEVA

Programa de Doctorado en Ingeniería Biomédica

Depto. Ingeniería de Sistemas, Automática e
Informática Industrial
UNIVERSIDAD POLITÉCNICA DE CATALUÑA
BARCELONA TECH

October 2012

A mis padres, Ernesto y Marlene

Agradecimientos

Han sido muchas las personas que indirecta o directamente han colaborado en la realización de esta tesis, incluso desde antes que se plantearan sus primeros cimientos y a los que de todo corazón agradezco.

Quisiera empezar por agradecer a mi director y guía durante estos años, Miguel Ángel Mañanas Villanueva, por compartir conmigo toda su experiencia en el campo científico y profesional, así como por sus acertados consejos y su conocimiento pero más que nada por su amistad, por todas las invaluables enseñanzas que me ha dejado a nivel personal y por su incansable preocupación a la hora de valorar todos mis esfuerzos. Gracias de verdad.

A mis compañeros y amigos en el doctorado tanto por sus consejos en temas relevantes al desarrollo de este trabajo como por su sincera amistad y compromiso, en especial a Mathieu, Joan Francesc, Mauricio, Agustín, Héctor, Leidy, Sergio, Michelle, Riccardo y Hamid.

A los voluntarios y pacientes que participaron en los diferentes estudios de mi tesis, en especial a los miembros del Departamento ESAII de la UPC, del LISiN del Politécnico de Torino y a los pacientes de la Mútua Egarsat que aceptaron participar en los protocolos experimentales. Gracias por su tiempo y su esfuerzo. A los doctores de la Mutua Egarsat, en particular a Quim y Carme por su soporte médico, su entusiasmo y por confiar en mí. También quisiera agradecer al Profesor Roberto Merletti por acogerme en su laboratorio, por permitirme colaborar con su grupo durante mi estancia en el LISiN y por su colaboración y orientación en el desarrollo de parte de la investigación de esta tesis.

También quisiera agradecer a los amigos que han compartido conmigo todas mis victorias, alegrías, angustias y frustraciones, a los de Colombia y también a los que he conocido en Barcelona, a mi prima Laura y a Moni que siempre han estado cerca de mí, a Juan, Jenny, Iris, Carla y Oscar y a mis amigos de Opción.

A mi familia, a mis padres Ernesto y Marlene y mis hermanos Augusto, Hernando y Sandra que me han apoyado siempre en todo lo que se me ocurre y que me han enseñado a persistir, una de las cualidades mas importantes en investigación. Mis padres siempre han sido mi guía, mi consuelo y mi constante motivación en el camino del esfuerzo. A Augusto que desde niña me quiso llevar por el camino de la investigación y a Hernando y Sandra que siempre me escuchan y que me han enseñado tantas otras cosas que me apasionan. Tampoco quiero olvidar a todos mis tíos, algunos que ya se han ido pero que siempre pensaron me apoyaron, en especial a Laura y Maruja. A Math por su cariño, su comprensión y su apoyo y por darme la estabilidad que necesitaba y necesito en los momentos más difíciles.

A todos mis sinceras gracias.

Resumen

Los movimientos voluntarios del cuerpo son controlados por el sistema nervioso central y periférico a través de la contracción de los músculos esqueléticos. La contracción se inicia al liberarse un neurotransmisor sobre la unión neuromuscular, iniciando la propagación de un biopotencial sobre la membrana de las fibras musculares que se desplaza hacia los tendones: el Potencial de Acción de la Unidad Motora (MUAP). La señal electromiográfica de superficie registra la activación continua de dichos potenciales sobre la superficie de la piel y constituye una valiosa herramienta para la investigación, diagnóstico y seguimiento clínico de trastornos musculares, así como para la identificación de la intención movimiento tanto en términos de dirección como de potencia.

En el estudio de las enfermedades del sistema neuromuscular es necesario analizar el nivel de actividad, la capacidad de producción de fuerza, la activación muscular conjunta y la predisposición a la fatiga muscular, todos ellos asociados con factores fisiológicos que determinan la resultante contracción mioeléctrica. Además, el uso de matrices de electrodos facilita la investigación de las propiedades periféricas de las unidades motoras activas, las características anatómicas del músculo y los cambios espaciales en su activación, ocasionados por el tipo de tarea motora o la potencia de la misma.

El objetivo principal de esta tesis es el diseño e implementación de protocolos experimentales y algoritmos de procesado para extraer información fiable de señales sEMG multicanal en 1 y 2 dimensiones del espacio. Dicha información ha sido interpretada y relacionada con dos patologías específicas de la extremidad superior: Epicondilitis Lateral y Lesión de Esfuerzo Repetitivo. También fue utilizada para identificar la dirección de movimiento y la fuerza asociada a la contracción muscular, cuyos patrones podrían ser de utilidad en aplicaciones donde la señal electromiográfica se utilice para controlar interfaces hombre-máquina como es el caso de terapia física basada en robots, entornos virtuales de rehabilitación o realimentación de la actividad muscular.

En resumen, las aportaciones más relevantes de esta tesis son:

- La definición de protocolos experimentales orientados al registro de señales sEMG en una región óptima del músculo.
- Definición de índices asociados a la co-activación de diferentes músculos
- Identificación de señales artefactuadas en registros multicanal
- Selección de los canales mas relevantes para el análisis
- Extracción de un conjunto de características que permita una alta exactitud en la identificación de tareas motoras

Los protocolos experimentales y los índices propuestos permitieron establecer que diversos desequilibrios entre músculos extrínsecos del antebrazo podrían desempeñar un papel clave en la fisiopatología de la epicondilitis lateral. Los resultados fueron consistentes en diferentes ejercicios y pueden definir un marco de evaluación para el seguimiento y evaluación de pacientes en programas de rehabilitación motora.

Por otra parte, se encontró que las características asociadas con la distribución espacial de los MUAPs mejoran la exactitud en la identificación de la intención de movimiento. Lo que es más, las características extraídas de registros sEMG de alta densidad son más robustas que las extraídas de señales bipolares simples, no sólo por la redundancia de contacto implicada en HD-EMG, sino también porque permite monitorizar las regiones del músculo donde la amplitud de la señal es máxima y que varían con el tipo de ejercicio, permitiendo así una mejor estimación de la activación muscular mediante el análisis de los canales mas relevantes.

Summary

Voluntary movements are achieved by the contraction of skeletal muscles controlled by the Central and Peripheral Nervous system. The contraction is initiated by the release of a neurotransmitter that promotes a reaction in the walls of the muscular fiber, producing a biopotential known as Motor Unit Action Potential (MUAP) that travels from the neuromuscular junction to the tendons. The surface electromyographic signal records the continuous activation of such potentials over the surface of the skin and constitutes a valuable tool for the diagnosis, monitoring and clinical research of muscular disorders as well as to infer motion intention not only regarding the direction of the movement but also its power. In the study of diseases of the neuromuscular system it is necessary to analyze the level of activity, the capacity of production of strength, the load-sharing between muscles and the probably predisposition to muscular fatigue, all of them associated with physiological factors determining the resultant muscular contraction. Moreover, the use of electrode arrays facilitate the investigation of the peripheral properties of the active Motor Units, the anatomical characteristics of the muscle and the spatial changes induced in their activation of as product of type of movement or power of the contraction.

The main objective of this thesis was the design and implementation of experimental protocols, and algorithms to extract information from multichannel sEMG signals in 1 and 2 dimensions of the space. Such information was interpreted and related to pathological events associated to two upper-limb conditions: Lateral Epicondylitis and Repetitive Strain Injury. It was also used to identify the direction of movement and contraction strength which could be useful in applications concerning the use of biofeedback from EMG like in robotic- aided therapies and computer-based rehabilitation training.

In summary, the most relevant contributions are:

- The definition of experimental protocols intended to find optimal regions for the recording of sEMG signals.

- The definition of indices associated to the co- activation of different muscles.
- The detection of low-quality signals in multichannel sEMG recordings.
- The selection of the most relevant EMG channels for the analysis
- The extraction of a set of features that led to high classification accuracy in the identification of tasks.

The experimental protocols and the proposed indices allowed establishing that imbalances between extrinsic muscles of the forearm could play a key role in the pathophysiology of lateral epicondylalgia. Results were consistent in different types of motor task and may define an assessment framework for the monitoring and evaluation of patients during rehabilitation programs.

On the other hand, it was found that features associated with the spatial distribution of the MUAPs improve the accuracy of the identification of motion intention. What is more, features extracted from high density EMG recordings are more robust not only because it implies contact redundancy but also because it allows the tracking of (task changing) skin surface areas where EMG amplitude is maximal and a better estimation of muscle activity by the proper selection of the most significant channels.

Table of Contents

List of Acronyms

Acc	Accuracy
ARV	Average rectified value
BB	Biceps Brachii
BR	Brachioradialis
CC	Cross-correlation
CG	Center of Gravity
CNS	Central Nervous System
CV	Conduction Velocity
DD	Double Differential Signals
DRL	Driven Right Leg
ECR	Extensor Carpi Radialis
ECU	Extensor Carpi Ulnaris
EDC	Extensor Digitorum Communis
EMG	Electromyography
FCR	Flexor Carpi Radialis
FN	False negatives
FP	False Positives
HD-EMG	High Density EMG
IED	Interelectrode distance
iEMG	Intramuscular EMG
IPI	Interimpulse Interval
IZ	Innervation Zone
LE	Lateral Epicondylalgia
μI	mean Intensity
maxI	maximum Intensity
MDF	Median Frequency
MNF	Mean Frequency

MU	Motor Unit
MUAP	Motor Unit Action Potential
MUAPt	Motor Unit Action Potential Train
MVC	Maximal Voluntary Contraction
NMJ	Neuro-muscular Junction
P	Precision
PNS	Peripheral Nervous System
PR	Precision-Recall representation
PSD	Power Spectral Density
PT	Pronator Teres
RMS	Root mean square value
ROC	Receiver Operating Characteristics
RSI	Repetitive Strain Injury
S	Sensitivity
SD	Single Differential Signals
sEMG	Surface EMG
SP	Specificity
TN	True Negatives
TP	True Positives
TR	Triceps Brachii

1

Introduction

Voluntary movements are achieved by the harmonious contraction and relaxation of skeletal muscles attached to bones by tendons and other tissues. When activated, they pull on the bones, either displacing or blocking the joints to produce movement or to stabilize a body segment, as for example during stand up. Muscles exert force by converting chemical energy into tension and contraction. Voluntary contraction is initiated when an action potential travelling down a motor neuron reaches the neuromuscular junction, triggering a chemical reaction that ends in the simultaneous shortening of a high number of long cells referred to as *muscle fibers*. Muscles are composed by bundles of muscle fibers, which in turn are composed by bundles of myofibrils composed by long chains of proteins, mainly actin and myosin. Myosin form thick filaments while actin form thin filaments. The sliding of the thin filaments past the thick filaments produces the shortening of muscle fiber, and so the *actual* muscular contraction and the movement.

1.1. Fundamentals of physiology of the neuromuscular system

1.1.1 The Neuromuscular system

The nervous system is divided into the Central Nervous System (CNS) and the peripheral nervous system (PNS).

The first consists in the brain and the spinal cord and collects, process and transmits all the information from and to the organs of the body in humans. The PNS consists of all ganglia and neural tracts that lie outside the brain or spinal cord and connect the CNS to the limbs and organs of the body.

Voluntary and involuntary movements are produced by spatial and temporal patterns of muscular contractions coordinated by the CNS. They are initiated by "lower" motor neurons (motor neurons-α) that directly innervate skeletal muscles which, in time, are

controlled by "upper" motor neurons in higher centers, enabling and coordinating complex sequences of movements. Finally, circuits in the basal ganglia and cerebellum (PNS) are responsible for the regulation of upper motor neurons, ensuring that movements are performed with spatial and temporal precision (Purves 2004). A schematic is presented in Figure 1.1. The combination of the nervous system and muscles, working together to allow movement, is known as the neuromuscular system.

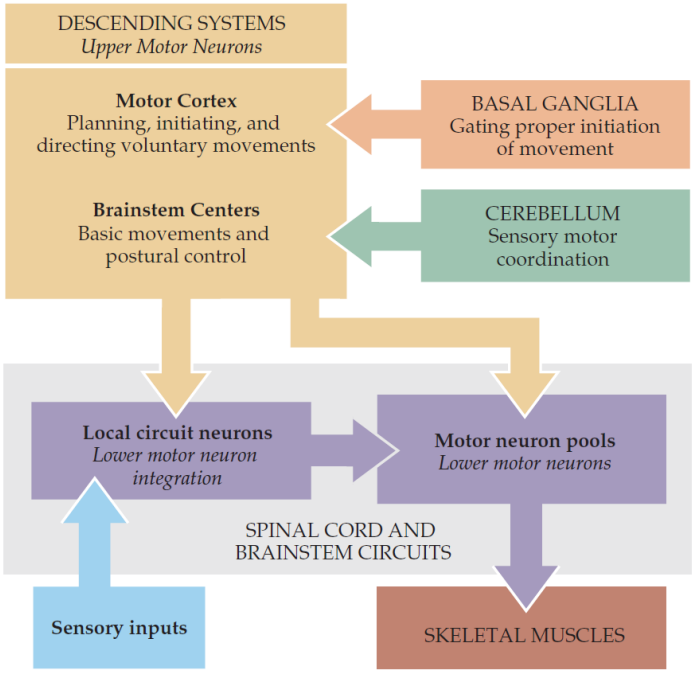

Figure 1.1. Overall organization of neural structures involved in the control of movement (extracted from (Purves 2004))

1.1.2 The Motor Unit

As mentioned before, the muscular fibers are stimulated by motor neurons-α coming from the spinal cord or the brainstem. A single neuron innervates several fibers at the same time. The set of fibbers plus a single motor neuron constitutes the smallest functional structure of the neuromuscular system: the motor unit (MU) (Figure 1.2). The stimulation takes place at the neuromuscular junction where the axons of the motor neurons end. From there, an action potential (the Motor Unit Action Potential- MUAP) propagates to both ends of the fibers at a certain Conduction Velocity CV depending on the type of fiber. The neuromuscular junctions are distributed in a region of the muscle that is referred to as the Innervation Zone, and it is normally located in the muscle belly. When a motor unit is activated, all the fibers within it contract simultaneously. In order to make a muscle move, different motor units of that muscle will group together and contract. This larger group of motor units is commonly referred to as *motor unit pool*.

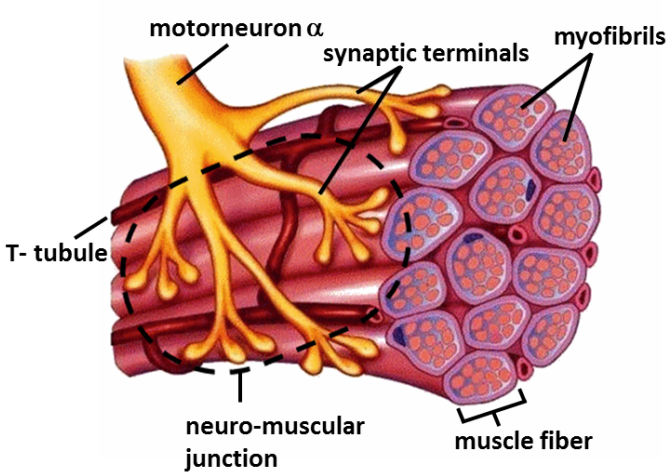

Figure 1.2. Motor Unit. Group of muscle fibers innervated by a single motorneuron.

Human muscle fibers can be classified into fast and low twitch response according to their biomechanical properties: Type I fibers have slow mechanical response and they are oxidative and fatigue resistant. Type IIb are glycolytic easily fatigable and have fast mechanical response. Type IIa are both glycolytic and oxidative, have fast response and are fatigue resistant (Merletti, Parker 2005). Each MU is composed by fibers of the same type, thus, the fiber type classification can be extended to MU. Type II MUs generate ATP for producing muscular contraction through anaerobic glycolysis, which in turn produces lactic acids and this is why they are more prone to fatigue (Merletti, Parker 2005). The diameter of glycolytic fibers is generally much higher than that of oxidative fibers. This fact has great significance for tension development: although the size of the cross sectional area of myosin and actin filaments per unit of cross-sectional area is about the same in all types of skeletal muscle fibers, their diameters are different. Thus, the larger the diameter of a muscle fiber, the greater the total number of protein filaments acting in parallel to produce force, and the greater the maximum tension the fiber can develop (greater strength) (Widmaier, Raff & Strang 2008). Consequently, type II motor units are capable of producing grater force than type I.

Finally, skeletal muscles are composed by different proportions of Type I and Type II MU depending on its function and when considering the same type of muscle, depending on the training status of a specific subject (Kadi et al. 2000).

For example, muscles of the back, which support the upright posture, must be able to maintain their activity for long periods of time without fatigue and thus contain large numbers of Type I and Type IIa MU. In contrast, the muscles in the arms capable of

producing large amounts of tension over a short time period, as when lift a heavy object, have a greater proportion of Type IIb fibers (Widmaier, Raff & Strang 2008).

1.1.3 The Motor Unit Action Potential

The motor neurons conduct nerve impulses from the anterior horn cells of the spinal cord to the nerve ending where the axonal potential releases a neurotransmitter called acetylcholine in the neuromuscular junction. As acetylcholine (Ach) binds the walls of the muscular fibers (i.e. the sarcolemma), sodium channels open creating miniature end-plate potentials. If sufficient Ach is released, the summation of all created end-plates reaches the excitation threshold and a fiber action potential propagates in opposite directions from its origin at the neuromuscular junction to the tendons. The travelling action potential spreads into the T-tubules and reaches the myofibril where calcium stored in the lateral sacs of the sarcoplasmic reticulum is released enabling the proteins myosin and actin to interact and contract (Henneberg 1999) (Figure 1.3). A cross-bridge cycle in which myosin attaches and detaches to actin is the responsible for the shortening of the muscle fiber. The summation of single fiber action potentials generate the Motor Unit Action Potential that propagates at a Conduction Velocity of 3 to 5 m/s in the direction of the muscular fibers (Pozzo, Farina & Merletti 2003)

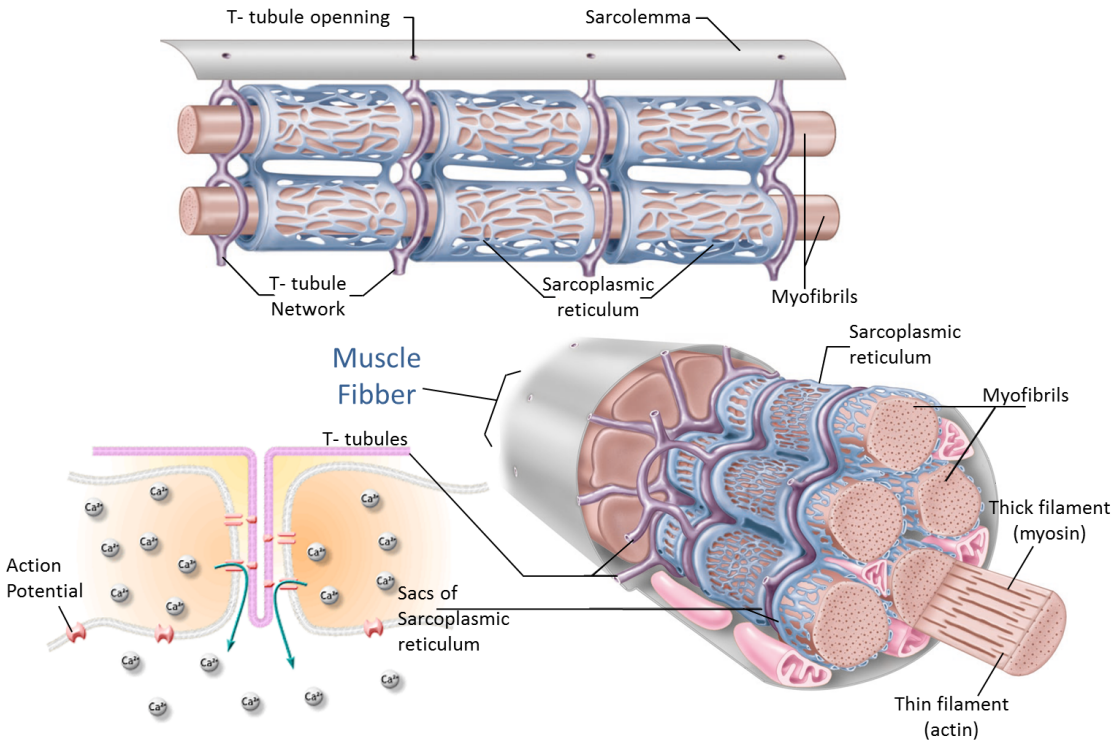

Figure 1.3. Diagrammatic representation of the sarcoplasmic reticulum, the transverse tubules, the myofibrils and the contractile proteins. Lateral and cross-section view are presented. The concept of calcium release is also represented. Extracted and modified from (Widmaier, Raff & Strang 2008)

Different MUs generate different MUAP shapes according to fiber type (I, IIa or IIb), and to the number and size of its constituent fibers (Figure 1.4). Each MUAP is unique, though some variations are induced mainly because not all the fibbers of the same MU activate at the same time instant. This variability is mainly reflected in the peak to peak amplitude and in the duration and the shape of the tails (Holobar, Zazula 2004). The frequency of activation is also related to the kind of MUs: MUs of type I have, in general, lower activation frequencies than MUs of type II.

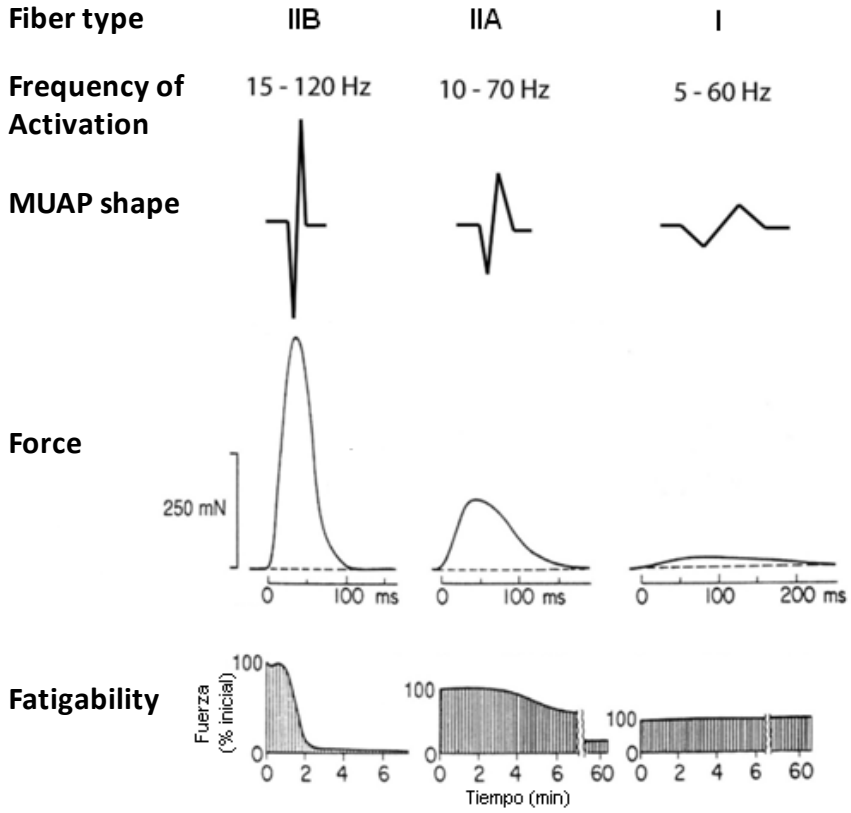

Figure 1.4. MUAP shapes and characteristics associated with the different kind of MUs. Retrieved and modified from (Ricard 2007)

The interval between two consecutive activations of the same MU is called IPI (Inter pulse Interval). Its distribution can be modeled as a Gaussian process where the mean value is the inverse of the activation frequency of the motor neuron. Typical values range around 50-120 ms with a standard deviation given by (Holobar, Zazula 2004):

$$\sigma = \sqrt{0.2IPI}$$

Typical values of σ are in between 0.1s and 0.33s (Merletti, Parker 2005).

1.1.4 Force Modulation

The Central Nervous System (CNS) controls the contraction of muscles, and thus, the force, with two different strategies: by increasing the number of active motor units (fiber recruitment) or by increasing the frequency of activation of each single motor unit. The greater the number of recruited MU and the higher their activation frequency, the greater the tension produced by the muscle. In early 1960s, Henneman formally proposed that the recruitment of MU was based in the "size principle", in which motor units innervated by the smallest motor neuron α were recruited at the beginning of the contraction followed by bigger motor units in increasing size, based on results obtained from electrical stimulation of cat motor neurons. The size principle states: "The amount of excitatory input required to discharge a motor-neuron, the energy it transmits as impulses, the number of fibers it supplies, the contractile properties of the motor unit it innervates, its mean rate of firing and even its rate of protein synthesis are all closely correlated with its size. This set of experimental facts and interrelations has been called the 'size principle'."(Henneman 1977). Figure 1.5 explains this concept: at the beginning of the contraction only type I MUs are recruited until there are no more left. As the contraction continues in time, type IIa MUs are recruited. Finally, if the requirement of force is very high, Type IIb MU become active, achieving the highest tension the muscle can exert by this mechanism.

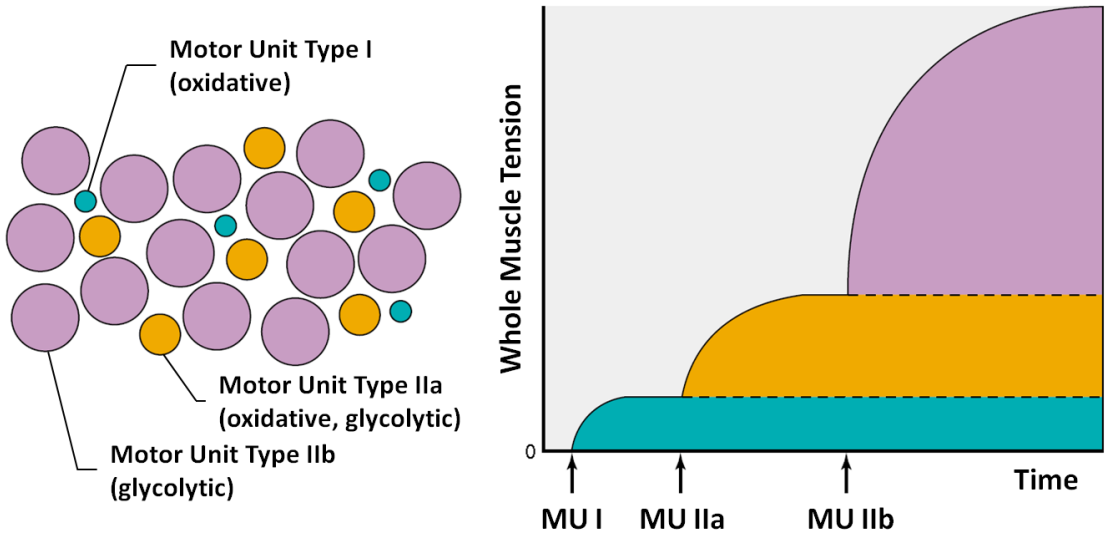

Figure 1.5. Diagram of a cross-section of a muscle (*left*), and size principle for recruitment of MU (*right*). Human skeletal muscle is composed by different proportions of MU types depending on its intended function. The higher muscle tension is achieved by the activation of type IIb MU which is the biggest and the strongest of the tree types. Extracted from (Widmaier, Raff & Strang 2008)

The force at which the largest motor unit is recruited corresponds to the upper limit of motor unit recruitment and varies from muscle to muscle. Beyond this threshold, only the

rate coding contributes to increments in the exerted force. For example all motor units in Adductor Pollicis are recruited at 50% of the maximal voluntary contraction (MVC) while upper recruitment limit in Biceps Brachii is around 80% MVC. Several studies have demonstrated that the relative contribution of the two mechanisms to muscle contraction depend on the amount of required force and on the speed of the movement (Duchateau, Enoka 2011).

1.2 Muscular fatigue

When a MU is repeatedly stimulated, the tension developed by their fibers eventually decreases even though the stimulation continues. This decline in the contractile activity is known as muscle fatigue and it is characterized by a decrease in the velocity of MUAP conduction and by a slower rate of relaxation (Widmaier, Raff & Strang 2008). It is a continuous process that starts the moment the MU is activated although its effects cannot be directly observed in a short time period. What can be observed is the *failure point* and corresponds to the time-instant when a muscle or a group of muscles are not able to maintain a given level of force (De Luca 1984). This point is also called the mechanical fatigue.

The onset of muscle fatigue (which is not to be confounded with the failure point) and its rate of development are different for different types of MUs, and, when referred to a whole muscle depends on its MU composition and on the degree of individuals' fitness. A fatigued muscle recovers its ability to contract after a resting period with its rate of recovery depending on the intensity and duration of the previous activity. Muscles with higher proportion of type II MU, like those of the forearm or hand fatigue earlier than muscles with higher proportions of type I MU (Kupa et al. 1995). Considering training exercise, high-intensity, short-duration contractions such as weight lifting induce muscular fatigue mainly on type II MU and is characterized by rapid onset of fatigue but also by short recovery periods. On the other hand, low-intensity, long-duration exercise such as long distance running requires much longer periods of rest often up to 24 h before muscles achieve complete recovery (Widmaier, Raff & Strang 2008).

A series of mechanisms are involved in fatigue induced by short-duration high-intensity contractions. They can be found at MU level in which case we refer to them as *peripheral fatigue* or can occur at a higher level in the CNS and they are referred to as *central fatigue*.

Different physiological changes occur when accounting for peripheral fatigue: the MUAP can fail to be conducted into the fiber along the T-tubules network halting the release of calcium and thus preventing the interaction of the contractile proteins. The repetitive activation leads to a persistent depolarization of the membrane potential as consequence of a high concentration of potassium ions in the small volume of the T-tubules (Figure 1.3) and thus its membrane is unable to produce action potentials (Widmaier, Raff & Strang 2008). Other factor is related to the acidification of the muscle: two different theories account for this: in the first, the production of ATP within the fiber causes the accumulation and the eventual release of lactic acid that increases the concentration of hydrogen ions inside and outside of the membrane and decreases the pH (De Luca 1984). However, a recent theory states that the accumulation of lactic acid actually retard acidosis (Gladden 2004) and is the lack of oxygen in association with the accumulation of hydrogen ions from the production of ATP which causes intramuscular acidification (Mesin et al. 2009). Either way, the acidification of the muscle membrane changes its excitability and slows the conduction of the MUAP across the fiber (De Luca 1984). The last factor is related to the build-up of ADP within the muscle fiber which delays the detachment of actin resulting in the slowing of the cross-bridge cycle and lastly reducing the shortening velocity (Widmaier, Raff & Strang 2008).

On the other hand, central fatigue is related to the synchronization of MUs (the tendency for MUs to discharge at, or nearly at, the same time) to increase the mechanical output once all available motor units have been recruited. It is the result of common pre-synaptic inputs to motor neurons within a motor neuron pool, showing a high time-dependency of action potentials from different MUs than expected by chance. Several works have reported this phenomenon (Mori 1973), (Kleine et al. 2001). It can occur during sustained long term contractions, as consequence of training or due to pathology.

Muscle training induces adaptations in the neural control of MUs in order to avoid or retard muscle fatigue. Skill or endurance training involving the fine control of a group of muscles during long periods of time like professional piano playing or long distance running promotes asynchronous recruitment of MUs. In contrast, strength- training involving high-force explosive contractions like weightlifting or Olympics high-jump practice promote synchronous recruitment of nearly all MUs in the muscle in a short period of time (Semmler, Nordstrom 1998).

Finally, although muscle fatigue can be beneficial in promoting muscle growth (Al-Mulla, Sepulveda & Colley 2011), and CNS recruitment as in the cases mentioned in the

previous paragraph, it is usually harmful and cause degenerative changes in the muscles, especially if highly repetitive contractions are considered (Larivière et al. 2010, Moore 2002)

1.3 Electromyographic signal (EMG)

The repetitive activation of MUs generates motor unit action potential trains (MUAPt) in time domain. It can be described as the convolution of the MUAP with a Dirac impulse train (δ) separated by the IPI of the MU. It can be expressed as (Dan 2001):

$$MUAPt_j(t) = \sum_{k=1}^{Mj} MUAP_{jk}(t - \delta_{jk})$$

Where $MUAPt_j$ is the train corresponding to MU *j*, $MUAPt_{jk}$ is the MUAP generated at time-instant *k*, *Mj* is the number of times the motor unit is activated and δ_{jk} is the impulse train defined by the IPI_j of MU_j.

Different trains of potentials add together to generate a signal in the time domain that can be recorded as the EMG signal (Figure 1.6) (Basmajian 1978)

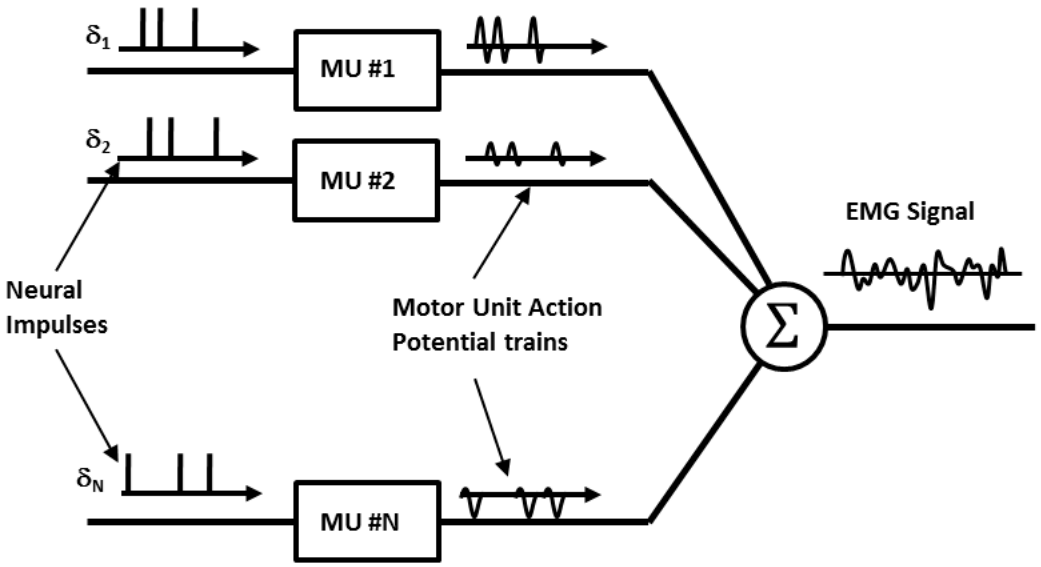

Figure 1.6. Model of the origin of the EMG signal. Each MUAP train can be seen as the convolution of the MUAP of a given MU with a train of neural impulses. The superposition of different trains creates the pattern of the EMG signal. Retrieved and modified from (Basmajian 1978)

If an invasive electrode is placed in a contracting muscle, the intra-muscular electromyogram (iEMG) can be detected as the spatial and temporal sum of potential contributions from a number of muscle fibers (some or almost all of the fibers of a given MU) depending on the type of electrode and on its size (Merletti, Parker 2005). On the

other hand, if an electrode is placed over the surface of the skin the surface EMG signal (sEMG) detects the electrical activity of a number of MU in a wider area, and thus, including information from a greater proportion of the muscle of interest than conventional iEMG. Moreover, the intramuscular action potentials are not representative of the entire MU because the needle is in contact with a reduced number of fibers (Stålberg 1980). Both, the amplitude and the spectral properties of the sEMG signal depend on the size of the active MUs and also on their depth with respect to the recording electrode. Analytically, it can be expressed as (Merlo, Farina & Merletti 2003):

$$sEMG(t) = \sum_{j} MUAPt_j(t) + n(t) = \sum_{k=1}^{Mj} a_j \cdot MUAP_j(\frac{t-\delta_j}{\alpha_j}) + n(t)$$

where *j* indicates a specific MU, δ is the impulse train modulating the occurrence of the MUAP, a_j and α_j are amplitude and scaling factors respectively and $n(t)$ is additive noise. The factor a accounts for the amplitude of the potential which depends on the number of fibers composing the MU *j*. On the other hand, observe that the scaling factor α directly affects the spectral properties of the signal. It stands for a number of tissues (i.e. the volume conductor) separating the sources and the recording electrodes, as for example connective tissue, fat layer, skin, other muscles, etc.

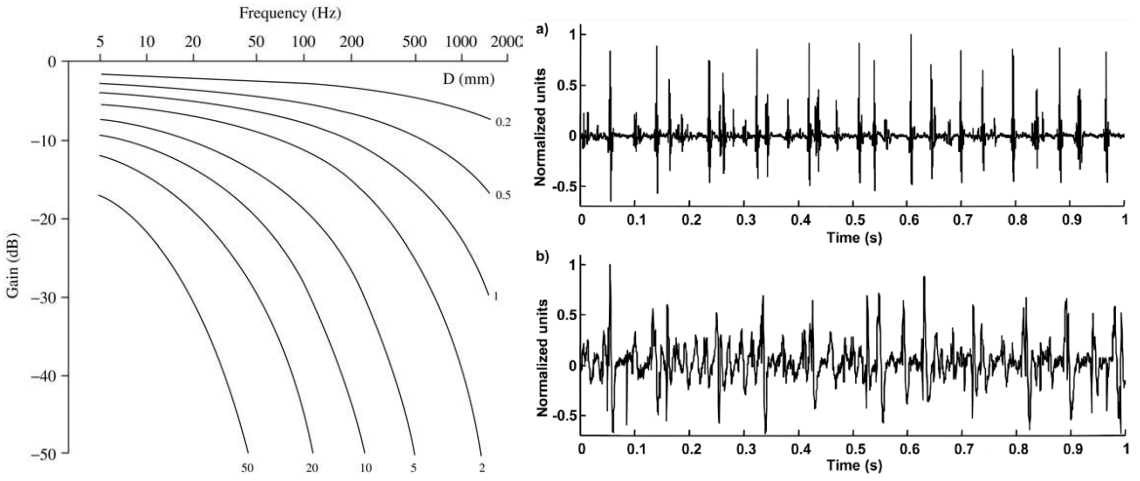

Figure 1.7. Left. Spatial transfer functions of a homogeneous volume conductor for different distanced D between the point of detection and the source. Right. Example of two EMG signals obtained from needle electrode (top) and surface electrode (bottom). Extracted from (Pozzo, Farina & Merletti 2003)

The transfer function of the volume conductor has the characteristics of a low-pass filter (Figure 1.7 left). While the iEMG signal has a bandwidth up to 5 kHz, the sEMG has frequency content below 300 Hz as result of the volume conductor between the recording electrode and the point of origin of the potential (Pozzo, Farina & Merletti 2003). An example is presented in Figure 1.7 right. It is possible to observe that the frequency content

of the iEMG signal is much higher than that of the sEMG. Additionally, in this last one it is also possible to observe a higher superposition of potentials as result of the detection in a wider area.

The amplitude of the EMG signal is stochastic in nature (De Luca 1997), regardless the recording method. However a signal recorded during an isometric contraction can be considered a wide sense stationary process if it is segmented in time-epochs of 0.5-1s (Balestra, Knaflitz & Merletti 1988). sEMG amplitude can range between 0 -10 mV peak-peak depending on the muscle and on the subject. In general, the dominant energy of the signal is up to 150 Hz. An example is presented in Figure 1.8.

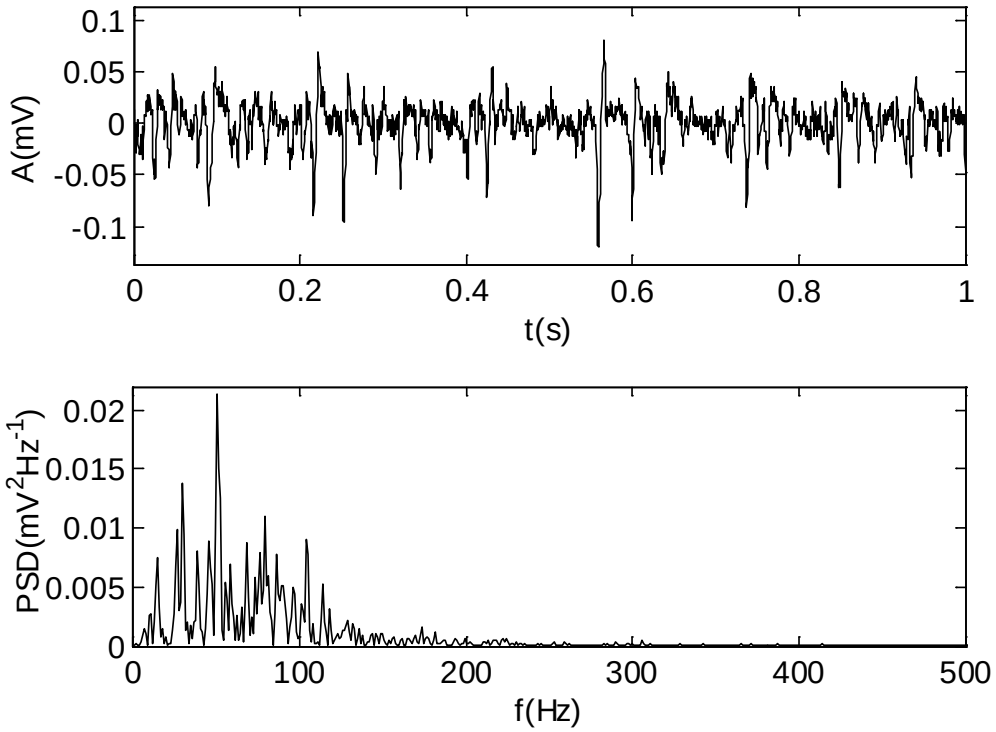

Figure 1.8. *top.* sEMG signal detected in the Biceps Brachii during a constant force contraction at medium level of effort. *bottom.* Frequency spectrum.

Although iEMG has been widely used in clinical applications, it has limitations in cases where needle insertion is not possible or not desirable. Some of them are related to subjects' condition as for example in the case of children, professional athletes or patients with transplanted limbs (Farina et al. 2008), while others are mainly related to discomfort as in the case of studies related to ergonomics, biomechanics, sport practice or rehabilitation monitoring. sEMG is usually analyzed as an interference signal from where properties of individual motor units are indirectly inferred from global variables, like for example, amplitude and power spectrum

Though sEMG does not substitute the conventional needle EMG, it offers complementary information. For instance, it allows the analysis of motor unit properties which are difficult to measure with invasive technology (Farina, Fortunato & Merletti 2000), such as muscle fiber conduction velocity which is intrinsically related to myoelectric fatigue and allows the determination of the anatomical characteristics of the muscle "in vivo", such as the location of the innervation zones (Rainoldi, Melchiorri & Caruso 2004, Enck et al. 2010).

1.3.1 Myoelectric manifestations of muscular fatigue in the EMG signal

As mentioned before, peripheral fatigue results in the reduction of the conduction velocity of active MUs. Changes at MU level are observed as a "slowing" of the EMG signal in the temporal domain which correspond to a scaling of the power density function (PDF) of the EMG signal towards lower frequencies in the frequency-domain (Merletti, Parker 2005). The shifting of the frequency content is observed long before reaching the mechanical fatigue (Figure 1.9) with its rate of decay depending on the muscle. Additionally, shifts toward lower frequencies are more pronounced at the beginning of the contraction and are better explained by peripheral than by central fatigue (De Luca 1984).

Central fatigue also contributes to frequency shift since the higher the activation frequencies (plus possible synchronizations), the higher the probability of MUAP superposition and the smother the shapes of the action potentials in the recorded signal. Finally, MUAP superposition increases the energy of the signal as the contraction progresses in time (De Luca 1984).

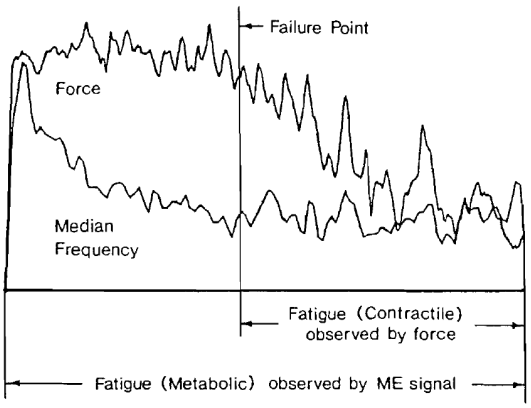

Figure 1.9. Decrease in the frequency content of the EMG signal during a constant force contraction and in the exerted force during a sustained contraction. Extracted from (De Luca 1984)

1.3.2 Types of contraction and EMG signal

Muscular contractions can be classified according to length changes in the muscle while developing tension (Hamill, Knutzen 2006):

- Isometric contraction: It is produced by exerting force against a resistance avoiding the movement of the joint. In isometric contractions no appreciable change in muscle length is observed, thus signals recorded with this method can be analyzed in segments that can be considered as wide- sense stationary processes
- Concentric contraction: Occurs when the muscle visibly shortens while generating tension. In concentric contraction, the net muscle forces producing movement change in the same direction as the joint angle. Concentric action is controlled by agonists muscles, i.e. those muscles whose specific function is involved in the movement being produced, for example, when contracting the biceps for flexing the arm from the standing position. In a flexion, the biceps is the agonist muscle and the triceps is the antagonist because the main function of the last is the opposite (i.e., extension)
- Eccentric contraction: In eccentric contraction, the net muscular forces producing the rotation are in the opposite direction of the change in joint angle and are the antagonist muscles that control the movement of the joint. Eccentric action causes a lengthening of the muscle while tension is produced in response to an external torque that is greater than the torque generated by the muscle. Eccentric contractions are produce in the leg muscles, for example, when walking down a hill.

The three types of contraction are displayed in Figure 1.10. As the concentric and eccentric actions involve the movement of the joint, they are also known as *dynamic* contractions. In time, they can also be classified into isotonic and isokinetic. In the first, the joint move through a range of motion against a constant resistance. Common examples are push-ups, sit-ups, and the lifting of weights. In the second, the joint angle change at a constant rate by varying the load or resistance at different joint angles to counteract the varying forces produced by the muscles.

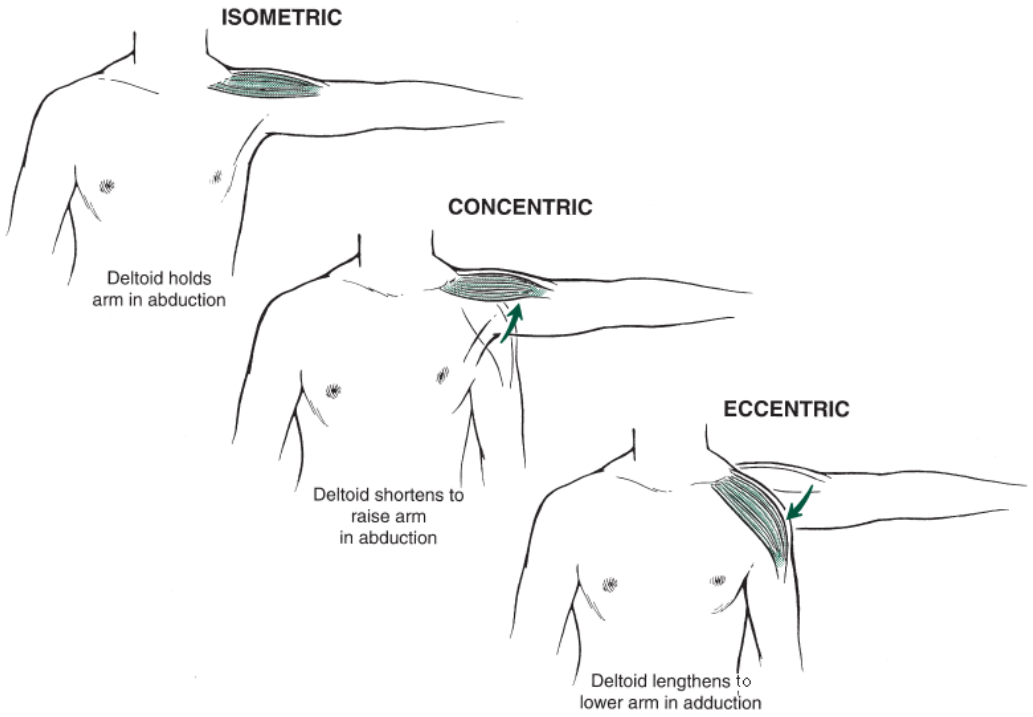

Figure 1.10. Types of contraction produced by skeletal muscles. Isometric contraction does not change the position of the joint. In the other two the muscle shortens or elongates in response to external forces acting over the body segment involved. Extracted from (Hamill, Knutzen 2006)

The three types of contraction are normally combined to produce movement rather than be used in isolation (Hamill, Knutzen 2006). However, in dynamic contractions, the distance between the origin of the MUAPs and the surface electrodes changes as the muscle fibers contract or elongate, hardening the interpretation of the sEMG signals and hindering their extrapolation to populations under study. Isometric signals, on the other hand, can be compared among different subjects if they are registered under controlled conditions that usually include the determination of the maximal voluntary contraction (MVC) (the maximal force a subject can exert during a specified task) and the feedback of the force being developed so the subject can maintain the same level of force during a period of time.

1.4 Electrode Arrays

Surface EMG signals are commonly recorded with bipolar electrodes in clinical environment. Such electrodes measure the voltage difference between two specific points, with its detection volume depending on the inter-electrode distance (IED). The differential configuration of the bipolar electrode implies a band-pass filter behavior that increases with increasing IED. Thus, the spectral characteristics of the signal are affected by the IED (Merletti, Parker 2005). Typical distances range between 15 mm and 45 mm and although lower distances should be desirable, the cited distances represent a compromise between

the need to enhance signal amplitude or signal/noise ratio and the need to limit spectral modifications in the signal. Besides, signals recorded with this kind of electrodes are highly affected by the relative position between the sensing region and the innervation zone and tendons when such information is not a-priori known. Information extracted from signals recorded in the proximity of these two muscular regions can be biased and must be avoided for correct interpretation of the results (Saitou et al. 2000).

An alternative is the use of electrode arrays. When referring to sEMG, an electrode arrays is a system that detects the signal at different points along the perpendicular and/or parallel directions of MUAPs propagation over the skin surface. Typical IED for electrode arrays range between 2.5 and 15 mm. If the electrode array is aligned with the transversal direction of the muscular fibbers, it allows the detection of MU distributed across the radial direction of the muscle while if aligned with the direction of fiber, it can record the electrical propagation of the potentials along the sarcolemma.

By using an electrode array it is possible to obtain a set of signals (one for each electrode) that gives specific information about the distribution of MUAPs on a given muscular region, allowing the observation of anatomical regions of the muscle like innervation zone and tendons. It also enables the estimation of the conduction velocity (CV) of the active MUs by calculating the delay between two signals detected at a known distance.

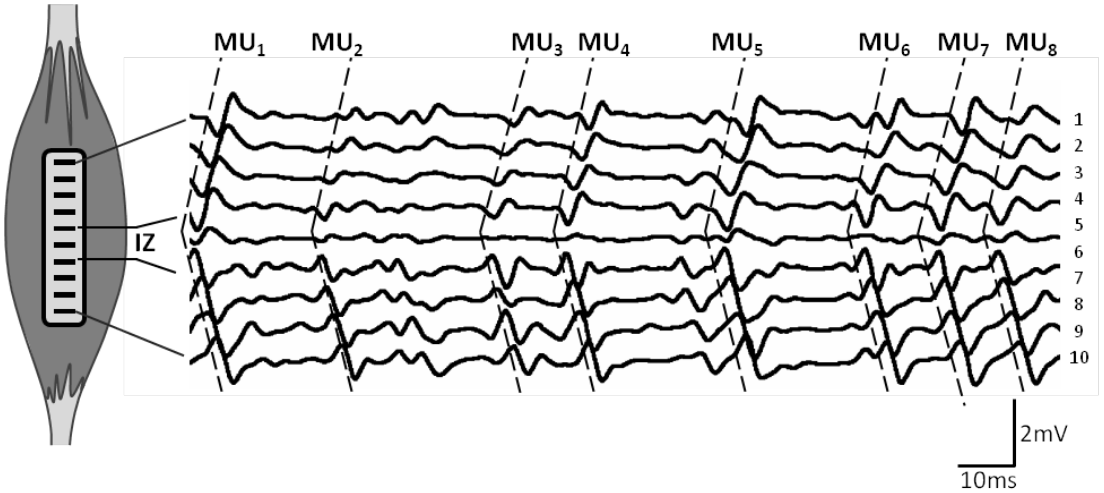

Figure 1.11. Multichannel sEMG signal registered with an electrode arrays over the Extensor Digitorum Communis Muscle. 10 bipolar channels are obtained form 11 Ag/AgCl electrode. It is possible to observe MUAP propagating from the IZ to the tendons.

A signal registered with a linear electrode array (1D) is presented in Figure 1.11. The location of the IZ and the propagation of MUAPs from there to the tendons where the extinction occurs can be observed. Note that both the amplitude and the shape of the

signals depend on the proximity between the recording electrode and the innervation zone.. Thus electrode positioning, either multichannel or specially bipolar, should be dependent on the location of innervation zones.

Different information can be extracted by using electrode arrays arranged in different fashions. The use of 2D arrays consisting in a set of electrodes distributed in the dimensions of the space and placed closely together allows a spatial sampling of MU activity over the surface of the muscle (Figure 1.12). The recorded signals, referred to as High Density EMG (HD-EMG), has four dimensions: two in the space, one in time and one in amplitude. This technique has gain attention during the last years for different applications such as signal decomposition (i.e. isolation and classification of individual MUAPs from the sEMG signal) (Merletti, Holobar & Farina 2008), the study of muscle compartmentalization (Vieira, Merletti & Mesin 2010) and of the changes in the spatial distribution of MUAPs with exercise or pain(Madeleine et al. 2006).

However, along with MUAPs from the muscle of interest, it is also possible to detect potentials originated in the activation of neighboring muscles or in the change of media (from muscle to tendon) obstructing the interpretation of the sEMG signals. These potentials, known as crosstalk, are due to the low-pass filter effect of the volume conductor and they can usually be observed as non- propagating potentials

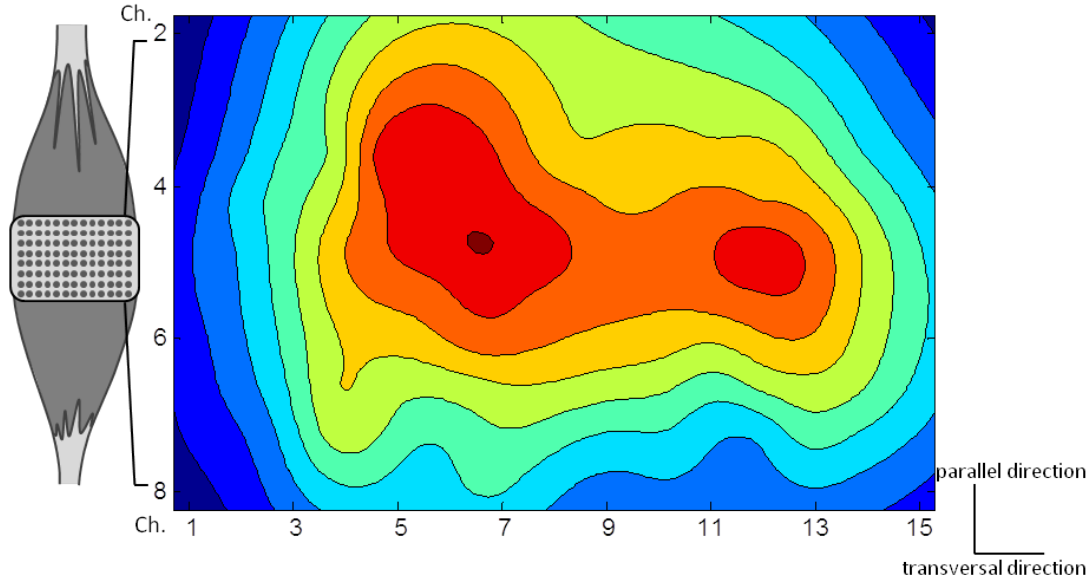

Figure 1.12. Contour intensity map of the electrical activity of Biceps muscle during a flexion at 50%MVC. A grid of 8×15 electrodes was used to register high density sEMG signals. It is possible to observe the activation of the 2- heads of the muscle and the extinction of the potentials in the transversal and radial directions.

On the other hand, the detection of sEMG can be enhanced by filtering in the spatial domain. Spatial filters can be applied online (when recording the signals) or offline (when analyzing the signals) (Farina et al. 2003). They are useful for reducing common-mode noise and crosstalk and to improve the pickup area of different MUAPs (Figure 1.13). MUAPs coming from MUs close to the skin surface have bigger contributions (in terms of amplitude) than MUAPs from deep MUs because of the attenuation caused by the volume conductor. The simplest consist in the subtraction of each channel from the next in the direction of propagation of the potentials (Single Differential detection- SD).

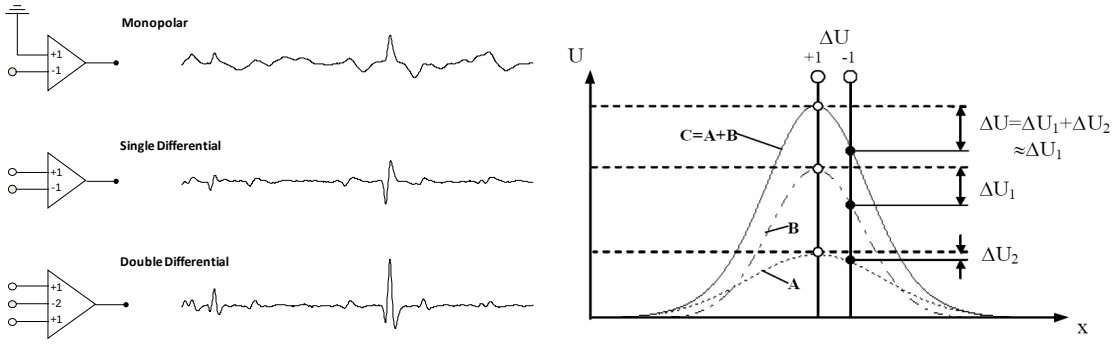

Figure 1.13. left. Signals obtained with different spatial filters. right. Single Differential detection. The sensitivity of the deepest potentials (A) is less than the most superficial potentials (B).

Figure 1.13 (right) shows the difference between single differential (SD) and monopolar configurations. The signal A (low amplitude and low frequency components) represent a signal originated on a MU located far away from B. In a monopolar arrangement, the detected signal will correspond to the sum of the signals A and B (signal C). However, a SD arrangement mainly detects variations on B. This is because of a slight change of amplitude of the potential A (ΔU_2) compared with a large change of amplitude of the potential B (ΔU_2), for small inter-electrode distances. Consequently, an SD configuration "isolates" the activity of the potential B (Grönlund 2006). On the other hand, by applying subsequent spatial filters like double differential-DD (i.e. by subtracting consecutive channels) in the case of 1D arrays or by weighting and subtracting neighboring channels in the case of 2D arrays, it is possible to reduce crosstalk because non- travelling potentials superimposed destructively and those that propagate remain.

1.5 References

Al-Mulla, M.R., Sepulveda, F. & Colley, M. 2011, "A Review of Non-Invasive Techniques to Detect and Predict Localised Muscle Fatigue", *Sensors,* vol. 11, no. 4, pp. 3545-3594.

Balestra, G., Knaflitz, M. & Merletti, R. 1988, "Stationarity of Voluntary and Electrically Elicited Surface Myoelectric Signals", *7th Congress of the International Soc. of Electrophysical kinesiology*, eds. W. Wallinga, H. Boom & J. Devries, , 1988, pp. 275-278.

Basmajian, J.V. 1978, *Muscles alive, their functions revealed by electromyography,* 4th edn, Williams & Wilkins.

Dan, S. 2001, "EMG signal decomposition: how can it be accomplished and used?", *Journal of Electromyography and Kinesiology,* vol. 11, no. 3, pp. 151-173.

De Luca, C.J. 1984, "Myoelectrical manifestations of localized muscular fatigue in humans.", *Critical Reviews in Biomedical Engineering,* vol. 11, no. 4, pp. 251.

De Luca, C.J. 1997, "The use of surface electromyography in biomechanics", *Journal of Applied Biomechanics,* vol. 13, no. 2, pp. 135-163.

Duchateau, J. & Enoka, R.M. 2011, "Human motor unit recordings: Origins and insight into the integrated motor system", *Brain research,* vol. 1409, no. 0, pp. 42-61.

Enck, P., Franz, H., Davico, E., Mastrangelo, F., Mesin, L. & Merletti, R. 2010, "Repeatability of innervation zone identification in the external anal sphincter muscle", *Neurourology and urodynamics,* vol. 29, no. 3, pp. 449-457.

Farina, D., Arendt-Nielsen, L., Merletti, R., Indino, B. & Graven-Nielsen, T. 2003, "Selectivity of spatial filters for surface EMG detection from the tibialis anterior muscle", *IEEE Transactions on Biomedical Engineering,* vol. 50, no. 3, pp. 354-364.

Farina, D., Fortunato, E. & Merletti, R. 2000, "Noninvasive estimation of motor unit conduction velocity distribution using linear electrode arrays", *Biomedical Engineering, IEEE Transactions on,* vol. 47, no. 3, pp. 380-388.

Farina, D., Pozzo, M., Lanzetta, M. & Enoka, R.M. 2008, "Discharge variability of motor units in an intrinsic muscle of transplanted hand", *Journal of neurophysiology,* vol. 99, no. 5, pp. 2232-2240.

Gladden, L.B. 2004, "Lactate metabolism: a new paradigm for the third millennium", *Journal of Physiology-London,* vol. 558, no. 1, pp. 5-30.

Grönlund, C. 2006, *Spatio-temporal processing of surface electromyographic signals: information on neuromuscular function and control*, Umeå universitet.

Hamill, J. & Knutzen, K.M. 2006, "Muscular Considerations for Movement" in *Biomechanical basis of human movement*, 2nd edn, Lippincott Williams & Wilkins.

Henneberg, K. 1999, "Principles of Electromyography" in *The Biomedical Engineering Handbook*, 2nd edn, CRC Press.

Henneman, E. 1977, "Functional organization of motoneuron pools: The size principle", *Int. Union Physiol. Sci.,* pp. 50.

Holobar, A. & Zazula, D. 2004, "Correlation-based decomposition of surface electromyograms at low contraction forces", *Medical & biological engineering & computing,* vol. 42, no. 4, pp. 487-495.

Kadi, F., Ahlgren, C., Waling, K., Sundelin, G. & Thornell, L.-. 2000, "The effects of different training programs on the trapezius muscle of women with work-related neck and shoulder myalgia", *Acta Neuropathologica,* vol. 100, no. 3, pp. 253-258.

Kleine, B.U., Stegeman, D.F., Mund, D. & Anders, C. 2001, "Influence of motoneuron firing synchronization on SEMG characteristics in dependence of electrode position", *Journal of applied physiology,* vol. 91, no. 4, pp. 1588-1599.

Kupa, E.J., Roy, S.H., Kandarian, S.C. & De Luca, C.J. 1995, "Effects of Muscle-Fiber Type and Size on Emg Median Frequency and Conduction-Velocity", *Journal of applied physiology,* vol. 79, no. 1, pp. 23-32.

Larivière, C., Forget, R., Vadeboncoeur, R., Bilodeau, M. & Mecheri, H. 2010, "The effect of sex and chronic low back pain on back muscle reflex responses", *European Journal of Applied Physiology,* vol. 109, no. 4, pp. 577-590.

Madeleine, P., Leclerc, F., Arendt-Nielsen, L., Ravier, P. & Farina, D. 2006, "Experimental muscle pain changes the spatial distribution of upper trapezius muscle activity during sustained contraction", *Clinical Neurophysiology,* vol. 117, no. 11, pp. 2436-2445.

Merletti, R. & Parker, P. 2005, *Electromyography: Physiology, Engineering, and Non-Invasive Applications*, IEEE Press in Biomedical Engineering.

Merletti, R., Holobar, A. & Farina, D. 2008, "Analysis of motor units with high-density surface electromyography", *Journal of Electromyography and Kinesiology,* vol. 18, no. 6, pp. 879-890.

Merlo, A., Farina, D. & Merletti, R. 2003, "A fast and reliable technique for muscle activity detection from surface EMG signals", *IEEE Transactions on Biomedical Engineering,* vol. 50, no. 3, pp. 316-323.

Mesin, L., Cescon, C., Gazzoni, M., Merletti, R. & Rainoldi, A. 2009, "A bi-dimensional index for the selective assessment of myoelectric manifestations of peripheral and central muscle fatigue", *Journal of Electromyography and Kinesiology,* vol. 19, no. 5, pp. 851-863.

Moore, J.S. 2002, "Biomechanical models for the pathogenesis of specific distal upper extremity disorders", *American Journal of Industrial Medicine,* vol. 41, no. 5, pp. 353-369.

Mori, S. 1973, "Discharge Patterns of Soleus Motor Units with Associated Changes in Force Exerted by Foot during Quiet Stance in Man", *Journal of neurophysiology,* vol. 36, no. 3, pp. 458-471.

Pozzo, M., Farina, D. & Merletti, R. 2003, "Electromyography: Detection, Processing, and Applications" in *Biomedical Technology and Devices Handbook* CRC Press, .

Purves, D. 2004, *Neuroscience,* 3rd edn, Sinauer Associates, Sunderland, Mass, U.S.A.

Rainoldi, A., Melchiorri, G. & Caruso, I. 2004, "A method for positioning electrodes during surface EMG recordings in lower limb muscles", *Journal of neuroscience methods,* vol. 134, no. 1, pp. 37-43.

Ricard, M. 2007, , *lectues notes on Advanced Physiology of Exercise*. Available at: http://www3.uta.edu/faculty/ricard/AdExPhysiol/AdExPhysiol.htm 11-20-2007].

Saitou, K., Masuda, T., Michikami, D., Kojima, R. & Okada, M. 2000, "Innervation zones of the upper and lower limb muscles estimated by using multichannel surface EMG.", *Journal of human ergology,* vol. 29, no. 1-2, pp. 35-52.

Semmler, J.G. & Nordstrom, M.A. 1998, "Motor unit discharge and force tremor in skill- and strength-trained individuals", *Experimental Brain Research,* vol. 119, no. 1, pp. 27-38.

Stålberg, E. 1980, "Macro EMG, a new recording technique.", *Journal of Neurology, Neurosurgery & Psychiatry,* vol. 43, no. 6, pp. 475-482.

Vieira, T.M.M., Merletti, R. & Mesin, L. 2010, "Automatic segmentation of surface EMG images: Improving the estimation of neuromuscular activity", *Journal of Biomechanics,* vol. 43, no. 11, pp. 2149-2158.

Widmaier, E.P., Raff, H. & Strang, K.T. 2008, "Muscle" in *Vander's human physiology: the mechanisms of body function*, 11th edn, McGraw-Hill Higher Education, , pp. 267-310.

2

Problem Statement

2.1 Introduction

Upper-limb conditions can be classified as anatomical or aetiological (Huckstep 1993). The first term includes numerous musculoskeletal conditions and disorders derived from the repetitive use of the upper extremity and affecting the shoulder, the elbow, and the hand/wrist complex. The second term includes other conditions derived from injuries to the brain or the spinal cord, in which case, can cause a total or partial paralysis of the limb.

Considering the non-invasive nature of sEMG and that of patients affected by medical conditions mentioned above, multichannel sEMG (i.e. with electrode arrays) constitutes a valuable tool for the diagnosis, monitoring and clinical research of these and other muscular disorders. Besides, the use of electrode arrays facilitate the investigation of the peripheral properties of the active MUs, such as its conduction velocity which can be determined from the time delay between two signals recorded at a known distance in the same direction of the muscle fibers. The assessment of CV is of particular importance for the study of pathological fatigue and its determinants (Merletti, Farina & Gazzoni 2003). Additionally, some anatomical characteristics of the muscle can only be investigated by multichannel sEMG, such as location of the innervation zones, fiber length and reinnervation processes (Merletti, Farina & Gazzoni 2003, Zwarts, Drost & Stegeman 2000). Recent research on multichannel EMG support the hypotheses of diversity in the distribution of motor units, inhomogeneities in fiber activation and muscle compartmentalization(Farina et al. 2008, Holtermann, Roeleveld & Karlsson 2005, Vieira, Merletti & Mesin 2010).These premises are related to bundles of fiber types organized in different regions within the muscle, each of them following different recruitment strategies according to Henneman's size principle (Holtermann, Roeleveld & Karlsson 2005) and also associated with the selective activation of anatomical compartments within the muscle that can be recruited independently and function as a separate entity(Vieira, Merletti & Mesin 2010).

2.2 Problem Statement

2.2.1 Upper Limb Disorders

Disorders of the upper limb include a wide range of inflammatory and degenerative conditions affecting muscles, tendons, ligaments, joints and/or peripheral nerves and causing pain and functional deficit. They are among the most common reasons for attendance to occupational physicians (Karjalainen, Niederlaender 2004) although they are not uniquely caused by work. This kind of disorders causes significant morbidity and incurs substantial costs not only related to their treatment but also to work absenteeism and disability. Numerous surveys on working populations have reported upper extremity symptom prevalence up to 30% (Punnett, Wegman 2004). Two common disorders are Lateral epicondylalgia and Repetitive Strain Injury and will be discussed next.

a. Lateral Epicondylalgia

Lateral Epicondylalgia (LE) is a common condition related to microtraumas of forearm muscles caused by sports or occupational activities involving quick repetitive movements of the wrist and forearm (Ciccotti, Charlton 2001, Pienimäki, Kauranen & Vanharanta 1997). Affects men and women equally and its annual incidence is around 1-3% (Allander 1974). It is characterized by loss of force and acute pain in the zone of the elbow affecting especially the muscles and tendons originated in the lateral epicondyle of the humerus: the extensor carpi radialis (ECR), the extensor digitorum communis (EDC) and the extensor carpi ulnaris (ECU) (Moore 2002), all of them involved in the extension of the wrist (Kendall F. P., Kendall McCreary E., and Provance P.G. 1993).

Pathological findings in LE often show thicker and denser extensor carpi radialis brevis tendon with hypervascularization, granulated tissue, edema, and occasional tear (Goldie 1964, Spencer, Herndon 1953, Nirschl, Pettrone 1979). Conspicuously, histological samples do not show inflammation (Kraushaar, Nirschl 1999). Acute cases usually improve with rest, anti-inflammatory drugs or local corticosteroid injections while chronic cases need active treatment for long-time periods (Pienimäki et al. 1996, Faro, Wolf 2007).

According to a biomechanical model proposed by Moore, LE is originated by overload of wrist extensor muscles in response to greater external forces, especially during eccentric contractions (Moore 2002). Muscle fatigability might also play a role in this condition. Consequently, several authors have promoted the use of strengthening exercises for treating LE (Bisset et al. 2005, Croisier et al. 2007, Smidt et al. 2003, Trudel et al. 2004) in order to induce changes in the mechanical properties of the muscles (Enoka 1996) and to

increase joint stability (Keays et al. 2003). Such studies are in agreement with others indicating that muscle conditioning induces changes in the diameter of the muscle fibers, in the proportion of MU types within the muscle (Kadi et al. 2000) and in the length-tension relationship of the exercised muscles, by increasing the number of sarcomeres(Lynn, Morgan 1994).

b. Repetitive Strain Injury in musicians

Repetitive Strain Injury (RSI) is a wide concept that involves chronic upper limb pain that cannot be related to a specific lesion of joints, tendons, or muscles. In advanced stages, it can lead to weakness and even to loss of response and control of the affected muscular groups, ending in disability (Cooke et al. 1993). RSI is extensively associated to repetitive low amplitude movements, though there is still a lack of scientific evidence proving its origin in repetitive contractions of a set of muscles which can eventually lead to tissue damage. What is more, there is not an agreement concerning an objective test for its diagnosis and treatment despite that the condition is highly prevalent in the working population (Winspur 2003). One of the most affected sectors is that of instrumentalist musicians affecting equally both, professional musicians and students, with its rate of incidence depending on practice time and load (Fry 1987).

In recent years some studies had associated RSI to changes at motor unit level, either because of changes in the proportion of the types of MU and mitochondrial abnormalities or because of alterations to the metabolism of muscle energy (Moreno-Torres et al. 2010). On the other hand, recent studies have shown that alterations in the muscles that can result in pain (myalgia) may be reflected in the electrical activation of muscles (Goudy, McLean 2006). Therefore, the use of noninvasive methods such as surface electromyography can allow the analysis of activation patterns and muscle fatigue that will be of great importance for prevention, diagnosis and treatment of patients with repetitive stress injuries.

2.2.2 Motion intention and human-machine interfaces in rehabilitation

As mentioned before, upper-limb conditions include those caused by injuries to the CNS as in the case of cerebral stroke or damage to the spinal cord. They can be originated by trauma or pathology and the degree of impact on the motor function depends on the extent and on the region of the injury. In some cases, the function of the upper-limb is not completely lost and can be enhanced by physical rehabilitation focused on functional goals engaging highly repetitive movements (Kwakkel, Kollen & Krebs 2008).

Rehabilitation of subjects with motor impairments is a labor-intensive process involving strong physical interaction between patient and therapist, and it is effectiveness is

subordinated to the active participation of the first (Hogan et al. 2006). Engineering approaches in the field of robotics have been extensively developed to assist in improving upper limb function in individuals such as the elderly, injured or disabled. The use of robotic devices and biofeedback systems facilitates rehabilitation therapies because they allow patients to train independently of a therapist and to improve on their own functional level by giving proper assistance. Robotic assistance and in general, human-machine interfaces like rehabilitation games or computer-based training, can help individuals with neural impairments or with weak muscles to start and follow a given movement in a range of motion, improving their own movement control and strength. Nevertheless, development of robotic devices that interact with patients is limited by the ability of the machine to sense volitional movement and either assist or resist the motion. Thus, the robotic device should be able to sense subject's ability and the force he can generate in the muscle to determine the assistance it must provide to facilitate the greatest functional change in muscle strength or coordination (Andreasen, Alien & Backus 2005). Such information can be extracted from the electrical activity of the muscle, considering that motor unit action potentials can be seen as natural, biological and selective amplifier of the neural code being transferred from the CNS to the muscles an so, of subject's movement intention.

2.3 Human Upper-limb

The upper limb comprises the region between the deltoid and the hand. Possible movements of the upper-limb are achieved by forces acting on three joints: the shoulder, the elbow and the wrist. The region between the shoulder and the elbow is referred to as the upper-arm, while the forearm comprises the region between the elbow and the wrist. The upper limb has multiple muscles that can be roughly divided into extensors and flexors. The firsts are located in the anterior compartment of the arm (i.e., in the front plane of the body) while the lasts are located in the posterior compartment. Movements of the upper-limb are achieved by orchestrated actions of these muscles.

Figure 2.1 shows a set of movements at the elbow joint and the wrist. Different upper-arm and forearm muscles are responsible for the flexion and extension at the elbow joint and the supination and pronation of the forearm and wrist (i.e. the rotation to turn the hand to face upwards or downwards respectively). Conversely, extensors and flexors of the forearm operate at wrist level flexing, extending and deviating the hand in different directions. They also extend and contract the digits and combine with other carpal muscles

to accomplish the gripping of the hand. Finally, movements at the shoulder joint are achieved by the combined activation of muscles in the upper-arm and trunk.

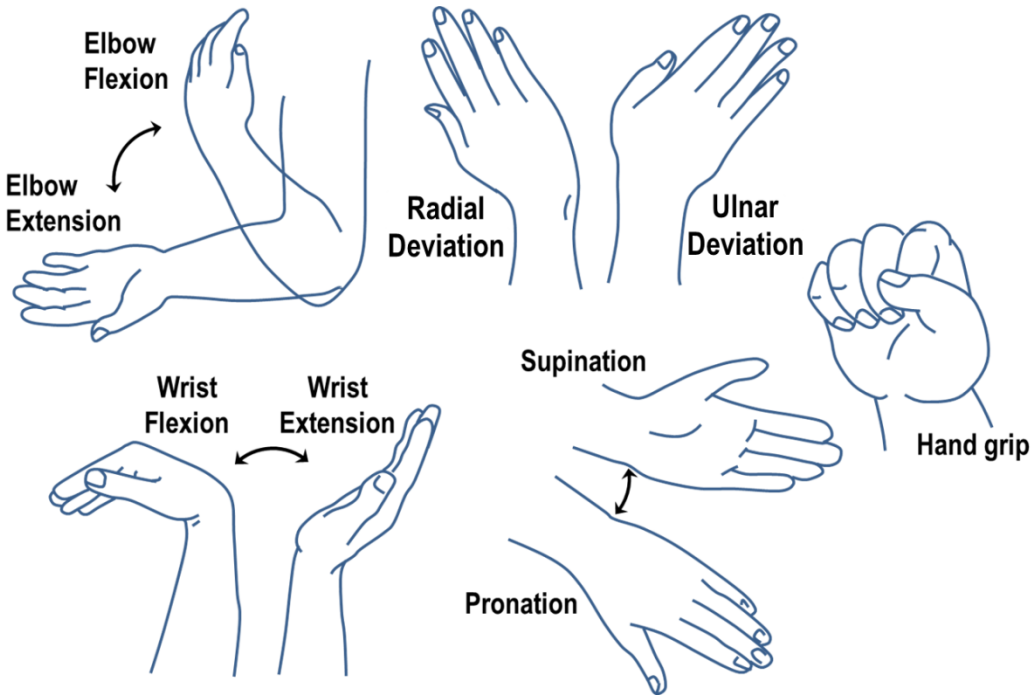

Figure 2.1. Different tasks accomplished by the contraction of muscles in the upper limb.

2.3.1 Forearm muscles

Most of the muscles that act at the wrist and finger joints originate outside the hand in the elbow joint. They are termed extrinsic muscles because their muscle belly is outside the hand in the forearm. These muscles provide considerable strength and dexterity to the fingers without adding muscle bulk to the hand, by pulling long tendons that in some cases end on the finger tips. A total of thirty nine muscles act in the wrist and fingers and none of them works alone. Agonist and antagonist work in pairs to produce even small and simple movements. Most of the muscles acting on the elbow are capable of producing as many as three movements not only at this joint but also at the wrist and phalangeal joints, although one movement is usually dominant (Hamill, Knutzen 2006b). Forearm muscles have multiple innervation zones distributed along its entire length and are thin and closely packed together. Additionally, location of IZ varies from subject to subject and thus, there is not a clear consensus on the location of surface electrodes for the analysis of EMG signals (Saitou et al. 2000), hardening the interpretation of results in clinical studies and the reliability of the same.

2.3.2 Upper-Arm muscles

Movements generated at the elbow assist the shoulder in applying force and in controlling the placement of the hand in space. The combination of shoulder and elbow movements affords the capacity to place the hand in many positions, allowing tremendous versatility (Hamill, Knutzen 2006a).

Spatial inhomogeneities have been observed on upper-arm muscles, that is, different regions of the muscle activate depending on different conditions like contraction level or type of task. They have been attributed to uneven fiber type distribution and neuromuscular compartmentalization (Holtermann, Roeleveld & Karlsson 2005, Segal 1992, Lucas-Osma, Collazos-Castro 2009).

Although upper arm muscles act on the shoulder and the elbow joints, in this work we will be referring only to muscles operating at the elbow and responsible for the positioning of the forearm and the hand in the space. Spatial inhomogeneities of upper-arm muscles will be analyzed and related to the degrees of freedom of the elbow joint.

2.4 Motivation

The quantitative analysis of EMG signals provides an objective measure of neuromuscular function. It allows the assessment of pathological conditions in the muscles themselves and in the neural paths involved in muscle contraction. Moreover surface EMG provides a non-invasive tool which is easy to apply and safe for subjects and patients with different pathological conditions. In the study of diseases of the neuro muscular system it is necessary to analyze the level of activity, the capacity of production of strength, the load-sharing between muscles and the probably predisposition to muscular fatigue, all of them associated with physiological factors determining the resultant muscular contraction. Such characteristics can be assessed by the analysis of sEMG signal, although its recording and interpretation must be carefully conducted because many external factors can bias the results. The use of electrode arrays improves the analysis of sEMG by recording the signal in multiple closely –spaced locations over the muscle allowing a better assessment of the spatial distribution of the potentials and when combined with spatial filters a major selectivity of MUs.

Regarding upper-limb rehabilitation, even when strengthening of forearm extensor muscles is a common approach in the treatment for upper-limb disorders, there is still a lack of information concerning weakness, muscular imbalance and fatigability of such muscles during voluntary contractions. Muscle imbalances, shortenings and weaknesses

have been identified as major biomechanical factors underlying cumulative trauma injuries (Benkibler, Chandler & Pace 1992, Wilder, Sethi 2004). Biomechanical deficits may both arise after an injury (in which case should be treated in the latter phases of rehabilitation) or precede the actual injury. On the other hand, continuous activation of forearm muscles could possibly lead to a higher level of specialization in subjects exposed to repetitive tasks that could end in decreased muscle endurance. Thus the identification of muscle imbalances and its predisposition to muscular fatigue is crucial in order to design rehabilitation/injury prevention programs that could help improve muscular condition of subjects, especially workers highly exposed to cumulative trauma injuries. In this context, multichannel sEMG constitute a valuable tool for the extraction of information related to biomechanical deficits mentioned above. On one side, the use of multiple electrodes allows the estimation of the CV of the active MUs and their changes associated to muscular fatigue. On the other side, forearm muscles are difficult to assess with traditional bipolar electrodes not only because of crosstalk (given the high number of muscles crossing the forearm), but also because the proximity to IZ may bias the estimation of the parameters extracted from the sEMG signal.

Regarding human-machine interfaces, sEMG signals are important to infer motion intention and therefore could be used to control devices such as exoskeletons, biofeedback systems or assistive devices (Nishikawa et al. 1999, Dipietro et al. 2005). Central to these goals is the extraction of information from myoelectric signal. Despite recent literature concerning the development and the application of electrode arrays (Holobar et al. 2010, Tucker et al. 2009, Östlund, Yu & Karlsson 2006, Zwarts, Stegeman 2003), the detection of surface EMG signals, both in ergonomics and in rehabilitation, is currently based almost exclusively on a single or a few electrode pairs. However EMG amplitude information provided by a single bipolar channel is unreliable and may be highly misleading because: a) The signal features are affected by electrode location and inter-electrode distance, b) Signal quality and power line interference may change with time due to increasing/decreasing unbalance of electrode-skin contact impedances, c) The quality of acquired EMG is position-dependent and alters significantly in the vicinity of innervation zones and tendons, d) Changing level of crosstalk from adjacent muscles, and , e) More than one muscle is involved in a specific task (Tkach, Huang & Kuiken 2010). On the other hand, the use of High Density EMG signals recorded with 2D electrode arrays provides a much larger amount of information, such as: a) The (time and task changing) skin surface areas where EMG amplitude is maximal, b) A better estimate of muscle force by proper

selection of the most significant channels and muscle area, c) it provides information of the spatial distribution of the potentials and its relation to muscle compartmentalization, and d) Better assessment of crosstalk and, in general, a better "understanding" of the signal from a 2-D image rather than from a single signal. Thus, HDEMG potentially has more discriminating power for the identification of movement intentions or tasks, providing a better signal to control robotic devices which is directly related to physiological processes within the neuromuscular system.

2.5 Multichannel sEMG on upper-limb muscles: State of the art

Multichannel sEMG, offers an alternative to conventional EMG facilitating the assessment of the physical propagation of the Motor Unit Action Potentials. Consequently, it allows not only the analysis of the time varying properties of the signal but also the analysis of important spatial aspects like location of innervation zones and extent and length of the muscle fibers, which are essential for the force-generating capacity of the muscle (Zwarts, Stegeman 2003).

Multichannel sEMG either in one or two dimensions permits to enhance selectivity by the application of spatial filters and can be used to estimate the Conduction Velocity of the active Motor Units. It can also be used to analyze inhomogeneities in muscle activation and allow the study of propagation and topographical aspects of MUs and its relation to pathology (Zwarts, Drost & Stegeman 2000). Thus, multichannel sEMG is a valuable tool for monitoring and understanding changes induced in the neuromuscular system by pathology or rehabilitation therapies of the upper-limb.

2.5.1 Assessment of Upper Limb Disorders

Conventional research on surface EMG for the assessment of upper-limb disorders or motion intention is based on signals extracted from invasive or single bipolar electrodes located at predetermined landmarks that do not take into account individual differences regarding anatomical characteristics of the muscle. What is more, previous studies have reveal that it is not possible to establish a landmark for the positioning of bipolar electrodes on some upper-limb muscles, especially extrinsic muscles of the forearm (Saitou et al. 2000, Signorino, Mandrile & Rainoldi 2006). Therefore a key aspect of surface EMG of forearm muscles is to choose an appropriate location for the extraction of reliable information before drawing conclusions on muscular pattern related to pathology or motion intention.

In general, both iEMG and sEMG have shown to be able to offer important insights into muscle pathology, physiology and anatomy (Sanjak et al. 2004, Duchateau, Enoka 2011, Ivanova, Garland & Miller 1997).

In the case of assessment of upper-limb disorders, changes in variables like integrated EMG value (Bauer, Murray 1999) or mean rectified value (Van Galen et al. 2002), both of them extracted from single EMG signals recorded in the surface of one or various muscles, were associated with pathology by the quantification of differences in muscle activation strategies with respect to those observed in control subjects. Other studies have also analyzed the muscular pattern at MU level by decomposing intramuscular signals into its constituent MUAPs and found differences in the recruitment strategies of MU in pathological subjects (Forsman et al. 2002).

Myoelectric fatigue in upper-limb disorders, on the other hand, has been usually assessed from spectral compression accompanying increases in sEMG amplitude(Roman-Liu, Tokarski & Wojcik 2004), disregarding that other factors different from physiological determinants of fatigue can induce changes in frequency or time-domain variables. However it can be assessed from Motor Unit Conduction Velocity of the active potentials which is directly related to changes in the contractile properties of the MU as induced by peripheral determinants of myoelectric fatigue (Widmaier, Raff & Strang 2008). Different methods can be used to estimate the MU conduction velocity (Sun I. Kim, Kang M. Lee 1990), though it can be measured straightforward from multichannel sEMG signals recorded at a known distance with an array of closely- spaced electrodes.

Multichannel EMG of forearm muscles has been used in the study of size and distribution of innervation zones (Saitou et al. 2000, Signorino, Mandrile & Rainoldi 2006), in the evaluation of crosstalk (Mogk, Keir 2003) and in the study of motor neuron disease (Wood et al. 2001). In the case of pathologies not related to the upper-limb, it has been used for example in the evaluation of CV in chronic neck pain (Falla, Farina 2005), in the assessment of low back pain (Reger et al. 2006) and in the analysis of myoelectric fatigue in temporomandibular disorders (Castroflorio et al. 2012). However, to the best knowledge of the author, it has not been used on the forearm for assessing muscular co-activation or myoelectric fatigue and on the analysis of upper-limb disorders.

2.5.2 Assessment of Motion Intention

Analysis of sEMG has been extensively investigated for more than 50 years in order to provide proportional and simultaneous control for human-machine interfaces, especially for prostheses. The simplest technique consists in mapping the activation of a given muscle

to a single function of the artificial device and the power of the detected signal to the velocity with which the device acts (Scott 1967). However, myoelectric control of multiple functions (or degrees of freedom) is rather more complex. Current approaches use pattern recognition techniques based on feature extraction from sEMG signals recorded in multiple muscles or sites with bipolar electrodes (Scheme, Englehart 2011, Parker, Englehart & Hudgins 2006, Englehart, Hudgins 2003). Pattern recognition relies in mapping repeatable patterns of activation to classes associated with different kinds of user's intended motions. In general, classification accuracy obtained from pattern recognition has been very high. For example, (Englehart, Hudgins 2003) reported accuracy higher than 95% in classifying four wrist functions from sEMG. However, most of the studies in this field were focused on the recognition of motion intention regardless of its strength. Additionally, in general, classification is based on features extracted from signals recorded while exerting a moderate force (Englehart, Hudgins 2003, Hargrove et al. 2009, Hargrove, Englehart & Hudgins 2007) whereas other recent studies have shown that classification accuracy worsens if the classifier is trained with a mixture of different levels of effort (Tkach, Huang & Kuiken 2010, Scheme, Englehart 2011).

In addition to the variations introduced by the exerted force, sEMG-based control is complex because of large inter-individual variability of sEMG features due to muscle size, subcutaneous tissue thickness and location of innervation zones which affect the amplitude of the recorded action potentials. Signal amplitude (and thus, power) changes because of muscle shift under the detection system and changing level of crosstalk from adjacent muscles (Tkach, Huang & Kuiken 2010, Parker, Englehart & Hudgins 2006). These variations are especially important when considering signals detected from one or few electrode pairs per muscle. These drawbacks can be reduced using High Density EMG (HD-EMG) obtained from 2D arrays and processing the signal in the space dimension ((Staudenmann et al. 2009) and (Zwarts, Stegeman 2003)). The processing of this kind of signals as a topographical image (HD-EMG map) provides a quantification of both the temporal and spatial characteristics of the electric muscle activity (Merletti et al. 2010a, Merletti et al. 2010b).Finally, it has been found that the spatial distribution of intensity in RMS maps changes with time (Tucker et al. 2009), pain (Madeleine et al. 2006) and force level (Holtermann, Roeleveld & Karlsson 2005). This change is related to "heterogeneity either in the distribution of the motor units within the muscle or in the strategy with which motor units are recruited" (Farina et al. 2008).

Very few studies have used HD-EMG and its spatial properties for the identification of motor intention. For example in (Man et al. 2011) HD-EMG was used for the proper selection of the most significant channels and (Tkach, Huang & Kuiken 2010) have used it to assess the stability of EMG features in the classification of motion intention but not for the extraction of features. In this thesis it would be analyzed how spatial information extracted from HD-EMG maps can improve pattern recognition from sEMG for the identification of movements of the upper-limb.

2.6 Objectives

2.6.1 Main objective

The main objective of this thesis is the design and implementation of experimental protocols, and algorithms to extract information from multichannel sEMG signals for the assessment of muscles of the upper-limb. Such information must be interpreted and related to different tasks and force levels as well as to pathological events associated to upper-limb conditions.

Expected results include quantitative indexes for the assessment of muscular co-activation patterns and fatigue in upper-extremity disorders. Such indexes will be promising for the design of rehabilitation and prevention programs and for monitoring changes during therapy. Co-activation patterns as well as spatial distribution of the electrical activity of the muscles from HDEMG signals are also expected to improve the automatic identification of tasks associated to possible movements of the upper limb based solely on sEMG signals. In the future, features extracted from HDEMG can be incorporated to devices intended to robotic-aided therapies or other devices requiring muscular biofeedback like rehabilitation games or computer-based training programs, and can also be related to pathological muscular patterns.

2.6.2 Specific objectives

- Design of different experimental protocols for the analysis of normal and pathological upper-limb function during isometric contractions: involves a selection of tasks, electronic instrumentation set-up, conditioning of mechanical and rehabilitation devices and software development.
- Recording of multichannel sEMG databases in muscles associated to Lateral Epicondylalgia and Repetitive Strain Injury.

- Definition and calculation of sEMG variables for determining the co-activation pattern of different muscles based on the amplitude of the sEMG signals and also in their distribution in the space.
- Assessment of myoelectric fatigue in different forearm muscles and its interpretation based on the type of task and/or the effect of Lateral Epicondylalgia.
- Comparative study of results between healthy subjects and patients with Lateral Epicondylalgia and determination of possible muscular imbalances and deficits.
- The design of a sensor system capable of adapting to the different anatomical regions of the upper-limb and to cover simultaneously the surface of various muscles. Such system will be able to reduce contact artifacts, especially for the recording of High Density EMG signals.
- The recording of High Density EMG signals in upper-limb muscles to analyze changes in the distribution of Motor Unit Action Potentials in the surface of the muscles according to different tasks and effort levels.
- Estimation of High Density EMG maps representative of four tasks associated to the degrees of freedom at the elbow joint during isometric contractions at different effort levels.
- Automatic identification of strength and direction of movement intention from HD-EMG signals.

2.7 Thesis Framework

This thesis has been supported by multiple funded projects:

1) Aplicación de técnicas avanzadas en adquisición y procesado de la señal EMG de superficie para la rehabilitación de la función muscular, Acción Integrada. Ministerio de Educación y Ciencia (Spain), Ministerio de Educación (Italy), 2004-2005.Thisproject was conducted in collaboration with the Mutua Egarsat and the LISiN of the Department of Electronics, Politecnico di Torino and its objective was to define the experimental protocols for the analysis of Lateral Epicondylalgia as well as the recording of signals in patients and controls.
2) Tratamiento e interpretación de señales biomédicas para la evaluación clínica y la rehabilitación, Comisión Interministerial de Ciencia y Tecnología (CICYT), Spain, ref. TEC2004-02274, 2004-2007. In this project, the multichannel EMG signals from controls and patients with Lateral Epicondylalgia recorded in the previous project were analyzed.

3) Signal Processing of multichannel surface EMG signals from upper and forearm muscles, Estancia de Investigación, Beca BE, AGAUR, Generalitat de Catalunya, 2008. Funding of this project was intended for a research internship for 6 months at the LISiN, Politecnico di Torino, Italy. During this period the initial sensorization system for HDEMG recording was developed and used to record signals from the upper-limb in tasks associated with the degrees of freedom at the elbow joint in healthy subjects.
4) R+D d'un sistema de neurorehabilitació de l'extremitat superior, NEUROREHAB 3E+D, ACC1Ó-CIDEM, Generalitat de Catalunya, 2009-2010. Work in this project focused in the analysis of HD-EMG signals in controls and in the definition of features for the differentiation of tasks, based on temporal and spatial characteristics of activation maps. Additionally, a signal database in patients with incomplete spinal cord injury was recorded, following the experimental protocol defined in the previous project.
5) Análisis de las Interacciones Dinámicas en Bioseñales No Invasivas Multicanal para la Terapia y la Rehabilitación, Ministerio de Ciencia e Innovación, Spain, ref.TEC2008-02754, 2008-2011. Design of an experimental protocol and analysis of multichannel sEMG signals for the assessment of Repetitive Stress Injuries in collaboration with the Institut de Fisiologia i Medicina de l'Art.
6) Biomedical Research Networking Center in Bioengineering, Biomaterials and Nanomedicine, CIBER-BBN, Instituto de Salud Carlos III, Spain.

Besides, it was developed with the collaboration of the following institutions:

- Department of Physical Medicine and Rehabilitation, Egarsat Hospital, Terrasa, Spain
- Laboratory of Engineering of Neuromuscular System and Motor Rehabilitation (LiSIN), Department of Electronics, Politecnico di Torino, Italy
- Institut de Fisiologia i Medicina de l'Art, Terrassa, Spain
- Biomedical Engineering Research Centre CREB, Division of Biomedical Signals and Systems (SISBIO), Department ESAII, Technical University of Catalonia (UPC), Barcelona, Spain.

2.8 References

Allander, E. 1974, "Prevalence, Incidence, and Remission Rates of some Common Rheumatic Diseases Or Syndromes", *Scandinavian journal of rheumatology,* vol. 3, no. 3, pp. 145-153.

Andreasen, D.S., Alien, S.K. & Backus, D.A. 2005, "Exoskeleton with EMG based active assistance for rehabilitation", *Proc. 9th International Conference on Rehabilitation Robotics, 2005*, pp. 333.

Bauer, J.A. & Murray, R.D. 1999, "Electromyographic patterns of individuals suffering from lateral tennis elbow", *Journal of Electromyography and Kinesiology,* vol. 9, no. 4, pp. 245-252.

Benkibler, W., Chandler, T.J. & Pace, B.K. 1992, "Principles of Rehabilitation After Chronic Tendon Injuries", *Clinics in sports medicine,* vol. 11, no. 3, pp. 661-671.

Bisset, L., Paungmali, A., Vicenzino, B. & Beller, E. 2005, "A systematic review and meta-analysis of clinical trials on physical interventions for lateral epicondylalgia", *British journal of sports medicine,* vol. 39, no. 7, pp. 411-422.

Bolgla, L.A., Malone, T.R., Umberger, B.R. & Uhl, T.L. 2010, "Reliability of electromyographic methods used for assessing hip and knee neuromuscular activity in females diagnosed with patellofemoral pain syndrome", *Journal of Electromyography and Kinesiology,* vol. 20, no. 1, pp. 142-147.

Castroflorio, T., Falla , D., Tartaglia, G.M., Sforza, C. & Deregibus, A. 2012, "Myoelectric manifestations of jaw elevator muscle fatigue and recovery in healthy and TMD subjects", *Journal of oral rehabilitation,* vol. 39, no. 9, pp. 648-658.

Ciccotti, M.G. & Charlton, W.P.H. 2001, "Epicondylitis in the athlete", *Clinics in sports medicine,* vol. 20, no. 1, pp. 77-93.

Cooke, E.D., Steinberg, M.D., Pearson, R.M., Fleming, C.E., Toms, S.L. & Elusade, J.A. 1993, "Reflex Sympathetic Dystrophy and Repetitive Strain Injury - Temperature and Microcirculatory Changes Following Mild Cold Stress", *Journal of the Royal Society of Medicine,* vol. 86, no. 12, pp. 690-693.

Croisier, J., Foidart-Dessalle, M., Tinant, F., Crielaard, J. & Forthomme, B. 2007, "An isokinetic eccentric programme for the management of chronic lateral epicondylar tendinopathy", *British journal of sports medicine,* vol. 41, no. 4, pp. 269-275.

Dipietro, L., Ferraro, M., Palazzolo, J.J., Krebs, H.I., Volpe, B.T. & Hogan, N. 2005, "Customized interactive robotic treatment for stroke: EMG-triggered therapy", *IEEE Transactions on Neural Systems and Rehabilitation Engineering,* vol. 13, no. 3, pp. 325-334.

Duchateau, J. & Enoka, R.M. 2011, "Human motor unit recordings: Origins and insight into the integrated motor system (vol 1409, pg 42, 2011)", *Brain research,* vol. 1421, pp. 121-121.

Englehart, K. & Hudgins, B. 2003, "A robust, real-time control scheme for multifunction myoelectric control", *IEEE Transactions on Biomedical Engineering,* vol. 50, no. 7, pp. 848-854.

Enoka, R.M. 1996, "Eccentric contractions require unique activation strategies by the nervous system", *Journal of applied physiology,* vol. 81, no. 6, pp. 2339-2346.

Falla, D. & Farina, D. 2005, "Muscle fiber conduction velocity of the upper trapezius muscle during dynamic contraction of the upper limb in patients with chronic neck pain", *Pain,* vol. 116, no. 1–2, pp. 138-145.

Farina, D., Leclerc, F., Arendt-Nielsen, L., Buttelli, O. & Madeleine, P. 2008, "The change in spatial distribution of upper trapezius muscle activity is correlated to contraction duration", *Journal of Electromyography and Kinesiology,* vol. 18, no. 1, pp. 16-25.

Faro, F. & Wolf, J.M. 2007, "Lateral Epicondylitis: Review and Current Concepts", *The Journal of hand surgery,* vol. 32, no. 8, pp. 1271-1279.

Forsman, M., Taoda, K., Thorn, S. & Zhang, Q.X. 2002, "Motor-unit recruitment during long-term isometric and wrist motion contractions: a study concerning muscular pain development in computer operators", *International Journal of Industrial Ergonomics,* vol. 30, no. 4-5, pp. 237-250.

Fry, H.J.H. 1987, "Prevalence of Overuse (Injury) Syndrome in Australian Music Schools", *British journal of industrial medicine,* vol. 44, no. 1, pp. 35-40.

Goldie, I. 1964, "Epicondylitis lateralis humeri: A pathogenetic study", *Acta Chir Scand Suppl,* vol. 339, pp. 1-119.

Goudy, N. & McLean, L. 2006, "Using myoelectric signal parameters to distinguish between computer workers with and without trapezius myalgia", *European journal of applied physiology,* vol. 97, no. 2, pp. 196-209.

Hamill, J. & Knutzen, K.M. 2006a, "Functional Anatomy of the Upper Extremity" in *Biomechanical basis of human movement*, 2nd edn, Lippincott Williams & Wilkins, .

Hamill, J. & Knutzen, K.M. 2006b, "Muscular Considerations for Movement" in *Biomechanical basis of human movement*, 2nd edn, Lippincott Williams & Wilkins, .

Hargrove, L.J., Englehart, K. & Hudgins, B. 2007, "A comparison of surface and intramuscular myoelectric signal classification", *IEEE Transactions on Biomedical Engineering,* vol. 54, no. 5, pp. 847-853.

Hargrove, L.J., Li, G., Englehart, K.B. & Hudgins, B.S. 2009, "Principal Components Analysis Preprocessing for Improved Classification Accuracies in Pattern-Recognition-Based Myoelectric Control", *IEEE Transactions on Biomedical Engineering,* vol. 56, no. 5, pp. 1407-1414.

Hogan, N., Krebs, H.I., Rohrer, B., Palazzolo, J.J., Dipietro, L., Fasoli, S.E., Stein, J., Hughes, R., Frontera, W.R., Lynch, D. & Volpe, B.T. 2006, "Motions or muscles? Some behavioral factors underlying robotic assistance of motor recovery", *Journal of Rehabilitation Research and Development,* vol. 43(5), pp. 605-18.

Holobar, A., Minetto, M.A., Botter, A., Negro, F. & Farina, D. 2010, "Experimental Analysis of Accuracy in the Identification of Motor Unit Spike Trains From High-Density Surface EMG", *IEEE Transactions on Neural Systems and Rehabilitation Engineering,* vol. 18, no. 3, pp. 221-229.

Holtermann, A., Roeleveld, K. & Karlsson, J.S. 2005, "Inhomogeneities in muscle activation reveal motor unit recruitment", *Journal of Electromyography and Kinesiology,* vol. 15, no. 2, pp. 131-137.

Huckstep, R.L. 1993, *A Simple Guide to Orthopaedics,* Churchill Livingstone, London.

Ivanova, T., Garland, S.J. & Miller, K.J. 1997, "Motor unit recruitment and discharge behavior in movements and isometric contractions", *Muscle & nerve,* vol. 20, no. 7, pp. 867-874.

Kadi, F., Ahlgren, C., Waling, K., Sundelin, G. & Thornell, L.-. 2000, "The effects of different training programs on the trapezius muscle of women with work-related neck and shoulder myalgia", *Acta Neuropathologica,* vol. 100, no. 3, pp. 253-258.

Karjalainen, A. & Niederlaender, E. 2004, *Occupational Diseases in Europe in 2001*.

Keays, S.L., Bullock-Saxton, J.E., Newcombe, P. & Keays, A.C. 2003, "The relationship between knee strength and functional stability before and after anterior cruciate ligament reconstruction", *Journal of Orthopaedic Research,* vol. 21, no. 2, pp. 231-237.

Kendall F. P., Kendall McCreary E., and Provance P.G. 1993, *Muscles: Testing and Function,* 4th edn, Williams & Wilkins.

Kraushaar, B.S. & Nirschl, R.P. 1999, "Tendinosis of the elbow (tennis elbow) - Clinical features and findings of histological, immunohistochemical, and electron microscopy studies", *Journal of Bone and Joint Surgery-American Volume,* vol. 81A, no. 2, pp. 259-278.

Kwakkel, G., Kollen, B.J. & Krebs, H.I. 2008, "Effects of Robot-Assisted Therapy on Upper Limb Recovery After Stroke: A Systematic Review", *Neurorehabilitation and neural repair,* vol. 22, no. 2, pp. 111-121.

Lucas-Osma, A.M. & Collazos-Castro, J.E. 2009, "Compartmentalization in the Triceps Brachii Motoneuron Nucleus and Its Relation to Muscle Architecture", *Journal of Comparative Neurology,* vol. 516, no. 3, pp. 226-239.

Lynn, R. & Morgan, D.L. 1994, "Decline Running Produces More Sarcomeres in Rat Vastus Intermedius Muscle-Fibers than does Incline Running", *Journal of applied physiology,* vol. 77, no. 3, pp. 1439-1444.

Madeleine, P., Leclerc, F., Arendt-Nielsen, L., Ravier, P. & Farina, D. 2006, "Experimental muscle pain changes the spatial distribution of upper trapezius muscle activity during sustained contraction", *Clinical Neurophysiology,* vol. 117, no. 11, pp. 2436-2445.

Man, S., Cescon, C., Vieira, T., Herle, S., Lazea, G. & Merletti, R. 2011, "Classification of electromyographic signals during finger isometric flexion: Using electrodes arrays", *E-Health and Bioengineering Conference (EHB), 2011*, pp. 1.

Merletti, R., Aventaggiato, M., Botter, A., Holobar, A., Marateb, H. & Vieira, T.M.M. 2010a, "Advances in surface EMG: recent progress in detection and processing techniques.", *Critical Reviews in Biomedical Engineering,* vol. 38, no. 4, pp. 305-45.

Merletti, R., Botter, A., Cescon, C., Minetto, M.A. & Vieira, T.M.M. 2010b, "Advances in surface EMG: recent progress in clinical research applications.", *Critical Reviews in Biomedical Engineering,* vol. 38, no. 4, pp. 347-79.

Merletti, R., Farina, D. & Gazzoni, M. 2003, "The linear electrode array: a useful tool with many applications", *Journal of Electromyography and Kinesiology,* vol. 13, no. 1, pp. 37-47.

Mogk, J.P.M. & Keir, P.J. 2003, "Crosstalk in surface electromyography of the proximal forearm during gripping tasks", *Journal of Electromyography and Kinesiology,* vol. 13, no. 1, pp. 63-71.

Moore, J.S. 2002, "Biomechanical models for the pathogenesis of specific distal upper extremity disorders", *American Journal of Industrial Medicine,* vol. 41, no. 5, pp. 353-369.

Moreno-Torres, A., Rosset-Llobet, J., Pujol, J., Fabregas, S. & Gonzalez-de-Suso, J. 2010, "Work-Related Pain in Extrinsic Finger Extensor Musculature of Instrumentalists Is Associated with Intracellular pH Compartmentation during Exercise", *Plos One,* vol. 5, no. 2, pp. e9091.

Nirschl, R.P. & Pettrone, F.A. 1979, "Tennis Elbow - Surgical Treatment of Lateral Epicondylitis", *Journal of Bone and Joint Surgery-American Volume,* vol. 61, no. 6, pp. 832-839.

Nishikawa, D., Wenwei Yu, Yokoi, H. & Kakazu, Y. 1999, "EMG prosthetic hand controller using real-time learning method", *Systems, Man, and Cybernetics, 1999. IEEE SMC '99 Conference Proceedings. 1999 IEEE International Conference on*, pp. 153.

Östlund, N., Yu, J. & Karlsson, J. 2006, "Adaptive spatio-temporal filtering of multichannel surface EMG signals", *Medical and Biological Engineering and Computing,* vol. 44, no. 3, pp. 209-215.

Parker, P., Englehart, K. & Hudgins, B. 2006, "Myoelectric signal processing for control of powered limb prostheses", *Journal of Electromyography and Kinesiology,* vol. 16, no. 6, pp. 541-548.

Pienimäki, T.T., Kauranen, K. & Vanharanta, H. 1997, "Bilaterally decreased motor performance of arms in patients with chronic tennis elbow", *Archives of Physical Medicine and Rehabilitation,* vol. 78, no. 10, pp. 1092-1095.

Pienimäki, T.T., Tarvainen, T.K., Siira, P.T. & Vanharanta, H. 1996, "Progressive Strengthening and Stretching Exercises and Ultrasound for Chronic Lateral Epicondylitis", *Physiotherapy,* vol. 82, no. 9, pp. 522-530.

Punnett, L. & Wegman, D.H. 2004, "Work-related musculoskeletal disorders: the epidemiologic evidence and the debate", *Journal of Electromyography and Kinesiology,* vol. 14, no. 1, pp. 13-23.

Reger, S.I., Shah, A., Adams, T.C., Endredi, J., Ranganathan, V., Yue, G.H., Sahgal, V. & Finneran, M.T. 2006, "Classification of large array surface myoelectric potentials from subjects with and without low back pain", *Journal of Electromyography and Kinesiology,* vol. 16, no. 4, pp. 392-401.

Roman-Liu, D., Tokarski, T. & Wojcik, K. 2004, "Quantitative assessment of upper limb muscle fatigue depending on the conditions of repetitive task load", *Journal of Electromyography and Kinesiology,* vol. 14, no. 6, pp. 671-682.

Saitou, K., Masuda, T., Michikami, D., Kojima, R. & Okada, M. 2000, "Innervation zones of the upper and lower limb muscles estimated by using multichannel surface EMG.", *Journal of human ergology,* vol. 29, no. 1-2, pp. 35-52.

Sanjak, M., Konopacki, R., Capasso, R., Roelke, K.A., Peper, S.M., Houdek, A.M., Waclawik, A. & Brooks, B.R. 2004, "Dissociation between mechanical and myoelectrical manifestation of muscle fatigue in amyotrophic lateral sclerosis", *Amyotrophic Lateral Sclerosis and Other Motor Neuron Disorders,* vol. 5, no. 1, pp. 26-32.

Scheme, E. & Englehart, K. 2011, "Electromyogram pattern recognition for control of powered upper-limb prostheses: State of the art and challenges for clinical use", *Journal of Rehabilitation Research and Development,* vol. 48, no. 6, pp. 643-659.

Scott, R.N. 1967, "Myoelectric Control of Prostheses and Orthoses", *Bull. Prothetics Res.,* vol. 10, no. 7, pp. 93-114.

Segal, R.L. 1992, "Neuromuscular Compartments in the Human Biceps Brachii Muscle", *Neuroscience letters,* vol. 140, no. 1, pp. 98-102.

Signorino, M., Mandrile, F. & Rainoldi, A. 2006, "Localization of innervation zones in forearm extensor muscles. A methodological study", *Proc. of the XVI International conference of the International Society of Electrophysiology and Kinesiology*, pp. 220.

Smidt, N., Assendelft, W., Arola, H., Malmivaara, A., Green, S., Buchbinder, R., van, d.W. & Bouter, L. 2003, "Effectiveness of physiotherapy for lateral epicondylitis: a systematic review", *Ann Med,* vol. 35, no. 1, pp. 51-62.

Spencer, G.E. & Herndon, C.H. 1953, "Surgical Treatment of Epicondylitis", *Journal of Bone and Joint Surgery-American Volume,* vol. 35-A, no. 2, pp. 421-424.

Staudenmann, D., Kingma, I., Daffertshofer, A., Stegeman, D.F. & van Dieën, J.H. 2009, "Heterogeneity of muscle activation in relation to force direction: A multi-channel surface electromyography study on the triceps surae muscle", *Journal of Electromyography and Kinesiology,* vol. 19, no. 5, pp. 882-895.

Sun I. Kim & Kang M. Lee 1990, "Mean Frequency Estimation Of Myoelectric Signal Using 2nd Order Maximum Entropy Method", *Proc. of the 12th Int. Conf. of the IEEE Engineering in Medicine and Biology Society*, pp. 2208.

Tkach, D., Huang, H. & Kuiken, T.A. 2010, "Study of stability of time-domain features for electromyographic pattern recognition", *Journal of Neuroengineering and Rehabilitation,* vol. 7, pp. 21.

Trudel, D., Duley, J., Zastrow, I., Kerr, E.W., Davidson, R. & MacDermid, J.C. 2004, "Rehabilitation for patients with lateral epicondylitis: a systematic review", *Journal of Hand Therapy,* vol. 17, no. 2, pp. 243-266.

Tucker, K., Falla, D., Graven-Nielsen, T. & Farina, D. 2009, "Electromyographic mapping of the erector spinae muscle with varying load and during sustained contraction", *Journal of Electromyography and Kinesiology,* vol. 19, no. 3, pp. 373-379.

Van Galen, G.P., Muller, M.L.T.M., Meulenbroek, R.G.J. & Van Gemmert, A.W.A. 2002, "Forearm EMG response activity during motor performance in individuals prone to increased stress reactivity", *American Journal of Industrial Medicine,* vol. 41, no. 5, pp. 406-419.

Vieira, T.M.M., Merletti, R. & Mesin, L. 2010, "Automatic segmentation of surface EMG images: Improving the estimation of neuromuscular activity", *Journal of Biomechanics,* vol. 43, no. 11, pp. 2149-2158.

Widmaier, E.P., Raff, H. & Strang, K.T. 2008, "Muscle" in *Vander's human physiology: the mechanisms of body function*, 11th edn, McGraw-Hill Higher Education, , pp. 267-310.

Wilder, R.P. & Sethi, S. 2004, "Overuse injuries: tendinopathies, stress fractures, compartment syndrome, and shin splints", *Clinics in sports medicine,* vol. 23, no. 1, pp. 55-81.

Winspur, I. 2003, "Controversies surrounding "misuse," "overuse," and "repetition" in musicians", *Hand clinics,* vol. 19, no. 2, pp. 325-+.

Wood, S.M., Jarratt, J.A., Barker, A.T. & Brown, B.H. 2001, "Surface electromyography using electrode arrays: A study of motor neuron disease", *Muscle & nerve,* vol. 24, no. 2, pp. 223-230.

Zwarts, M.J., Drost, G. & Stegeman, D.F. 2000, "Recent progress in the diagnostic use of surface EMG for neurological diseases", *Journal of Electromyography and Kinesiology,* vol. 10, no. 5, pp. 287-291.

Zwarts, M.J. & Stegeman, D.F. 2003, "Multichannel surface EMG: Basic aspects and clinical utility", *Muscle & nerve,* vol. 28, no. 1, pp. 1-17.

3

Linear Electrode Arrays Experimental Protocols and Setup

3.1 Introduction

This chapter focuses in the description of the experimental protocols designed for the assessment of upper limb disorders caused by repetitive contractions. The analysis is based on the processing of sEMG signals recorded with linear electrode arrays. As described in the Introduction, a linear electrode array is a system that allows the recording of sEMG signals in different points over the surface of the muscle. In this case, the electrodes were distributed along a line oriented in the same direction of the muscular fibers and separated by a fixed inter-electrode distance. This technique facilitates the selection of channels away from the innervation zones and tendons and the estimation of the global conduction velocity of the muscular fibbers, which in time is related to physiological changes determining muscle fatigue. The instrumentation setup and a software tool designed for the protocol will be described as well.

3.2 Experimental Protocols

According to a biomechanical model proposed by Moore (Moore 2002), Lateral Epicondylalgia is caused by microtraumas with impaired healing at the origin of wrist extensor muscles. They result from repetitive contractions of forearm muscles involving elbow extension, supination, pronation and hand gripping. Absolute values of maximum strength of the later are commonly used to evaluate muscular deficits in Lateral Epicondylalgia (LE) (Bhargava, Eapen & Kumar 2010) while strengthening exercises comprising hand extension have been used for rehabilitation purposes (Croisier et al. 2007).

On the other side, extrinsic muscles of the forearm have been associated with repetitive stress injuries (RSI) in instrumental musicians, especially in guitar and piano-players (Bejjani, Kaye & Benham 1996). A recent study analyzed intracellular changes at

muscle-fiber level and concluded that pH comparmentation during exercise was associated to pain in extrinsic extensors of the forearm (Moreno-Torres et al. 2010). They also hypothesized that such changes were related to a reduction in the oxidative capacity of the muscles as consequence of muscular fatigue.

Therefore, muscular pattern of extrinsic muscles of the forearm was analyzed through multichannel sEMG. The study involved isometric contractions associated to Lateral Epicondylitis and others similar to piano-playing. In the former case, a software interface intended for feedback of the exerted force during piano-like contractions was developed.

Three types of tasks were considered: wrist extension, hand grip and finger pressing. The first two were linked to LE while the third was linked to RSI in musicians.

3.2.1 Tasks and Subject positioning

In general, isometric contractions at low, medium and high levels of effort were considered.

Hand actions associated to LE and assessed by the experimental protocol are shown in Figure 3.1.

a. Wrist extension

During the experiment, subjects sat with the back straight and the forearm of the dominant limb placed in total pronation inside a mechanical brace (Figure 3.3 top-left). The elbow joint was kept at an angle of $\gamma=90^{o}$, the shoulder in horizontal adduction at $\alpha\sim15^{o}$ and the wrist aligned with the main axis of the forearm ($\delta=0^{o}$). In this position, subjects were asked to extend the wrist in neutral deviation (i.e. perpendicular to the main axis of the forearm) keeping the fingers relaxed. Wrist extension requires the co-activation of forearm extensor muscles rather than the contraction of an isolated one. Lateral Epicondylalgia manifests as localized pain in the origin of wrist extensor muscles. Therefore, the analysis of these muscles during hand extension is of interest for the assessment of muscular deficits and imbalances.

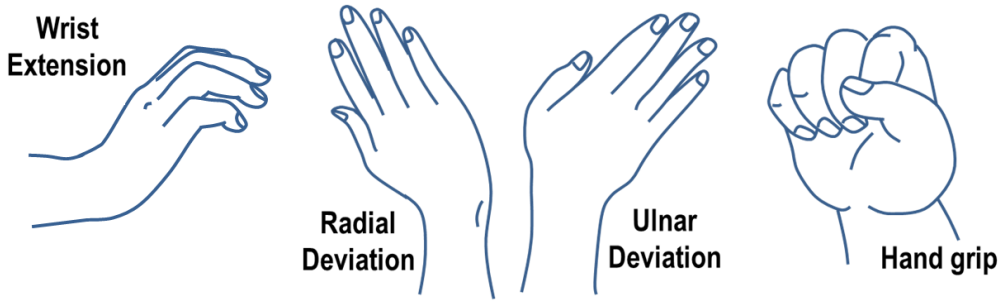

Figure 3.1. Tasks in the experimental protocol oriented to the study of Lateral Epicondylalgia

b. Hand gripping

Subjects kept the same position as in the task of wrist extension. Gripping work was performed on a hydraulic hand dynamometer in order to produce and maintain isometric contractions. The position of the subject during the experimental session can be observed in Figure 3.3 top. Gripping has been associated with lateral epicondylalgia as both, a mechanism that induces the pathology (Moore 2002, Snijders et al. 1987) and as an index related to the functional integrity of the upper-arm following recovery (Bhargava, Eapen & Kumar 2010). Hand gripping is produced by the simultaneous activation of flexors and extensors of the forearm. Although grip force is mainly generated by flexor muscles, extensor activation is important in stabilizing the wrist and maintaining the optimal position of the flexors (Shimose, Matsunaga & Muro 2011)

c. Finger pressing

Finger actions associated to Repetitive Strain injuries in musicians are shown in Figure 3.2. Contractions of this kind involve movement of the wrist and fingers depending on where the pressure has to be exerted. Movements at the wrist include radial and ulnar deviation and flexion and extension. As mentioned before, this kind of task involves a complex activation of forearms' extrinsic and intrinsic muscles. In this work only radial and ulnar deviations were assed.

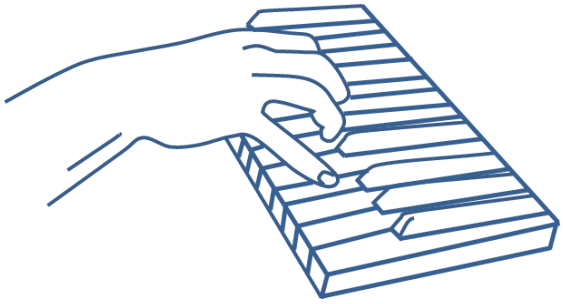

Figure 3.2. Tasks in the experimental protocol oriented to the assessment of repetitive strain injuries in musicians

During the different tasks, subjects kept the same position as in wrist extension and hand gripping (Figure 3.3- bottom). In this position, subjects were asked to push against a transverse bar connecting the right and left arms of the mechanical brace either simultaneously with all of the fingers or with one finger at a time. Regarding this last exercise, two possible activations were considered: one implicating no movement of the wrist (it was kept at 0º of ulnar deviation) by pressing with each finger in its natural position, and the other involving a rotation of the wrist (in radial and ulnar directions) by

pressing on a common point accessible to all fingers (at middle finger level). This exercise was designed to exert isometric contractions similar to piano-playing: each contraction lasted for a short time period and was followed by a short rest. Each time, the subject had to complete a predefined number of repetitions at the target force level, where the level was relative to the MVC for each finger, if the task consisted in the isolated activation of the fingers, or relative to the MVC exerted when pressing with all fingers simultaneously if that was the case. In all cases, the wrist was aligned with the axis of the torquemeters and no movement of the forearm was allowed during the experimental protocol.

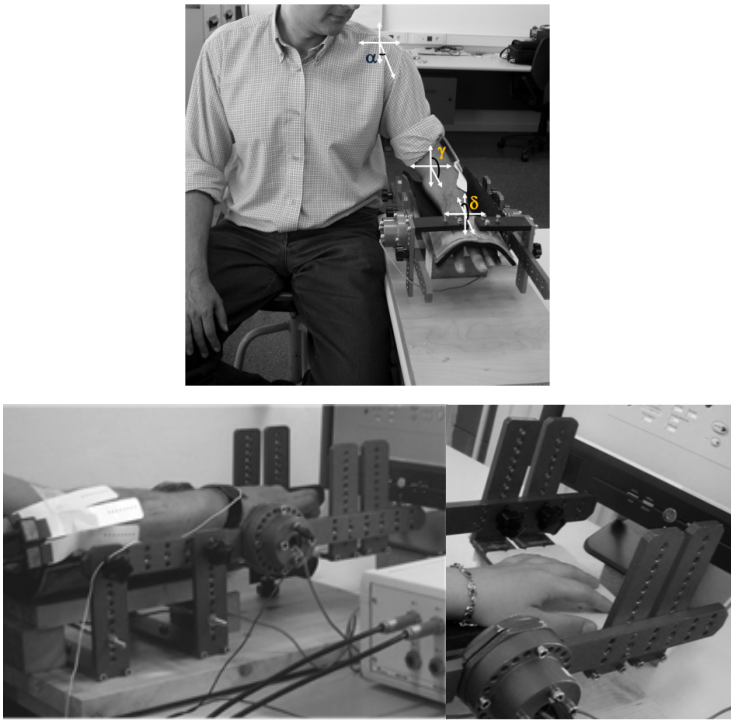

Figure 3.3. Subject position during wrist extension and hand gripping (top) and finger pressure (bottom). The position of the three joints is showed at the top figure and was common for the three tasks: shoulder at α~15 in horizontal adduction, elbow at γ=90º and wrist at δ=0º of ulnar deviation (δ was constant except for the case of finger pressing with rotation of the wrist). The forearm was kept in full pronation for all tasks. The position of the hand for the finger pressing task is presented at the bottom. The wrist was aligned with the main axis of the torquemeters and the force was exerted over a transverse bar connecting the two arms of the mechanical brace.

3.2.2 Muscles

Extrinsic muscles of the forearm were assessed through multichannel sEMG in order to analyze muscle function in upper limb disorders.

Among forearm muscles three units primarily extend the wrist: the Extensor Carpi Radialis Longus and brevis (ECR), the Extensor Carpi Ulnaris (ECU) and the Extensor Digitorum Communis (EDC) (Moore 2002). These muscles also assist forearm flexors during hand gripping although power grip is primarily achieved by the contraction of

flexor muscles (Hamill, Knutzen 2006). Extensor and Flexor muscles also assist the movements of the fingers.

Function of the different extrinsic muscles considered in this work is summarized in Table 3-1 (Hamill, Knutzen 2006, Kendall F. P., Kendall McCreary E., and Provance P.G. 1993) and are described as following:

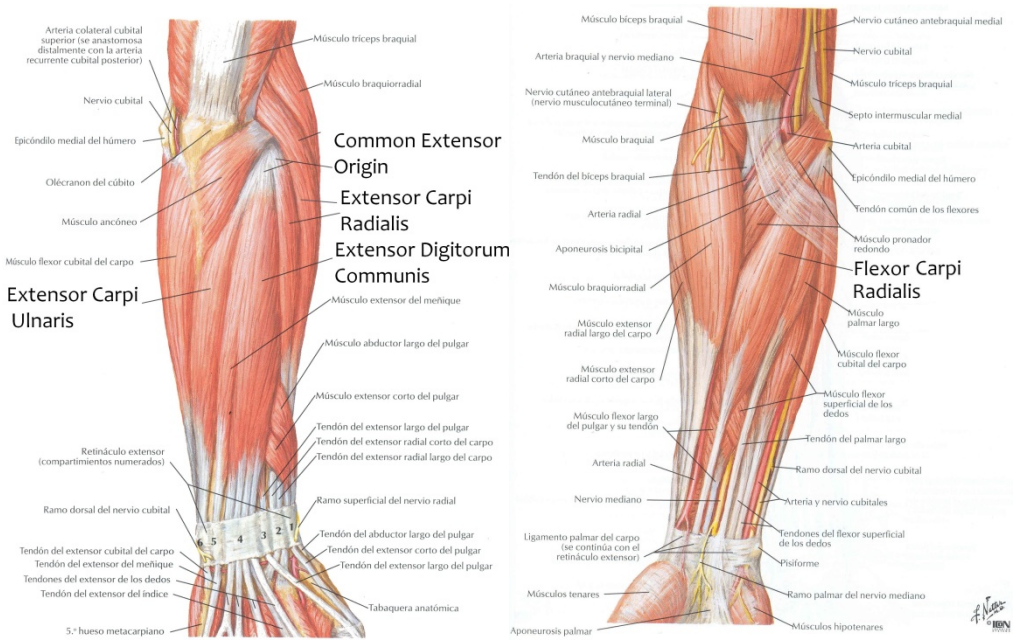

Figure 3.4. Extrinsic forearm muscles. Posterior view (palmar) and anterior view (dorsal) are shown at left and right respectively. Muscles analyzed in the present study are highlighted in big fonts. Images were extracted and modified from (Netter 2006).

a. Extensor Carpi Radialis

The extensor carpi radialis muscle in one of the main extensors of the wrist. Its principal function is the deviation of the hand in radial direction. It is originated at the lateral epicondyle of the humerus and becomes a long tendon about half-way of the forearm before its insertion into the second and third metacarpal bones. This muscle is actually considered as two independent units: the extensor carpi radialis longus and the extensor carpi radialis brevis, although it is very difficult to differentiate between the action of one or the other. In sEMG is commonly assessed as a unit.

Several studies have linked this muscle with the onset of lateral epicondylalgia (Moore 2002) as well as with repetitive strain injuries in musicians (Moreno-Torres et al. 2010).

b. Extensor Digitorum Communis

The Extensor digitorum communis originates at the lateral epicondyle of the humerus. At the distal forearm, it divides into four tendons which pass through a separate compartment of the dorsal carpal ligament and enter the hand where it inserts into the

second and third phalanges of the fingers. Its main function is the extension of the fingers and also assists the extension of the wrist.

c. Extensor Carpi Ulnaris

Extensor Carpi Ulnaris is also originated at the lateral epicondyle of the humerus as the extensor carpi radialis and the extensor digitorum communis. It runs along the ulna and inserts into the fifth metacarpal bone. Its main functions are the extension of the wrist and the deviation of the hand in the ulnar direction (Figure 3.4.)

The three extensor muscles describe above act as flexors of the elbow and are also active during hand gripping either by positioning the hand on a given direction in the space or to stabilize the wrist. They are commonly linked to upper-limb disorders because they are highly active during common tasks related to repetitive contractions of the hand and fingers.

d. Flexor Carpi Radialis

The Flexor Carpi Radialis originates at the Medial Epicondyle and inserts into the base of the 2nd and 3rd metacarpal bones. It produces wrist flexion along with other extrinsic flexors of the forearm and the radial deviation of the hand. As in the case of many extrinsic muscles, it becomes a tendon halfway along the forearm before reaching the hand.

The anatomical locations of the described muscles can be observed in Figure 3.4.

TABLE 3-1. MUSCLES INCLUDED IN THE EXPERIMENTAL PROTOCOL AND THEIR FUNCTION

Muscle	Wrist Extension	Wrist Flexion	Ulnar Deviation	Radial Deviation	Hand Gripping	Finger Extension	Finger Flexion
Extensor Carpi Radialis	Main function			Main function	Assist	Assist	
Extensor Carpi Ulnaris	Main function		Main function		Assist	Assist	
Extensor Digitorum Communis	Assist				Assist	Main Function	
Flexor Carpi Radialis		Main function			Main function		Assist

The following muscles in each type of task were analyzed

- Wrist extension: Extensor Carpi Radialis, Extensor Carpi Ulnaris and Extensor Digitorum Communis

- Hand Grip: Extensor Carpi Radialis, Extensor Carpi Ulnaris, Extensor Digitorum Communis and Flexor Carpi Radialis
- Finger Pressing: Extensor Carpi Radialis, Extensor Carpi Ulnaris and Extensor Digitorum Communis: The activation of extensor muscles was compared to the activation of Flexor Carpi Radialis

3.3 Instrumentation

3.3.1 Electrode arrays and positioning

As previously mentioned forearm muscles present multiple innervations zones and their assessment is hardened by the proximity of other neighbor muscles that cause multiple crosstalk potentials. Therefore, the first concern was to determine the proper zone for the location of the electrodes in each muscle. For this purpose a linear array of 16 electrodes spaced by 5 mm (LISiN- OT Bioeletronica) (Figure 3.5 left) was used to identify the direction of propagation of Motor Unit Action Potentials and the location of innervation zones. Once the direction was determined, an adhesive array was employed (Figure 3.5 right). The array was placed over a line connecting the origin and insertion of each muscle. An example is presented in Figure 3.6. sEMG signals correspond to the Extensor Digitorum Communis. It is possible to observe a phase inversion of MUAPs in the proximity of innervation zones IZ_1 and IZ_2 (channels 9 and 7 respectively) as well as a change in the direction of propagation (solid lines) from left- right to right- left. Additionally, MUAPs extinguish near the tendon in the proximal forearm (channels 3 to 1).

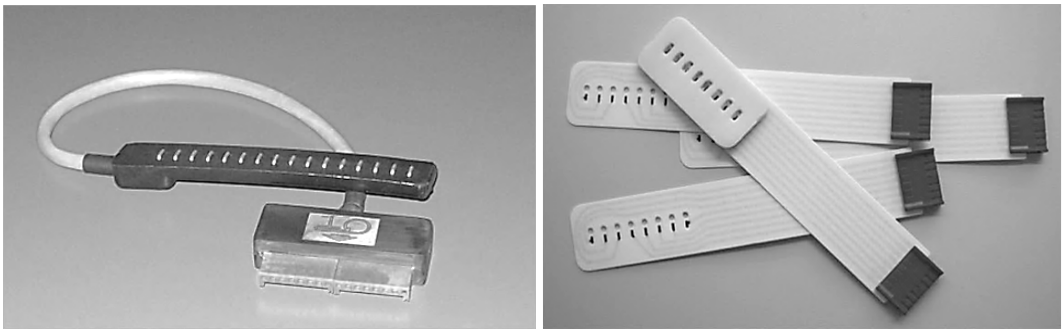

Figure 3.5. Linear Electrode Arrays employed for the assessment of muscles in the forearm. The 16-electrodes array at the left was used to find a proper location for the 8-electrode adhesive arrays (right) in each muscle. IED= 5 mm in both cases

A preliminary study showed that best locations, away from innervation zones and tendons, were proximal for ECR, ECU and FCR and distal for EDC (Signorino, Mandrile & Rainoldi 2006, Mananas et al. 2005). Around these regions final locations for 8- electrode arrays (IED=0.5 mm, LISiN- OT Bioeletronica) (Figure 3.5 right) were selected by

inspection of sEMG signals. Propagation of Motor Unit Action Potentials (MUAP) and small wave-shape differences between subsequent signals were used as criteria for the correct alignment of the array with the muscle fibres.

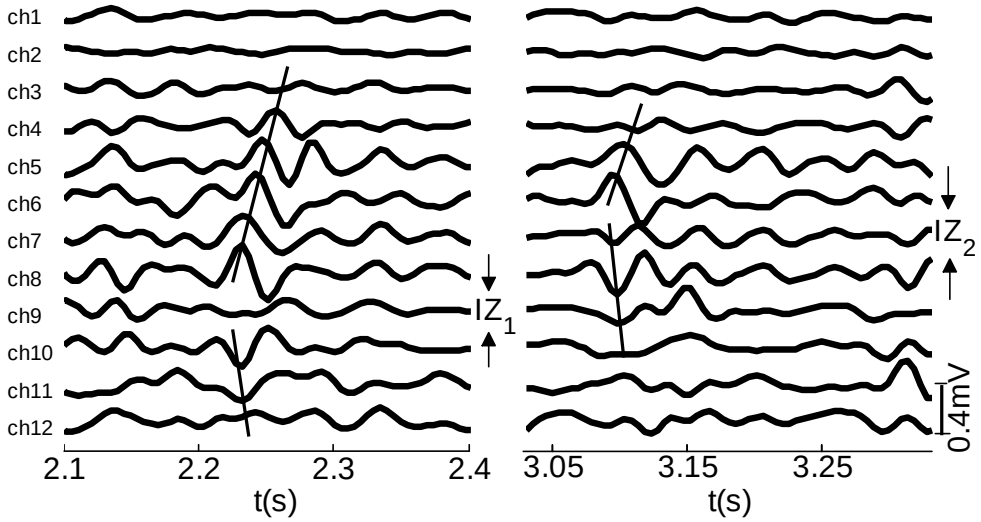

Figure 3.6. sEMG signal registered with a linear 16-electrode array (IED=0.5mm) in the muscle Extensor Digitorum Communis. Twelve channels are displayed. It is possible to observe two different innevation zones, one near channel 9 (IZ_1) and the other near channel 7 (IZ_2). Both the phase and the direction of propagation (in solid lines) changes in the proximity of innervation zones. The extinction of pontentials near the tendon can be observed in channels 1-3.

3.3.2 Force Measurement

Isometric contractions were executed by means of two devices (Figure 3.7): a mechanical brace for hand extension (OT Bioelettronica, range 150 N.m, resolution 2.5mV/V) and finger flexion and a JAMAR® hydraulic hand dynamometer for the gripping task (Baseline®, Fabrication Enterprises Inc., U.S.A.).

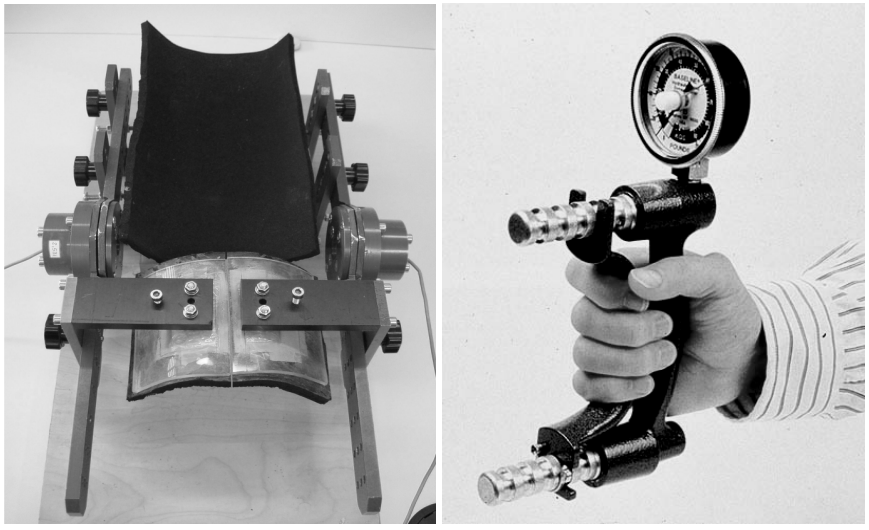

Figure 3.7. *Left.* Mechanical brace. *Right.* Hydraulic hand dynamometer

The mechanical brace consisted on a set of bars fixed to a table at right and left to resist the movement of the joint (Figure 3.7 left). On each side, the torque applied at the end of one of two independent bars was measured by a transducer placed in the coupling joint.

In the case of wrist extension, torque measurement was independent on each side in order to prevent pronation and supination of the hand and the consequent activation of other forearm muscles employed in these kinds of contractions. During the experiment subjects were trained and asked to maintain similar levels of torque at both sides (see section 3.3.3)

In the case of finger pressing, the measurement was coupled on both sides by using a transverse bar (Figure 3.3. bottom).

3.3.3 Instrumentation setup

The general instrumentation setup is shown in Figure 3.8. Biofeedback for the subject was accomplished by software implemented in LabView. For each kind of task, the subject was asked to reach the Maximal Voluntary Contraction (MVC), which was measured by the torquemeters in each side. These values were then used as reference for submaximal efforts, and the signals at right and left sides of the mechanical brace were sensed and presented to the subject in real time. In this way the subject was able to maintain the same level of force in both sides.

Torque signals from each torquemeter were sampled at 100 Hz and stored in this first system by using a data acquisition card (NI PCI 1200). The EMG signals were acquired using a second system composed by two 16-channels amplifiers (ASE16, LISiN-SEMA Elettronica, Torino, Italy). Surface EMG signals were recorded in single differential mode (SD), bandpass filtered (3-dB bandwidth 10–450 Hz), sampled at a rate of 2048 Hz and stored on a PC after 12-bit analog-to-digital conversion (National Instrument NI-DAQ 6024E and NI-DAQ AI-16E4 A/D cards).

An example of the feedback presented to the subject during piano playing-like contractions is presented in Figure 3.9. This case is underlined because it presented a higher complexity when compared to the other two tasks, since it has to use different references for different fingers, and even had to use as reference the torque signal on one or the other transducer when pressing with each finger in its natural position. In this case, the torquemeter closest to the active finger was used as reference. Besides, the purpose was to simulate piano playing in a way that the isometric contraction for each or all of the fingers lasted only for a few seconds and was followed by a short period of relaxation. For

this purpose, the software interface emitted a musical tone during a short time-interval (one of the musical scale for each finger), so that the subject exerted the corresponding finger pressure for the duration of that tone. Silence was associated to rest and the feedback was presented independently for every finger (Figure 3.9 left).

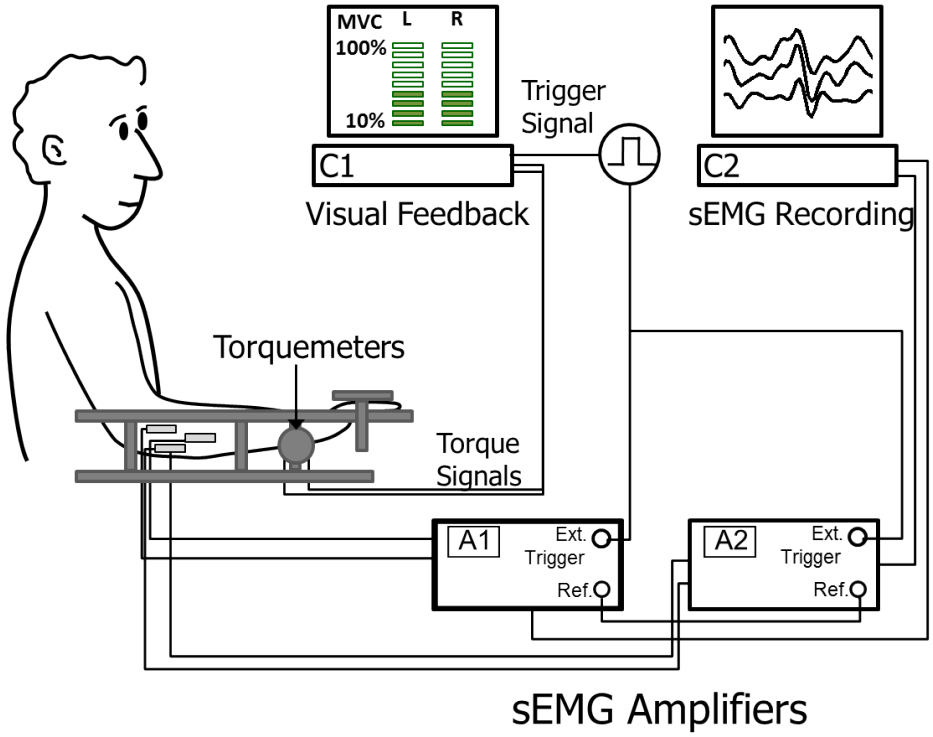

Figure 3.8. Instrumentation setup for tasks in the different experimental protocols. In the case of hand grip, the mechanical brace was replaced by a hand dynamometer.

The feedback software (either wrist or piano) controlled both, the recording of torque signals and the trigger pulse for the synchronization of the different systems in Figure 3.8. The recording of sEMG signals from amplifiers A1 and A2 in computer C1 and of torque signals in computer C2 was triggered with the rising edge of a TTL pulse.

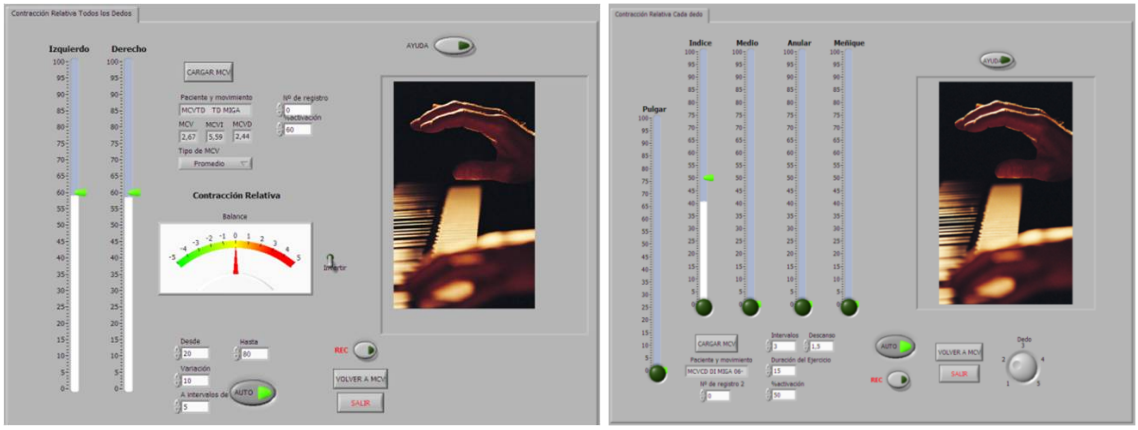

Figure 3.9. Biofeedback for the subject during the task of finger pressing. Feedback is presented as the relative torque exerted in both torquemeters with all fingers (left) or independently for each finger (right).

3.4 Experimental session and signal recording

Each session consisted in the following steps:

- Find the proper location for the electrodes in the selected muscles. As described earlier, forearm muscles are difficult to assess because they are characterized by multiple innervation zones and they are very close to one another which increases crosstalk in the recorded signal. This step was critical for the correct interpretation of the signals. In order to find the best position for signal detection a dry linear array of 16 silver bar electrodes was displaced along a line traced between the origin and insertion of each muscle (Kendall F. P., Kendall McCreary E., and Provance P.G. 1993). Then, the subject was asked to perform short contractions in order to locate the innervation zones (IZ) and to find a portion of the muscle between IZs and away from tendons in which it was possible to detect propagating potentials with similar shape on different EMG channels. Selective contractions for each of the muscles were performed to maximize their activation: radial deviation for enhancing the activity of the Extensor Carpi Radialis and finger extension and ulnar deviation for enhancing the activations of Extensor Digitorum Communis and Extensor Carpi Ulnaris respectively. The activation of Flexor Carpi Radialis was assessed during wrist flexion while accomplishing a hand grip. Propagation of Motor Unit Action Potentials (MUAP) and small shape differences between subsequent signals were used as criteria for the correct alignment of a linear electrode array with the muscular fibers.
- Skin preparation including shaving and cleaning with abrasive paste and water. This procedure permitted to reduce the electrode-skin impedance.
- Fixation of semi-disposable 8-electrode arrays with an IED of 5 mm (Figure 3.5 right).
- Guidelines for the subject about the exercises to be performed.
- Isometric task and signal recording: In the initial phase, Maximal Voluntary Contraction was measured as the maximum value of three different explosive trials separated by three minutes of rest. In the cases of wrist extension, hand grip, and pressure with all fingers, MVC measurement was followed by contractions at 20%, 50% and 80% MVC after 5 minutes rest. Each submaximal contraction lasted for 15 seconds. For isolated finger pressure (either with rotation or not), submaximal contractions were performed by pressing sequentially with each finger (starting from thumb to little finger) until five complete repetitions were recorded. Subjects pressured with each finger for 2 seconds at a time and this task was accompanied with a different musical tone emitted by the

biofeedback software so that the subject was able to follow the sequence maintaining the target force for such time interval. A two seconds rest was imposed between consecutive finger pressures. This procedure was repeated for the three effort levels (20%, 50% and 80% MVC) and for all considered tasks. Submaximal contractions were performed in randomized order to avoid bias in the results and every contraction was followed by a resting period of 3 minutes in order to avoid the effects of cumulative fatigue.

- Finally, at the end of the session subjects were asked to perform an endurance contraction at 50% MVC until exhaustion for every task (wrist extension, hand grip and finger pressure).

3.5 Subjects

The experimental protocols intended for the assessment of Lateral Epicondylitis were conducted on a group of patients and on a control group of healthy volunteers. The experimental protocol intended for the analysis of Repetitive Strain Injuries in musicians was applied only on healthy subjects.

Healthy subjects did not report any history of musculoskeletal and/or neuromuscular disorders of the upper extremity. Patients had been clinically diagnosed for Lateral Epicondylalgia in the past and were treated with conservative therapy including physical modalities and exercise (surgery excluded). In all cases, the injury had been induced by repetitive contractions related to physical effort required by their daily work activities. They were free of symptoms and pain at the time of their participation and were actively working for at least six months. None of the subjects (control or patients) were involved in regular training or sports activities focused on the use of the upper limb. By chance, all the analyzed subjects were right-handed. Sample sizes (N) and anthropometric measures for the different subjects in the database are summarized in Table 3-2.

TABLE 3-2. SAMPLE SIZES AND ANTHROPOMETRIC MEASURES FOR SUBJECTS IN THE DATABASE.

		N	Age (years)	Height (cm)	Weight (kg)	MGS (k)
Wrist Extension	**Control**	10	31.5 ± 5.0	176.4 ± 6.2	76.3 ±5.5	43.5 ± 4.1
	Patients	10	33.3 ± 4.6	174.6 ± 5.8	76.92 ± 12.8	44.3 ± 4.1
Hand Grip	**Control**	10	32.5 ± 4.2	177.4 ± 6.0	79.4 ± 6.6	43.9 ± 5.34
	Patients	10	32.6 ± 4.3	169 ± 24.3	88 ± 36.3	45.7 ± 5.42
Finger Pressing	**Control**	5	33 ± 8.0	172.5 ± 6.3	77.5 ± 5.8	—
	Patients	0	—	—	—	—

Maximal strength during hand gripping was measured in the groups associated to the study of Lateral Epicondylitis. This measure is commonly used as index of the functional integrity of the upper extremity in clinical environments (Bhargava, Eapen & Kumar 2010). Maximal Grip Strength (MGS) was measured using the JAMAR® hand dynamometer in kilograms-force. Results are summarized in Table 3-2. No statistical differences were found between healthy subjects or patients, regarding age, body mass index or functional integrity of the upper limb. Differences were evaluated through a Mann-Whitney's U test.

3.6 References

Bejjani, F.J., Kaye, G.M. & Benham, M. 1996, "Musculoskeletal and neuromuscular conditions of instrumental musicians", *Archives of Physical Medicine and Rehabilitation,* vol. 77, no. 4, pp. 406-413.

Bhargava, A., Eapen, C. & Kumar, S. 2010, "Grip strength measurements at two different wrist extension positions in chronic lateral epicondylitis-comparison of involved vs. uninvolved side in athletes and non athletes: a case-control study", *Sports Medicine, Arthroscopy, Rehabilitation, Therapy & Technology,* vol. 2, no. 1, pp. 22.

Croisier, J., Foidart-Dessalle, M., Tinant, F., Crielaard, J. & Forthomme, B. 2007, "An isokinetic eccentric programme for the management of chronic lateral epicondylar tendinopathy", *British journal of sports medicine,* vol. 41, no. 4, pp. 269-275.

Hamill, J. & Knutzen, K.M. 2006, "Functional Anatomy of the Upper Extremity" in *Biomechanical basis of human movement*, 2nd edn, Lippincott Williams & Wilkins, .

Kendall F. P., Kendall McCreary E., and Provance P.G. 1993, *Muscles: Testing and Function,* 4th edn, Williams & Wilkins.

Mananas, M.A., Rojas, M., Mandrile, F. & Chaler, J. 2005, "Evaluation of muscle activity and fatigue in extensor forearm muscles during isometric contractions", *Proc. 27th Annual International Conference of the Engineering in Medicine and Biology Society, 2005. IEEE-EMBS 2005*, pp. 5824.

Moore, J.S. 2002, "Biomechanical models for the pathogenesis of specific distal upper extremity disorders", *American Journal of Industrial Medicine,* vol. 41, no. 5, pp. 353-369.

Moreno-Torres, A., Rosset-Llobet, J., Pujol, J., Fabregas, S. & Gonzalez-de-Suso, J. 2010, "Work-Related Pain in Extrinsic Finger Extensor Musculature of Instrumentalists Is Associated with Intracellular pH Compartmentation during Exercise", *Plos One,* vol. 5, no. 2, pp. e9091.

Netter, F.H. 2006, *Atlas of human anatomy,* Saunders/Elsevier.

Shimose, R., Matsunaga, A. & Muro, M. 2011, "Effect of submaximal isometric wrist extension training on grip strength", *European journal of applied physiology,* vol. 111, no. 3, pp. 557-565.

Signorino, M., Mandrile, F. & Rainoldi, A. 2006, "Localization of innervation zones in forearm extensor muscles. A methodological study", *Proc. of the XVI International conference of the International Society of Electrophysiology and Kinesiology*, pp. 220.

Snijders, C., Volkers, A., Mechelse, K. & Vleeming, A. 1987, "Provocation of Epicondylalgia Lateralis (Tennis Elbow) by Power Grip Or Pinching", *Medicine and science in sports and exercise,* vol. 19, no. 5, pp. 518-523.

4

Linear Electrode Arrays sEMG analysis

4.1 Introduction

Multichannel surface EMG was used to analyse muscular co-activation and myoelectric manifestations of fatigue in contractions associated to common upper-limb disorders. This chapter is intended to the analysis of signals recorded in extrinsic forearm muscles during the experimental protocols described in Chapter 3. Different surface EMG variables were extracted from the signals after applying a Double Differential filter on a triplet that was selected on the basis of similarity between different channels and where it was possible to observe propagation of Motor Unit Action Potentials. This technique guarantees the correct interpretation of results considering the difficulty of assessing muscles in the forearm.

Different indices related to co-activation patterns and fatigue were calculated from sEMG variables. Such indices were related to muscular imbalances and deficits on patients affected by upper limb disorders. Findings of this series of studies can be used in the design and follow up of rehabilitation therapies intended to Upper Limb Disorders.

4.2 Methods

4.2.1 Signal processing

As first step, the multichannel sEMG signals were filtered between 12 and 350 Hz with a 4th order Butterworth filter in forward and backward direction in order to correct for phase distortion. Double Differential signals were calculated from the different SD channels in order to enhance selectivity of the recorded signals, by reducing crosstalk and non-propagating components (Mesin et al. 2009).

All variables extracted from the signals were calculated in fifty percent overlapping windows (epochs) of 500 ms and averaged on signal segments of 3 s where the observed

torque was between ±5% of the target level. Epoch length was chosen to meet stationary conditions as described in (Merletti, Parker 2005)and elsewhere.

a. Triplet Selection

Parameters were obtained from a triplet, that is, three consecutive SD channels resulting in two DD signals. Triplet selection was based on the cross-correlation coefficient (CC) between the DD channels and on the time delay estimated between signals to guarantee the propagation of MUAPs in the recorded signals and the correct alignment with the muscular fibers. Triplets for further analysis were chosen among those that exhibited a CC>0.70 and whose time-delay corresponded to a conduction velocity (Eq. 4-5 and Eq. 4-6) that ranged between 3 m/s and 8 m/s according to physiological expected values.

b. EMG Variables

Parameters related to power and spectrum of the EMG signal (associated to the number and conduction velocity of the active MU respectively), were analyzed in order to establish the level of activity of the muscles involved in the contraction.

- **Amplitude variables**

Information from power and amplitude of EMG signal was obtained by means of root mean square (RMS) and average rectified value (ARV), respectively.

$$RMS = \sqrt{\frac{1}{N}\sum_{i=1}^{N} x_i^2} \qquad ARV = \frac{1}{N}\sum_{i=1}^{N} |x_i| \quad \text{(Eq. 4-1)}$$

Where x_i is the *i-th* DD signal in the selected triplet and N is the total number of samples in the analyzed epoch.

- **Frequency variables**

The power spectral density of the signal is affected by the distance between the recording electrodes *d* and the conduction velocity of MUAPs as (Sun I. Kim, Kang M. Lee 1990):

$$P(f) = \frac{1}{CV^2} G\left(\frac{f \cdot d}{CV}\right) \quad \text{(Eq. 4-2)}$$

Where *P* represents the Power Spectral Density (PSD) of the signal, *d* is the electrode distance, *CV* the conduction velocity and *G(f)* determine the shape of the power spectrum.

Variables used to evaluate shifts in the PSD of the signals included the mean frequency (MNF) and the median or central frequency (MDF) and were calculated by using the following expressions:

$$MNF = \frac{\sum_{i=1}^{M} f_i P_i}{\sum_{i}^{M} P_i} \qquad \sum_{i=1}^{MDF} P_i = \sum_{i=MDF}^{M} P_i = \frac{1}{2}\sum_{i=1}^{M} P_i \quad \text{(Eq. 4-3)}$$

Where P_i represents i-*th* bin of the PSD and M is the highest harmonic considered (Farina, Merletti 2000).

- **Global Conduction Velocity**

Muscle fiber conduction velocity (CV) was estimated through the spectral matching algorithm in the frequency domain (McGill, Dorfman 1984). The algorithm is based on the following property of the Fourier Transform:

$$x\left[n+\hat{\theta}\right] \xleftrightarrow{F} X(\Omega)e^{j2\pi\hat{\theta}/N} \quad \text{(Eq. 4-4)}$$

Where $x(n)$ represents an EMG signal recorded on a given channel, $X(\Omega)$ is its Fourier transform, and $\hat{\theta}$ is the temporal delay introduced by the frequency shift $e^{j2\pi\hat{\theta}/N}$. Thus, the temporal delay $\hat{\theta}$ between two consecutive channels assumed to have identical shapes (except for noise) can be obtained by least squares minimization as:

$$e_t(\hat{\theta}) = \sum_{n=1}^{N}\left[x_2\left(n+\hat{\theta}\right) - x_1(n)\right]^2 = \frac{2}{N}\sum_{k=1}^{N/2} | X_2(\Omega)e^{j2\pi k\hat{\theta}/N} - X_1(\Omega) | \quad \text{(Eq. 4-5)}$$

Where $x_1(n)$ and $x_2(n)$ are two consecutive DD signals, their Fourier transforms are represented by $X_1(\Omega)$ and $X_2(\Omega)$ and N is the total number of samples of the epoch. Finally, the conduction velocity was obtained as:

$$CV = \frac{d}{\hat{\theta}} \quad \text{(Eq. 4-6)}$$

4.2.2 Muscular Co-Activation

The coordination of extensor and/or flexor muscles during the different tasks and contraction levels was assessed by analyzing the amplitude (ARV) or the power (RMS) of the observed signals. As mentioned earlier, ARV or RMS values were extracted from epochs of 500 ms and were averaged on a signal segment of 3 seconds.

Two different sets of indices were used, the co-activation index *CI* and the orientation angles θ and φ of a set of vectors in the *contraction level- space*. This last set of indices was analyzed only during hand grip considering that this task is produced by the simultaneous

activation of flexor and extensor muscles (Hamill, Knutzen 2006) and comparable activation levels were expected. That was not the case of the other two tasks where one group of muscles (i.e. extensors or flexor) or the other was expected to present higher activations.

a. Co-activation Index- CI

Muscle co-activation, in terms of relative contributions of each muscle to a given exercise, was analyzed by normalizing the ARV or RMS values obtained in the each muscle with respect to the sum of the values obtained in the four muscles for each exercise as:

$$CI_m\Big|_{lev} = \frac{A_i}{\sum_{m=1}^{M} A_m}\Bigg|_{lev} \quad \text{(Eq. 4-7)}$$

Where m = [1, 2, 3,... , M] is the identifier of any of the muscles from the analyzed subset ms = [ECR, EDC, ECU or FCR] depending on the task (wrist extension, hand grip or finger pressing), M is the length of the subset ms and lev is any of the contraction levels lev = [20%, 50%, 80%] MVC (see Chapter 3) . In the case of analysis of wrist extension A corresponded to the average ARV of the signal segment and for hand grip and finger pressing A corresponded to the average RMS value.

Finally, an especial case involves the analysis of activation of extrinsic muscles when pressing with different fingers. For each muscle m from the subset ms = [ECR, EDC, ECU, FCR] and each level lev, a co-activation index CI^f similar to CI in (Eq. 4-7) was defined as:

$$CI_m^{f_j}\Big|_{lev} = \frac{RMS_m^{f_j}}{RMS_m^{f_3}}\Bigg|_{lev} \quad \text{(Eq. 4-8)}$$

Where f_j is one of the fingers of the set fs = [1. Thumb, 2. Index, 3. Middle, 4. Ring, 5. Little].

b. Orientation Angles θ and φ

Considering that the absolute amplitude of the signal is subject to many external factors such as intersubject variability, electrode-skin impedance, conduction volume and electrode location among others, an approach inspired in the works proposed by Valero-Cuevas et al, and Danna-Dos Santos et al in (Valero-Cuevas 2000, Danna-Dos Santos et al. 2010) was adopted. This kind of approach avoids normalizations with respect to the amplitude of EMG signal during maximal voluntary contraction (MVC) which can result in inaccurate associations to the exerted muscle force(Gatti et al. 2008) not only because of

uncertainty in MVC measurements itself (Buchanan et al. 2004) but also because negative superposition of MUAPs during contractions at high level of effort can be expected to affect the amplitude of the obtained signal (Day, Hulliger 2001, Keenan et al. 2005). Thus, a nonlinear relationship between force and amplitude of sEMG signal can be expected (Herda et al. 2011). The power of the signals at different contraction levels was used to assemble a vector in the $\mathbb{R}^3$ space as:

$$\mathbf{u_m} = [RMSm_{20\%},\ RMSm_{50\%},\ RMSm_{80\%}] \quad \text{(Eq. 4-9)}$$

Where each dimension corresponded to the power observed at a given effort level. The vector **u** was defined for every muscle *m* = [*ecr, edc, ecu, fcr*] and its orientation in the *contraction level* space depended on amplitude changes from a given contraction level to the next (i.e. from 20%MVC to 50%MVC and from 50%MVC to 80%MVC). The rationale behind the analysis was that if changes were not uniform in for different muscles, or even for different population groups, they would be reflected in the orientation of such vectors.

Moreover, interactions between different muscles can also be observed from differences in the relative orientation of the set of vectors **u**. Several authors have reported differences in the force exerted by flexors and extensors of the forearm between patients with upper-limb disorders and normal subjects, but those differences were based in the exerted force or torque (Forthomme et al. 2002, Alizadehkhaiyat et al. 2007, Alizadehkhaiyat et al. 2007). In this work, muscular imbalances were assessed by calculating a second set of vectors in $\mathbb{R}^3$ as:

$$\mathbf{v_n} = \mathbf{u_n}\text{-}\mathbf{u_{fcr}} \quad \text{(Eq. 4-10)}$$

Where vectors **u** were defined as in (Eq. 4-9) and *n* is any element of the subset *n* corresponding to extensor muscles, *n=[ecr, edc, ecu]*.

Differences in the angle between flexor and extensor vectors can be mapped to muscular imbalances in patients with upper-limb disorders.

Finally, the orientation of the sets of vectors u and v in $\mathbb{R}^3$, was evaluated by the elevation (θ) and azimuth (φ) angles (Figure 4.1), after applying a transformation from Cartesian to Spherical coordinates (Eq. 4-11).

$$\theta = \tan^{-1}(y/x),\ \varphi = \tan^{-1}\left(z/\sqrt[2]{x^2+y^2}\right),\ r^2 = x^2+y^2+z^2 \quad \text{(Eq. 4-11)}$$

where x, y, and z axis corresponded to 20%, 50% and 80% MVC respectively (Figure 4.1).

Unlike relative angles defined in (Valero-Cuevas 2000) and (Danna-Dos Santos et al. 2010), θ and φ are absolute angles and are always measured in the same direction (from the x axis and from the x-y plane respectively) in the Spherical coordinate system (Figure 4.1).

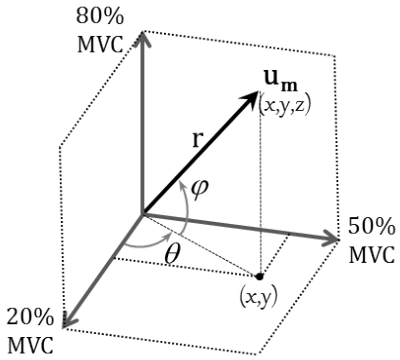

Figure 4.1.Transformation from coordinates in the Cartesian system to coordinates in the Spherical system.

4.2.3 Assessment of Muscular Fatigue

Myoelectric fatigue was assessed by the temporal evolution of the variables described in section 1.2.1.b. Such evolution is commonly represented in a fatigue plot. An example of the changes observed on CV, MNF and MDF during a sustained contraction at 50%MVC is presented in Figure 4.2.

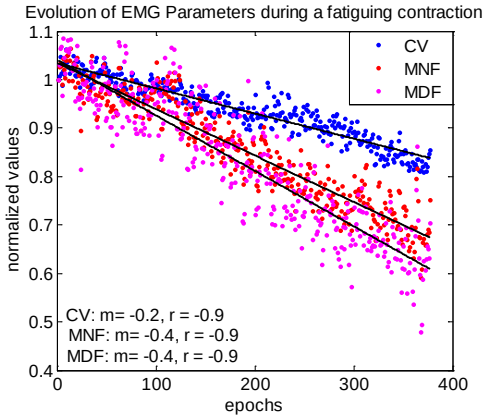

Figure 4.2. Fatigue plot. The evolution of the variables CV, MNF and MDF during a sustained isometric contraction is presented as well as the slope of the regression (m) and the regression coefficient (r).

As explained earlier, the frequency spectrum shifts to low frequencies, decreasing the values observed on the variables MNF and MDF as consequence of localized fatigue, involving changes in the CV of the MUs among others. Thus, a decrease in the observed CV is also expected. Finally, the amplitude of the signal (ARV or RMS) is expected to increase because of an increasing superposition of MUAPs caused by the recruitment of new MUs or by an increase in the activation frequency of the recruited MUs.

Time changes were evaluated from the rate of change *m* (i.e. the slope) of the linear regression of each variable normalized with respect to the initial value across the total

endurance time (Merletti, Parker 2005), that is, the time instant (break point) where the subject could no longer maintain the contraction at the desired level of effort.

4.2.4 Statistical Methods

Differences between groups (healthy subjects vs. recovered patients) were assessed through non-parametric Mann–Whitney U test while intragroup differences were analyzed by Wilcoxon signed test.

In the case of hand-grip, Repeated Measures Analysis of variance (ANOVA) was used for analyze differences in the orientation angles (i.e. the co-activation pattern) at 3 levels of effort (20%, 50% and 80%MVC). It was also used to analyze the trend of CV for each muscle during the sustained contraction at 50%MVC. In this case, 11 levels were defined, each of them corresponding to the value observed every 10% of the total endurance time from 0% to 100%. Finally, Multivariate Analysis of Variance (MANOVA) was applied to evaluate differences in the orientation angles θ and φ in the contraction level space for the set of vectors **u** and **v** (Eq. 4-9 and Eq. 4-10).

Effects and differences were considered significant at $p=0.05$.

4.3 Results

4.3.1 Wrist Extension

The following results were obtained during wrist extension for 10 healthy subjects and 10 patients with Lateral Epicondylalgia. No significant differences concerning anthropometric measures or upper-limb functional index (MGS) were found between groups. For a description of subjects in the database, please refer to section 3.5 in Chapter 3. EMG variables were extracted from three extensor muscles (Extensor Carpi Radialis- ECR, Extensor Digitorum Communis- EDC and Extensor Carpi Ulnaris- ECU) and three different effort levels relative to the Maximal Voluntary Contraction at 20%, 50% and 80% MVC (see protocol description and muscle selection in Chapter 3).

a. Conduction Velocity and cross-correlation coefficients

No significant differences in CV estimates were found between muscles or exercises in the same group (control or patients) neither when comparing the same muscles at different contraction levels and/or between groups.

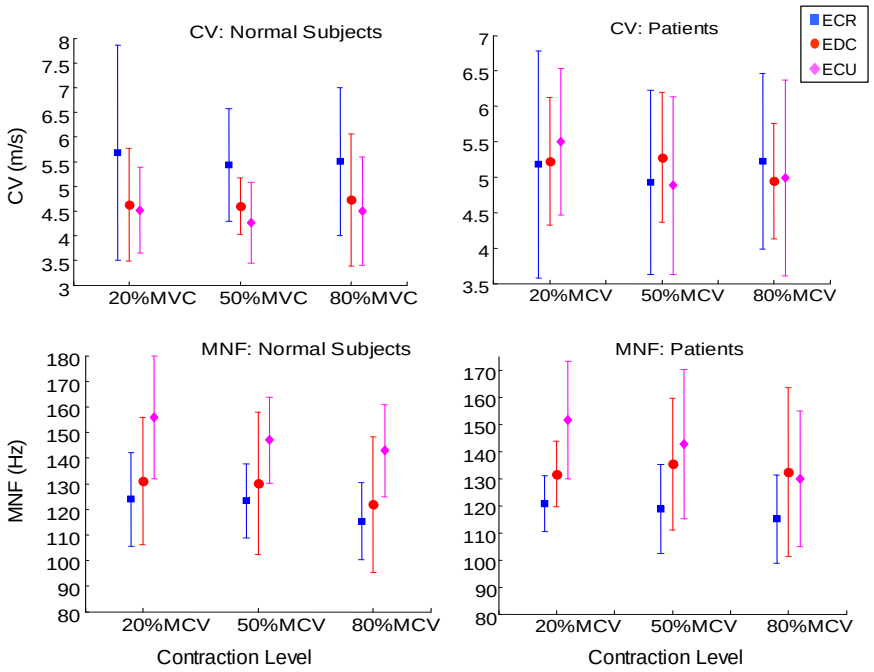

Figure 4.3. Conduction Velocity (top) and Median Frequency (bottom) estimated for the control group (left) and patients (right) during wrist extension at different levels of effort.

Regarding spectral parameters, it was found that ECU signals presented higher frequencies with respect to signals recorded in the ECR for the control group ($p<0.05$ in all cases) but not for patients, where this relationship maintained only for the case of the contraction at 20% MVC ($p<0.01$). Results are presented in Figure 4.3.

b. Co-Activation Index *CI*

Six exercises were analyzed: radial, finger and ulnar extension (*selective contractions* for each muscle), and three wrist extensions at submaximal level. In the case of patients and for selective contractions, *CI* in the muscle whose activity was enhanced was significantly higher than the value obtained in the other muscles ($p<0.03$ for ECR and $p<0.004$ for EDC and ECU) (Fig. 2b). In the case of healthy subjects it happened only in radial and ulnar extension but not in finger extension where the ECR was also active.

The main contribution to the joint activation is carried out by different muscles in different groups. Results are presented in Figure 4.4.

In the case of selective contractions in patients, CI of the muscle whose activity was enhanced was significantly greater than in the other ones ($p<0.03$ for ECR and $p<0.004$ for EDC and ECU). In the case of healthy subjects it happened only in radial and ulnar extension but not in finger extension where the ECR was also active ($p<0.01$).

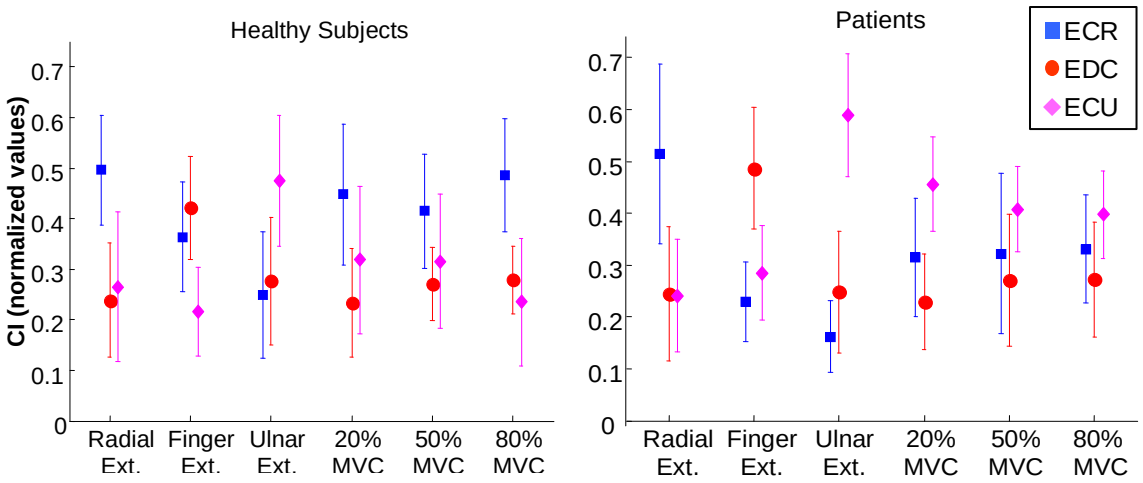

Figure 4.4. Co-activation Index CI based on the ARV of the signal in the different extensor muscles. Selective contractions as well as wrist extension at different effort levels are presented. Values are presented as mean and standard deviation for the control group (left) and patients (right)

Significant differences were also found in wrist extension at different effort levels. In the control group, *CI* in ECR was higher than in EDC at all levels of effort and also higher than in ECU at 80% MVC ($p<0.04$ in all cases). Regarding the patient group, *CI* in ECU was higher than in EDC at 20, 50 and 80% MVC ($p<0.02$) and also than in ECR at 20%MVC ($p<0.05$). Additionally when comparing *CI* for each muscle between the two populations, it was found that the average contribution of ECR was higher for healthy subjects than for patients ($p<0.02$). On the contrary, the average contribution of ECU was higher for patients than for healthy subjects ($p<0.02$).

c. Fatigue Indices

Time evolution of sEMG variables is presented in Figure 4.5. Results are presented in mean and standard deviation for subjects in each group at intervals of 10% of the total endurance time.

A significant decrease of CV with time was observed during the endurance exercise in all muscles and in both groups ($p<0.02$ for healthy subjects and $p<0.01$ for patients). However, significant changes for MNF and MDF variables and ARV were only observed in the group of patients ($p<0.04$ in all variables).

When comparing between groups, ARV in ECR, ECU and EDC presented higher fatigue indices for patients than for healthy subjects ($p<0.02$, $p<0.01$, $p<0.03$ respectively). Conversely, the rate of change of CV was higher for patients than for healthy subjects for EDC ($p<0.04$) and especially for ECR ($p<0.01$).

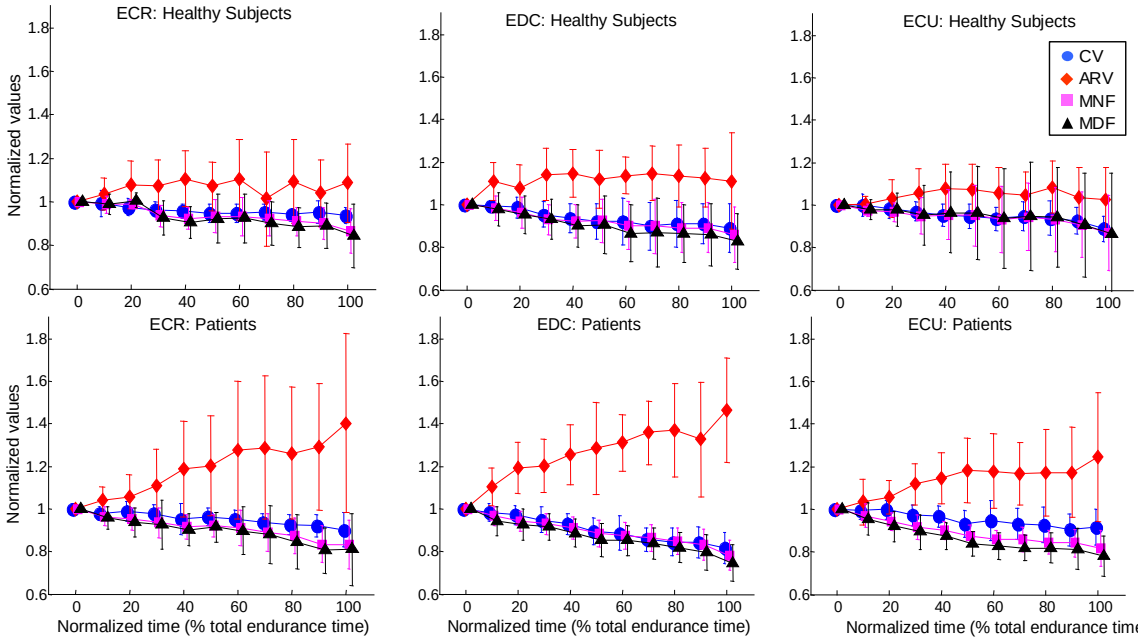

Figure 4.5. Fatigue plots for ECR, EDC and ECU for healthy subjects (top) and patients with lateral epicondylalgia (bottom). Results are presented in mean and standard deviation for each group.

4.3.2 Hand Grip

The following results are reported for 10 subjects in each group (control and patients with Lateral Epicondylalgia after recovery). No significant differences concerning anthropometric measures or MGS index were found between groups. Four muscles among forearm extensors and flexors were analyzed: Extensor Carpi Radialis- ECR, Extensor Digitorum Communis- EDC, Extensor Carpi Ulnaris- ECU and Flexor Carpi Radialis- FCR. Three levels of effort during hand grip were considered: 20%, 50% and 80% relative to the MVC.

a. Cross correlation Coefficients and Conduction Velocity

Conduction velocity for all of the muscles ranged between 2 m/s and 8 m/s (Figure 4.6) and their correspondent cross-correlation coefficients (in median and [IQR]) were 76.81[13.52]% and 77.80[18.48]% for healthy subjects and patients respectively. Regarding CV, no differences were found between groups or between muscles or effort levels in the same group. These results were expected, given that the absolute value of this parameter has a high dependence on the alignment of the electrodes and the muscular fibers.

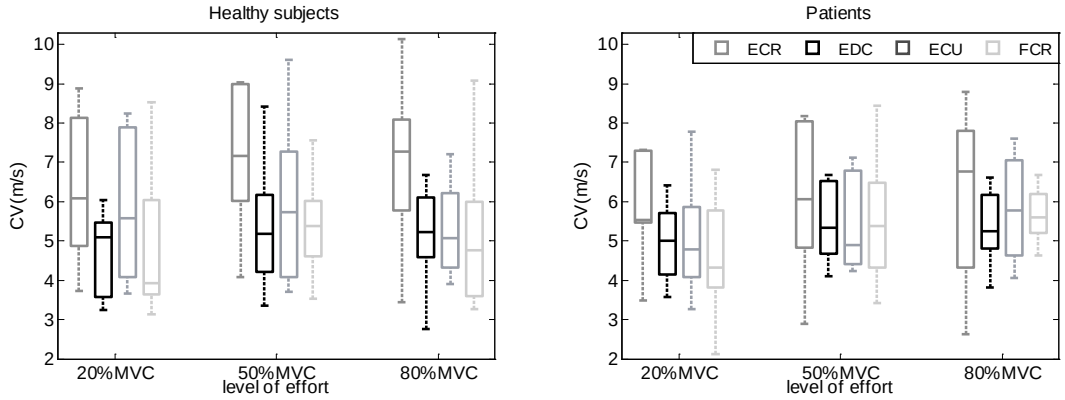

Figure 4.6. Box-plots for conduction velocity in healthy subjects (left) and patients (right). The four muscles are presented in shadows of gray for the 3 levels of effort performed in the experiment. Results are displayed for 10 subjects in each group. Outliers are represented with a cross (+)

b. Co-activation Indices

Multivariate analysis of variance- MANOVA was applied to the angles corresponding to azimuth (θ) and elevation (φ) of the set of vectors **u** (Eq. 4-11) in the spherical coordinate system (Figure 4.7). Previous to the analysis, equality of variances was tested through Levene's test and it was found that azimuth angle corresponding to EDC (θ_{edc}) did not satisfy the condition of equal variances in the two groups. Consequently, both angles: azimuth and elevation (θ_{edc},φ_{edc}) for the vector $\mathbf{u_{edc}}$ were removed from the analysis.

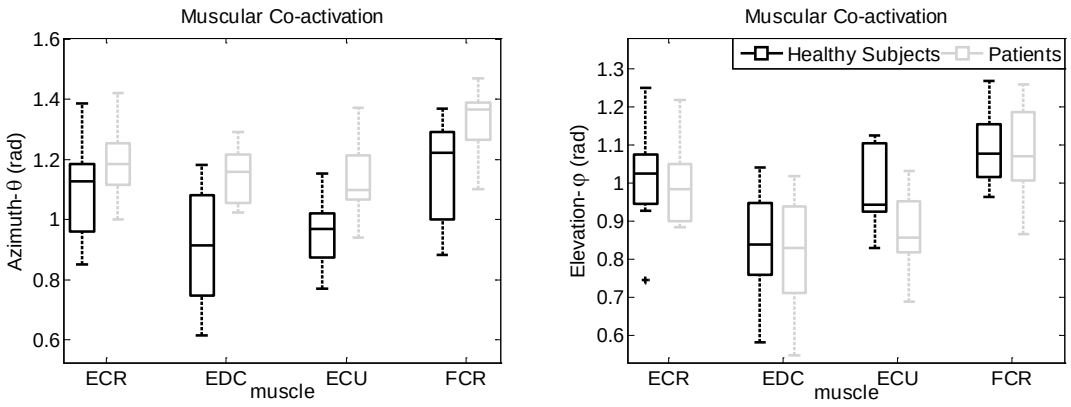

Figure 4.7. Box-plots for Azimuth-θ (left) and Elevation-φ (right) of the set of vectors u in the spherical coordinate system. Outliers are displayed with a cross (+).

A significant interaction for the factor "group" was found ($p<0.026$) as estimated form Pillai's Trace or Wilks' Lambda. Additionally, ANOVA revealed significant differences between the two groups in azimuth for θ_{ecu} and θ_{fcr} and in elevation for φ_{ecu} ($p<0.027$ in all cases).

Co-activation Index-*CI* (Eq. 4-7) was evaluated for each group independently. Results are presented in Figure 4.8. It was found that the co-activation index for FCR was lower

than for the other 3 muscles at 20%MVC for both, healthy subjects and patients ($p<0.02$ in all cases). However, the co-activation index for ECU was also higher than the index for ECR and EDC ($p<0.05$) for patients but not for healthy subjects (p.n.s). Moreover, the same situation replies at 50%MVC ($p<0.05$ comparing ECU with other muscles). No differences between muscles were found for healthy subjects. Finally, at 80%MVC no differences were found for the *CI* of the analyzed muscles except for EDC whose index was lower than ECR and ECU ($p<0.01$ for healthy subjects and $p<0.003$ for patients).

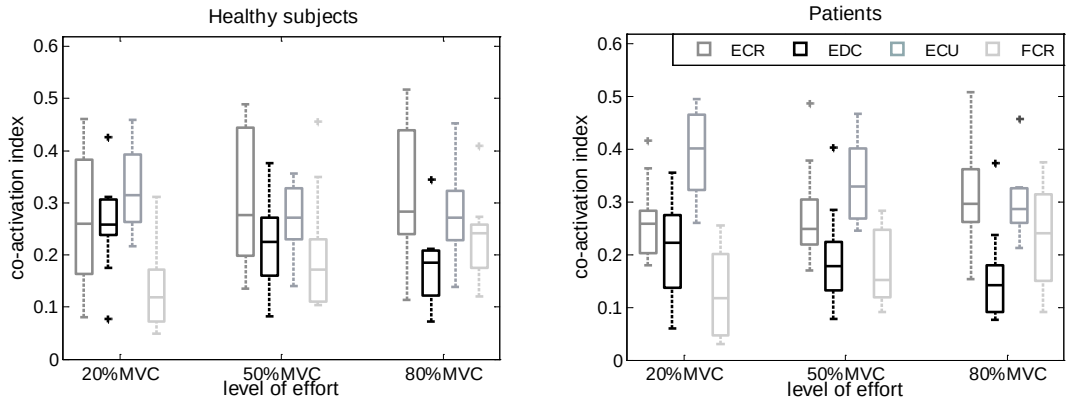

Figure 4.8. Box-plots for muscle co-activation in healthy subjects (left) and patients (right). The four muscles are presented in shadows of gray for the 3 levels of effort performed in the experiment.

Finally, flexor-extensor imbalances represented by the set of vectors **v** were also analyzed through MANOVA test. Box-plots for the dependent variables are presented in Figure 4.9. Angles corresponding to vector $\mathbf{v}_{\mathbf{edc\text{-}fcr}}$ were once more removed from the MANOVA since azimuth$\boldsymbol{\theta}_{\mathbf{edc\text{-}fcr}}$ did not satisfy the condition of equality of variance according to Levene's test.

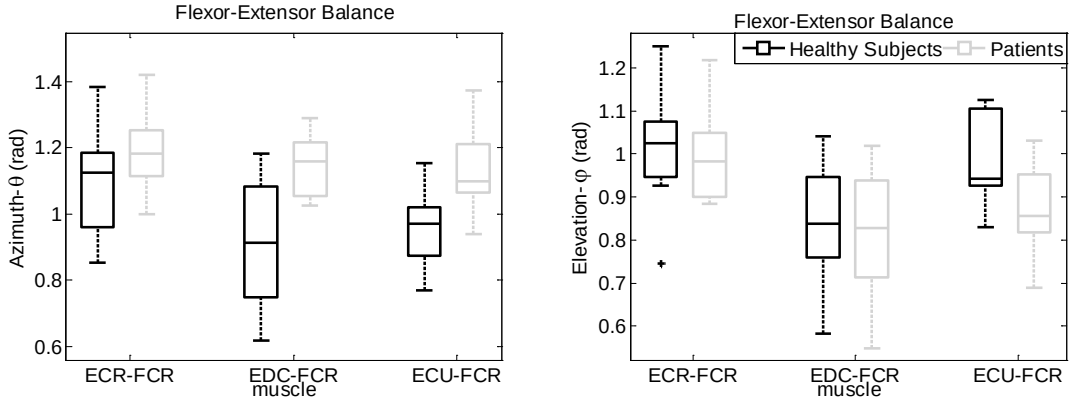

Figure 4.9. Box-plots for Azimuth-θ (left) and Elevation-φ (right) of the set of vectors **v** in the spherical coordinate system, representing muscular balance between flexors and extensors. Results are displayed for 10 subjects in each group. Outliers are represented with a cross (+)

Significant differences were found for the interaction with the factor group ($p<0.012$). Additionally, significant differences between healthy subjects and patients were found for $\theta_{ecu\text{-}fcr}$ and $\varphi_{ecu\text{-}fcr}$ ($p<0.008$ and $p<0.027$ respectively) from the ANOVA test of each angle θ or φ of the set of vectors **v**.

c. Power Spectrum

Mean and Median frequency (MNF and MDF) of the recorded signals in each muscle and effort level are presented in Figure 4.10.In healthy subjects, no differences were found between muscles except for ECU whose MNF was higher than that of the other three muscles regardless the level of effort ($p<0.01$ in all cases). As for patients, the values obtained for MNF for both ECU and EDC in all exercises were higher than for ECR and FCR ($p<0.005$ and $p<0.03$, respectively) but no differences were found when comparing ECU and EDC. Similar behavior was found for MDF. Finally, differences were found for power spectrum variables when comparing its values between groups (healthy subjects and patients) at 80%MVC in EDC ($p<0.026$).

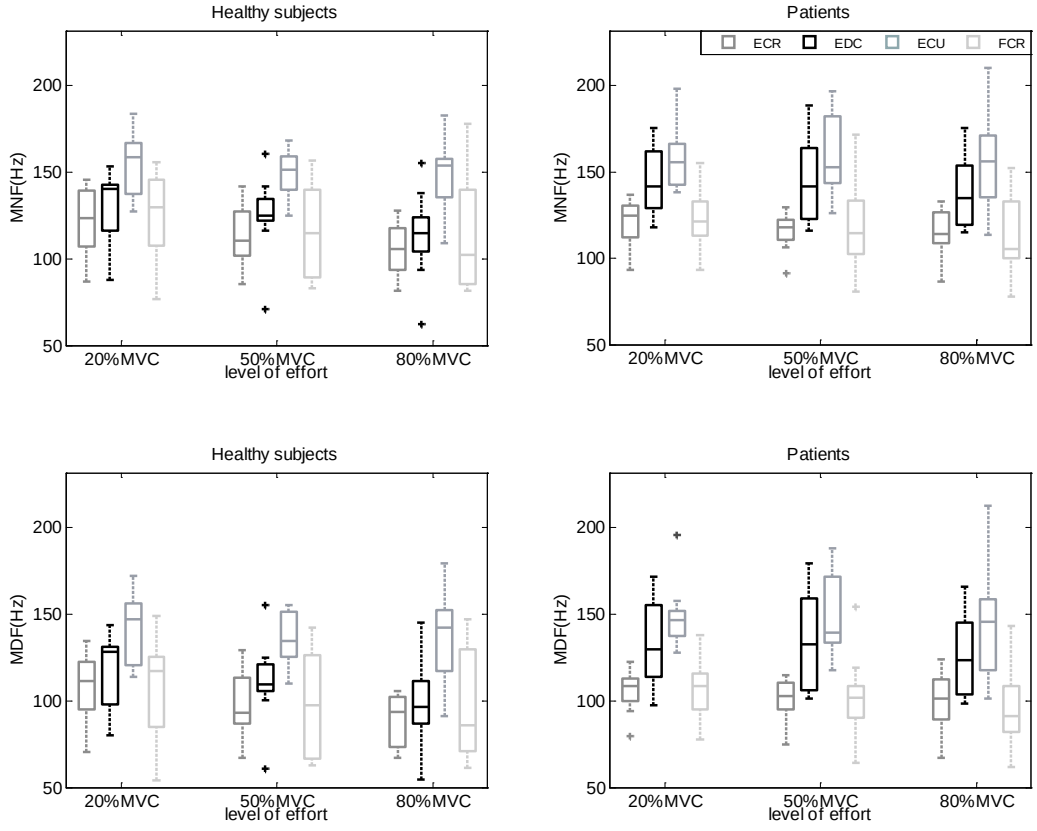

Figure 4.10.Box plots for Mean (MNF) and Median (MDF) frequency (top and bottom respectively) for healthy subjects (left) and patients (right).The four muscles are presented in shadows of gray for the 3 levels of effort performed in the experiment. Results are displayed for 10 subjects in each group. Outliers are represented with a cross (+).

d. Fatigue Indices

Myoelectric manifestations of muscle fatigue, as analyzed from the rate of change of sEMG parameters across the total duration of the exercise, was observed for all muscles in each of the groups ($p<0.027$ for all cases). Most significant values were obtained for CV ($p<0.004$ for both groups in the four analyzed muscles). On the other hand, no significant differences were obtained in the slopes of any of the parameters between different muscles regardless the group. Additionally, no significant differences were found in the absolute initial values (before normalizing) between healthy subjects and recovered patients, which is consistent with results presented in the previous section for the contraction at 50% MVC.

Moreover, differences were found when comparing the slope associated to CV in ECR, EDC and FCR between the two populations ($p<0.03$). No differences were found for ECU. Results are presented in Figure 4.11.

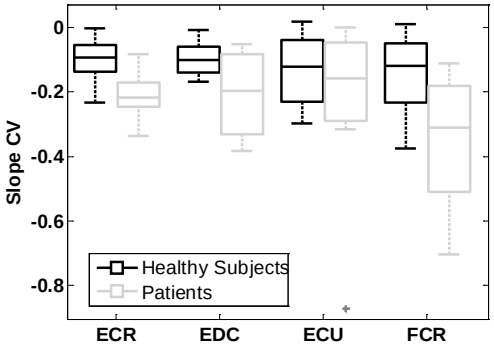

Figure 4.11. Box-plots for fatigue indices obtained from Conduction Velocity in ECR, EDC, ECU, and FCR for healthy subjects (in black) and patients (gray). In each box, the central mark represents the median. The 25th and 75th percentiles as well as most extreme values (whiskers) are represented. Outliers are represented with a cross. Results were obtained from 10 subjects in each population.

A repeated measures ANOVA test conducted on each muscle independently revealed a significant interaction for the factor group for ECR, EDC and FCR ($p<0.03$ in all cases), after applying the Greenhouse-Geisser correction for violations of the sphericity of the data. Profile plots for each muscle are presented in Figure 4.12.

Finally, when comparing normalized CV through Mann-Whitney's U test between groups every 10% from 0% to 100%of the total endurance time (ET)it was found that differences started around 30% ET for ECR ($p<0.01$)and after 50%ET for EDC and ECU ($p<0.04$ and $p<0.03$ respectively). Additionally, after calculating the cumulative normalized CV from 100% to 0% ET every 10%, it was found that this value was always lower for

recovered patients than for healthy subjects across the entire endurance time in ECR and EDC ($p<0.001$ and $p<0.04$ respectively) and starting from 60% ET for FCR ($p<0.05$).

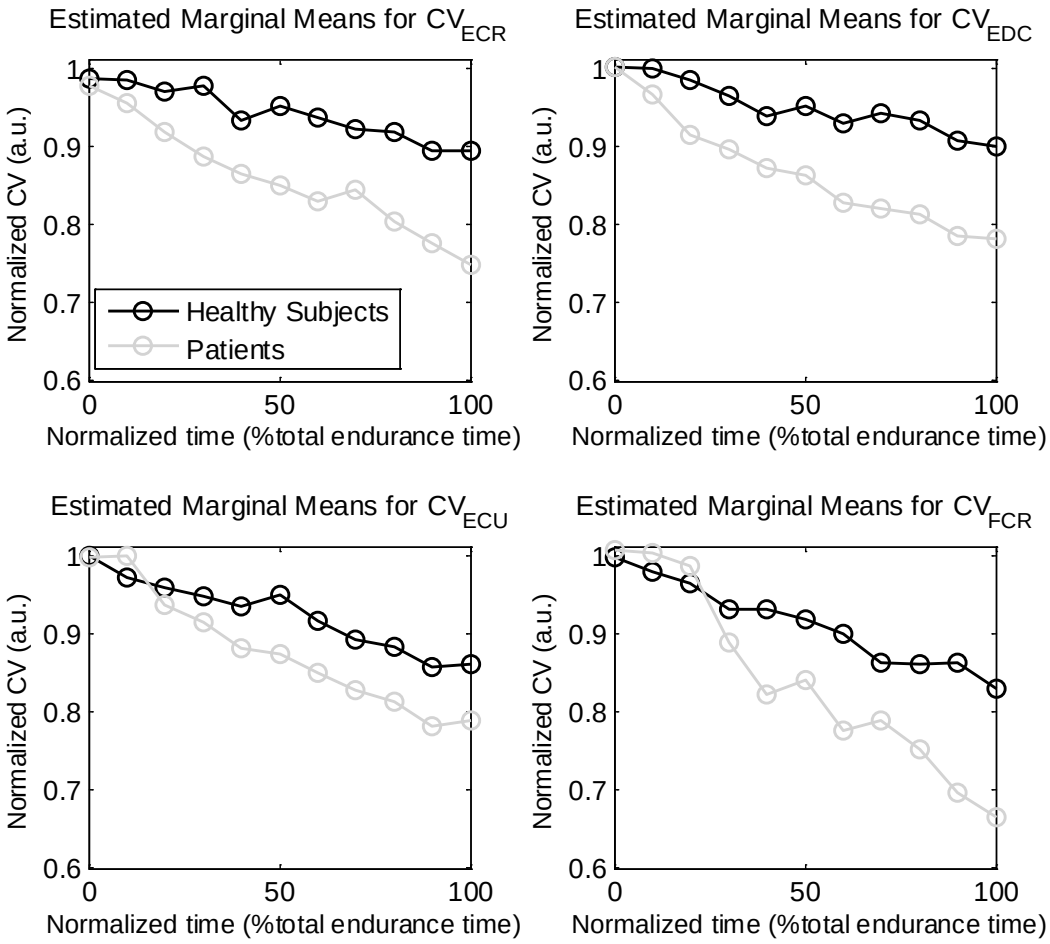

Figure 4.12. Profile plots for the estimated marginal means for ECR (top-left), EDC (tor-right), ECU (bottom-left) and FCR (bottom-right). Curves display the normalized CV every 10% of the total endurance time for healthy subjects (black) and former patients (gray) and 10 subjects in each group.

4.3.3 Finger Pressing

The following results were obtained in a group of five healthy subjects. For a detailed description of subjects in the database, please refer to section 3.5 in Chapter 3. EMG signals were recorded and analysed in four forearm muscles: Extensor Carpi Radialis- ECR, Extensor Digitorum Communis- EDC, Extensor Carpi Ulnaris- ECU and Flexor Carpi Radialis- FCR. The experimental protocol considered isometric contractions associated to pressure on a bar with all fingers simultaneously or with each finger independently in a way similar to piano playing. For this task only, statistic differences were analysed with a t-test.

a. sEMG signals corresponding to the activation of different fingers

The activation of each muscle was different when pressing with different fingers. This pattern was similar in all subjects and was analyzed through the co-activation indices *CI* and

CI^f (Eq. 4-7 and Eq. 4-8 respectively). An example is presented in Figure 4.13. It is possible to observe that the amplitude of the signals depends on which finger is active, especially for ECU. On the other hand, no variations in the amplitude of the ECR muscle were observed. This was consistent for all subjects in all tasks: pressing with all of the fingers at the same time, or pressing with each finger independently. Thus the ECR muscle was excluded in subsequent analysis of the sEMG signals

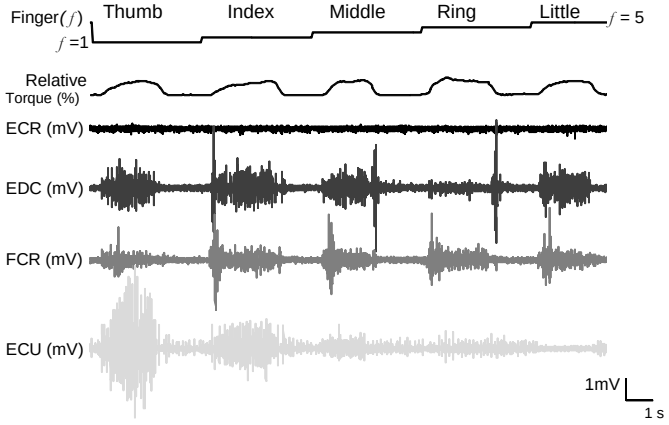

Figure 4.13. sEMG signals recorded on ECR, EDC, FCR and ECU when pushing independently with each of the fingers at 50%MVC.

b. Conduction Velocity

CVs estimated in ECU, FCR and EDC when pressing with all fingers and with each finger independently are presented in Figure 4.14 and Figure 4.15 respectively. The last figure present results for the case of wrist rotation, given that similar results were obtained for finger pressing without rotation. In all cases (except for the ECU when pressing with the little finger where its level of activation is very low), the CV was within the physiological range, confirming the propagation of MUAPs and the correct alignment of the electrodes. No significant differences were found between muscles or resulting the activation of different fingers.

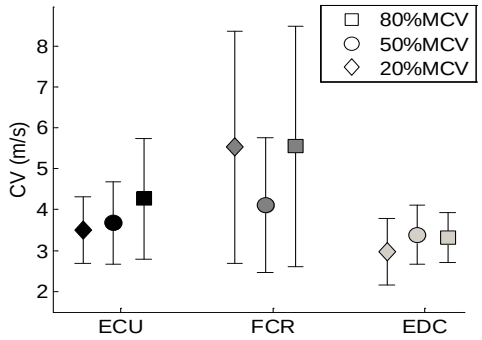

Figure 4.14. CV estimated in the active muscles when pressing simultaneously with all fingers at different levels of contraction (in different symbols). Results are presented in mean and standard deviation for 5 subjects.

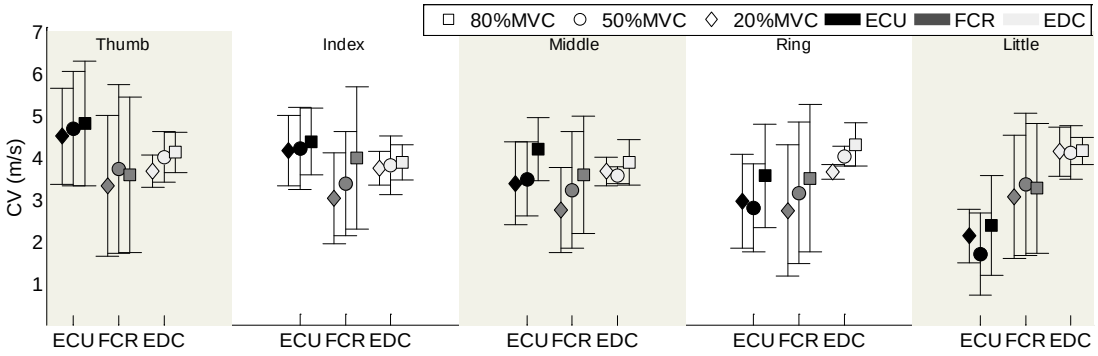

Figure 4.15 CV estimated in the active muscles when pressing independently with each finger and involving wrist rotation. Three levels of contraction are shown in different symbols. Results are reported in mean and standard deviation for 5 subjects.

c. Co- activation index CI

The *CI* in the analyzed muscles was similar for different levels of contraction (20%, 50% and 80% MVC) as can be observed in Figure 4.16 and Figure 4.17. However significant differences were found for different muscles when pressing with all fingers: CI_{EDC} was lower than CI_{ECU} and CI_{FCR}, especially at 80 %MVC ($p<0.02$, Figure 4.16), although no differences between these last two were found.

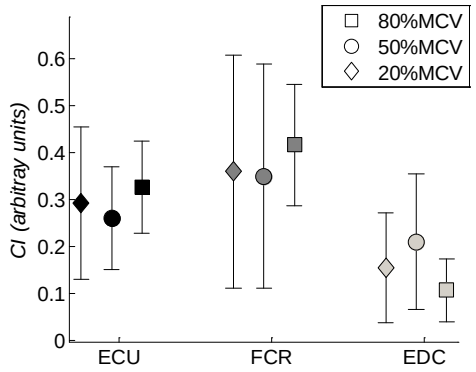

Figure 4.16. *CI* for each muscle when pressing simultaneously with all fingers. Results are presented in mean and standard deviation for all subjects in the database

Similar results were obtained from tasks comprising the isolated activation of fingers as can be appreciated in Figure 4.17. In order to simplify the analysis, findings will be presented and discussed in light of results obtained from the task of combined activation of fingers with wrist rotation which represents the most general case. For example, no significant differences were found between CI_{ECU} for thumb when pressing in its natural position or when rotating the wrist to reach the common point. Results are summarized as following: CI_{ECU} presented the highest value when pressing with the thumb exhibiting decreasing values as the activation moved away from thumb to the little finger ($p<0.007$, Figure 4.17 top) where the ECU presented the lowest contribution to the contraction. The action of the ECU was compensated by the activation of the FCR and EDC as can be

inferred from CI_{FCR} ($p<0.02$) and especially from CI_{EDC} in such digits closest to the little finger ($p<0.001$).

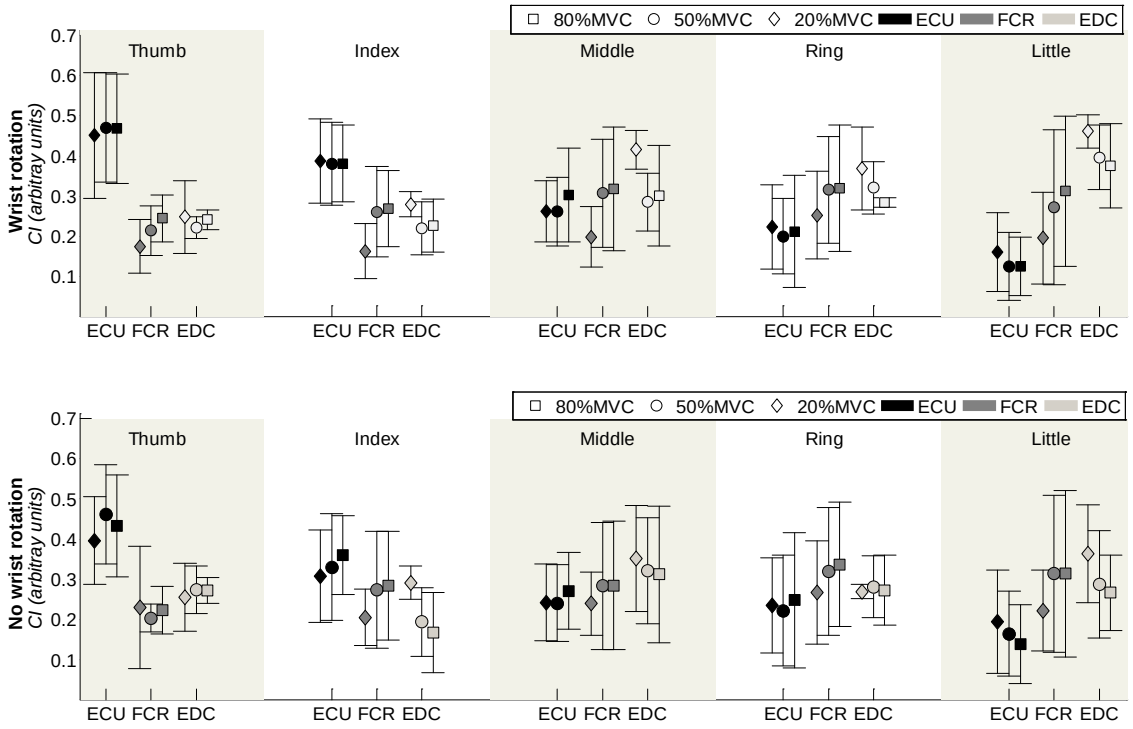

Figure 4.17. *CI* for each muscle and finger while pressing independently with each finger with wrist rotation (top) and when maintaining the wrist at 0º of ulnar deviation (bottom). Results are presented in mean and standard deviation for all subjects in the database

d. Co- activation index CI^f

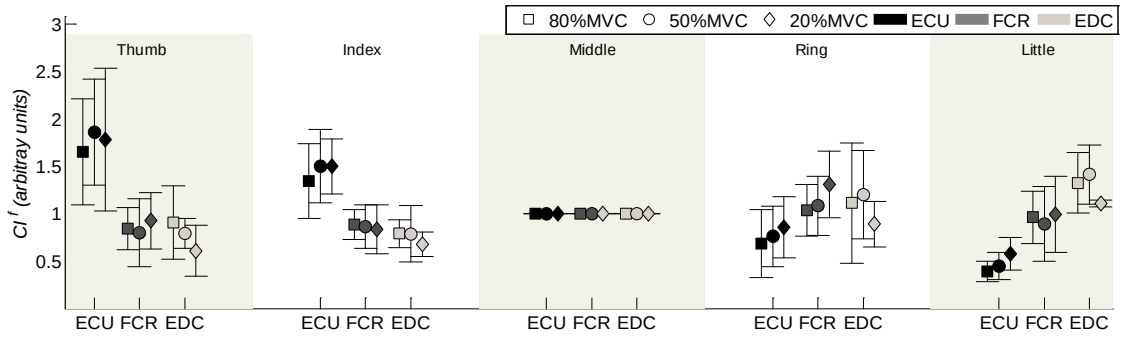

Figure 4.18. CI^f index for ECR, FCR and ECU for the isolated activation of the fingers. Results are presented for the task involving wrist rotation, in mean and standard deviation for all the subjects in the database.

The CI^f index permitted to analyze the relative contribution of each muscle when pressing with a given finger (Figure 4.18). Similarly to *CI*, CI^f_{ECU} was higher for digits close to the thumb, where the highest values with respect to the other two muscles were observed ($p<0.0001$ when compared to CI^{thumb}_{EDC} or CI^{thumb}_{FCR}), while CI^{little}_{ECU} presented the lowest value when pressing with the little- finger ($p<0.002$ compared to both EDC and FCR). However, CI^f values for EDC and FCR were similar showing no significant

differences between them two or between one or the other as compared across different digits, with the exception of a small difference at 20% MVC when comparing between CI^{ring}_{EDC} and $CI^{ring}_{FCR,}$ and CI^{f}_{EDC} and CI^{f}_{FCR} (f = [thumb or index], $p<0.02$ in all cases).

e. Fatigue Indices

Myoelectric fatigue was assessed trough the regression slope of the variables RMS, MDF and CV during the endurance exercise. Examples of fatigue plots for FCR during simultaneous and independent finger pressing are presented in Figure 4.19. Negative slopes were obtained for all of the muscles and the different fingers when considering the task of isolated activation of fingers. However, no changes in the slopes were observed when pressing with all of the fingers.

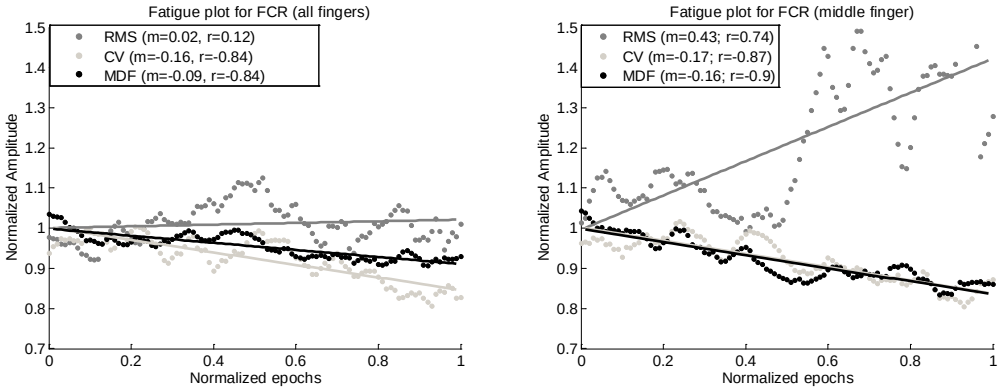

Figure 4.19. Fatigue plot for FCR during the simultaneous (right) and independent (left) finger pressing exercise. The different variables were normalized with respect to the initial value and the points correspond to a normalized number of epochs. Results are presented in mean for all subjects in the database.

4.4 Discussion

4.4.1 Assessment of Lateral Epicondylalgia

a. Functional integrity of the upper-arm

In this work, no differences were found in the functional integrity index MGS (Table 3-2) between controls and patients with Lateral Epicondylalgia. This result differ from those reported by Alizadehkhaiyat et al. where LE patients (Alizadehkhaiyat et al. 2007) and even recovered patients, females is this case (Alizadehkhaiyat et al. 2009), exhibited significant lower grip forces at MVC. In this two works, MVC was measured as the mean value for 3s-long contractions, while in our work MVC was measured as the peak force obtained during explosive contractions (<1s).

b. Submaximal contractions

Regarding sEMG parameters during submaximal contractions, no differences in CV estimates between muscles or even between groups were observed. However, MNF and MDF estimates for ECU were higher than for the other forearm muscles (ECR, EDC and FCR) in the group of healthy subjects both, during hand grip and wrist extension. Additionally, MNF and MDF estimates were higher for ECU and EDC than those obtained for ECR and FCR in the group of recovered patients during hand grip. Although no differences were found for CV estimates from different muscles, high MNF estimates have been associated to predominance of type-II fibers in in-vitro studies of rat muscles, and confirmed with histochemical analysis (Kupa et al. 1995). Similar results were found for patients with choric neck pain (Falla et al. 2003) and once more, this difference was attributed to a higher percentage of type II fibers with respect to type I fibers (or a greater role of the firsts in any case). This can be explained in terms of muscular adaptation to overload of upper extremity as required by work activities in patients. Finally, the fact that these observations cannot be corroborated from CV could be because estimates of this parameter can be biased by several methodological factors such as the alignment of recording electrodes with respect to the direction of propagation of MUAPs in the muscular fibers (Farina, Cescon & Merletti 2002).

c. Muscle Co-activation

Selective contractions (Figure 4.4) like those described in this work can enhance significantly the action of isolated muscles in the case of patients but not in the case of control subjects. This can be understood in terms of a higher level of specialization of forearm muscles due to continuous training of the upper extremity during work activities. Regarding muscular co-activation, different behavior in patients can be inferred from *CIs* associated to ECU at all effort levels during wrist extension and from *CIs* for ECU at 20% and 50%MVC during hand grip. However, the Mann-Whitney's U test showed no significant differences between groups. On the other side, such differences were confirmed from the orientation angles θ and φ analyzed during hand grip, not only for ECU but also for FCR. These results are consistent with those obtained for the set of vectors **v,** defined to identify flexor-extensor imbalances in the same space.

d. Myoelectric manifestations of fatigue

Myoelectric manifestations of fatigue were observed in both groups from slopes of CV, MNF, MDF and RMS, obtained by linear regression of the normalized values in each

epoch across the total endurance time. These findings were consistent in tasks oriented to the analysis of LE (i.e. wrist extension and hand grip). No differences were found between muscles regardless the analyzed group (control or recovered patients). Likewise, no differences were found when comparing the initial absolute values (not normalized) of any of the parameters between the two groups. This is consistent with results presented in section 1.4.1.a and 1.4.2.a for submaximal contractions at 50% MVC. However, when comparing slopes obtained for CV, higher indices (i.e. more negative) were found for ECR, EDC and FCR indicating greater fatigability of these muscles in recovered patients, despite the absence of symptoms. Note that the slope m was estimated from values normalized with respect to the initial value. It must be said that although the slope of CV in ECU showed no significant differences between healthy subjects and patients, this may be related to a higher percentage of type II fibers in ECU as mentioned in section 4.4.1.b, which would make this muscle easily fatigable both in healthy subjects and patients.

Finally, repeated measures analysis for ECR, EDC and FCR during hand grip confirmed that recovered patients are more prone to myoelectric fatigue than healthy subjects. This kind of analysis is more reliable since liner regression assumes that the scatter plot of parameters CV, RMS, MNF or MDF is linear but it may be curvilinear as well (Merletti, Parker 2005).

4.4.2 Muscular pattern related to Repetitive Strain Injury in musicians

a. Submaximal contractions

Although no significant differences were found for CV estimates between different muscles, the absolute value of the parameter varied when pressing with different fingers. Such differences could be related to variations in the load-sharing of the muscles when pressing with a given finger, as was later confirmed from *CI* and CI^f indices. It could also be related to crosstalk originated in other forearm muscles. Nevertheless, it was possible to obtain a set of three consecutive signals (a triplet) where propagation of MUAP was observed and where it was possible to extract sEMG variables.

b. Co- activation Indices *CI* and CI^f

The ECR was not active during the isometric contractions associated to finger pressing either with all or with every digit, as analyzed in this study. This result can be related to the angle of the wrist defined for the experimental protocol and differs from other studies were physiological changes in this muscle were associated with repetitive contractions involving finger pressing (Moreno-Torres et al. 2010). Nevertheless, the former study

found physiological changes only on patients with repetitive strain injuries that were also experienced instrumentalists. Thus, a different muscular pattern in ECR in patients should not be disregarded and may be a matter of analysis in a future study.

On the other hand, the contribution of ECU depended on the active finger, presenting higher *CI* and CI^f indices when pressing with the digit located at the opposite side, that is, the thumb. Such activation is not only related to the rotation of the wrist as can be inferred from Figure 4.17 and it was consistent in both tasks involving independent finger pressing. ECU also presented high *CI* indices when pressing with all of the fingers were its contribution was comparable to that of FCR. EDC presented a similar behavior but in the opposite direction, from little finger to thumb. On the contrary, FCR presented similar co-activation indices for different digits and even for different levels of contraction.

c. Myoelectric manifestations of fatigue

From fatigue indices it can be deduced that the set of muscles is highly prone to myoelectric fatigue in contractions similar to those proposed in the present study. Future studies should be focused in the assessment of similar indices in patients in order to analyze possible patterns leading to rapid manifestations of fatigue.

4.5 Conclusions

4.5.1 Lateral Epicondylalgia

Two biomechanical models have been proposed for lateral epicondylalgia: one emphasizing the role of eccentric exertions and the other emphasizing the contact pressure of the radial head (Moore 2002). The present study shows new findings which could complete those models since several differences between controls and patients in muscle activation pattern have been identified.

Differences in the co-activation pattern of wrist extensor muscles (namely, *CI* or orientation angles in the contraction level space) may indicate a muscular imbalance underlying the lateral epicondyle overuse condition. Biomechanical factors such as muscle imbalances, shortenings and weaknesses have been associated to cumulative trauma injuries in the past (Benkibler, Chandler & Pace 1992).

Biomechanical deficits may both arise after an injury (in which case should be treated in the latter phases of rehabilitation) or precede the actual injury. In any case, the identification of biomechanical deficits is crucial in order to design rehabilitation/injury prevention programs. By pointing the target muscles to be specifically trained, findings

explained above might provide new insights for the design of rehabilitation and/or prevention programs for lateral epicondylalgia.

Regarding fatigue parameters, we found significantly higher CV fatigue indices for three of the analyzed muscles in recovered patients. Surprisingly, higher fatigue indices were found not only for extensor muscles originated in the extensors common origin (i.e. the lateral epicondyle) but also for the flexor carpi radialis. Frequently, only extensor muscles are considered for the diagnosis and treatment of lateral epicondylalgia. Fatigue findings could also be related to muscular imbalances depicted from this study. It is, to our best knowledge, the first time that such a relationship has been found.

Differences in fatigue indices might be related to a higher composition of type II fibers in muscles of recovered patients, though this should be confirmed by biopsy or histochemical analysis, which is beyond the reach of the present study.

In summary, findings in the present study indicate a different muscle pattern of contraction during wrist extension or hand grip in former patients when compared to healthy volunteers. The latter also showed significantly lower fatigability in both wrist extensor and flexor muscles. This is a conspicuous finding indicating that lateral epicondylalgia might be viewed not as a mere wrist dorsal flexor muscle dysfunction problem but as a whole forearm one (including extrinsic flexors). Consequently, a strengthening program designed to increase the percentage of fatigue resistant fibers in both muscular groups may be desirable in LE patients or in populations at risk. Regarding resistance training, several studies have reported increases in the cross sectional area of type I fibers following such kind of programs (for example in (Kosek et al. 2006)). What's more, Andersen et al. in (Andersen, Aagaard 2000) suggested that resistive training decreases the proportion of type IIb fibers (fast and easily fatigable) while reciprocally increasing the percentage of type IIa fibers (also fast but resistant to fatigue).

Further research will be done in order to check muscle performance during dynamic contractions (both concentric and eccentric).

4.5.2 Repetitive Strain Injury in musicians (protocol evaluation)

The protocol designed for the assessment of repetitive strain injury was tested and validated. Isometric contractions similar to those exerted during dynamic contractions in tasks similar to piano playing were evaluated with multichannel sEMG. Differentiated muscular patterns associated to extrinsic muscles and to the activation of different fingers were achieved. What is more, no differences, concerning either muscles or fingers, between the two tasks aimed for independent finger pressing (i.e. with or without rotation of the

wrist) were found. Thus, it is possible to infer that both, the protocol and the proposed indices are highly repetitive. Such results are encouraging and motivate the use of techniques based on multichannel sEMG for the study of repetitive strain injuries in experienced musicians. This kind of analysis will be useful in establishing possible mechanisms underlying this syndrome as well as its possible prevention and treatment.

4.6 References

Alizadehkhaiyat, O., Fisher, A.C., Kemp, G.J. & Frostick, S.P. 2007, "Strength and fatigability of selected muscles in upper limb: Assessing muscle imbalance relevant to tennis elbow", *Journal of Electromyography and Kinesiology,* vol. 17, no. 4, pp. 428-436.

Alizadehkhaiyat, O., Fisher, A.C., Kemp, G.J., Vishwanathan, K. & Frostick, S.P. 2009, "Assessment of functional recovery in tennis elbow", *Journal of Electromyography and Kinesiology,* vol. 19, no. 4, pp. 631-638.

Alizadehkhaiyat, O., Fisher, A.C., Kemp, G.J., Vishwanathan, K. & Frostick, S.P. 2007, "Upper limb muscle imbalance in tennis elbow: A functional and electromyographic assessment", *Journal of Orthopaedic Research,* vol. 25, no. 12, pp. 1651-1657.

Andersen, J.L. & Aagaard, P. 2000, "Myosin heavy chain IIX overshoot in human skeletal muscle", *Muscle & nerve,* vol. 23, no. 7, pp. 1095-1104.

Benkibler, W., Chandler, T.J. & Pace, B.K. 1992, "Principles of Rehabilitation After Chronic Tendon Injuries", *Clinics in sports medicine,* vol. 11, no. 3, pp. 661-671.

Buchanan, T.S., Lloyd, D.G., Manal, K. & Besier, T.F. 2004, "Neuromusculoskeletal modeling: estimation of muscle forces and joint moments and movements from measurements of neural command.", *Journal of Applied Biomechanics,* vol. 20, no. 4, pp. 367-95.

Danna-Dos Santos, A., Poston, B., Jesunathadas, M., Bobich, L.R., Hamm, T.M. & Santello, M. 2010, "Influence of Fatigue on Hand Muscle Coordination and EMG-EMG Coherence During Three-Digit Grasping", *Journal of Neurophysiology,* vol. 104, no. 6, pp. 3576-3587.

Day, S.J. & Hulliger, M. 2001, "Experimental Simulation of Cat Electromyogram: Evidence for Algebraic Summation of Motor-Unit Action-Potential Trains", *Journal of neurophysiology,* vol. 86, no. 5, pp. 2144-2158.

Falla, D., Rainoldi, A., Merletti, R. & Jull, G. 2003, "Myoelectric manifestations of sternocleidomastoid and anterior scalene muscle fatigue in chronic neck pain patients", *Clinical Neurophysiology,* vol. 114, no. 3, pp. 488-495.

Farina, D. & Merletti, R. 2000, "Comparison of algorithms for estimation of EMG variables during voluntary isometric contractions", *Journal of Electromyography and Kinesiology,* vol. 10, no. 5, pp. 337-349.

Farina, D., Cescon, C. & Merletti, R. 2002, "Influence of anatomical, physical, and detection-system parameters on surface EMG", *Biological cybernetics,* vol. 86, no. 6, pp. 445-456.

Forthomme, B., Croisier, J.L., Foidart-Dessalle, M. & Crielaard, J.M. 2002, "Isokinetic assessment of the forearm and wrist muscles", *Isokinetics and Exercise Science,* vol. 10, no. 3, pp. 121-128.

Gatti, C.J., Doro, L.C., Langenderfer, J.E., Mell, A.G., Maratt, J.D., Carpenter, J.E. & Hughes, R.E. 2008, "Evaluation of three methods for determining EMG-muscle force parameter estimates for the shoulder muscles", *Clinical Biomechanics,* vol. 23, no. 2, pp. 166-174.

Hamill, J. & Knutzen, K.M. 2006, "Functional Anatomy of the Upper Extremity" in *Biomechanical basis of human movement*, 2nd edn, Lippincott Williams & Wilkins, .

Herda, T.J., Walter, A.A., Costa, P.B., Ryan, E.D., Stout, J.R. & Cramer, J.T. 2011, "Differences in the log-transformed electromyographic-force relationships of the plantar flexors between high- and moderate-activated subjects", *Journal of Electromyography and Kinesiology,* vol. 21, no. 5, pp. 841-846.

Keenan, K.G., Farina, D., Maluf, K.S., Merletti, R. & Enoka, R.M. 2005, "Influence of amplitude cancellation on the simulated surface electromyogram", *Journal of applied physiology,* vol. 98, no. 1, pp. 120-131.

Kosek, D.J., Kim, J., Petrella, J.K., Cross, J.M. & Bamman, M.M. 2006, "Efficacy of 3 days/wk resistance training on myofiber hypertrophy and myogenic mechanisms in young vs. older adults", *Journal of applied physiology,* vol. 101, no. 2, pp. 531-544.

Kupa, E.J., Roy, S.H., Kandarian, S.C. & De Luca, C.J. 1995, "Effects of Muscle-Fiber Type and Size on Emg Median Frequency and Conduction-Velocity", *Journal of applied physiology,* vol. 79, no. 1, pp. 23-32.

McGill, K.C. & Dorfman, L.J. 1984, "High-Resolution Alignment of Sampled Waveforms", *IEEE Transactions on Biomedical Engineering ,* vol. BME-31, no. 6, pp. 462-468.

Merletti, R. & Parker, P. 2005, *Electromyography: Physiology, Engineering, and Non-Invasive Applications*, IEEE Press in Biomedical Engineering.

Mesin, L., Smith, S., Hugo, S., Viljoen, S. & Hanekom, T. 2009, "Effect of spatial filtering on crosstalk reduction in surface EMG recordings", *Medical engineering & physics,* vol. 31, no. 3, pp. 374-383.

Moore, J.S. 2002, "Biomechanical models for the pathogenesis of specific distal upper extremity disorders", *American Journal of Industrial Medicine,* vol. 41, no. 5, pp. 353-369.

Moreno-Torres, A., Rosset-Llobet, J., Pujol, J., Fabregas, S. & Gonzalez-de-Suso, J. 2010, "Work-Related Pain in Extrinsic Finger Extensor Musculature of Instrumentalists Is Associated with Intracellular pH Compartmentation during Exercise", *Plos One,* vol. 5, no. 2, pp. e9091.

Sun I. Kim & Kang M. Lee 1990, "Mean Frequency Estimation Of Myoelectric Signal Using 2nd Order Maximum Entropy Method", *Proc. of the 12th Int. Conf. of the IEEE Engineering in Medicine and Biology Society,* pp. 2208.

Valero-Cuevas, F.J. 2000, "Predictive Modulation of Muscle Coordination Pattern Magnitude Scales Fingertip Force Magnitude Over the Voluntary Range", *Journal of Neurophysiology,* vol. 83, no. 3, pp. 1469-1479.

5

High- Density EMG Experimental Protocol and Setup

5.1 Introduction

Neuromuscular activity recoded by sEMG can be used to track CNS strategies for the control of movements, based on the correlation between the amplitude of the sEMG signal and the force exerted on a given joint. This relationship has been used in the past to control robotic devices for different purposes like biofeedback devices for rehabilitation (Dipietro et al. 2005), exoskeletons (Fleischer et al. 2006), medical assistance devices (Pierrot et al. 1999), powered prosthesis (Parker et al. 2006) or wheelchairs (Galindo, Gonzalez & Fernandez-Madrigal 2006). Central to these goals is the extraction of information from myoelectric signal which is commonly detected with electrode pairs.

As mentioned before, the main disadvantage of bipolar signals is that its amplitude depends on the distance between the active motor units and the recording electrodes (Drost et al. 2004). Due to the low spatial resolution of the bipolar signal, the standard surface EMG reflects the activity of a number of motor units (MU) within a delimited area of the muscle. However, amplitude variations are expected in both, the parallel and the perpendicular directions of propagation of the MU action potentials (MUAP): in the former, the amplitude of the signal varies with the proximity to innervation zones and tendons, while in the latter the amplitude is attenuated because of the propagation properties of the conductor volume (Kleine et al. 2007). As pointed out by Zwarts et al. in (Zwarts, Stegeman 2003), single channel approaches do not reflect the physical propagation of the potentials and therefore only the time-varying properties of the signals are usually analyzed, disregarding important spatial aspects of the propagation like extent and length of the muscle fibers, which are essential for the force-generating capacity of the muscle, and, if not well addressed can lead to incorrect conclusions. In recent years, on the other hand, the development and application of electrode arrays in one or two dimensions have allowed the study of the sEMG signal in the temporal and the spatial domain, opening new

possibilities to the study of the neuromuscular system (Zwarts, Stegeman 2003, Holobar et al. 2010, Merletti et al. 2008) and to the field of myoelectric control (Farina et al. 2010).

What is more, recent studies have demonstrated that the muscles do not activate homogeneously, that is, distinct regions of the muscle are activated differentially depending on the position of the joint (Vieira et al. 2010) and the duration (Tucker et al. 2009) and strength of the contraction (Holtermann et al. 2005). Such activation may be related to bundles of fiber types organized in different regions within the muscle, each of them following different recruitment strategies according to Henneman's size principle (Holtermann et al. 2005).

Therefore, EMG amplitude information provided by a single bipolar channel is highly dependent on the location of the recording electrodes, even when they are well located away from innervation zones and tendons and it does not offer the possibility of tracking inhomogeneities in the activation of the muscles.

The recording of sEMG signals with 2D arrays in a wide area of the muscles and the processing of the signal in the space dimension (Zwarts, Stegeman 2003, Staudenmann et al. 2009) can overcome some of the drawbacks of single-channel approaches, providing information regarding the proper selection of the most significant channels and a quantification of the temporal and spatial properties of the electrical muscle activity (Merletti et al. 2010a, Merletti et al. 2010b). Therefore, the system must cover a large surface of the muscles of interest, adapt to the individual, detect and remove interference signals and artifacts, check signal quality, and finally, extract useful information contained in the signal related to the co-activation patterns of the muscles.

In this chapter, the experimental protocol designed for the assessment of possible movements at the elbow joint by HD-EMG is described. The design of 2D- electrode arrays for this purpose and the instrumentation set-up used during recording sessions is also discussed.

5.2 Experimental protocol

The experimental protocol considered isometric contractions of upper-am and forearm muscles at different levels of effort. Isometric contractions were preferred over

dynamic, in order to be able to transfer findings in this study to the general population, although in this case, only healthy subjects were involved.

5.2.1 Tasks and Subject positioning

The experimental protocol considered four possible tasks related to the degrees of freedom at the elbow joint: flexion and extension of the elbow and supination and pronation of the forearm (Figure 5.1). Isometric contractions at different levels of effort were carried out by means of a mechanical brace modified to measure rotational force.

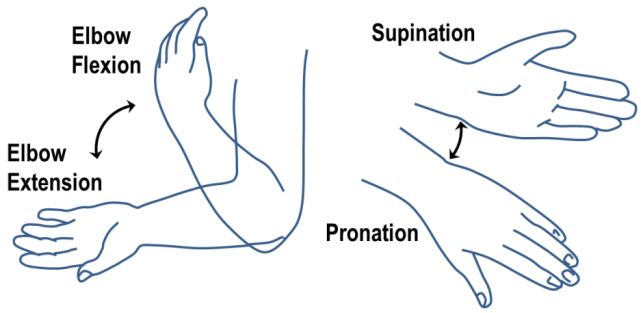

Figure 5.1. Possible movements at the elbow joint.

During the experiment, subjects sat in front of the mechanical brace with the back straight, the elbow joint flexed at γ=45º measured from the transversal plane, shoulder abducted at α=0º from the coronal plane (parallel to the sagittal plane) and at β=90º parallel to the transversal plane, and forearm rotated δ=90º, midway between supination and pronation (Figure 5.2). This position was selected to minimize the activation of upper-arm muscles on the shoulder joint and to study possible synergies between forearm and upper arm muscles (Hamill, Knutzen 2006).

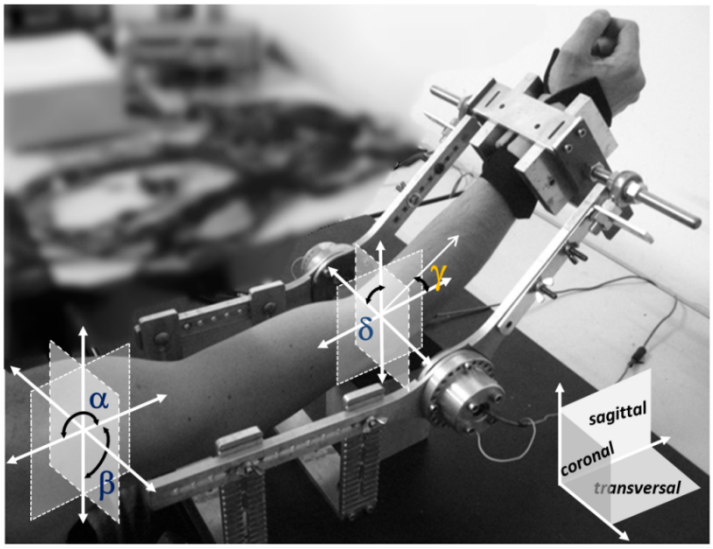

Figure 5.2. Joint angles in the experimental protocol. Shoulder, α=0º (parallel to the sagittal plane), β=90° parallel to the transversal plane. Elbow, γ = 45° from the transverse plane and δ= 90° (midway between pronation and supination)

5.2.2 Muscles

The co-activation pattern corresponding to tasks described in the previous section was assessed through electromyographic signals registered on five superficial muscles: biceps brachii, triceps brachii, brachioradialis, anconeus and pronator teres. Their function is summarized in Table 5-1 (Hamill, Knutzen 2006, Kendall F. P. et al. 1993).

Figure 5.4 to Figure 5.6 show the anatomical location of muscles in the upper-arm. Muscles analyzed in this work are highlighted in big letters and are described as follows (Hamill, Knutzen 2006):

a. Biceps Brachii

The biceps brachii is composed by two units: the short head and the long head. It originates on the supraglenoid tubercle and in the corocoid process and insert into the radial tuberosity in the forearm. Biceps brachii acts at the shoulder and elbow joints, either abducting the upper limb or flexing the forearm. However, because its tendon wraps around the radius, the biceps brachii is most effective as flexor when the forearm is in full supination; otherwise, its tendon is twisted under the radius. It is also a powerful supinator of the forearm when the elbow is flexed, especially at 90º of flexion. Slow, and unresisted supination actions are produced only by the Supinator muscle in the deep substrate of the forearm, but this muscle in not accessible by sEMG.

b. Triceps Brachii

The triceps brachii is composed by three portions: the lateral, the medial and the long heads. Of these three, only the long head crosses the shoulder joint, making it dependent partially on shoulder position for its effectiveness. The strongest head is the lateral, especially in movements against resistance.

It is originated at the infraglenoid tubercle on scapula, the mid posterior shaft of humerus and the lower shaft of humerus and inserts into the olecranon process. The triceps brachii is the strongest muscle within elbow extensors. Its output is not influenced by supination or pronation of the forearm.

c. Anconeus

The anconeus is a small muscle located at the proximal forearm. It originates at the lateral epicondyle of the humerus. Its main function is the extension of the elbow and acts like an auxiliary muscle during pronation and supination depending on the rotation angle of the ulna.

d. Brachioradialis

The brachioradialis originate at the supracondylar ridge of humerus in the upper-arm and inserts into the styloid process of radius. Its main function is elbow flexion. It has the smallest cross-sectional area of the elbow flexors but has the best mechanical advantage because of a longer moment arm. The brachioradialis flexes the elbow most effectively when the forearm is in halfway between pronation and supination. It also assists during pronation and supination

e. Pronator Teres

The pronator teres originates at the medial epicondyle along with the forearm flexors, and inserts into the midlateral surface of radius. Its main function is the pronation of the forearm but it also assists during elbow flexion. Forearm pronation is accomplished by two muscles: pronator quadratus in the deep substrate and pronator teres. Although the pronator quadratus is more active regardless of forearm position, pronator teres becomes more active when the pronation action is rapid or against a high load.

Possible tasks at the elbow joint can be evaluated by the analysis of the co-activation pattern of this set of muscles. In all cases at least one of the muscles in the set has a predominant action related to one of the proposed tasks (flexion extension, supination or pronation). There is also at least one muscle that assists the contraction of the main muscle. Supination, however, is an exception because it is mainly achieved by the activation of the *supinator* muscle which is not superficial. However, the biceps brachii acts as a supinator when the elbow is flexed (Hamill, Knutzen 2006, Kendall et al. 1993).

TABLE 5-1. ACTIONS OF THE MUSCLES INCLUDED IN THE EXPERIMENTAL PROTOCOL DURING THE ANALYZED TASKS: FLEXION AND EXTENSION OF THE ELBOW AND SUPINATION AND PRONATION OF THE FOREARM.

Muscle	Flexion	Extension	Supination	Pronation
Biceps Brachii	Main function		if the elbow is flexed	
Triceps Brachii		Main function		
Brachioradialis	Main function		Assist	Assist
Anconeus		Main function	Stabilize ulna	Stabilize ulna
Pronator Teres	Assist			Main function

5.3 Instrumentation

5.3.1 Electrode arrays and positioning

Three 2-D electrode arrays were fabricated in hydrophobic fabric (Gore-Tex ®) for the recording of high density surface EMG signals- HDEMG: one for the biceps (A2), one for the triceps (A3) and one for the forearm (A1) which was intended for the analysis of brachioradialis, anconeus and pronator teres (Figure 5.3).

Arrays consisted in silver-plated and gel-filled eyelets (external diameter of 5 mm) equally spaced by 10 mm in rows and columns (inter-electrode distance, IED=1cm). Rows were aligned in the proximal-distal direction(*y*) while columns were aligned in the medial-lateral direction (*x*). Textile semi-elastic fabric (Gore-Tex ®) was used as substrate for eyelets allowing the arrays to adapt to the geometry of the muscle while maintaining inter-electrode distance. The substrate was both, hydrophobic and transpirable in order to avoid possible cross-bridges between channels of the array caused by gel or sweat. Finally, adhesion to the skin was provided by elastic straps located at the sides of the arrays.

The size of each array was determined from a preliminary study on the muscles described in the previous section. Results for length and perimeter of the limb segments involved are summarized in (Table 5-2). Lengths and circumferences of the upper-arm and forearm segments were measured as follows: the length of the ventral side of the upper-arm (i.e. for biceps) was measured from the acromion to the fossa cubit whereas the length of its dorsal side (i.e. for triceps) was measured from the posterior crista of the acromion to the olecranon. The length of the forearm was measured from the medial epicondyle to the apophysis of the radius. Circumferences were measured in the belly of the involved muscles while contracting at high effort levels: distal and proximal upper-arm circumferences were measured over biceps and triceps during flexion and extension respectively and the proximal forearm circumference was measured over the brachioradialis during flexion. The length of the transversal section of the surface of biceps and triceps was estimated as C=½ circumference of the limb segment. The final dimensions for the electrode arrays are summarized in the last column of Table 5-2.

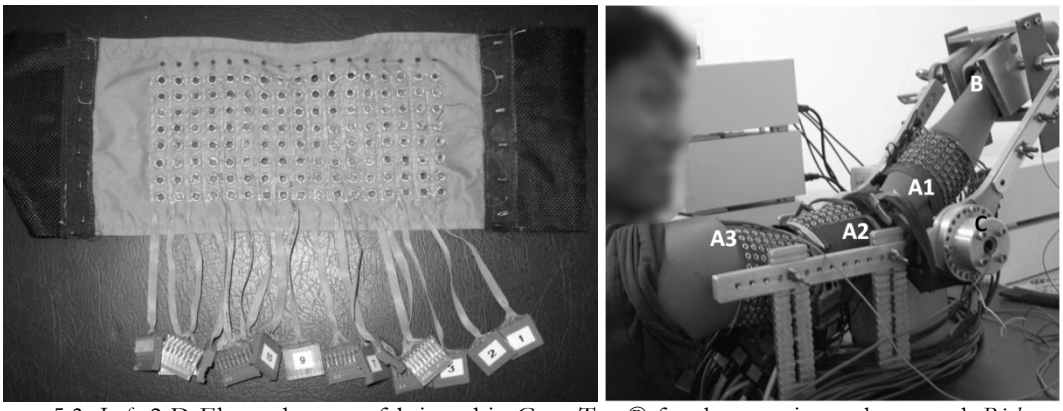

Figure 5.3. *Left.* 2-D Electrode arrays fabricated in Gore-Tex ® for the experimental protocol. *Right.* Positioning of the electrode arrays during the experimental protocol

In the case of biceps, the electrode array covered approximately 87% of the transversal section of the muscle and 25% of its longitudinal section. It covered the long and short heads of biceps. For triceps, the array covered approximately 87% and 20% of its transversal and longitudinal sections respectively. In this case, only the long and lateral heads were considered. Finally, the forearm array covered approximately 100% and 20% of the transversal and longitudinal sections of the forearm covering different portions of the muscles pronator teres, brachioradialis and anconeus. The forearm array was designed to have 18 or 19 columns depending on the limb of the subject.

In the case of biceps and triceps, the central points of the arrays were aligned to landmarks proposed by SEMIAM project (Freriks, Hermens 1999): for biceps over the line connecting the anterior process of the acromion and the fossa cubit at $^1/_3$ of the distance between these two points ($d_{acr\text{-}fc}$). In triceps, over the line connecting the posterior process of the acromion and the olecranon at ½ of the distance between these two points ($d_{acr\text{-}ole}$). In the case of the forearm, the array was located 2 cm below the elbow crease. The locations of the electrode arrays can be observed in detail in Figures 5.4 to 5.6.

TABLE 5-2. DIMENSIONS OF UPPER-LIMB SEGMENTS OBTAINED IN A PRELIMINARY STUDY AND SIZES OF THE ELECTRODE ARRAYS ACCORDING TO THEM

	Length (cm)	**Transversal segment (cm)**	**Array dimensions (rows × columns, IED=1 cm)**
Proximal Upper-arm (triceps)	36.2±2.5	16±1.3	8 × 15
Distal Upper-arm (biceps)	34.3±2.8	16±1.1	8 × 15
Forearm (brachioradialis, anconeus, Pronator teres)	28±1.9	17±2.5	6 × 18-19

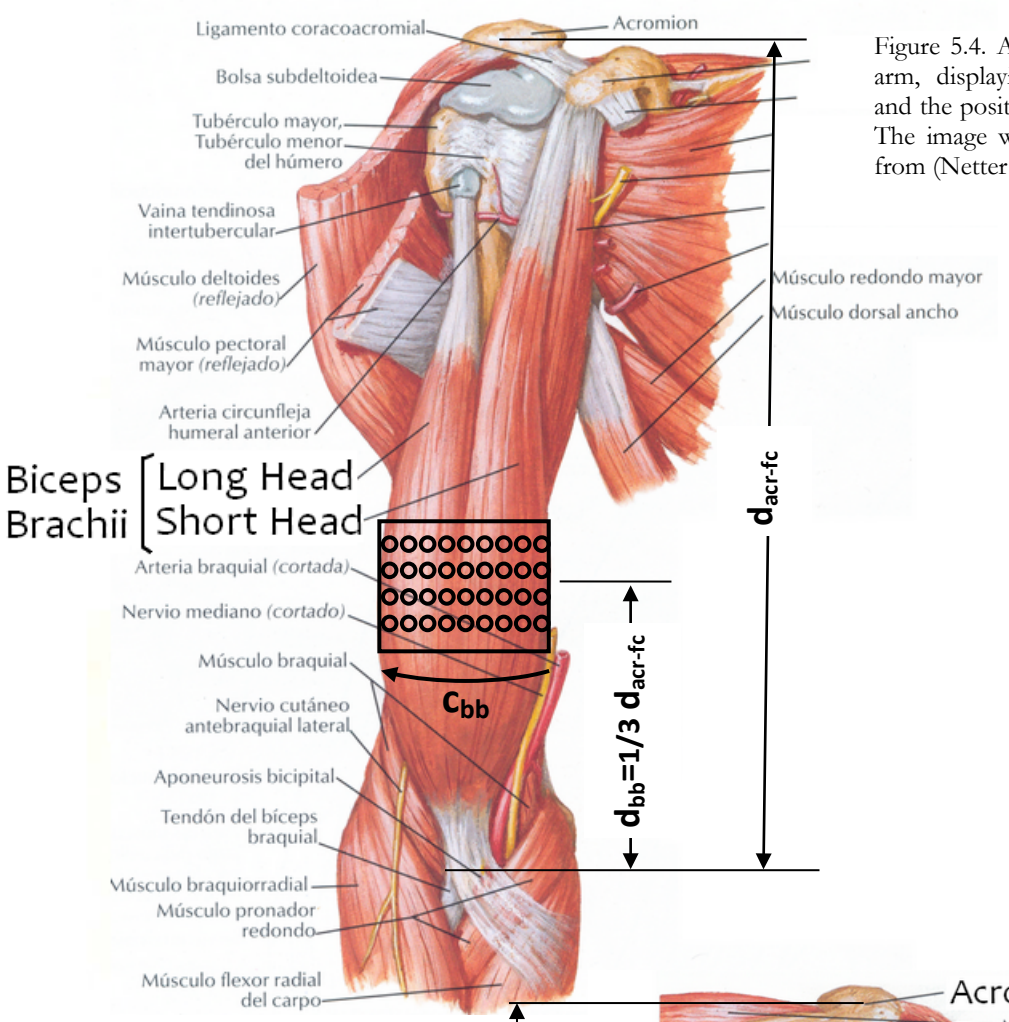

Figure 5.4. Anterior view of the upper-arm, displaying biceps brachii muscle and the positioning of the 2D electrode. The image was extracted and modified from (Netter 2006)

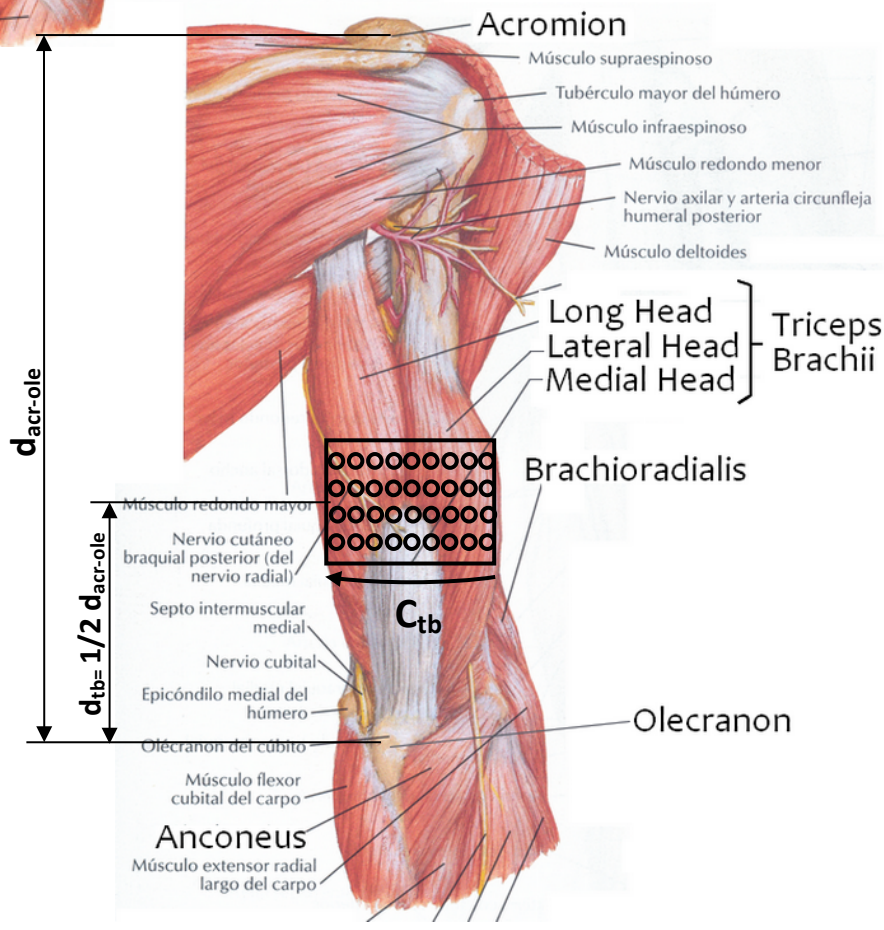

Figure 5.5. Posterior view of the upper-arm displaying triceps brachii muscle and the positioning of the 2D electrode. The image was extracted and modified from (Netter 2006)

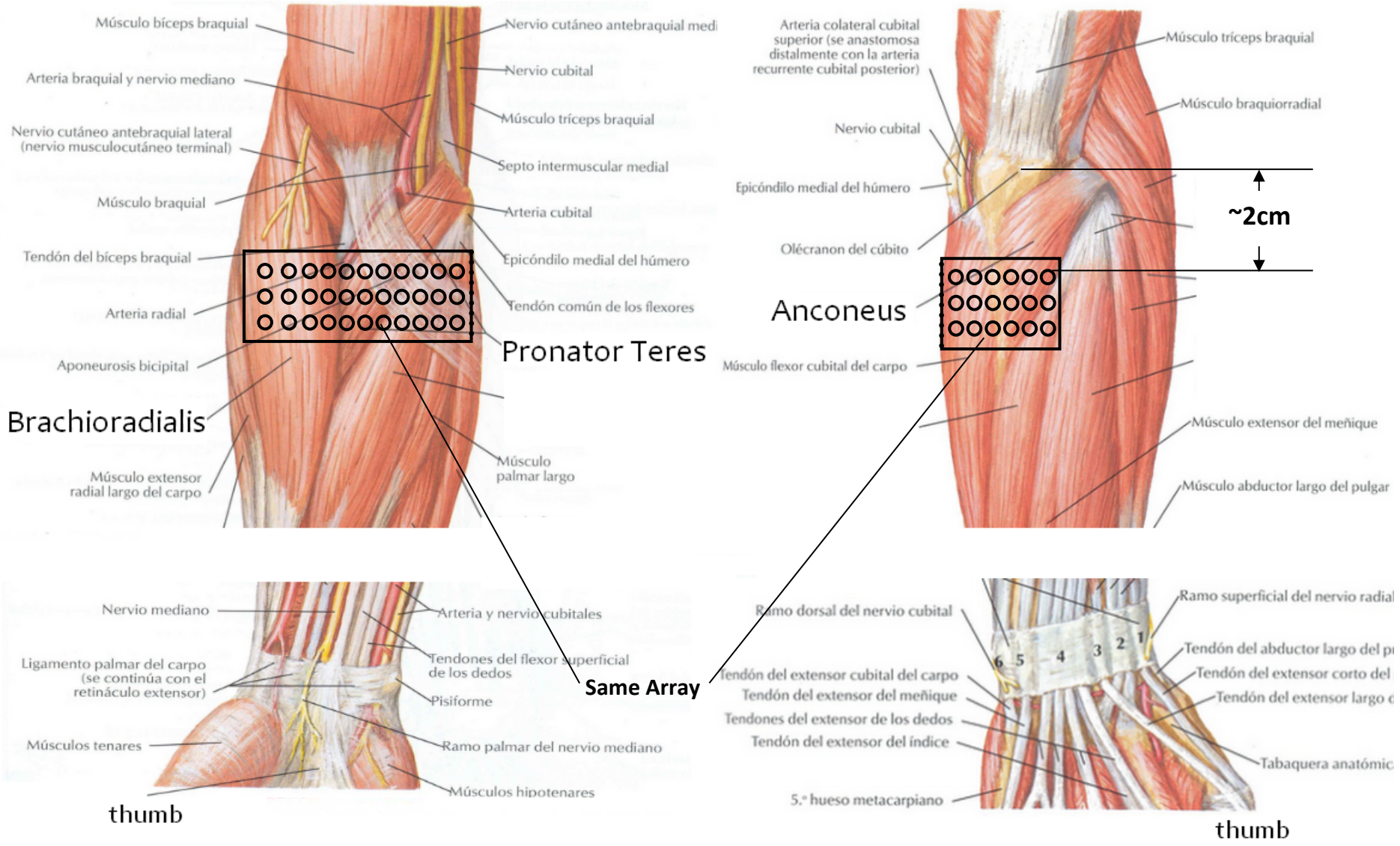

Figure 5.6.Anterior view (left) and Posterior view (right) of the forearm. Anconeus, Pronator Teres (rotondo) and Brachioradialis muscles are shown. The positioning of the 2D electrode is also shown. Images were extracted and modified from (Netter 2006)

5.3.2 Mechanical Brace

Isometric contractions were measured by means of a mechanical brace that prevented muscle elongation and movement of the elbow and the wrist. The mechanical brace had two parallel arms, each of them composed by two bars connected by a joint on which a torque transducer (OT Bioelettronica, range 150 N.m, resolution 2.5mV/V) was placed. The upper-limb of the subject was positioned between the arms of the brace in a way that the elbow laid on the axes of the transducers. Finally, the moment force exerted at the free ends of the mechanical brace was measured.

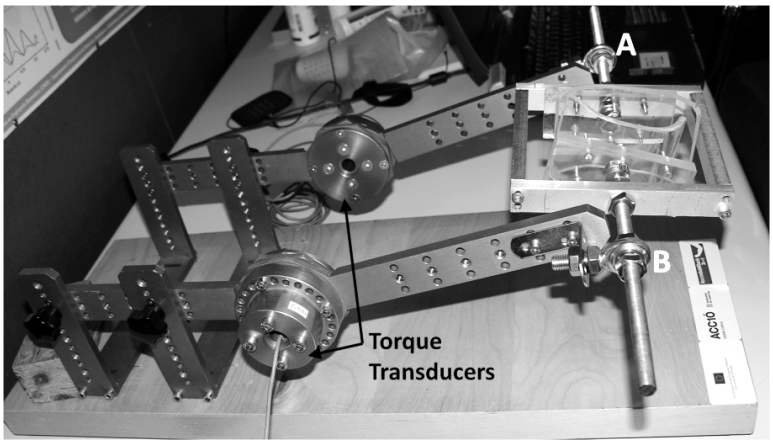

Figure 5.7. Mechanical Brace used in the experimental protocol

The action of the hand and fingers was avoided by using a bracelet-like piece designed to fasten the forearm at its distal end and to transmit the force exerted over two independent plates within this piece, to the ends of the free bars of the mechanical brace, thus maintaining independent measures in both transducers. Rotational forces were transduced by spherical bearings that moved freely at the end of each brace arm (A and B in Figure 5.7). This mechanism avoided hand gripping (Figure 5.3 right), and in general, the activation of flexors and extensors of the wrist.

5.3.3 Instrumentation Setup

The acquisition system consisted on three amplifiers (*EMG-USB- 128* channels, sampling frequency of 2048 Hz, 3dB bandwidth 10-750 Hz, programmable gains of 100, 200, 500, 1000, 2000, 5000 and 10000, LISiN-OT Bioelettronica) with synchronized sampling provided by an external signal. Amplifier #1 recorded signals from the triceps and amplifier #2 from biceps. Amplifier #3 recorded signals from the forearm muscles together with torque signals sensed by the torque transducers in the mechanical brace. The torque signals were amplified and displayed to the subject for biofeedback purposes (*Miso*

II, LISiN-OT Bioelettronica, Torino, Italy). A schematic view of the connections of the different instruments is presented in Figure 5.8.

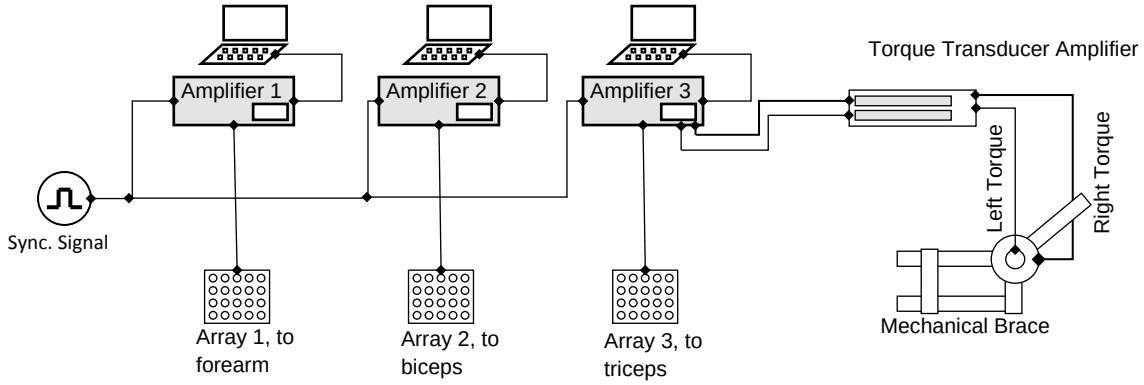

Figure 5.8. Instrumentation set up for the experimental protocol.

5.4 Experimental session and signal recording

Each experimental session consisted on:

- Drawing a line connecting the origin and insertion of each muscle over the surface of the skin to confirm that all of them were covered by at least 3 columns of electrodes (especially in the forearm). This information was later used for the definition of reference systems for each muscle when processing the activations maps.
- Positioning of the electrode arrays after skin preparation that included shaving and cleaning with abrasive paste to reduce contact impedance.
- An initial training on how to avoid the activation of wrist and fingers providing feedback of the EMG signals to the subjects
- Measurement of the Maximal Voluntary Contraction (MVC) during explosive contractions. Three consecutive trials separated by 3-minute rest were completed for each task and the maximum of the three was selected as the MVC for a given task. Subjects were instructed to maintain similar torque outputs in both transducers for flexion and extension while supination and pronation were associated to only one torque signal.
- A set of contractions in randomized order at 10%, 30% and 50%MVC for the four tasks of interest, each of them lasting for 10 seconds and followed by 2 minutes rest. The random order was included to avoid biasing in the results and the rest period was used to avoid the effects of cumulative fatigue.

- At the end of the experimental session, muscle fatigue was assessed by a long-term contraction at 50%MVC up to subjects' exhaustion. This test was performed for each task with 10 minute rest between contractions.

Monopolar signals were recorded simultaneously on the three amplifiers and power line interference was reduced by using a "driven right leg" (DRL) circuit (Metting et al. 1990). Additionally, the amplifiers were modified to provide a virtual ground to the subject in order to enhance the quality of the signals (Darby, Hammond 1979). Reference electrodes were placed at the clavicle, wrist, and shoulder of the same (dominant) side. The schematic is presented in Figure 5.9.

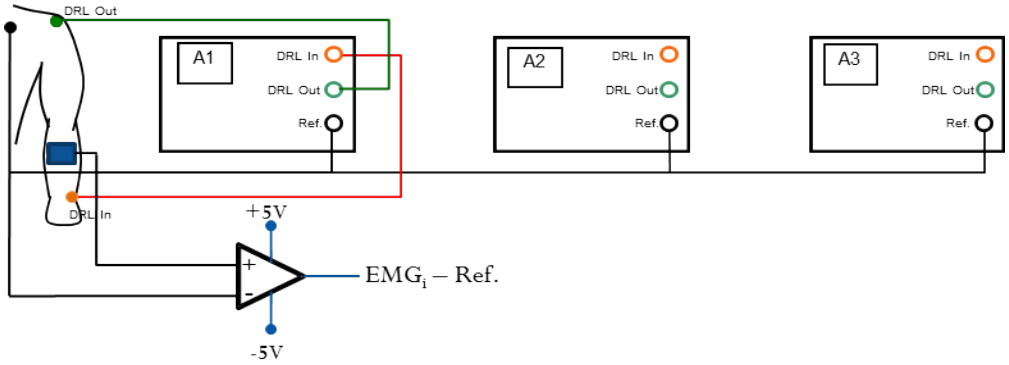

Figure 5.9. Schematics of the acquisition of monopolar signals. A DRL circuit was used to reduce common mode noise.

5.5 Subjects

Twelve healthy male volunteers participated in the experiment. Subjects did not have any history of neuromuscular disorders, pain or regular training of the upper limb. All subjects gave informed consent to participate to the experimental procedure.

TABLE 5-3. BIOMETRIC MEASURES OF SUBJECTS PARTICIPATING IN THE EXPERIMENTAL PROTOCOL

				Biceps		**Triceps**		**Forearm**	
	Age (years)	Height (cm)	Weight (cm)	L (cm)	Φ (cm)	L (cm)	Φ (cm)	L (cm)	Φ (cm)
s1	28	176	76	31	33	31	40	26	30
s2	29	183	90	36	33	34	39	32	30
s3	21	183	83	37	33,5	34	41	32	30
s4	31	175	68	30,5	30	29	34	27	29
s5	28	176	70	29	30	28	34	20	28
s6	22	187	82	32	30	30	40	28	31
s7	22	175	72	33	31	30	38	27	29
s8	27	171	68	34	34	30	37	29	30
s9	28	168	75	32,5	30	34	37	27	28
s10	40	178	83	33	32,5	34	37,5	28	26,5
s11	29	173	64	31	31,5	29	36,5	26,5	25
s12	37	179	65	29	32	29,5	37	27	28,5
Mean (std)	29 (5.7)	177 (5.4)	75 (8.3)	32 (2.5)	32 (1.5)	31 (2.3)	38 (2.2)	27 (3.1)	29 (1.7)

By chance, all subjects were right-handed. Data concerning age, height and weight of each subject as well as length (L) and the circumference (Φ) of the limb segments involved are summarized on Table 5-3.

5.6 Activation Maps

The HD-EMG signals recorded in the two dimensions of the space can be represented as an image *I(x,y)*, where *x* and *y* represent the coordinates of the channels in the reference system and *I(x, y)* is referred to the amplitude of the signal in that point, either as measured at a "sample by sample" scale or as "averaged" on a signal segment. The firsts allow the identification characteristics of individual motor unit action potential, like for example its propagation direction and its conduction velocity, and the second permits to map variations of the values of intensity to variations in the amplitude of the signals recorded in each channel, allowing an insight in the distribution of potentials along the surface of the muscle. An example of an averaged activation map from HD-EMG signals is presented in Figure 5.10.

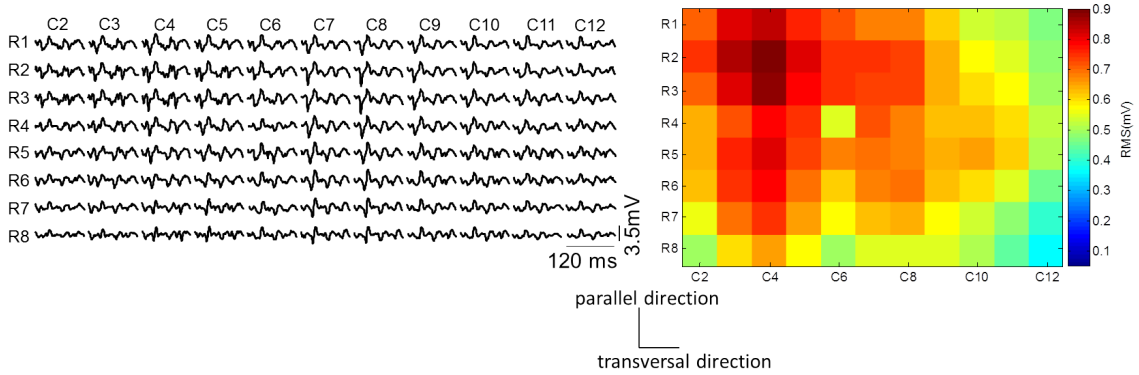

Figure 5.10. Example of HD-EMG signals and its correspondent averaged map *I* from Biceps during flexion at 50% MVC. Segments of 120 ms of the original signals are displayed according to their location in the electrode- array (left). The map *I* was obtained from the averaged RMS value of each channel in segments of 3s (right)

The averaged activation map can be expressed as:

$$I(x,y) = \frac{1}{M}\sum_{m=1}^{M} A_m(x,y) \quad \text{Eq. 5-1}$$

Where *x* and *y* are the spatial coordinates of the map (in the transversal or parallel directions with respect to the muscular fibers), *A* is a variable associated to the amplitude of the signal (ARV or RMS in Eq. 4-1 in Chapter 4) estimated on an epoch, recalling that the EMG signals is not stationary, and M is the total number of epochs in the analyzed segment.

In the following chapters of this thesis, averaged activation maps obtained from HD-EMG signals recorded using the protocol described in the present chapter will be analyzed.

5.7 References

Darby, C. & Hammond, P. 1979, "A patient virtual earth and electrical-interference monitor", Medical and Biological Engineering and Computing, vol. 17, no. 1, pp. 107-109.

Dipietro, L., Ferraro, M., Palazzolo, J.J., Krebs, H.I., Volpe, B.T. & Hogan, N. 2005, "Customized interactive robotic treatment for stroke: EMG-triggered therapy", *IEEE Transactions on Neural Systems and Rehabilitation Engineering,* vol. 13, no. 3, pp. 325-334.

Drost, G., Stegeman, D.F., Schillings, M.L., Horemans, H.L.D., Janssen, H.M.H.A., Massa, M., Nollet, F. & Zwarts, M.J. 2004, "Motor unit characteristics in healthy subjects and those with postpoliomyelitis syndrome: A high-density surface EMG study", *Muscle & nerve,* vol. 30, no. 3, pp. 269-276.

Farina, D., Lorrain, T., Negro, F. & Jiang, N. 2010, "High-density EMG E-Textile systems for the control of active prostheses", *Engineering in Medicine and Biology Society (EMBC), 2010 Annual International Conference of the IEEE*, pp. 3591.

Fleischer, C., Wege, A., Kondak, K. & Hommel, G. 2006, "Application of EMG signals for controlling exoskeleton robots", *Biomedizinische Technik/Biomedical Engineering,* vol. 51, no. 5, pp. 314-319.

Freriks, B. & Hermens, H.J. 1999, *SENIAM 9: European Recommendations for Surface ElectroMyoGraphy, results of the SENIAM project (CD),* Roessingh Research and Development b. v.

Galindo, C., Gonzalez, J. & Fernandez-Madrigal, J.-. 2006, "Control Architecture for Human–Robot Integration: Application to a Robotic Wheelchair", *Systems, Man, and Cybernetics, Part B: Cybernetics, IEEE Transactions on,* vol. 36, no. 5, pp. 1053-1067.

Hamill, J. & Knutzen, K.M. 2006, "Functional Anatomy of the Upper Extremity" in *Biomechanical basis of human movement*, 2nd edn, Lippincott Williams & Wilkins, .

Holobar, A., Minetto, M.A., Botter, A., Negro, F. & Farina, D. 2010, "Experimental Analysis of Accuracy in the Identification of Motor Unit Spike Trains From High-Density Surface EMG", *IEEE Transactions on Neural Systems and Rehabilitation Engineering,* vol. 18, no. 3, pp. 221-229.

Holtermann, A., Roeleveld, K. & Karlsson, J.S. 2005, "Inhomogeneities in muscle activation reveal motor unit recruitment", *Journal of Electromyography and Kinesiology,* vol. 15, no. 2, pp. 131-137.

Kendall F. P., Kendall McCreary E., and Provance P.G. 1993, *Muscles: Testing and Function,* 4th edn, Williams & Wilkins.

Kleine, B.U., van Dijk, J.P., Lapatki, B.G., Zwarts, M.J. & Stegeman, D.F. 2007, "Using two-dimensional spatial information in decomposition of surface EMG signals", *Journal of Electromyography and Kinesiology,* vol. 17, no. 5, pp. 535-548.

Merletti, R., Aventaggiato, M., Botter, A., Holobar, A., Marateb, H. & Vieira, T.M.M. 2010a, "Advances in surface EMG: recent progress in detection and processing techniques.", *Critical Reviews in Biomedical Engineering,* vol. 38, no. 4, pp. 305-45.

Merletti, R., Botter, A., Cescon, C., Minetto, M.A. & Vieira, T.M.M. 2010b, "Advances in surface EMG: recent progress in clinical research applications.", *Critical Reviews in Biomedical Engineering,* vol. 38, no. 4, pp. 347-79.

Merletti, R., Holobar, A. & Farina, D. 2008, "Analysis of motor units with high-density surface electromyography", *Journal of Electromyography and Kinesiology,* vol. 18, no. 6, pp. 879-890.

Metting van Rijn, A., Peper, A. & Grimbergen, C. 1990, "High-quality recording of bioelectric events", *Medical and Biological Engineering and Computing,* vol. 28, no. 5, pp. 389-397.

Parker, P., Englehart, K. & Hudgins, B. 2006, "Myoelectric signal processing for control of powered limb prostheses", *Journal of Electromyography and Kinesiology,* vol. 16, no. 6, pp. 541-548.

Pierrot, F., Dombre, E., Dégoulange, E., Urbain, L., Caron, P., Boudet, S., Gariépy, J. & Mégnien, J. 1999, "Hippocrate: a safe robot arm for medical applications with force feedback", *Medical image analysis,* vol. 3, no. 3, pp. 285-300.

Staudenmann, D., Kingma, I., Daffertshofer, A., Stegeman, D.F. & van Dieën, J.H. 2009, "Heterogeneity of muscle activation in relation to force direction: A multi-channel surface electromyography study on the triceps surae muscle", *Journal of Electromyography and Kinesiology,* vol. 19, no. 5, pp. 882-895.

Tucker, K., Falla, D., Graven-Nielsen, T. & Farina, D. 2009, "Electromyographic mapping of the erector spinae muscle with varying load and during sustained contraction", *Journal of Electromyography and Kinesiology,* vol. 19, no. 3, pp. 373-379.

Vieira, T.M.M., Merletti, R. & Mesin, L. 2010, "Automatic segmentation of surface EMG images: Improving the estimation of neuromuscular activity", *Journal of Biomechanics,* vol. 43, no. 11, pp. 2149-2158.

Zwarts, M.J. & Stegeman, D.F. 2003, "Multichannel surface EMG: Basic aspects and clinical utility", *Muscle & nerve,* vol. 28, no. 1, pp. 1-17.

6

High- Density EMG Activation Maps at the Elbow Joint

6.1 Introduction

This chapter is devoted to the calculation of activation maps for the upper arm and forearm. As mentioned in Chapter 5, activation maps obtained with HD-EMG provide a larger amount of information related to the tracking of (task changing) skin surface areas where EMG amplitude is maximal and a better estimation of muscle activity by the proper selection of the most significant channels. The main objective of this chapter was to analyze patterns in the activation maps associating them with the four movement directions at the elbow joint and by considering different strengths of those movements. Moreover, such activation pattern was compared with that extracted from bipolar electrodes.

In addition, this chapter also deals with the necessary preprocessing of HD-EMG signals: identification of outlier signals and segmentation of global activation areas. The first is associated to the recording of large number of physiological signals where it is very likely to observe some low quality channels affected by artifacts due to movement, poor contact or power line interference. For this purpose different algorithms based on the spatial spread of the potentials over the skin surface have been proposed in the literature (Gronlund et al. 2005, Marateb et al. 2012). Such algorithms considered only the information of the bulk of data for the detection of outliers in 2D multichannel recordings. The approach proposed here takes into account features extracted from channels in the close- proximity neighborhood to evaluate the quality of a given signal and to interpolate its value from neighboring channels when needed. Besides, the method was designed to compromise between precision and sensitivity of the detection in order to reduce the number of misclassifications of good-quality signals.

In the second case it was necessary to select the regions associated to the main activity within the recording since large inter-individual variability can be expected (especially concerning the size of the muscles) before extracting information associated to the global

activation of the maps and averaging between subjects. Watershed image segmentation has been proposed in the past for determining the regions of activity in HD-EMG recordings (Vieira et al. 2010), however this method is prone to over-segmentation in the presence of multiple discontinuities (Vincent 1993), particularly, those introduced by dissimilarities in the electrode-skin impedance of the different channels. The segmentation proposed here offers an alternative, being less sensitive to local maxima. Results show that features extracted from HD-EMG maps could be useful in the identification of movement intention.

6.2 Methodology

6.2.1 Detection of low quality signals

a. Features Extraction

Human experts can identify artifact signals with high accuracy, based on their amplitude, frequency pattern (as in the case of power-line interference) and in their similarity. However, visual inspection of outliers ("bad" channels presenting low-quality signals) is time-consuming and depends on the expertise of the operators (Minium et al. 1999). Thus, it becomes necessary to apply an automatic method to identify such signals (and perform adequate processing if necessary) before any kind of information extraction.

These channels are characterized by: a) high-power low frequency components, b) high power components at power-line harmonics due to high-impedance contacts and stray capacitive couplings, and c) their energy may be much higher or lower than that of neighboring monopolar channels, especially if parallel-fibber muscles are considered. An example of poor quality monopolar signals and its normalized Power Spectral Density (PSD) is presented in Figure 6.1. Low quality signals commonly present lower or higher amplitude (for example R1C1 and R6C2 in Figure 6.1a respectively) when compared to neighboring channels. They can also present large baseline fluctuations caused by relative motions of the electrode over the skin, or periodic patterns mainly caused by power-line interference. These two later artifacts are reflected in the power spectrum of the signals (for example R6C2 and R3C3 in Figure 6.1b)

An artifact detection method based merely on the amplitude of the signal is not sufficient because the surface of the array covers different muscles with quite different ranges of EMG amplitude (Figure 6.1a). Taking this into account, no assumption on the power of the non-artifact signals can be made. On the other side, the normalized power

spectrum of non-artifacts can be similar to that of artifact signals. An example is presented in Figure 6.1c. Signal recorded in channel R1C1 is an artifact whereas signal in channel R6C3 is not. Both, the power spectrum and the amplitude of these two signals are similar but R1C1 can be identified as an artifact when compared to neighbor channels in time domain.

Three features for the detection of artifactual signals were defined as:

1. Relative power of low frequency components, $P_{l/t}$, from 0 to 12 Hz,

2. Relative power of power-line components $P_{line/t}$, corresponding to 50Hz and its first four harmonics, and

3. Signal power calculated from the root mean square (RMS) of the signal

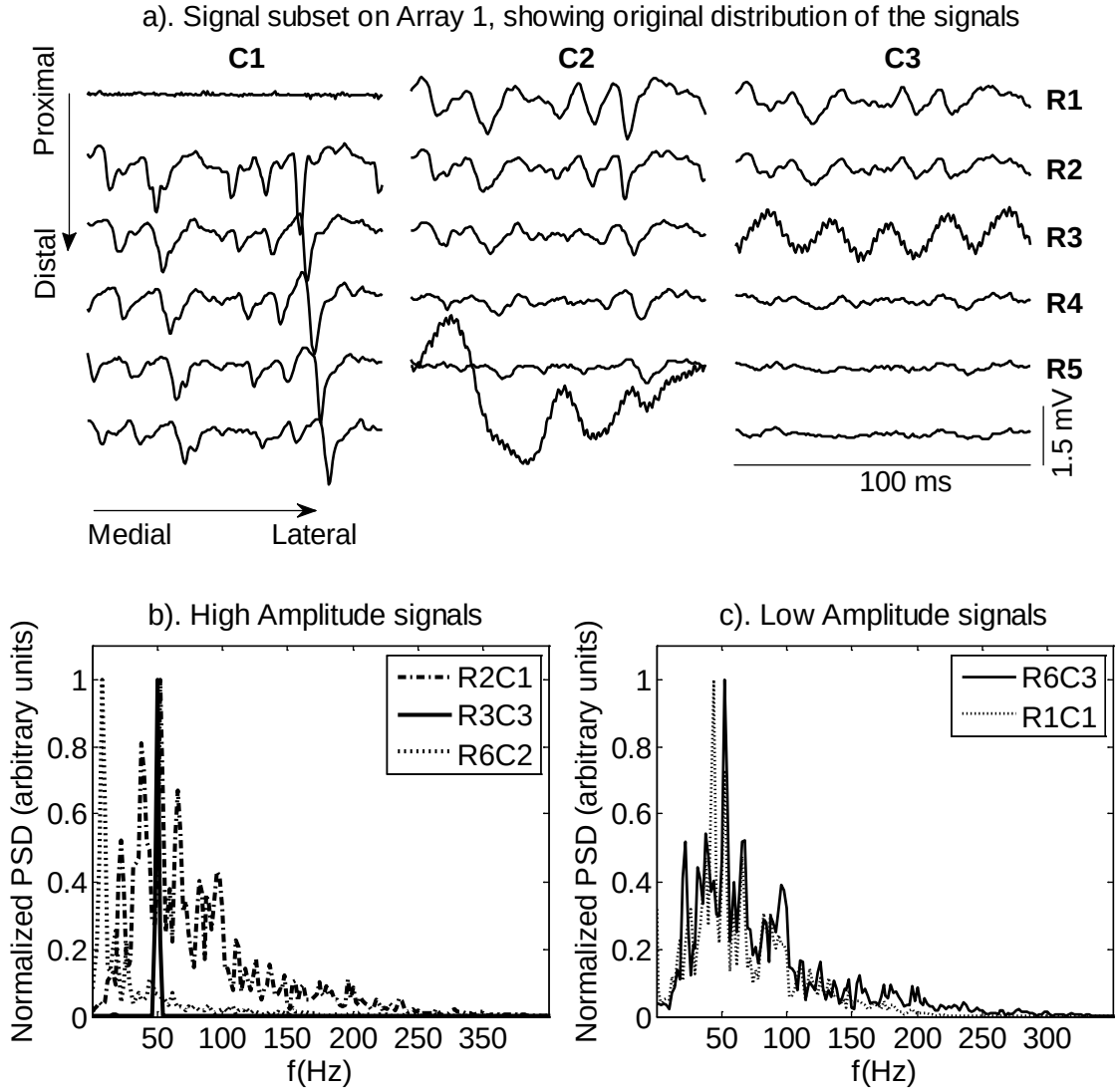

Figure 6.1. a).Signal subset recorded in array A1 (forearm) during elbow flexion at 50%MVC. Three columns (C1 to C3) and six rows (R1 to R6) are shown. Different kinds of artifacts are observed in C1R1, C2R6, and C3R3. It is also possible to observe that the energy of the signals changes in both x and y directions. Normalized Power Spectral Density for different signals are displayed in the bottom. Each spectrum is normalized with respect to its peak value. Artifactual channels can present higher or lower amplitude when

compared to neighbor channels. b). High amplitude signals. It is possible to observe power-line components on the artifactual channel R3C3 and low frequency components on the artifactual channel R6C2. The attenuation of the analogue filter in the amplifier is not sufficient to remove the movement artifact on channel R6C2. c). Low amplitude signals. Thought normalized PSD is similar for R6C3 and R1C1, the later can be identified as an artifact when compared to neighbor channels in the temporal domain.

The Power Spectral Density of the signal was estimated with the FFT in non-overlapping signal epochs of 500ms. Features ($P_{l/t}$, $P_{line/t}$ and RMS) were computed for each channel as the mean of the values obtained from six epochs over segments of 3 s where the exerted force remained constant.

b. Automatic Algorithm for artifact removal

An expert system based on thresholds associated with the three features described previously was designed.

The algorithm was applied to a signals set, *S,* composed by signals $s_{i,j}$ recorded in the rows (*i*) and columns (*j*) of a given electrode array A1 to A3 as described on Chapter 5 (*i=[1,2,…,6] and j=[1,2,…,17] or j=[1,2,…,19]* for array A1 depending on the size of the forearm of the subject, and *i=[1,2,...,8]* and *j=[1,2,…,15]* for arrays A2 and A3 in the upper-arm). A schematic of the decision algorithm is presented in Figure 6.2.

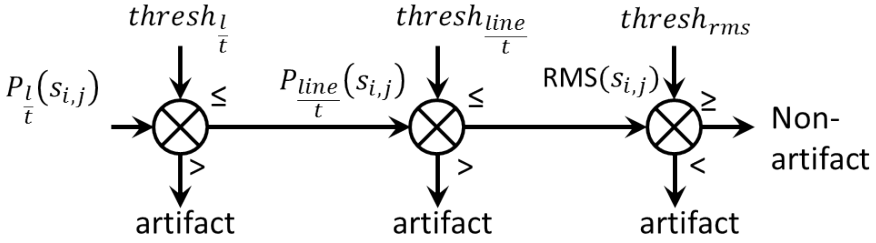

Figure 6.2. Schematics of the algorithm for the detection of low quality signals. The symbols (>) or (<) represent the cases where the feature was expected to be higher or lower than the specified threshold in order to determine if a given signal was labeled as artifact.

Thresholds $thresh_{l/t}$, $thresh_{line/t}$ and $thresh_{rms}$ were calculated from a subset of *S* composed of signals called reference (*ref)* that satisfied the following two conditions:

$$ref = \begin{cases} abs\left(P_{\frac{l}{t}}(ref) - median\left(P_{\frac{l}{t}}(S)\right)\right) < 1.5IQR\left(P_{\frac{l}{t}}(S)\right) \\ abs\left(P_{\frac{line}{t}}(ref) - median\left(P_{\frac{line}{t}}(S)\right)\right) < 1.5IQR\left(P_{\frac{line}{t}}(S)\right) \end{cases} \quad \text{(Eq. 6-1)}$$

where IQR represents the Interquartile Range. The median was chosen instead of the mean because of its lower sensitivity to outliers since it considers the highest breakpoint (50%), that is, the smallest percentage of outliers that can cause an estimator to take arbitrary large values (Hampel 1971).

The thresholds were calculated as following:

- $$thresh_{\underline{l}\atop t} = k_1\left(median\left(P_{\underline{l}\atop t}(ref) \right) + 1.5IQR\left(P_{\underline{l}\atop t}(ref) \right) \right) \quad \text{(Eq. 6-2)}$$

where the constant k_l was subjected to an optimization criterion in order to improve the performance of the detection method as it is explained in the next section.

- $$thresh_{\underline{line}\atop t} = k_{line}\left[median\left(P_{\underline{line}\atop t}(ref) \right) + 1.5IQR\left(P_{\underline{line}\atop t}(ref) \right) \right] \quad \text{(Eq. 6-3)}$$

where the constant k_{line} was subjected to a sensitivity analysis (see Table 6-1) and set to 2.5, as tradeoff between the capacity of $thresh_{line/t}$ to identify the highest proportion of signals presenting power-line harmonics and the capacity to correctly identify such signals avoiding the misdetection of good-quality signals. In any case, $thresh_{line/t}$ was always constrained to 0.85, that is, signals presenting more than 85% of the signal power in the bands related to power-line harmonics were considered as artifacts.

TABLE 6-1. SENSITIVITY ANALYSIS FOR CONSTANT k_{line} FOR THE DETECTION OF POWER-LINE ARTIFACTS

k_{line} (2.5)	1	2	3	5	7
Acc	99,74	99,79	99,79	99,74	99,79
S	83,33	83,33	83,33	75,00	75,00
SP	99,83	99,87	99,87	99,87	99,91
P	71,43	76,92	76,92	75,00	81,82

k_{line} in Eq. 6-3 was chosen as 2.5 (presented in parenthesis). Increasing values of k_{line} reduced the sensitivity (S) of the threshold $thresh_{line/t}$, whereas decreasing values decreased the precision (P). Variations in these two indexes affected the Accuracy (Acc) and the Specificity (SP). k_{line} = 2.5 is a good compromise between S and P

- $$thresh_{rms} = \min\{\mu_{pa}, \mu_{pb}, \mu_{pc}\} + k_2 \max\{std_{pa}, std_{pb}, std_{pc}\} \quad \text{(Eq. 6-4)}$$

where μ and *std* are the average and standard deviation, respectively, of the RMS of the following three neighbor-pairs in the proximity of a given channel $s_{i,j}$: $p_a = [RMS_{i-1,j}, RMS_{i+1,j}]$ in the longitudinal direction, and $p_b = [RMS_{i-1,j-1}, RMS_{i+1,j+1}]$ and $p_c = [RMS_{i+1,j-1}, RMS_{i-1,j+1}]$ in the diagonal directions. This third condition distinguished low amplitude signals corresponding to innervations zones or non- active regions (for

example R4C3, R5C3 and R6C3 in Figure 6.1 from isolated low amplitude signals (for example R1C1 in Figure 6.1) that were considered as artifacts. Hence, the threshold in Eq. 6-4 takes into account the spatial direction of propagation of Motor Unit Action Potentials. Finally, the constant k_2 in Eq. 6-4 was tuned in order to improve the performance of the method as it is explained in next section.

c. Training and Validation

Constant values of k_1 and k_2 on Eq. 6-2 and Eq. 6-4, allowed to increase the performance of the detection method, especially its sensitivity (or the capacity of the method to identify the highest proportion of low-quality signals) and the precision (or the capacity to correctly identify low-quality signals avoiding the misdetection of good signals as low-quality). Thus, the performance of the method was measured in terms of Sensitivity(S), Specificity (SP), Precision (P) and Accuracy (A) (Farina et al. 2001) as:

$$S = \frac{TP}{TP+FN} \quad SP = \frac{TN}{TN+FP} \quad P = \frac{TP}{TP+FP} \quad A = \frac{TP+TN}{TP+FP+TN+FN} \quad \text{(Eq. 6-5)}$$

where TP and TN is the number of channels correctly identified as low and good-quality signals respectively, FN is the number of low-quality signals not identified by the method and FP is the number of good-quality signals identified as low-quality.

Signals were visually classified as low-quality or not by three experts based on the observation of similarity between different channels and on the examination of baseline fluctuations or periodicity patterns (related to movement artifacts and power-line interference respectively, see Figure 6.1a as an example). Two databases for training and validation were obtained, each composed of 20 signal sets selected from different contractions, effort levels and arrays 1 to 3. Fleiss' Kappa index (Fleiss 1971) was used to measure agreement between experts, scoring 82.63% and 86.19% for the training and validation databases respectively and indicating an "almost perfect agreement". Results of the three experts were selected according to the majority vote in each case (i.e. the statistical mode of the three opinions) in order to obtain a binary classification-label as artifact (1) or non-artifact (0) for each single-channel in the set *S*.

Optimal values for k_1 and k_2 were selected according to the following criteria: 1) by Receiver Operating Characteristic (ROC) curves (S vs. 1-SP), widely used in classic signal detection theory and clinical diagnostics (Fawcett 2006) and, 2) by Precision-Recall representations (P vs. SP), which are commonly used in machine learning (Landgrebe et al. 2006). Both methods assessed the accuracy of the prediction (or outcome) of the described method based on its Sensitivity, Specificity and Precision. The optimal classifier is found as a tradeoff between hit rates and false alarm rates. In the first case the optimal can

be found as the minimum distance between the curve (S vs. 1-SP) and the point (0, 1), and in the second case, as the minimum distance between curve (P vs. SP) and the point (1, 1).

6.2.2 Segmentation of HD-EMG Maps

Areas corresponding to electrodes lying over an active region of a muscle or a set of muscles can change between subjects. In addition, for each of the five selected muscles, activity of neighbor muscles can also be observed during the task. Therefore, it was useful to extract the region related to each muscle of interest from the individual maps before averaging between subjects, in order to finally obtain a general activation map associated only with each of the selected muscles. Thus, an algorithm for the segmentation of active regions was proposed in this study. An *activation map I* in the 2D space was obtained from HD-EMG signals as:

$$I_{i,j} = \frac{1}{M}\sum_{m=1}^{M}\left(\frac{1}{N}\sum_{n=1}^{N} s_{i,j}^2(n)\right) = \frac{1}{M}\sum_{m=1}^{M} RMS(s_{i,j}) \quad \text{(Eq. 6-6)}$$

where *s* is an EMG signal in the channel located at the position *i, j* of the 2D array (as explained before), N is the total number of samples in an epoch of 500 ms and the RMS value was averaged in M=6 non overlapped epochs corresponding to three seconds of signal. Prior to the calculation of RMS values, the EMG signals were filtered between 12 and 350 Hz with a 4th order Butterworth filter in forward and backward direction in order to correct for phase distortion, following SENIAM recommendations for the processing of surface EMG signals (Hermens et al. 1998). RMS values corresponding to signals previously identified as artifacts were replaced by triangle-based cubic interpolation based on Delaunay Triangulation for surface fitting proposed in (Bradford et al. 1996).

Each channel in the map can be considered as a pixel located at the positions *i* and *j* of the electrode array whose intensity is given by $I_{i,j}$. In other words, the map I can be thought of three dimensions where the intensity values represent elevations as in a topographical map. Intensity levels in the maps correspond to the activation level of a muscle (or a set of muscles) during the development of a specific task.

The activation map was segmented by applying an h-dome transform $D_h(I)$ over the image *I*, as proposed by L. Vincent (Vincent 1993). This transform extracted regional maxima and minima by the morphological reconstruction of the original image *I* (the mask) using as marker a second image *J* which was derived from *I* by subtracting a constant value *h:*

$$D_{h_{i,j}}(I_{i,j}) = I_{i,j} - \rho_I(J_{i,j}) = I_{i,j} - \rho_I(I_{i,j} - h) \quad \text{(Eq. 6-7)}$$

where the operator ρ_I stand for morphological reconstruction (Serra 1982), and *J* is derived from *I* by subtracting a constant value *h*. This transformation preserved all the domes above the height *h*, including those that contain various local maxima. In the case of activation maps, such local maxima could correspond to local variations on the amplitude of the 2D maps due to distinct contact impedances in the various electrodes. The concept is explained in Figure 6.3.

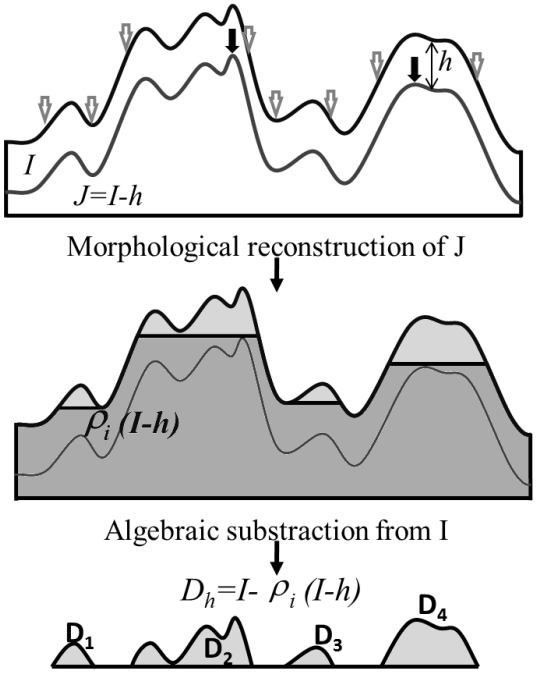

Figure 6.3. H-dome transform- D_h. The concept is explained on a topographical representation of the image *I*. Observe that the segmentation is not affected by local maxima or minima present in each of the domes D_h

Additionally, a morphological opening (γ) was applied to the resulting image Dh in order to avoid the segmentation of isolated peaks, small in area, and which corresponded to pixels with an amplitude slightly higher than that of the surrounding channels. This was the case in "flat" maps (particularly at low-effort levels) where the activation is mainly reflected on the synergistic muscles with levels comparable to background noise and where only marginal activation can be observed in antagonist muscles. Therefore, the final segmented image $Is_{i,j}$ was obtained as:

$$Is_{i,j} = \gamma(D_{h_{i,j}}) = D_{h_{i,j}} \circ b = \left(D_{h_{i,j}} \ominus b\right) \oplus b \quad \text{(Eq. 6-8)}$$

where *b*, the structuring element, is a disc of radius 1 and $\ominus$ and $\oplus$ are the operators for dilation and erosion respectively (Serra 1982).

6.2.3 Average HD-EMG Maps

Average maps for the 12 subjects who participated in the study were obtained by averaging individually segmented maps, in order to obtain useful information related to muscle co-activation pattern in terms of intensity values and its spatial distribution which were expected to be different for different kind of tasks and/or levels of effort. Considering that upper-limb dimensions in terms of circumference and muscle length are different for every subject, it was necessary to normalize and interpolate the image in the 2D space so that results could be comparable among subjects, allowing the calculation of an average map for the population. In the case of arrays 2 and 3 (biceps and triceps), the zero of the coordinate system was defined to correspond to landmarks defined by SEMIAM project (Freriks, Hermens 1999). In the case of forearm muscles, the origin of the *x-axis* laid in the intersection of the line connecting the origin and insertion of each muscle (Anconeus, Brachioradialis or Pronator Teres) and an arch traced around the forearm, 2 cm below the elbow crease which in turn was the zero of the *y-axis*. Values in the *x* dimension were normalized with respect to the circumferences of the different limb segments: proximal forearm for array 1, distal upper-arm for array 2 and proximal upper-arm for array 3, and values in the *y* dimension were normalized with respect to the length of the segments between reference points as described in section 5.3.1 of Chapter 5. Data on the dimensions of subjects' upper-limb segments are summarized in Table 6-2.

TABLE 6-2. UPPER-LIMB DIMENSIONS FOR SUBJECTS IN THE DATABASE.

	Length (cm)*	**Circumference (cm)***
Proximal Upper Arm (ventral)	38±2.2	31±2.3
Distal Upper Arm (dorsal)	32±1.5	32±2.5
Proximal Forearm	29±1.7	27±3.1

* Length was measured between reference points: Acromion and Fossa Cubit for Proximal Upper Arm, posterior crista of the acromion and Olecranon for Distal Upper Arm and Medial Epicondyle and Apofisis of the Radius for Forearm. Circumference was measured during strong contractions of Biceps, Triceps and Brachioradialis for the three segments respectively. Results are presented as mean ± Standard Deviation for 12 subjects.

In order to obtain individual maps with the same (*i, j*) coordinates for the calculation of population's average map, RMS values in the 2-D space were re-sampled in the *x* and *y* directions by using cubic splines interpolation, considering units relative to the total length and total circumference of the upper-limb segment as explained in the previous paragraph.

Intensity of the maps was parameterized by the average RMS value ($RMS_{av\text{-}HD}$) for the segmented area. In addition, spatial distribution of the maps was parameterized according

to the median of its projection over the *x* and *y* axes, that is, $x=\mu x$ or y= μy where such projection was divided into two regions of equal area, as following:

$$\sum_{k=1}^{\mu_{dim}} Q_k^{dim} = \sum_{k=\mu_{dim}}^{M} Q_k^{dim} = \frac{1}{2}\sum_{k=1}^{M} Q_k^{dim} \text{ where } Q_k^{dim} = \max(Is_k, dim) \quad \text{(Eq. 6-9)}$$

where Q_k^{dim} is the value of the projection of the maximum of the segmented map *Is* at the k^{th} coordinate along the dimension dim=*x* or dim=*y* and μ_{dim} corresponds to the median of the projection Q_k^{dim}. The median of the projections permitted to evaluate spatial shifts along the *x* and *y*-axes of the maps, both of them associated with changes in effort levels or even with different tasks.

On the other hand, data similar to that obtained with bipolar electrodes was extracted by selecting two monopolar channels for each muscle in the 2D arrays: the first electrode corresponded to the one located at the origin of the coordinate system (following SENIAM recommendations (Freriks, Hermens 1999) as described previously for each muscle, and the second one was located 10 mm apart in the direction of the muscular fibers. A single differential signal was obtained from these two channels for each muscle and its corresponding RMS_{av-bip} value was calculated at the same time-interval as in the case of HD-EMG maps. The variables $RMS_{av\text{-}bip}$ and $RMS_{av\text{-}HD}$ (from bipolar or HD-EMG configurations) were used in the identification of tasks and their performances were compared as later explained.

6.2.4 Statistical Analysis

The statistical analysis was intended to assess differences between information extracted from single bipolar signals or from HD-EMG maps and also to analyze differences due to type of task and effort level. Such analysis was based in the variables determined in the previous section, that is, $RMS_{av\text{-}bip}$ and $RMS_{av\text{-}HD}$ both of them related to the signal power, and μ_x and μ_y associated with the spatial distribution of the maps.

Factors considered in the statistical analysis were: 1) the type of electrode (bipolar or HD-EMG), 2) The type of task, that is, flexion, extension, supination and pronation, and contraction level (10%, 30% and 50% MVC), and 3) Muscle (i.e. biceps, triceps, brachioradialis, anconeus and pronator teres).

Differences between $RMS_{av\text{-}bip}$ and $RMS_{av\text{-}HD}$ were evaluated with the non-parametric Friedman test in two-way layout. In order to avoid differences between the type of recording (bipolar and monopolar), both variables in each muscle were normalized with respect to the mean value obtained in all tasks and contraction levels. Data corresponding to different tasks and effort levels were pooled together by considering blocks with

replication of cells of the factor muscle according to the procedure described in (Zar 2010) and implemented in the statistical toolbox of MATLAB®.

On the other hand, the capacity of the extracted variables ($RMS_{av\text{-}bip}$ or $RMS_{av\text{-}HD}$) for the identification of tasks and/or effort levels was evaluated by classifying the data into different groups based on linear discriminant analysis (Krzanowski 1988) and cross-validation with the Leaving One Out Method (Kearns, Ron 1999). Data was classified into four or twelve groups corresponding to type of task or to type of task and effort level respectively. In the former case, samples corresponding to the three levels of effort were pooled together for each type of task. The overall classification performance was obtained in terms of Accuracy, Sensitivity, Specificity and Precision as described in (Farina et al. 2001) and (Eq. 6-5). For this analysis TP were data samples well classified into any of the classes, FN corresponded to the number of missing samples in any of the classes, that is, samples belonging to a given class but that were classified in another, TN were not misclassified samples, and FP were samples misclassified in any of the classes.

In addition, changes in the spatial distribution of the maps due to type of task and effort level were analyzed with a non-parametric repeated measures design based on the Friedman test. In this case, variations of the variables μ_x and μ_y were evaluated in 12 different measures corresponding to four types of task by three levels of effort each. A Bonferroni correction was applied in order to take into account the multiple comparisons.

Finally, pair-wise comparisons were analyzed trough non-parametric Wilcoxon signed rank test.

Statistical significance was set to p=0.05. In the Friedman test, χ^2 statistics was considered significant for χ^2 (d.o.f=1)> 3.84 for one degree of freedom (d.o.f = 2 types of electrode -1) and for χ^2 (d.o.f=11)> 27.28 for eleven degrees of freedom (d.o.f=12 measures -1) after the Bonferroni correction.

6.3 Results

6.3.1 Detection of Low-Quality Signals

Sensitivity analysis for constant k_{line} in (Eq. 6-3) in the training database is presented in Table 6-1. Higher values of k_{line} increased the number of TP and FP affecting both, the sensitivity and the precision of the detection. As it can be observed on Table 6-1, k_{line} between 2 and 3 is a good compromise between sensitivity and precision as it can be confirmed from accuracy and specificity of the detection, where the highest values were

obtained. For values lower than 2, precision decreases whereas for values higher than 3 sensitivity decreases.

Performance indexes for the detection of artifacts in the training and validation databases using ROC and PR are shown in Table 6-3. Although results were similar when comparing both criteria, the precision was higher for the PR approach at the expense of slightly lower sensitivity because of the introduction of a number of FN. The sensitivity was higher when considering the ROC criterion but this led to an increase in the number of FP (as compared to PR). The specificity was always very high (above 99%) because the number of non-artifact signals is much higher than the number of low-quality signals. A sensitivity analysis for k_1 and k_2 in the training database is presented in Table 6-3. Different values of k_2 produced the same sensitivity for increasing values of k_1 whereas the precision varied at high values of k_1 (because of the inclusion of FP). Precision and sensitivity increased and decreased respectively for increasing values of k_1. The values adopted for $k_1$and k_2 in this work represent a good tradeoff between sensitivity, specificity and precision.

TABLE 6-3.OPTIMUM VALUES OF k_1 AND k_2 (Eq. 6-2 AND Eq. 6-4) AND THEIR PERFORMANCE INDICES.

		(k_1, k_2)	Acc (%)	S (%)	SP (%)	P (%)
Training	ROC	(7.1, 0.2)	99.61	97.67	99.69	92.31
	PR	(11.2, 0.2)	99.66	94.19	99.87	96.43
Validation	ROC	(7.1, 0.2)	99.40	97.94	99.46	88.78
	PR	(11.2, 0.2)	99.48	92.78	99.77	94.73

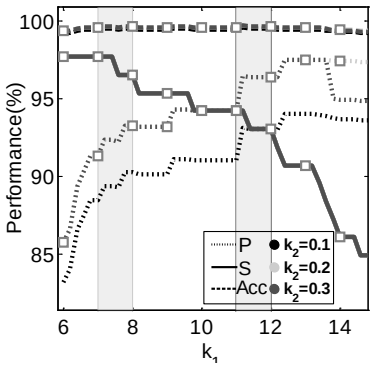

Performance measures for combinations of k_1 and k_2: Accuracy (Acc), Sensitivity (S), Specificity (SP) and Precision (P) for the training (20 sets) and validation (20 sets) databases. The two methods proposed for outlier detection are presented (ROC, Receiver Operating characteristics and PR, Precision-Recall). Sensitivity analysis for k_1 and k_2 in the training database is shown in the figure. Constant k_1 is represented along the x-axis. Curves (in shades of gray) are shown for k_2. Higher values of k_1 increased P (in dot lines) but decreased S (in solid lines). Acc (dash lines) remained almost constant for different values of k_1 and k_2. Optimal values for k_1 were found as a compromise between S and SP; and S and P in the ranges in gray. Performance indexes corresponding to the selected k_2=0.2 are shown in squares.

Although high Sensitivity (S) and Specificity (SP) were desired, a lower number of FP became important when considering the next step of the analysis where RMS values of artifacts were interpolated from neighbor channels. If too many channels in the neighborhood were wrongly labeled as "artifacts" (i.e. too many FP), then the interpolation process was not possible. Because of the lower Precision of the algorithm with the ROC

criterion (Table 6-3), constants k_1 and k_2 were finally selected according to optimization results obtained by Precision- Recall.

The algorithm for artifact detection had low computational complexity. The execution time of the algorithm, (mean and standard deviation for joint training and validation databases), was 201.2 ± 12.85ms, [min: 187.5 ms, max 234.4 ms] per signal set on a 2.13 GHz Intel® Core2™ processor. Each set had comprised signals with a total duration of 3s and was composed by a different number of channels between 109 and 120 channels.

6.3.2 Segmentation

Channels affected by artifacts were identified and replaced before the segmentation of the activation maps. An example is presented in Figure 6.4. It is possible to observe that RMS values corresponding to artifacts were correctly replaced even at the edges of the map. An example of the segmentation on different maps obtained for flexion, extension, pronation and supination in the five muscles is presented in Figure 6.5. The shape of the segmented area depended on the intensity of the peaks.

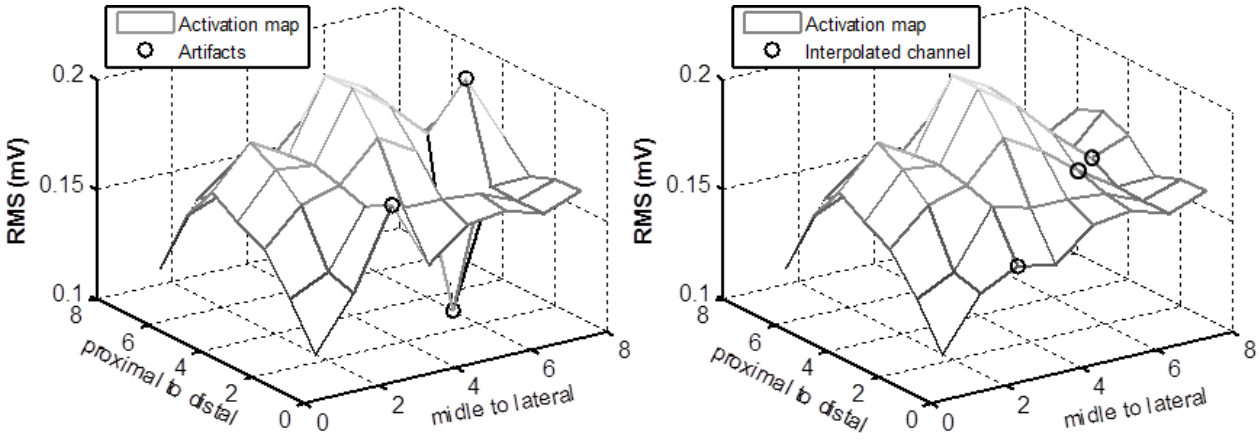

Figure 6.4. Substitution of RMS values due to artifact signals. RMS values of artifact channels are replaced by fitting the surface described by nearby non-artifact channels. Left. Sharp peaks caused by artifacts are marked with a circle. Right. Fitted surface obtained after replacing RMS values detected as artifacts (marked with a circle). Such points were replaced by fitting the surface described by non-artifact neighboring channels

The segmentation produced intensity maps for each muscle and subject, and allowed the calculation of average HDEMG maps representative for the 12 subjects in the study.

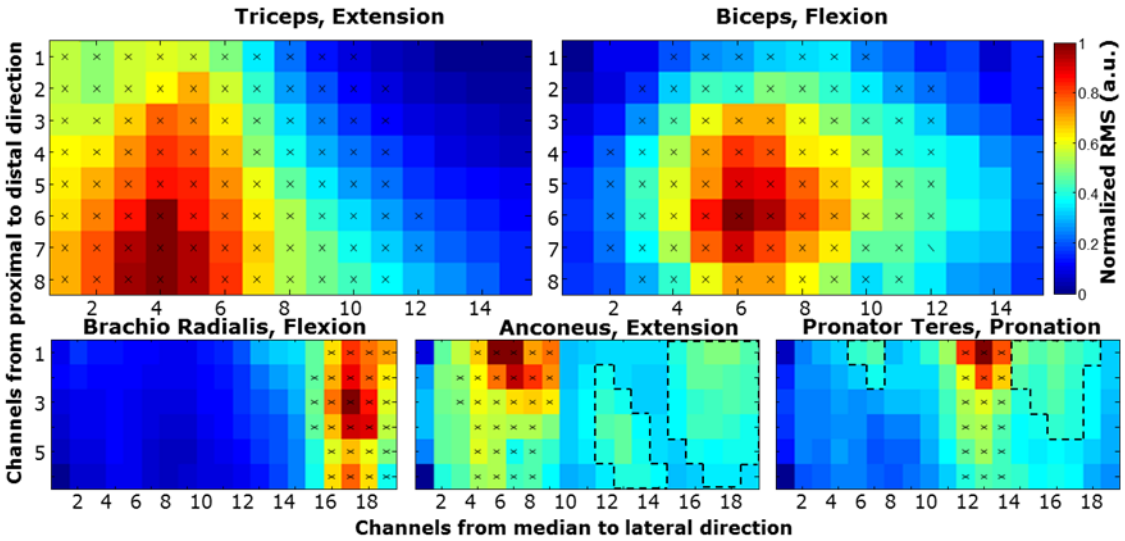

Figure 6.5. Example of segmentation of HD- EMG Maps from the right arm of subject 5: Triceps (top left), Biceps (top right), Brachio Radialis (bottom left), Anconeus (bottom middle), and Pronator Teres (bottom right). Maps corresponding to 50% MVC in exercises associated with the main function of each muscle are presented. Final segmented regions are presented with crosses. Regions limited by dash lines were also segmented and considered as belonging to neighboring muscles and were not taken into account to obtain the average map for the 12 subjects.

6.3.3 Bipolar vs. High-Density EMG signals

Significant differences were observed for the two-way Friedman test between $RMS_{av\text{-}bip}$ and $RMS_{av\text{-}HD}$ using the factor *muscle* as blocking factor (χ^2 (1) = 16.55, $p<0.001$). Thus, significant differences were observed when characterizing the different tasks and effort levels with information extracted from one or the other type of sensor.

Results for the overall classification into four or twelve groups are presented in Figure 6.6 for the variables $RMS_{av\text{-}bip}$ and $RMS_{av\text{-}HD}$.

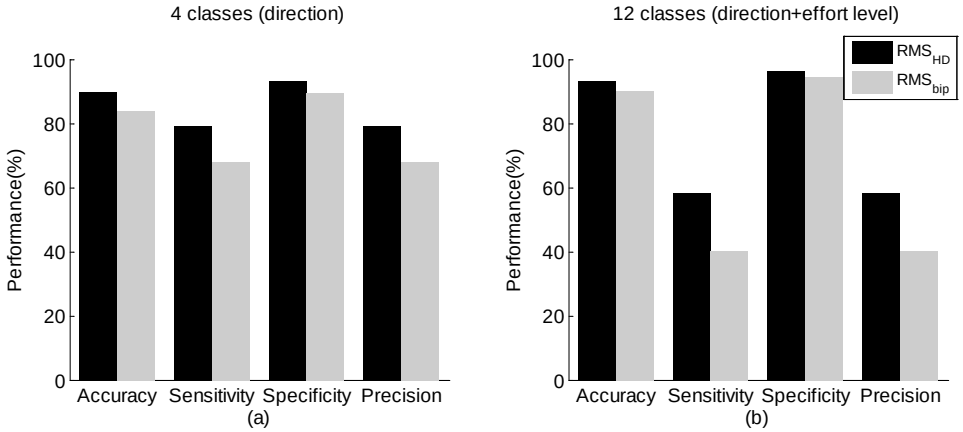

Figure 6.6. Classification performance using the feature $RMS_{av\text{-}HD}$ (in black) extracted from HD-EMG maps or $RMS_{av\text{-}bip}$ (in gray) extracted from single bipolar EMG signals. a). Four classes corresponding to type of task (flexion, extension, pronation and supination) or b). Twelve classes corresponding to type of task and effort level (10%, 30% or 50% MVC)

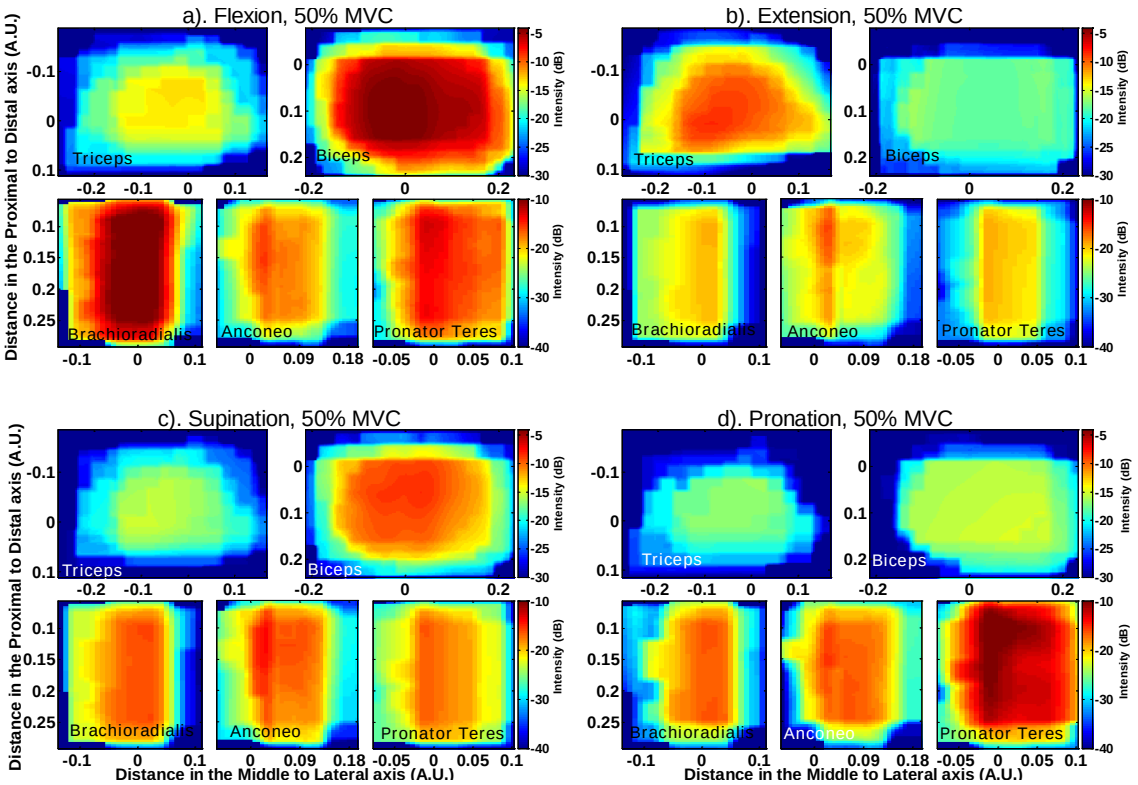

Figure 6.7. Average HD-EMG maps across subjects in the five assessed muscles: Triceps (top left), Biceps (top right), Brachioradialis (bottom left), Anconeus (bottom middle) and Pronator Teres (bottom right). Maps are displayed in db. The color scale for biceps and triceps is presented at the top of each figure and the color scale for brachioradialis, anconeus and pronator teres is presented at the bottom. a). Flexion at 50% MVC, b.) Extension at 50%MVC, c.) Supination at 50%MVC. d.) Pronation at 50%MVC

6.3.4 Average HD-EMG Maps

Average activation maps for the 12 subjects at 10, 30 and 50% MVC for each of the four tasks under study were obtained by averaging the individual maps of each subject. Results on average maps at 50%MVC are displayed in Figure 6.7.

TABLE 6-4. VARIABILITY BETWEEN THE 12 INDIVIDUAL MAPS ASSOCIATED WITH THE AVERAGE HD-EMG MAPS

	10%	30%	50%
Biceps (mean, [min max])	0.085, [0.07, 0.11]	0.18, [0.16, 0.2]	0.29, [0.23, 0.39]
Triceps (mean, [min max])	0.13, [0.084, 0.23]	0.15, [0.089, 0.2]	0.24, [0.11, 0.36]
Brachio Radialis (mean, [min max])	0.14, [0.063, 0.25]	0.16, [0.13, 0.21]	0.23, [0.17, 0.26]
Anconeus (mean, [min max])	0.13, [0.11, 0.14]	0.18, [0.12, 0.22]	0.2, [0.15, 0.23]
Pronator Teres (mean, [min max])	0.12, [0.063, 0.2]	0.16, [0.11, 0.2]	0.22, [0.15, 0.29]

Variability was measured through the standard deviation divided by the intensity for each pixel of the average map. Mean variability is shown by averaging the variability values over the segmented region for the four tasks. Results are presented as mean for 12 subjects including minimum and maximum values. This average was carried out for each muscle and each level of effort

Variability between subjects was measured through the standard deviation divided by the intensity for each pixel of the average map. Results are presented in Table 6-4.

In addition to the average maps at 50%MVC, their projections Q_k^x at 10%, 30% and 50%MVC for the two most active muscles in each type of task are presented in Figure 6.8. Each projection was normalized with respect to the maximum value reached at 50% MVC in order to observe changes of the intensity as a function of effort level and to compare among muscles and/or tasks. Changes observed are summarized as following:

- Flexion: Intensity decreased with decreasing levels of effort (from 50 to 10%MVC) in Biceps and Brachioradialis ($p<0.0005$), preserving a similar proportion in both muscles (Figure 6.8a).
- Extension: Intensity in Triceps decayed proportionally from 50% to 10% MVC ($p<0.0005$), but not in the Anconeus, where the maximum of the distribution was significantly different between 10% and 30% MVC ($p<0.009$) but not between 30% and 50%MVC. (Figure 6.8b)
- Supination: Intensity decreased from 50 to 10%MVC in Biceps and Anconeus ($p<0.0005$) but not in the same proportion in both muscles. Changes in the activation of the Anconeus were proportionally higher at 10% and 30%MVC when compared to changes in biceps, ($p<0.003$), although the former continued being the most active muscle in the contraction. (Figure 6.8c)
- Pronation: Intensity levels in Pronator Teres and Anconeus decreased similarly from 50 to 10%MVC. However, the normalized levels for Anconeus at 10%MVC were higher than those for Pronator Teres ($p<0.001$) showing that the contribution of the former was higher at lower levels of contraction. (Figure 6.8d)

The identification of movement intention by muscle co-activation is usual in pattern recognition approaches (Tkach, Huang & Kuiken 2010). Although such co-activation pattern has already been assessed with bipolar electrodes, performance of the identification

of tasks and even of the intended effort level were improved when considering HD-EMG maps from the upper-arm and forearm (see Figure 6.6). Additionally, differences in the co-activation of muscles were also reflected in the spatial distribution of the maps. Results for the repeated measures Friedman test for the spatial distribution variables μ_x and μ_y extracted from HD-EMG maps are presented in Table 6-5. It is possible to observe that the obtained χ^2 values were significant for four of the five analyzed muscles confirming possible changes in the spatial distribution with different tasks and/or effort levels.

TABLE 6-5.RESULTS FOR THE REPEATED MEASURES FRIEDMAN TEST FOR THE VARIABLES μ_x AND μ_y EXTRACTED FROM HD-EMG MAPS. THE TABLE PRESENTS THE $\chi^2(11,12)$ STATISTICS FOR 11 D.O.F. AND N=12 SAMPLES, AND ITS ASSOCIATED SIGNIFICANCE VALUE P FOR THE FIVE MUSCLES. STATISTICAL DIFFERENCES ARE MARKED WITH (*)

	$\chi^2(11,12)$		p	
	μ_x	μ_y	μ_x	μ_y
Biceps	47.84*	28.94*	<0.001*	<0.002*
Triceps	33.18*	42.98*	<0.001*	<0.001*
Brachioradialis	8.99	23.52	n.s.	n.s.
Anconeus	8.68	27.43*	n.s.	<0.004*
Pronator Teres	45.08*	31.96*	<0.001*	<0.001*

Furthermore, pair-wise comparisons between spatial-distribution variables obtained for different effort levels of the same task on a given muscle in Figure 6.8 were assessed by applying a Wilcoxon signed rank test to the medians. For example, μ_x in the Biceps, shifted to the left with increasing levels of contraction during flexion ($p<0.02$) and during supination ($p<0.05$). Such shifts were likely due to differences in the activation of the two heads of this muscle. Additionally, significant shifts were also found for the Pronator Teres during pronation ($p<0.05$).

Finally, interesting results were obtained when comparing spatial distributions between different kinds of task for the same muscle. Intensity levels can be very similar, with no significant differences in the absolute maxima of the projections, but differences were found in the spatial distribution along the x-axis. An example is presented for Biceps during supination at 50%MVC and flexion at 30%MVC in Figure 6.9a: The maxima of the projections Q_k^x were not significantly different (p.n.s) but their spatial distribution differed

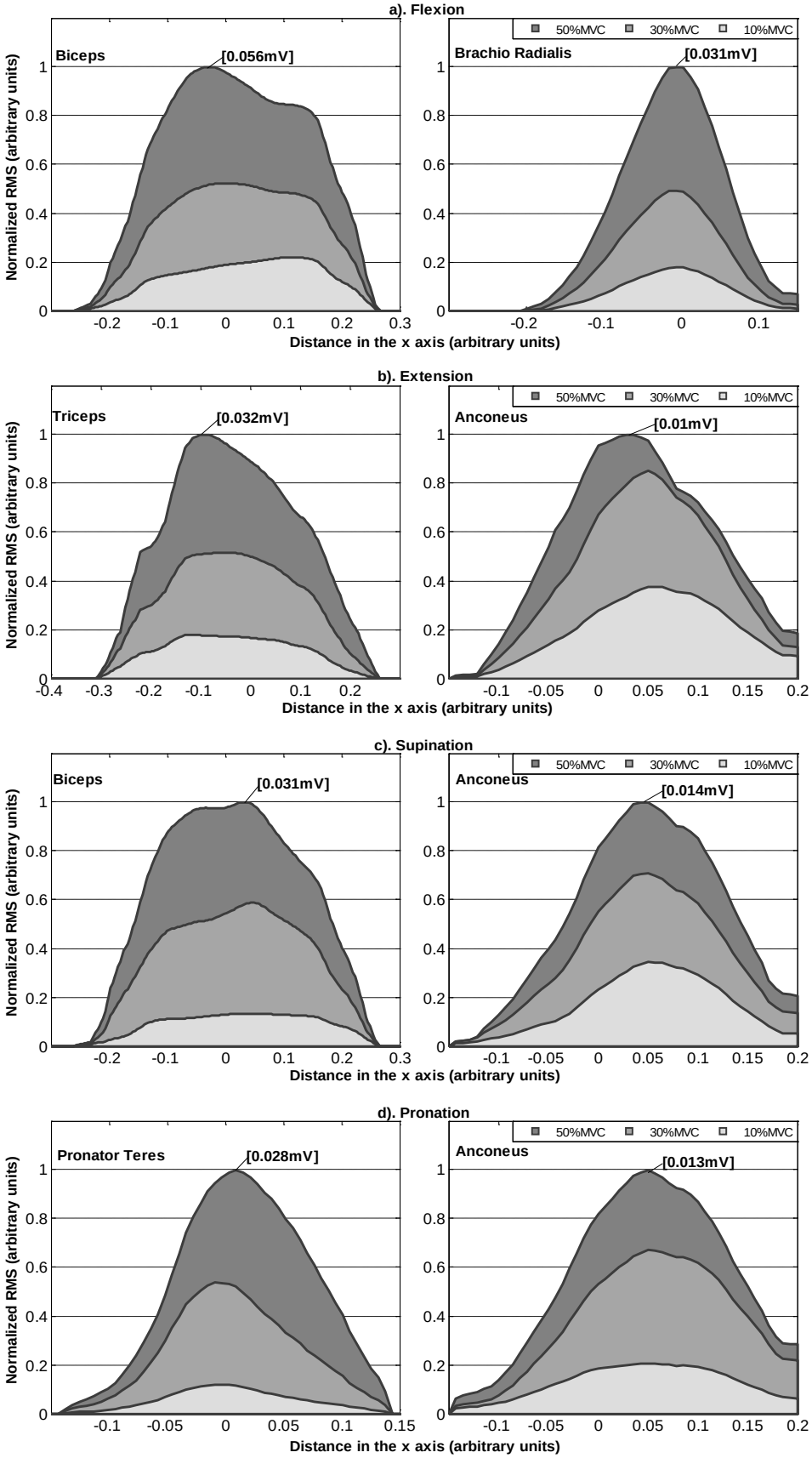

Figure 6.8. Contour distribution from the two most active muscles for each kind of exercise. Curves are normalized with respect to the maximum intensity reached at 50%MVC (showed with a label in each plot). a). Flexion in Biceps and Brachio Radialis, b.) Extension in Triceps and Anconeus. c.) Supination in Biceps and Anconeus, and d.) Pronation in Pronator Teres and Anconeus.

(i.e. different median μ_x, $p<0.04$). This effect was also observed in the Anconeus (Figure 6.9b.) when considering an extension and a pronation, both at 30% MVC ($p<0.05$ for the location of μ_x). Therefore, even when in these two examples the same muscle is active with similar levels of intensity, only the spatial distribution permitted to observe differences between tasks.

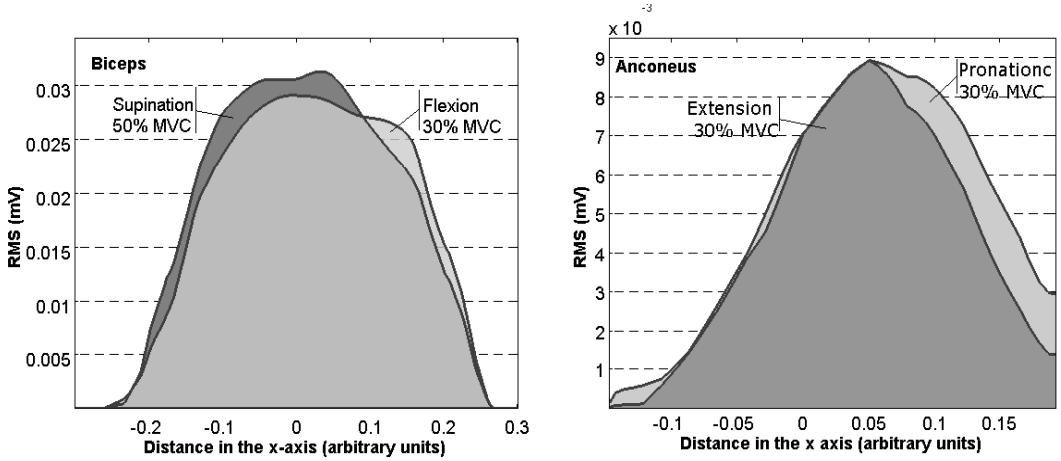

Figure 6.9. Contour distribution in the x-axis for Biceps during Supination at 50%MVC and Flexion at 30%MVC (left) and Anconeus during extension at 30%MVC and Pronation at 30%MVC (right). Although the maximum and the area under each curve were similar for different exercises (p.n.s), their contour distribution shifted laterally depending on the exercise kind.

6.4 Discussion and Conclusions

The main objective of the study was to extract information from HD-EMG maps that could be associated with four tasks at the elbow joint (forearm pronation and supination, and elbow flexion and extension) at different effort levels. This objective has been reached using 2D arrays of electrodes on five muscles in the upper-arm and forearm. It was shown no only that the average signal power extracted from HD-EMG maps may improve the differentiation of tasks and effort levels but also that the spatial distribution of the maps differed between tasks. Variables related with the spatial distribution of the intensity may complement the information provided by the amplitude of the signals in the identification of motion intention. Additionally, average HD-EMG maps for the four types of tasks and for the group of 12 voluntary subjects were obtained.

6.4.1 Detection of low-quality signals

Due to the high number of sEMG channels, an algorithm for the automatic detection of low quality signals was developed. In this study, the artifactual channels were removed and interpolated based on RMS values of neighbor channels in the HD-EMG maps.

As the number of channels affected by artifacts is usually much lower than the number of non- artifact channels, the number of TN is usually high, so the accuracy and especially, the specificity, is in general very high (>99%). In this study, the percentage of low quality signals was between 0 and 13% of the total number of channels of each set in the training database. For this reason, the ROC method, which was intended to compromise between specificity and sensitivity, provided an overestimated value of the former (the latter was always very high as it was explained above) at the expense of reducing the precision of the algorithm. On the other hand, PR method maximized the sensitivity while preserving the precision. Considering that both, the specificity and the accuracy were always very high, the use of PR was more convenient in our case since we were dealing with offline detection and interpolation of artifacts. In addition, the accuracy was slightly higher with the PR method. Other applications, especially those intended for online detection, should consider the ROC approach in order to increase the sensitivity as much as possible.

In addition, the sensitivity analysis for the constants k_{line}, k_1 and k_2 in Table 6-1 and 6-3 showed that the selected values represented a good compromise between the Precision and Sensitivity of the detection.

Different approaches have also been suggested for the detection of low quality signals. In (Marateb et al. 2012), a non-supervised method based on local distance-based outlier factor was proposed for HD-EMG signals recorded from the same muscles and electrodes arrays. That method did not required a training process and successfully detected low-quality signals with an average Accuracy of 91.9%, Sensitivity of 96.9% and Specificity of 96.4%. If the latter index is considered (refer to SP in Eq. 6-5), it is possible that such

method was prone to the inclusion of FP, given that the number of TN is always very high as explained before. This condition was not desired in our study because intensity values associated with low quality signals were later replaced in the maps based on neighbor channels, and if the latter were wrongly identified as artifacts (FP), the interpolation for the replacement was not possible. Thus, another method intended to minimize the number of FP while preserving the accuracy of the detection was proposed in the present work. Moreover, the method in (Marateb et al. 2012) did not take into account information provided by neighbor channels as in the present work.

A different study by Gronlund et al. in (Gronlund et al. 2005) assumed unimodal distribution of the amplitude of the signals and therefore it was not applicable to cases where the multichannel recording involved various regions with different levels of activity (as in Fig. 2) or even with no activity at all. The latter corresponded to regions localized far away from the main activation areas or to muscles marginally active during the contraction (an example can be observed in Figure 6.5 bottom-left for the signals recorded in array A1-forearm during flexion). In contrast, the algorithm proposed in the present work labeled a signal as an artifact based on the amplitude information of 6 neighboring channels (Eq. 6-4), avoiding general assumptions on the distribution of the potentials recorded in the array as proposed in (Gronlund et al. 2005).

Finally, the algorithm reached very high values for the performance indexes in the validation dataset (see Table 6-3). In addition, the channels identified as artifacts were correctly interpolated from the information of neighboring non-artifact channels even at the edges of the map (see Figure 6.4), which provided a smooth surface for subsequent stages of the analysis. Therefore, both the proposed methodology and features showed a very good performance for the detection and off-line replacement of low-quality signals.

6.4.2 Segmentation of HD-EMG maps

An automatic algorithm for the segmentation of active zones was proposed. This segmentation allowed the calculation of average HD-EMG maps for the population of 12 subjects by determining the ranges of active zones in the *x* and *y* axes relative to upper-limb circumference and muscle length respectively, and referred to the electrode location recommended for sEMG recording on the analyzed muscles.

Other methods have been previously proposed for the segmentation of activation maps. Particularly Vieira et al. in (Vieira, Merletti & Mesin 2010) proposed a method based on watershed for assessing muscle compartmentalization. Such segmentation was aimed at the extraction of zones associated with local variations in the level of neuromuscular activity in the same muscle and it was applied successfully with this objective on the gastrocnemius. However, we were interested in obtaining activation maps for each muscle associated with different types of contractions and levels of effort. This purpose required the isolation of muscle activity from background in individual maps before their average. Thus, the segmentation algorithm had to extract global activate regions, even if those were composed by several regional maxima. This last condition would lead to an over-segmentation in terms of the purpose of our study when using Watershed techniques (see Figure 6.10). On the other hand, h-dome was applicable straightforward without need of previous equalization or transformation of the original image and was not sensitive to regional maxima (28). For this reason the *h-dome* transformation was preferred in this work.

Furthermore, it is important to note that maps segmentation was not the aim of this study neither the determination of anatomical muscle regions but was an intermediate step in order to obtain average maps. It is known that potentials' amplitude diffuses across skin surface, so the actual size of active muscle regions might be overestimated by the segmentation proposed. In spite of this, the segmentation permitted the extraction of surface areas corresponding to different muscles in individual maps and also permitted to

focus on the regions of major activation, avoiding other active neighboring areas that could be more affected by the activity of nearby muscles (see Figure 6.5). By averaging individual segmented maps, it was possible to obtain representative HD-EMG maps associated with the activation of each muscle during the different tasks and effort levels. In this sense, the segmentation worked properly.

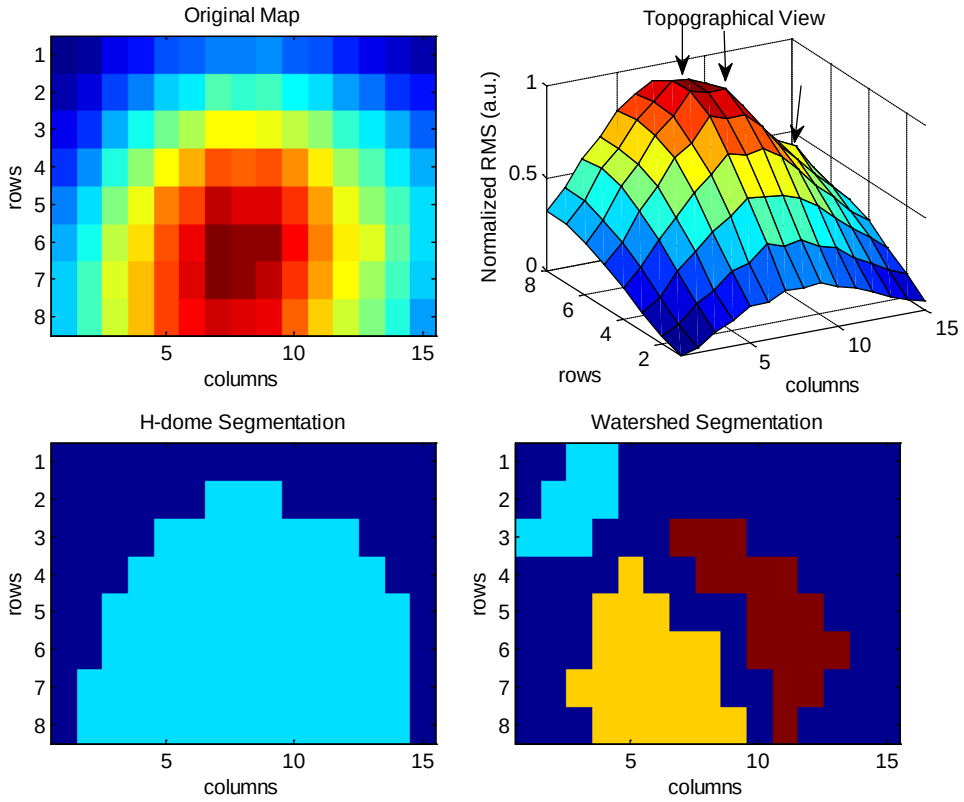

Figure 6.10. Segmentation of HD-EMG map from biceps of subject 2 during flexion at 10%MVC. The original map and its topographical view is presented at the top of the figure (left and right respectively). The segmentation obtained by H-dome transform is presented at bottom-left. The active zone in light blue is correctly isolated from the background image (displayed in dark blue). The watershed segmentation obtained 3 different zones: light blue, yellow and dark red (bottom-right) as consequence of multiple regional maxima indicated by arrows in the topographical view of the map. The final result of the segmentation is obtained after discarding those pixels whose intensity value is below 70% of the maximum intensity in each of the segmented zones. Such pixels correspond to the background (dark blue).

6.4.3 Average HD-EMG maps

Variability in the levels of intensity between subjects with respect to the average HD-EMG maps (Table 6-4) was found to be low enough to consider such maps as representative for the 12 subjects. The obtained differences were higher for higher levels of contraction (between 20% and 29% in the four tasks at 50%MVC) and being less than 12% for contractions at 10%MVC (see Table 6-4). In the average activation maps depicted in

Figure 6.7, it is possible to observe changes in the activation pattern corresponding to different tasks. Such differences were confirmed with the classification by LDA shown in Figure 6.6. Consequently, results concerning the spatial distribution and the levels of intensity from average maps can be considered as globally associated with the muscle function and to the activation pattern of the subjects in the study.

On the other hand, the classification performance was higher for the average power extracted from HD-EMG maps ($RMS_{av\text{-}HD}$) than from bipolar electrodes ($RMS_{av\text{-}bip}$) either for four or twelve classes, especially when considering the precision and sensitivity of the classification. Therefore it is possible to conclude that information extracted from the amplitude of signals recorded in high-dimensional configuration has more power to differentiate between tasks and even effort levels than single bipolar signals. With this respect, a recent study by Tkach et al. (Tkach, Huang & Kuiken 2010) and based on information extracted from bipolar signals, showed that the classification accuracy for the identification of motor tasks worsens when considering distinct strengths of the same motion. Substantial drops were observed when training and testing the classifier with data of mixed high and low effort levels obtaining a maximal accuracy of ~80% for the classification into the four tasks described in the present work. In our case, an overall classification accuracy of approximately 90% for 4 motor tasks with mixed data from very-low to medium-high effort levels (10%, 30% and 50% MVC) was obtained. What is more, classification accuracy for 12 classes was also in the order of 90%. However, in both cases the precision and sensitivity were not very high, thus additional data transformations or other features are necessary in order to improve the identification performance. In this sense, the Friedman test showed that variables related to the spatial distribution of the maps (μ_x and μ_y, see Table 6-5) may also assist in the discrimination between types of tasks and effort levels.

In addition, Tkach et al. also found that classification accuracy dropped when bipolar electrodes shifted by15 mm (Tkach, Huang & Kuiken 2010). Such shifts could be due to relative movements between the recording electrodes and the skin or because of errors when positioning the sensors, for example in different days. Thus another advantage of HD-EMG maps relies on the contact redundancy implied by the recording of a number of signals over a large surface of the muscle, as well as in the possibility of extracting features associated with spatial-changes induced by the central nervous system in the control of the muscles (Holtermann, Roeleveld & Karlsson 2005). All of this makes HD-EMG maps more robust to errors introduced by contact artifacts and by the relative location of the electrodes with respect to the origin of the potentials, especially in contractions involving joints movement or sensors repositioning.

When analyzing variables associated with the activation maps for the 12 subjects, it was possible to observe differences in the co-activation pattern of the muscles according to the kind of task and the effort level. For example during flexion at 50%MVC (see Figure 6.5), the Biceps, and the Brachioradialis were the most active muscles (as expected) but there was also an important activation of the Anconeus and of the Pronator Teres likely to stabilize the elbow joint and to compensate for the supination action of the biceps. The extension at 50%MVC was mainly produced by the Triceps and the Anconeus but the other two analyzed muscles in the forearm were also active. All selected muscles but Triceps were involved during Supination at 50%MVC with similar intensity levels among them. Finally, during Pronation at 50%MVC, naturally the most active muscle was the Pronator Teres but both the Anconeus and the Brachioradialis were also active while the muscles of the upper-arm appeared not to be active during the contraction. Additionally, when considering activation patterns for contractions at 30% and 10%MVC it was found that the levels of intensity did not decreased proportionally with effort level in all of the muscles, showing changes in the load-sharing of the involved muscles.

Differences in the average maps between 10%, 30% and 50%MVC were not only related to the levels of intensity but also to its spatial distribution. It was possible to observe differences in their projection over the *x*-axis (see Figure 6.8 and 6.9 and Table 6-5) for different effort levels depending on the task. These variations corresponded to shifts in the lateral to medial axis when the level of effort changed from 10% to 50% MVC. Furthermore, similar values of intensity were obtained for different kind of tasks in some muscles and differences were only found in the spatial distributions of the maps.

For all of this, HD-EMG maps instead of single bipolar signals, and variables related to maps intensity and spatial distribution might be useful in applications where identification of movement intention is needed: for example in robotic-aided therapies focused on the improvement of muscle coordination where the interaction between patient and machine is involved and where the robot has to be able to sense patient's intention (Hogan et al. 2006). Additionally, other applications implying proportional control for devices like powered- prostheses or orthoses could benefit from information provided by HD-EMG maps regarding not only the task but also its strength.

6.5 References

Bradford Barber, C., Dobkin, D.P. & Huhdanpaa, H. 1996, "The quickhull algorithm for convex hulls", *ACM Trans.Math.Softw.,* vol. 22, no. 4, pp. 469–483.

Farina, D., Colombo, R., Merletti, R. & Baare Olsen, H. 2001, "Evaluation of intra-muscular EMG signal decomposition algorithms", *Journal of Electromyography and Kinesiology,* vol. 11, no. 3, pp. 175-187.

Fawcett, T. 2006, "An introduction to ROC analysis", *Pattern Recognition Letters,* vol. 27, no. 8, pp. 861-874.

Fleiss, J.L. 1971, "Measuring nominal scale agreement among many raters", *Psychological bulletin,* vol. 76, no. 5, pp. 378-382.

Freriks, B. & Hermens, H.J. 1999, *SENIAM 9: European Recommendations for Surface ElectroMyoGraphy, results of the SENIAM project (CD),* Roessingh Research and Development b. v.

Gronlund, C., Roeleveld, K., Holtermann, A. & Karlsson, J.S. 2005, "On-line signal quality estimation of multichannel surface electromyograms", *Medical & biological engineering & computing,* vol. 43, no. 3, pp. 357-364.

Hampel, F.R. 1971, "A General Qualitative Definition of Robustness", *The Annals of Mathematical Statistics,* vol. 42, no. 6, pp. 1887-1896.

Hermens, H.J., Rau, G., Disselhorst-Klug, C. & Freriks, B. 1998, "Standards for Surface Electromyography: the European project (SENIAM). Surface Electromyography Application Areas and Parameters", *Proceedings of the Third General SENIAM Workshop on Surface Electromyography*Aachen, Germany.

Hogan, N., Krebs, H.I., Rohrer, B., Palazzolo, J.J., Dipietro, L., Fasoli, S.E., Stein, J., Hughes, R., Frontera, W.R., Lynch, D. & Volpe, B.T. 2006, "Motions or muscles? Some behavioral factors underlying robotic assistance of motor recovery", *Journal of Rehabilitation Research and Development,* vol. 43(5), pp. 605-18.

Holtermann, A., Roeleveld, K. & Karlsson, J.S. 2005, "Inhomogeneities in muscle activation reveal motor unit recruitment", *Journal of Electromyography and Kinesiology,* vol. 15, no. 2, pp. 131-137.

Kearns, M. & Ron, D. 1999, "Algorithmic stability and sanity-check bounds for leave-one-out cross-validation", *Neural computation,* vol. 11, no. 6, pp. 1427-1453.

Krzanowski, W.J. 1988, *Principles of Multivariate Analysis: A User's Perspective,* Oxford University Press, New York.

Landgrebe, T.C.W., Paclik, P., Duin, R.P.W. & Bradley, A.P. 2006, "Precision-recall operating characteristic (P-ROC) curves in imprecise environments", *Proc. of the 18th International Conference on Pattern Recognition*, pp. 123.

Marateb, H.R., Rojas-Martinez, M., Mansourian, M., Merletti, R. & Mananas Villanueva, M.A. 2012, "Outlier detection in high-density surface electromyographic signals", *Medical & biological engineering & computing,* vol. 50, no. 1, pp. 79-89.

Minium, E.W., Clarke, R.B. & Coladarci, T. 1999, *Elements of Statistical Reasoning,* Wiley NY, New York.

Serra, J. 1982, *Image Analysis and Mathematical Morphology,* Academic Press, London.

Tkach, D., Huang, H. & Kuiken, T.A. 2010, "Study of stability of time-domain features for electromyographic pattern recognition", *Journal of Neuroengineering and Rehabilitation,* vol. 7, pp. 21.

Vieira, T.M.M., Merletti, R. & Mesin, L. 2010, "Automatic segmentation of surface EMG images: Improving the estimation of neuromuscular activity", *Journal of Biomechanics,* vol. 43, no. 11, pp. 2149-2158.

Vincent, L. 1993, "Morphological grayscale reconstruction in image analysis: applications and efficient algorithms", *Image Processing, IEEE Transactions on,* vol. 2, no. 2, pp. 176-201.

Zar, J.H. 2010, *Biostatistical analysis,* 5th edn, Prentice Hall, New Jersey.

7

High- Density EMG Tasks Identification

7.1 Introduction

Surface electromyography (sEMG) records the superposition of the motor unit action potentials (MUAP) originated by discharges of the motor neurons during a voluntary muscular contraction. It can be used as a natural biological signal to infer motion intention of the user regarding the direction of the movement as well as its strength. sEMG signals have been widely used as control source for different devices in the field of human-machine interfaces including powered- prostheses and orthoses (Englehart, Hudgins 2003, Khokhar, Xiao & Menon 2010), rehabilitation robots (Dipietro et al. 2005) and assistive devices (Hogan et al. 2006).Therefore, when considering the control of a robotic device, the basic challenge consists in the extraction of a set of features from sEMG signals to be used as input information for the control of robotic systems. This procedure reduces the dimensionality of the raw sEMG signal by obtaining a feature vector that can later be used for pattern recognition, that is, for classifying the features related to different muscles or anatomical locations into classes associated to different kinds of user's intended motions or even to different strengths of that motion. The main advantage of establishing the interface at the neuromuscular level is the ability to estimate the forces that will be generated by the muscles before these effects can be directly measured by kinematic interfaces. This also applies to highly-impaired patients, who are unable to produce movement but are still able to weakly activate their muscles (Dipietro et al. 2005). This information could be fed into an exoskeleton system, so that when the muscles contract the exoskeleton amplifies the joint moment by a preselected gain factor. What is more, the identification of effort, (in terms of strength and direction) is also necessary in other applications involving games or rehabilitation exercises (De Biase et al. 2011) in order to

provide the subject with biofeedback. In this way, the subject can try to improve its performance or to reach a given target or goal.

Pattern recognition from sEMG signals has been extensively investigated during the past 50 years, especially for the control of powered prosthesis (Englehart, Hudgins 2003, Scheme, Englehart 2011, Parker et al. 2006). In general, classification accuracy obtained from pattern recognition has been very high. For example, (Englehart, Hudgins 2003) reported accuracy higher than 95% in classifying four wrist functions from sEMG. However, most of the studies in this field were focused on the recognition of motion intention regardless of its strength and distribution. We extend previous experience to the identification of the degree of exerted force and from EMG signals. Such information could be beneficial for the control of rehabilitation games, therapeutic or assistive devices (Khokhar et al. 2010). Moreover, in most of the studies, classification is based on features extracted from signals recorded while exerting a moderate force (Englehart, Hudgins 2003, Hargrove et al. 2009, Hargrove et al. 2007) whereas other recent studies have shown that classification accuracy worsens if the classifier is trained with a mixture of different levels of effort (Scheme, Englehart 2011, Tkach et al. 2010). In pattern recognition control, repeatable patterns of EMG activity are mapped to classes associated with multiple degrees of freedom-DOF based on the co-activation of different muscles for a given task (Scheme, Englehart 2011). However, such patterns may change at different force levels because of variations in the load-sharing of synergistic muscles or even because of differences in their motor unit recruitment thresholds (Merletti, Parker 2004). Thus, the correct identification of the activation level for proportional control (or simply for showing the user a map of activation) is still an open subject that needs to be solved before translating pattern-recognition approaches to clinical environment (Englehart, Hudgins 2003, Scheme, Englehart 2011, Parker et al. 2006), especially when considering applications to devices that are not necessarily prostheses.

In addition to the variations introduced by the exerted force, sEMG-based control is complex because of the large inter-individual variability of sEMG features due to muscle size, subcutaneous tissue thickness and location of innervation zones which affect the amplitude of the recorded action potentials. Additionally, signal amplitude changes because of muscle shift under the detection system and changing level of crosstalk from adjacent muscles (Parker, Englehart & Hudgins 2006, Tkach, Huang & Kuiken 2010). These variations are especially important when considering signals detected from one or few electrode pairs per muscle. These drawbacks can be reduced using High Density EMG

(HD-EMG) obtained from 2D arrays and processing the signal in the space dimension (Staudenmann et al. 2009 and Zwarts, Stegeman 2003). The processing of this kind of signals as a topographical image (HD-EMG map) provides a quantification of both the temporal and spatial characteristics of the electric muscle activity (Merletti et al. 2010a, Merletti et al. 2010b). It has been found that the spatial distribution of intensity in RMS maps changes with time (Tucker et al. 2009), pain (Madeleine et al. 2006) and force level (Holtermann, Roeleveld & Karlsson 2005). This change is related to "heterogeneity either in the distribution of the motor units within the muscle or in the strategy with which motor units are recruited" (Farina et al. 2008).Thus, spatial information can improve pattern recognition from sEMG when different effort levels are considered.

The main goal of the present study was the automatic identification of four types of isometric tasks associated to the DOF of the elbow: flexion, extension, supination and pronation and also the differentiation between levels of voluntary contraction at low-medium efforts. The classifier was trained and tested using pooled data corresponding to different levels of effort. The identification was attempted based on a new set of features extracted from HD-EMG maps, incorporating not only traditional time-domain variables, but also features associated to the distribution of potentials in the space of HD-EMG maps. This set of features showed very positive results for the classification of tasks, in spite of taking into account different levels of force, and even for the identification of the effort level associated to a single task.

This chapter deals with the extraction of a set of features related to HD-EMG maps from the forearm and upper-arm, to their distribution in the 2D space and with the use of a two-steps classifier based on linear discriminant analysis and muscle function information for each type of contraction for the identification of contractions at the elbow joint.

7.2 Methodology

7.2.1 Reference system

A reference coordinate system was defined for each muscle separately (biceps, triceps, etc.) in order to homogenize the coordinates of the recording electrodes locations among subjects. In all cases, the *x-axis* was parallel to the medial- lateral direction and the *y-axis* was parallel to the proximal-distal direction. Coordinates in both axes were normalized with respect to the circumference and length of the different limb segments where the electrode arrays were placed. *x- coordinates* for the reference systems were normalized with respect to:

- the circumference of the proximal forearm during a strong flexion contraction for the array 1;
- the circumference of the distal upper-arm during a strong flexion contraction for the array 2;
- the circumference of the proximal upper-arm during a strong extension contraction for the array 3.

Circumference was measured over the muscle belly of Brachioradialis, Biceps and Triceps respectively.

On the other hand, *y-coordinates* for the reference systems were normalized with respect to:

- the distance from the medial Epicondyle to the Apofisis of the radius for the array 1;
- the distance between reference points proposed by SENIAM project for the triceps and biceps in arrays 2 and 3 respectively: from the Acromion to the Fossa Cubit (d_1) for the former, and from the Acromion to the Olecranon (d_2) for the latter (Freriks, Hermens 1999).

The origin of the coordinate axes of the reference system for each muscle was defined as follows:

- For muscles recorded on array 1 the origin of the *x-axis* laid in the intersection between the line that connects the origin and insertion of each muscle of the forearm (Kendall F. P., Kendall McCreary E., and Provance P.G. 1993) and the arc traced around the forearm 2 cm below the elbow crease. The origin of the *y-axis* was placed on this arch.
- the origin of the reference coordinate systems for biceps and triceps corresponded to landmarks proposed by SENIAM project: at the points located at ¾ d_1 and at ½ d_2 respectively over the lines that connect the origin and insertion of such muscles (Freriks, Hermens 1999).

7.2.2 Feature Extraction

Features for the identification of tasks and levels of effort were related to the level of intensity and to the distribution of such intensity of HD-EMG maps in the space. Four features were extracted from the segmented area for each of the five selected muscles: Mean and Maximum Intensities (μI and *maxI*, respectively), and the coordinates of Centre of gravity and Maximum (**CG** and **MX,** respectively). Intensity- based features (μI and

maxI) are related to the amplitude of EMG signal, which is commonly used in the control of prosthesis and other human- machine interfaces (see for example (Dipietro et al. 2005, Andreasen, Alien & Backus 2005). The inclusion of spatial-based features (**CG** and **MX**) was motivated by previous findings (see Chapter 6), and by the work of Holterman et al. who found that the spatial distribution of HD-EMG maps changed with force level (Holtermann, Roeleveld & Karlsson 2005).

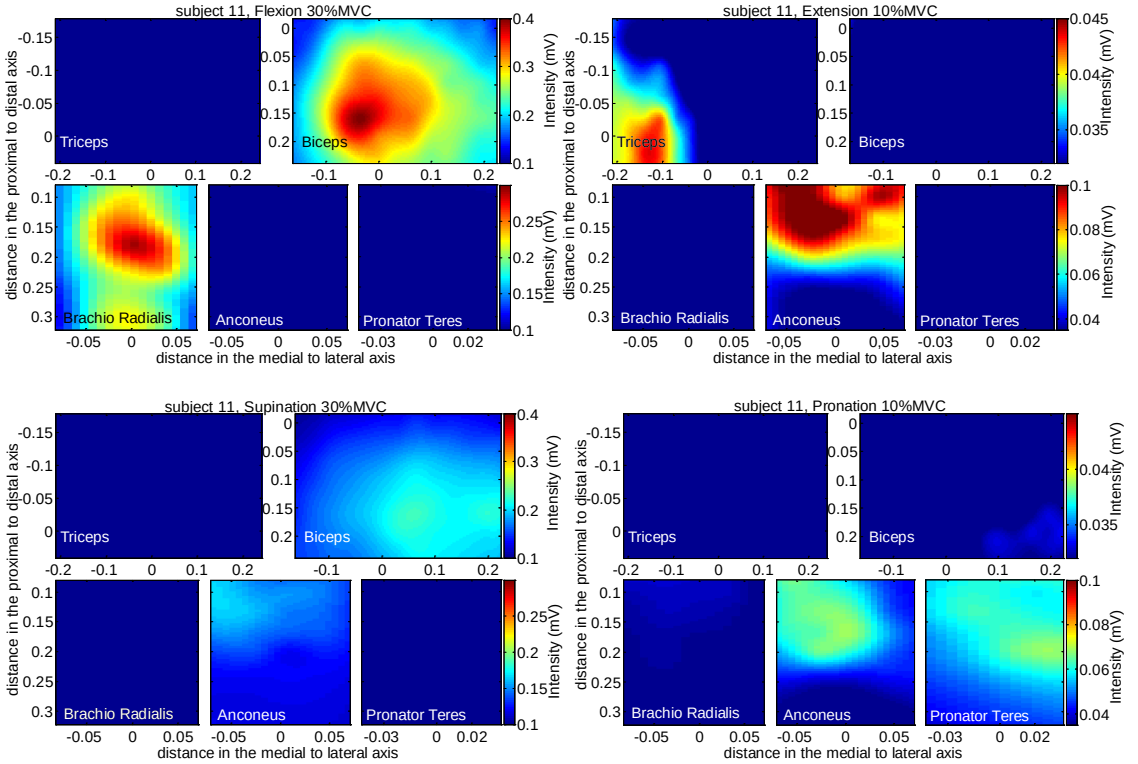

Figure 7.1. Monopolar HD-EMG maps for subject 11 obtained for the five muscles under study: triceps, biceps, brachioradialis, anconeus and pronator teres. The full maps are presented. The four tasks are indicated: flexion at 30%MVC (top- left), extension at 10%MVC (top right), supination at 30%MVC (bottom-left) and pronation at 10%MVC (bottom-right). The maps are interpolated in both dimensions in space for visualization purposes only. It is possible to observe differences in the average intensity as well as in the spatial distribution of the maps. Note that the scales are linear and different scales were used for maps at 30%MVC and maps at 10%MVC in order to appreciate the spatial distribution of the RMS of the signals at low effort levels. The maps are represented in the reference system for each muscle as described in Methods.

Examples of different HD-EMG maps obtained for subject 11 are presented in Figure 7.1. Maps corresponding to the five analyzed muscles and to the four tasks are displayed. Two effort levels at 10% and 30% MVC are shown in order to illustrate graphically the described differences, not only with respect to the average intensity of the maps but also with respect to their spatial distribution. It is possible to observe that different muscles are active according to the intensity levels of the maps and depending on both, the task and the effort level. It is also possible to observe spatial shifts in the intensity values or the

maximum, for example when comparing flexion and supination both at 30%MVC in Biceps.

Spatial features were computed by two methods: one considered the global segmented area ("global mass" method) while the other one considered only the areas with the highest intensity ("isolated masses" method).

In the "global mass" method, all pixels were considered for computing the center of gravity of the segmented area as:

$$\mathbf{CG^{GM}} = \frac{1}{GM}\sum_{n=1}^{N} H_n \cdot \mathbf{u}_n, \mathbf{MX^{GM}} = \mathbf{v} \text{ (Eq. 7-1)}$$

where H corresponded to the value of intensity (i.e. RMS) of channel n located at the positions (i, j) of the map $Is_{i,j}$ (please refer to Eq. 6-8 in Chapter6), whose position in the new reference coordinate system (x, y) is described by the vector **u**, N is the number of elements in the total segmented area and $GM = \sum_{n=1}^{N} H_n$ is the total sum of the values of intensity across N elements (i.e., the "global mass" of the segmented area of the map) . On the other hand, the vector **v** described the position of the electrode with maximum intensity in the map. Both, **u** and **v** had components in x and y and so, $\mathbf{CG^{GM}}$ and $\mathbf{MX^{GM}}$ were defined as bi-variate features. Nevertheless, this method was sensitive to local variations in the amplitude of the signals on a given neighborhood (which were reflected in the RMS value obtained from individual channels) especially if the activation was low (10%MVC). These variations could be explained by differences in the electrode-skin impedance of different channels, noise, or even by crosstalk from adjacent muscles. Besides, the method was also dependent on the location of innervation zones and on the geometry of the segmented area.

In the second method, the coordinates of the maximum intensity (MXm) and of the center of gravity (CGm) were obtained by analyzing Isi,j as a set of "isolated masses" corresponding to isolated regions of high intensity (peaks) within the map. Additionally, using a constraint related to the minimum size of the masses, it was possible to obtain a better estimation of the maximum intensity (maxIm) and its location within the map, avoiding bright spots caused by dramatic variations in RMS values as described in the previous paragraph that could not have been considered as artifacts.

The "isolated masses" method consisted in:

1). Extraction of T intensity peaks within the map by applying an *h-dome* transformation intended for the segmentation of isolated areas with high intensity .The

image *I* was viewed as a topographical map with different elevations corresponding to peaks of intensity or *domes*, which were extracted from the background by a morphological reconstruction of the Image. Details are described in (Vincent 1993) and an application is described in Chapter 6. Isolated domes extracted from the image were used to arrange a system of T isolated masses.

2). Estimation of the center of gravity of the system of masses and the position of the maximum intensity as

$$\mathbf{CG^m} = \frac{1}{\sum_{t=1}^{T} m_t} \sum_{t=1}^{T} m_t \cdot \mathbf{cg}_t\,, \quad \mathbf{MX^m} = \mathbf{w} \text{ (Eq. 7-2)}$$

Where m_t and $\mathbf{cg_t}$ represent the mass and the coordinates of center of gravity calculated analogously to (Eq. 7-1) across K pixels for each isolated mass t=1, 2…T, and $\mathbf{w}$ is the position vector of the maximum value of intensity considering only the T masses.

An example of both approaches is presented in Figure 7.2. The map displays an activation of both heads of Biceps during flexion at 50% MVC. It is possible to observe a valley in the middle of the activation zone affecting the estimation of the center of gravity obtained by applying the "global mass" method. On the other side, the center of gravity is attracted to the masses at the left (m_1 and m_2) when applying the "isolated masses" method.

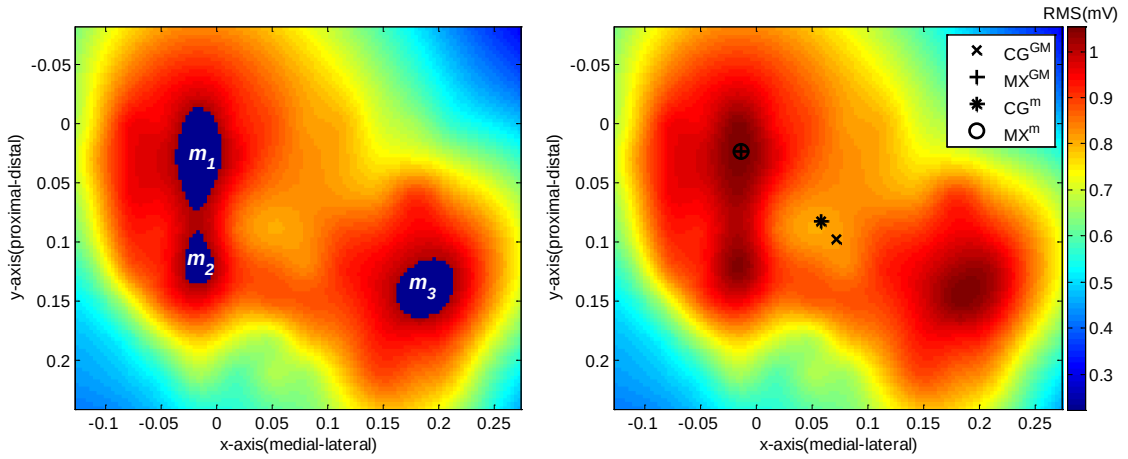

Figure 7.2. Example of monopolar HD-EMG Intensity map *I* from Biceps during flexion at 50% MVC. A system of T=3, [m_1, m_2, m_3] masses is obtained after the *h-dome* transformation (left). The center of gravity- $\mathbf{CG^m}$ obtained from the "isolated masses" method (*) is closer to the brightest area (i.e. the two masses m_1 and m_2 at the left) than the $\mathbf{CG^{GM}}$ obtained from the "global mass" method (×) (right). The maps are represented in the reference system for biceps as described in Methods.

On the other hand, and considering that the relationship between exerted force and EMG amplitude is not necessarily linear (Staudenmann et al. 2010), the Intensity level of each map was parameterized according to the logarithm of the maximum value ($maxI^{GM}$, $maxI^{m}$) and of the mean value (μI) of intensity of the maps. The former was calculated

using both approaches explained above: $maxI^{GM}$ and $maxI^{m}$ by the "global mass" and "isolated masses" methods respectively:

$$maxI^{GM} = log_{10}\left[\max\left(Is_{i,j}\right)\right] \ , maxI^{m} = log_{10}[\max(Ip_t)] \ \forall\, t = 1..T$$

$$\mu I = log_{10}\left[\frac{1}{N}\sum_i \sum_j Is_{i,j}\right] \quad \text{(Eq. 7-3)}$$

where Is_{ij} was defined in Eq. 6-8 for the N pixels of the segmented area and I_p is each of the segmented peaks *t* after the h-dome transform. Log-transformations have been found useful for characterizing the force-EMG relationship in the past (Herda et al. 2011).

7.2.3 Classification

The main research question of the study was if it is possible to differentiate among tasks and effort levels involving isometric contractions related to flexion, extension, supination and pronation at three submaximal contractions on the basis of HD-EMG maps.

A linear discriminant classifier (LDC) (Krzanowski 1988) based on the spatial distribution and intensity of the activation maps was proposed. Different sets of features defined in the previous section were used: coordinates of $\mathbf{CG^{GM}}$, $\mathbf{CG^{m}}$, $\mathbf{MX^{GM}}$ and $\mathbf{MX^{m}}$ and intensity descriptors μI, $maxI^{GM}$ and $maxI^{m}$ for each of the five areas corresponding to the five selected muscles. The classification was carried out by applying the Leaving One Out method (Kearns, Ron 1999). Two approaches were considered in order to define two classifiers for the discrimination between tasks and/or between levels of effort from intensity-based features and/or spatial-based features.

The first approach, called 1-step LDC, classified simultaneously both task and level of effort, that is, 12 groups. In this case, features extracted from all of the five muscles were considered.

The second approach was based on a two-steps classification and was called 2-steps LDC. Firstly, features were classified according to the four types of task (i.e. flexion, extension, supination or pronation) considering different combinations of the described features from the five muscles. Then, a second classification according to the level of effort was carried out. This second step was based solely on the features obtained from those muscles that were expected to be involved during that particular task (identified during the first step). Such subset of muscles was chosen to be composed by at least one agonist and one antagonist as follows: Biceps and Triceps for both flexion and extension, Biceps, Brachioradialis and Anconeus for supination and Pronator Teres and Anconeus for

pronation. The inclusion of these subsets of muscles was also supported by previous results (Rojas-Martínez et al. 2012), where significant differences were found for both intensity levels and their spatial distribution as obtained for variations in the levels of effort relative to the maximal voluntary contraction in the selected muscles during these tasks.

Performance of the automatic classification was defined in terms of Sensitivity(S), Specificity (SP), Precision (P) and Accuracy (Acc) (Farina et al. 2001) as:

$$S = \frac{TP}{TP+FN} \quad SP = \frac{TN}{TN+FP} \quad P = \frac{TP}{TP+FP} \quad Acc = \frac{TP+TN}{TP+FP+TN+FN} \quad \text{(Eq. 7-4)}$$

where True Positives (TP) is the number of elements of group *x* classified as belonging to class *x*, False Positives (FP) is the number of elements belonging to other groups and classified as class *x*, False Negatives (FN) is the number of elements of group *x* classified as belonging to other groups and True Negatives (TN) is the number of elements of other groups that were not classified as belonging to class *x*.

7.3 Results

7.3.1 Classification based on Spatial Distribution of HD-EMG maps

First of all, a Multivariate Analysis of Variance was applied to the features $\mathbf{CG^m}$ and $\mathbf{CG^{GM}}$ obtained from the five muscles in order to assess their power in discriminating the four types of task. A significant interaction for the factor "group" (i.e. type of task) was found as estimated from Pillai's Trace (Anderson 1984), obtaining a much lower significance for the case of feature $\mathbf{CG^m}$ ($p<<0.0001$) than for $\mathbf{CG^{GM}}$ ($p<0.04$). These results confirmed the expected differences between the two methods when calculating the spatial distribution-based features.

TABLE 7-1. PERFORMANCES INDEXES FOR THE CLASSIFICATION ACCORDING TO TYPE OF TASK BASED ON SPATIAL-BASED FEATURES. RESULTS PRESENT THE AVERAGE PERFORMANCE INDEXES FOR THE CLASSIFICATION IN FOUR GROUPS AS MEAN ± STANDARD DEVIATION FOR 144 OBSERVATIONS (12 SUBJECTS × 4 TASKS × 3 EFFORT LEVELS).

	Accuracy (%)	Sensitivity (%)	Specificity (%)	Precision (%)
$\mathbf{CG^m}$	78.1±3.8	56.3±6.9	85.4±4.0	56.7±8.2
$\mathbf{MX^m}$	78.8±2.8	57.6±11.2	85.9±2.4	57.4±5.7

Since the method of "isolated masses" proved to be more sensitive than the one based on distributed masses, in further classifications, only features $\mathbf{CG^m}$, $\mathbf{MX^m}$, $maxI^m$ and μI will be used instead of the ones obtained from the classical "global mass" method.

Finally, spatial-based features **CG^m** and **MX^m** were used for the discrimination of type of tasks (flexion, extension, supination and pronation) in order to evaluate its performance when used in isolation avoiding the inclusion of any other type of feature. Results are summarized in Table 7-1 as mean ± standard deviation for the four types of task.

7.3.2 Classification based on Intensity of HD-EMG maps

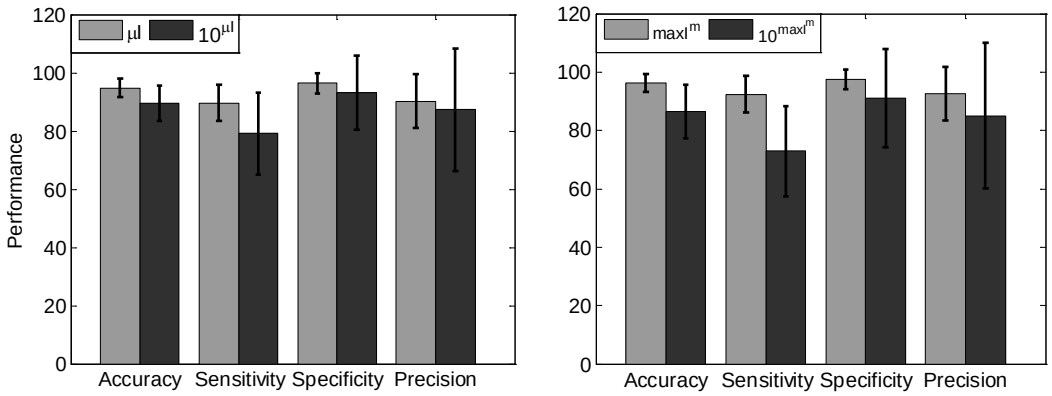

Figure 7.3. Performance indexes for the classification according to type of task: flexion, extension, supination or pronation. The LDC classifier used the Log Intensity-based features μI or maxI^m (Eq. 7-3). Performance indexes obtained without applying the log-transformation are also presented (i.e.10μI or 10maxIm). Results present the performance of the classification in four tasks as mean ± standard deviation of the four Performance Indexes.

Features μI and $maxI^m$ were used for differentiating between flexion, extension, supination and pronation. Performance of the classification by using the 1-step LDC is presented in Figure 7.3 for the log-transformed features μI and $maxI^m$ as well as for the non-transformed ones for comparison purposes. Higher accuracy is observed for the former with respect to the latter. This could be because the relationship between force and EMG is not linear and its better explained by log-transformations of the amplitude (Herda et al. 2011). Hence, log-transformed intensity features (see Eq. 7-3) will be used for further classifications.

TABLE 7-2. PERFORMANCE INDEXES FOR THE CLASSIFICATION IN TYPE OF TASK + EFFORT LEVEL BASED ONLY ON INTENSITY-BASED FEATURES (μI OR maxI^m). THE CLASSIFICATION IS PERFORMED USING THE TWO CLASSIFIERS: 1- STEP LDC AND 2-STEPS LDC. RESULTS PRESENT THE AVERAGE PERFORMANCE INDEXES FOR THE 12 CLASSES CORRESPONDING TO IDENTIFIED TASKS AND ITS LEVELS OF CONTRACTION AS MEAN ± STANDARD DEVIATION FOR 144 OBSERVATIONS(12 SUBJECTS × 4 TASKS ×3 LEVELS) ..

Class. Meth.	Feature	Accuracy (%)	Sensitivity (%)	Specificity (%)	Precision (%)
1- step LDC	μI	92.8 ± 2.4	56.9 ± 13.2	96.1 ± 1.80	57.9 ± 13.8
	$maxI^m$	93.3 ± 2.0	59.7 ± 11.1	96.3 ± 1.5	60.6 ± 13.9
2- steps LDC	μI	94.3 ± 2.2	66.0 ± 14.0	96.9 ± 1.5	66.5 ± 14.5
	$maxI^m$	94.8 ± 2.1	68.8 ± 14.3	97.2 ± 1.4	69.2 ± 13.1

Table 7-2 presents the performance indexes obtained by using the 1-step and 2-steps LDC for the joint classification of four tasks and three effort levels using the features μI or $maxI^m$. Results are shown as mean and standard deviation among the 12 groups.

7.3.3 Classification based on Combined Intensity and Spatial distribution of HD-EMG maps

Different combinations of intensity-based (μI or $maxI^m$) and spatial- based features ($\mathbf{CG^m}$ or $\mathbf{MX^m}$) were used as inputs for the LDC (one or two steps) to discriminate between tasks or tasks and their corresponding effort levels. Regarding task identification, similar results were obtained for all the combinations obtaining an accuracy and sensitivity higher that 95% and 90% respectively. Results for the combination $maxI^m$+$\mathbf{MX^m}$ which presented the best average performance are shown in Table 7-3. In this case, the task extension presented a perfect discrimination (Acc=100%) while supination was the most difficult to differentiate with an Acc= 94.4% and S=P=88.9%.

TABLE 7-3. PERFORMANCE INDEXES FOR THE CLASSIFICATION IN FLEXION, EXTENSION, SUPINATION OR PRONATION. THE LDC CLASSIFIER USED THE COMBINATION OF FEATURES maxI^m+$\mathbf{MX^m}$. RESULTS PRESENT THE TOTAL PERFORMANCE OF THE CLASSIFICATION AND THE AVERAGE OF THE FOUR GROUPS AS MEAN ± STANDARD DEVIATION FOR 144 OBSERVATIONS (12 SUBJECTS × 4 TASKS × 3 EFFORT LEVELS)

Type of task	Accuracy (%)	Sensitivity (%)	Specificity (%)	Precision (%)
Flexion	97.2	97.2	97.2	92.1
Extension	100	100	100	100
Supination	94.4	88.9	96.3	88.9
Pronation	95.8	88.9	98.2	94.1
Average	**96.9±2.4**	**93.8±5.7**	**97.9±1.6**	**93.8±4.7**

Results for the classification in 12 groups corresponding to type of exercise and level of effort are presented in Table 7-4. The LDC classifier was applied in one or two steps. According to results in the previous paragraph, the pair of features $maxI^m$ + $\mathbf{MX^m}$ was used for both, the 1-step LDC and for the identification of type of task in the first layer of the 2-steps LDC. Once the type of task was determined, the 2-steps LDC used all possible combinations of features between μI or $maxI^m$ and $\mathbf{CG^m}$ or $\mathbf{MX^m}$. The best performance was obtained by using the features $maxI^m$+ $\mathbf{CG^m}$ for the differentiation of effort levels during flexion and extension and from μI+$\mathbf{MX^m}$ for determining the effort levels during supination and pronation.

TABLE 7-4. PERFORMANCE INDEXES FOR THE CLASSIFICATION IN 12 GROUPS OBTAINED FROM LDC IN ONE AND TWO STEPS. THE FIRST STEP USED THE COMBINATION $\max I^m + \mathbf{MX}^m$. RESULTS ARE PRESENTED AS MEAN ±STANDARD DEVIATION FOR THE THREE LEVELS OF EFFORT COMPRISING 36 OBSERVATIONS IN EACH TASK (12 SUBJECTS × 3 EFFORT LEVELS). THE AVERAGE PERFORMANCE IS ALSO PRESENTED AT THE BOTTOM OF EACH SUBTABLE.

Classifier	Type of task	Accuracy (%)	Sensitivity (%)	Specificity (%)	Precision (%)
1- step LDC	Flexion	94.2 ± 2.4	66.7 ± 14.4	96.7 ± 1.6	65.4 ± 15.9
	Extension	92.4 ± 5.4	52.8 ± 34.7	96.0 ± 3.1	53.6 ± 33.0
	Supination	92.0 ± 2.4	55.6 ± 17.4	95.2 ± 1.2	50.9 ± 12.9
	Pronation	91.0 ± 3.0	41.7 ± 25.0	95.5 ± 1.5	43.4 ± 21.3
	Average	**92.4 ± 3.3**	**54.2 ± 22.6**	**95.8 ± 1.8**	**53.3 ± 20.6**
2- steps LDC	Flexion	97.7 ± 0.8	88.9 ± 9.6	98.5 ± 1.5	86.1 ±12.7
	Extension	95.4 ± 2.4	72.2 ±21.0	97.5 ± 0.9	71.3 ±12.4
	Supination	96.3± 1.1	77.8 ± 4.8	98.0 ± 1.6	79.5 ±11.8
	Pronation	95.8 ± 1.2	72.2 ± 9.6	98.0 ± 0.4	76.3 ± 6.1
	Average	**96.3 ± 1.6**	**77.8 ±13.0**	**98.0 ± 1.1**	**78.3 ±11.0**

The major problem was observed to separate between contraction levels at 30% and 50% MVC because such levels of effort are similar. In order to quantify this situation and to evaluate the capability of the LDC to differentiate between low and medium levels of effort, the contractions at 30% and 50% MVC were pooled and differentiated from those at 10% MVC. Results for the 2-steps LDC are presented in Table 7-5 where an important improvement in the performance of the classifier can be observed.

TABLE 7-5. PERFORMANCE INDEXES FOR THE CLASSIFICATION INTO EIGHT GROUPS BY USING THE 2-STEPS LDC. RESULTS ARE PRESENTED AS MEAN ±STANDARD DEVIATION FOR THE 2 LEVELS OF EFFORT (10% AND 30%-50%MVC) COMPRISING 36 OBSERVATIONS (12 SUBJECTS × (1+2) EFFORT LEVELS) IN EACH TASK. THE PRIORS OF THE 2 STEPS CLASSIFIER WERE MODIFIED IN ORDER TO TAKE INTO ACCOUNT THE DIFFERENT SIZE OF THE GROUPS PROVIDING THAT CONTRACTIONS AT 50% AND 30% MVC WERE POOLED TOGETHER.

Type of task	Accuracy (%)	Sensitivity (%)	Specificity (%)	Precision (%)
Flexion	97.9 ± 1.0	91.7 ± 11.8	98.4 ± 0.1	87.8 ± 6.4
Extension	97.9 ± 0	91.7 ± 0	98.8 ± 0.5	90.1 ± 7.8
Supination	96.5 ± 0	85.4 ± 3.0	98.0 ± 0.4	84.1 ± 10.2
Pronation	96.5 ±1.0	83.3 ± 0	98.5 ± 2.1	85.7 ± 20.2
Average	**97.2 ± 0.9**	**88.0 ± 6.1**	**98.4 ± 0.9**	**87.0 ± 9.7**

7.3.4 Classification using smaller sets of electrode arrays

Identification of tasks and levels of efforts using smaller electrodes arrays was also considered in order to evaluate the classification performance using a lower number of electrodes located around a generic anatomical point. A subset of the arrays corresponding to a square grid of 3×3 channels centered at the average of the $\mathbf{CG}^m$ and $\mathbf{MX}^m$ for the 12

subjects for each muscle was used for the calculation of intensity-based feature $maxI^m$. This feature was considered since its classification performance was better than with the other intensity-based feature μI (see Figure 7.3 and Table 7-2) when using the total segmented area of the arrays. Thus, a total number of 45 electrodes were considered to obtain EMG signals from the five muscles. The coordinates of the center of the 3×3 grid of electrodes for each muscle are presented in Table 7-6 considering two anatomical possible reference locations: at the average $\mathbf{CG}^{\mathbf{m}}$ or at the average $\mathbf{MX}^{\mathbf{m}}$ for the 12 subjects.

TABLE 7-6. REFERENCE ELECTRODE LOCATIONS BASED ON THE AVERAGE COORDINATES OF THE CENTER OF GRAVITY ($\mathbf{CG}^{\mathbf{m}}$) OR OF THE MAXIMUM VALUE ($\mathbf{MX}^{\mathbf{m}}$) FOR THE 12 SUBJECTS. RESULTS ARE RELATIVE TO THE DIMENSIONS OF THE LIMB. THE ORIGIN OF THE SYSTEM IS DESCRIBED IN SECTION 7.2.1 OF METHODS

		Biceps (%)	Triceps (%)	Brachioradialis (%)	Anconeus (%)	Pronator Teres (%)
$\mathbf{CG}^{\mathbf{m}}_{\mathbf{average}}$	x	3.1	-5.9	0.1	3.6	1
	y	8.9	-3.0	15.8	15.9	13.5
$\mathbf{MX}^{\mathbf{m}}_{\mathbf{average}}$	x	5.6	-3.5	0	3.4	1.2
	y	9.6	-3.6	13.9	15.0	11.7

The classification in four or 12 classes associated to type of task or to the joint classification in tasks and effort levels at 10%, 30% and 50% MVC is summarized in Table 7-7. The two locations of the 3×3 grid of electrodes arrays over each muscle as described above were considered.

TABLE 7-7. PERFORMANCE INDEXES FOR THE CLASSIFICATION IN FOUR CLASSES CORRESPONDING TO TYPE OF TASK (FLEXION, EXTENSION, PRONATION AND SUPINATION) AND IN 12 CLASSES (2-STEPS LDC) INVOLVING 3 DIFFERENT EFFORT LEVELS FOR EACH TASK. CLASSIFICATION IS BASED ON $maxI^M$ FROM A 3X3 GRID CENTERED AT $\mathbf{CG}^{\mathbf{m}}_{\mathbf{average}}$ OR AT $\mathbf{MX}^{\mathbf{m}}_{\mathbf{average}}$

Electrode-array location	No. of Classes	Accuracy (%)	Sensitivity (%)	Specificity (%)	Precision (%)
$\mathbf{CG}^{\mathbf{m}}_{\mathbf{average}}$	**4**	93.8 ± 3.3	87.5 ± 9.2	95.8 ± 1.9	87.5 ± 6.1
	12	93.6 ± 2.5	61.8 ± 18.6	96.5 ± 1.5	61.5 ± 15.9
$\mathbf{MX}^{\mathbf{m}}_{\mathbf{average}}$	**4**	95.1 ± 2.3	90.3 ± 5.8	96.8 ± 1.8	90.4 ± 5.1
	12	94.2 ± 2.4	65.3 ± 15.4	96.8 ± 1.4	65.5 ± 14.9

7.4 Discussion

The HD-EMG maps were parameterized using their levels of intensity and their distribution in the 2D space. Regarding the distribution, it was found that features estimated trough the "*isolated masses*" method proposed in this work provided greater

discriminating power ($p<<0.001$ for a MANOVA) than the classical "global mass" method and, thus, more capacity to classify or separate between tasks and their associated effort levels. These findings are consistent with results presented by Tucker et al. (Tucker et al. 2009) that reported changes in the spatial distribution of activation maps with varying loads.

The proposed features and classification methods have shown to be valid for the discrimination of contractions at the elbow joint. The simple 1-step LDC can discriminate between the four different tasks with high accuracy when using intensity-based features (S=92.4%, P=92.6%, Sp=97.5%, Acc=96.2 % with $maxI^m$) and with even slightly better performance(S=P=93.8%, Sp=97.9%, Acc=96.9%) when using combinations of the intensity and spatial distribution-based features $maxI^m$ **+** $\mathbf{MX^m}$ over the segmented area for each muscle (see Figure 7.3 and Table 7-3, respectively).

Several studies have used pattern recognition based on bipolar sEMG signals to control prostheses with multiple degrees of freedom, focusing on the identification of movement rather than on the proportional control of such movements to regulate the output force. Therefore, the classifiers are usually trained and validated with similar levels of effort reaching very high accuracies. For example, in (Englehart, Hudgins 2003, Hargrove et al. 2009, Hargrove, Englehart & Hudgins 2007),various strategies were used for the identification of degrees of freedom at the wrist and/or the hand comprising different features, classifiers, pattern-recognition from intramuscular signals and even feature-projections obtained by principal component analysis. In all of these studies, the highest accuracies reached values between 90% and 98%. However, none of them took into account that tasks were carried out at different effort levels, and the classifier was trained and tested with similar forces at medium levels of contraction, whereas different effort levels are considered in the objectives of our study.

Regarding this issue, a recent study by Scheme and Englehart (Scheme, Englehart 2011), analyzed the stability of classification due to changes in the force for ten classes of motion at the wrist and hand using eight electrode pairs. In that case subjects were asked to perform contractions at different levels of force between 20% and 80% of the strongest contraction they felt comfortable producing (SCC). The best classification accuracy (around 93%) was obtained at 70% SCC when testing at the same force level as training but this decreased dramatically to 72% when training with such force level and then testing with all levels of force. These two accuracies were worse at lower levels of effort reaching values of 81% and 54% respectively, at 20% SCC. It is important to remark that a very low

level of effort at10% MVC is considered in our study, and despite this, the classification performance is very good. Finally, the classification accuracy obtained in (Scheme, Englehart 2011) when training and testing with pooled data from all force levels, which is similar to our study, reached only 83% and authors suggested this procedure of mixing different force levels when training and testing for the identification of tasks in order to reduce error in the recognition of motor intention.

Similarly, Tkach and Kuiken (Tkach, Huang & Kuiken 2010) analyzed the classification accuracy for the recognition of DOF at the elbow joint, as in our study, using different time-domain features extracted from bipolar signals recorded at 25% and 65% MVC. When considering training and validation with features extracted from a mixture of both levels of contraction, in a way similar to our study, accuracy ranged between 50%-80% depending on the feature. Moreover, they also studied the influence of disturbances such as electrodes shift on the classification and the accuracy decreased further up to ~35%.

Thus, very recent studies like (Tkach, Huang & Kuiken 2010) or (Scheme, Englehart 2011) have shown the need for continuing the research on pattern recognition from sEMG signals including more difficult conditions as mentioned previously. In this sense, our study showed that features extracted from HD-EMG maps substantially improve the identification of tasks obtaining classification accuracies of ~ 97% when considering data sets extracted from different effort levels between 10% and 50% MVC. These results were obtained at the expense of considerably increasing the number of recorded EMG signals, however, the classification performance was very good even when using a small grid of 3×3 electrodes properly located at the anatomical points proposed in Table 7-6 (S>87%, P>87%, Sp>95%, Acc>93%, see Table 7-7).

In our study we were interested in identifying not only motion tasks but also the level of intended force. Moreover, the use of features extracted from HD-EMG signals provides contact redundancy being less sensitive to shifts in electrode location. Scheme and Englehart (Scheme, Englehart 2011), remarked that error rate (ER=100%-Acc) introduced by different levels of effort should not exceed 10% for the user to comfortably operate a system in the usable range of forces. They also concluded that training and validation of the classifier should consider a mixture of different levels of effort to reduce ER. In our case average ER is lower than 4% for the joint identification of type of task and effort level. This information could be used by a robotic device, providing proportional control related to the force intended by the user. It can also be used for biofeedback purposes in applications intended for motor rehabilitation and based on virtual games or any kind of

interaction between a patient and a computer system in which the user is encouraged to follow a rehabilitation exercise.

Two approaches were considered for the classification: the 1-step LDC is poor when analyzing the joint discrimination among tasks and effort levels (S=59.7%, P=60.6%, Sp=96.3% and Acc=93.3% and using $maxI^m$). On the contrary, the second approach, called 2-steps LDC, which consists in using a sequential classifier, is much more efficient. In the initial step, the observations are divided into different tasks, and after the task identification they are separated into sub-groups related to 10%, 30% and 50% MVC during a second step of the classifier, using only a subset of muscles assumed to be involved in each kind of task. Higher performance indexes (S= 77.8%, P= 78.3%, SP = 98% and Acc= 96.3% see Table 7-4) compared to 1-step LDC were obtained when combining intensity and spatial distribution based features in 2-steps LDC, using features as follows: a) a combination of $maxI^m$ +$\mathbf{MX}^\mathbf{m}$ for the identification of the four tasks in the first step of the classifier and b) a combination of features $maxI^m$+ $\mathbf{CG}^\mathbf{m}$ in flexion and extension and the features μI+$\mathbf{MX}^\mathbf{m}$ for supination and pronation in the second step for the identification of effort levels. Note that this LDC used the muscles selection and the appropriate features during the second step based on the task identification provided during the first one. When comparing among tasks, best results were found for flexion (S= 88.9%, P= 86.1 %, Sp= 98.5%, Acc= 97.7), and worst identification was found for the different effort levels of *extension* (S= 72.2%, P= 71.3%, Sp= 97.5%, Acc= 95.4%), in spite that the latter presented a perfect classification (Acc=100%) when identifying the task (see Table 7-3). This highlights that extension contractions are easy to classify but it is more difficult to differentiate between their intensity levels, mainly because of the similarity of EMG maps obtained at levels of 30% and 50% MVC, resulting in higher numbers of FP and FN. This effect was also observed, although in lesser extent, in the other three tasks. Performance indexes were much higher when differentiating between low-medium (30-50% MVC) and very low (10%MVC) levels of effort (S= 88 %, P= 87%, SP= 98.4%, Acc= 97.2%). Such increase was mainly reflected in the Sensitivity (S) and in the Precision (P) of the classification.

Average anatomical locations for the center of gravity and coordinates of the point of maximal EMG amplitude were provided for each muscle. This information can be used as reference for electrode placement in future studies involving similar protocols. A subset of the arrays corresponding to a square grid of 3×3 channels (IED=10 mm) centered at these locations, which are the same for all subjects, was also used in order to evaluate the

possibility of task identification using a much smaller number of electrodes. In this case, slightly better results were found when placing the grid around the coordinates of the average maximum (see Table 7-7). With such grid the identification of tasks was very good (S> 87%, P>87%, SP>95%, Acc>93%) using $maxI^M$, being only 2% less than using the original arrays with all the electrodes and the intensity-based features. The subsequent identification of effort level was more difficult (S> 61%, P> 61%, SP> 96%, Acc> 93%), however these indexes were only slightly lower than when using the total segmented area and $maxI^m$. Thus, despite using a much smaller number of electrodes, the capacity for classification remains but only when considering intensity-based features. Due to the small region covered in each muscle, spatial distribution-based features do not improve the performance of the classification as in the case of using all the electrodes where they significantly increase the performance indexes.

7.5 Conclusions

Surface EMG maps from five muscles of the upper limb were analyzed in order to identify differences in the muscle activation patterns associated to four tasks and three effort levels for each task. A Linear Discriminant classifier was described using an original method based on features associated to the intensity and distribution of monopolar HD-EMG maps based on the selective use of information from different muscles depending on the identified task. Features associated to EMG distribution themselves are not sufficient to differentiate between tasks or the effort level with acceptable accuracy; however, when used in combination with intensity based features, they improve the performance of the classifier. It is important to note that this improvement is not obtained when the intensity based features are calculated classically ("global mass" method) but it is obtained with the "isolated masses" method proposed in this study. This is because the latter is more robust with respect to several local maxima (peaks) and minima (valleys as in Fig. 3). Once the task has been identified, the center of gravity is more suitable to determine the effort level for flexion and extension whereas the coordinates of the maximum present better performance for pronation and supination. The identification of flexion-extension is based on biceps and triceps while the identification of pronation and supination is mainly based on forearm muscles. Biceps and triceps are composed of two and three well separated compartments respectively. This may be the reason why the coordinates of the maximum, which is located in one of the compartments, is less appropriate than the center of gravity which depends on the intensity over the total

segmented area, (that is, more than one compartment). The 2-steps LDC is easy to implement and results showed high accuracy. The classification according to the type of task achieved high performance indexes, even when the HD-EMG signals related to tasks comprised contractions at different levels and therefore included different ranges of amplitude. The best automatic classification was obtained using a combination of intensity and spatial-distribution features defined in this study and the proposed 2-steps LDC.

The most difficult task to assess was *supination*. This is probably due to the fact that supination is not the main function of any of the analyzed muscles. The most involved muscles in the supination of the forearm are the *Supinator* which is not superficial (and so, it cannot be assessed with sEMG) and the Biceps, but the main function of this last is the flexion at the elbow joint. However, good results were obtained for the identification of supination contractions by combining intensity and spatial distribution-based features. On the other hand, when trying to differentiate between levels of effort, the *extension* task is the most difficult to assess.

The Accuracy in task identification remains very high even with a properly positioned smaller set of electrodes (3×3 grids), however the classification of the effort levels does not reach the performance obtained when all the electrodes are considered (being the *supination* class the most affected).

Regarding statistical indexes associated with performance of the classification, Accuracy and Specificity are not the most appropriate to be considered in multiple classifications (four, eight and 12 groups in our study) in spite of being commonly used in the control of powered prosthesis (Tkach, Huang & Kuiken 2010, Scheme, Englehart 2011). Although they increased with increasing values of Sensitivity and Precision, these two measures are biased by the usually very high number of observations not belonging to a given group and correctly identified as members of the other groups (TN), regardless of whether they were assigned to the correct group or not. Consequently, these two measures are always very high (>90%). On the contrary, both Sensitivity (S) and Precision (P) are more appropriate because they are more affected by changes in the classification performance and since they take into account the number of observations for each group that were correctly classified with respect to the number of those that were wrongly classified (FN), and with respect to those that were incorrectly classified as members of the group (FP) respectively.

The results presented in this work are based on RMS maps. These RMS values present large variability of amplitude and distribution among different subjects. In spite of this

difficulty, the overall performance of the best classifier for the identification of both the task and the effort level, is very good (Acc=96.3%, S= 77.8%, P=78.3%, SP=98%, see Table 7-4). These results, together with the algorithms ability to differentiate between low (10% MVC) and medium (30%-50% MVC) levels (S= 88%, P=87%, Acc=97.2%, SP=98.4%, see Table 7-5), support the feasibility of the proposed set of features together with LDC to help in the estimation of motion intention during robotic-aided rehabilitation and other applications concerning the use of biofeedback from EMG signals like virtual games or computer-based rehabilitation training.

7.6 References

Anderson, T.W. 1984, *An Introduction to Multivariate Statistical Analysis, 2nd Edition,* 2nd edn, Wiley.

Andreasen, D.S., Alien, S.K. & Backus, D.A. 2005, "Exoskeleton with EMG based active assistance for rehabilitation", *Proc. 9th International Conference on Rehabilitation Robotics, 2005*, pp. 333.

De Biase, M.E.M., Politti, F., Palomari, E.T., Barros-Filho, T.E.P. & De Camargo, O.P. 2011, "Increased EMG response following electromyographic biofeedback treatment of rectus femoris muscle after spinal cord injury", *Physiotherapy,* vol. 97, no. 2, pp. 175-179.

Dipietro, L., Ferraro, M., Palazzolo, J.J., Krebs, H.I., Volpe, B.T. & Hogan, N. 2005, "Customized interactive robotic treatment for stroke: EMG-triggered therapy", *IEEE Transactions on Neural Systems and Rehabilitation Engineering,* vol. 13, no. 3, pp. 325-334.

Englehart, K. & Hudgins, B. 2003, "A robust, real-time control scheme for multifunction myoelectric control", *IEEE Transactions on Biomedical Engineering,* vol. 50, no. 7, pp. 848-854.

Farina, D., Leclerc, F., Arendt-Nielsen, L., Buttelli, O. & Madeleine, P. 2008, "The change in spatial distribution of upper trapezius muscle activity is correlated to contraction duration", *Journal of Electromyography and Kinesiology,* vol. 18, no. 1, pp. 16-25.

Freriks, B. & Hermens, H.J. 1999, *SENIAM 9: European Recommendations for Surface ElectroMyoGraphy, results of the SENIAM project (CD),* Roessingh Research and Development b. v.

Hargrove, L.J., Englehart, K. & Hudgins, B. 2007, "A comparison of surface and intramuscular myoelectric signal classification", *IEEE Transactions on Biomedical Engineering,* vol. 54, no. 5, pp. 847-853.

Hargrove, L.J., Li, G., Englehart, K.B. & Hudgins, B.S. 2009, "Principal Components Analysis Preprocessing for Improved Classification Accuracies in Pattern-

Recognition-Based Myoelectric Control", *IEEE Transactions on Biomedical Engineering,* vol. 56, no. 5, pp. 1407-1414.

Herda, T.J., Walter, A.A., Costa, P.B., Ryan, E.D., Stout, J.R. & Cramer, J.T. 2011, "Differences in the log-transformed electromyographic-force relationships of the plantar flexors between high- and moderate-activated subjects", *Journal of Electromyography and Kinesiology,* vol. 21, no. 5, pp. 841-846.

Hogan, N., Krebs, H.I., Rohrer, B., Palazzolo, J.J., Dipietro, L., Fasoli, S.E., Stein, J., Hughes, R., Frontera, W.R., Lynch, D. & Volpe, B.T. 2006, "Motions or muscles? Some behavioral factors underlying robotic assistance of motor recovery", *Journal of Rehabilitation Research and Development,* vol. 43(5), pp. 605-18.

Holtermann, A., Roeleveld, K. & Karlsson, J.S. 2005, "Inhomogeneities in muscle activation reveal motor unit recruitment", *Journal of Electromyography and Kinesiology,* vol. 15, no. 2, pp. 131-137.

Kendall F. P., Kendall McCreary E., and Provance P.G. 1993, *Muscles: Testing and Function,* 4th edn, Williams & Wilkins.

Khokhar, Z.O., Xiao, Z.G. & Menon, C. 2010, "Surface EMG pattern recognition for real-time control of a wrist exoskeleton", *Biomedical Engineering Online,* vol. 9, pp. 41.

Madeleine, P., Leclerc, F., Arendt-Nielsen, L., Ravier, P. & Farina, D. 2006, "Experimental muscle pain changes the spatial distribution of upper trapezius muscle activity during sustained contraction", *Clinical Neurophysiology,* vol. 117, no. 11, pp. 2436-2445.

Merletti, R., Aventaggiato, M., Botter, A., Holobar, A., Marateb, H. & Vieira, T.M.M. 2010a, "Advances in surface EMG: recent progress in detection and processing techniques.", *Critical Reviews in Biomedical Engineering,* vol. 38, no. 4, pp. 305-45.

Merletti, R., Botter, A., Cescon, C., Minetto, M.A. & Vieira, T.M.M. 2010b, "Advances in surface EMG: recent progress in clinical research applications.", *Critical Reviews in Biomedical Engineering,* vol. 38, no. 4, pp. 347-79.

Parker, P., Englehart, K. & Hudgins, B. 2006, "Myoelectric signal processing for control of powered limb prostheses", *Journal of Electromyography and Kinesiology,* vol. 16, no. 6, pp. 541-548.

Scheme, E. & Englehart, K. 2011, "Electromyogram pattern recognition for control of powered upper-limb prostheses: State of the art and challenges for clinical use", *Journal of Rehabilitation Research and Development,* vol. 48, no. 6, pp. 643-659.

Staudenmann, D., Kingma, I., Daffertshofer, A., Stegeman, D.F. & van Dieën, J.H. 2009, "Heterogeneity of muscle activation in relation to force direction: A multi-channel surface electromyography study on the triceps surae muscle", *Journal of Electromyography and Kinesiology,* vol. 19, no. 5, pp. 882-895.

Staudenmann, D., Roeleveld, K., Stegeman, D.F. & van Dieen, J.H. 2010, "Methodological aspects of SEMG recordings for force estimation - A tutorial and review", *Journal of Electromyography and Kinesiology,* vol. 20, no. 3, pp. 375-387.

Tkach, D., Huang, H. & Kuiken, T.A. 2010, "Study of stability of time-domain features for electromyographic pattern recognition", *Journal of Neuroengineering and Rehabilitation,* vol. 7, pp. 21.

Tucker, K., Falla, D., Graven-Nielsen, T. & Farina, D. 2009, "Electromyographic mapping of the erector spinae muscle with varying load and during sustained contraction", *Journal of Electromyography and Kinesiology,* vol. 19, no. 3, pp. 373-379.

Vincent, L. 1993, "Morphological grayscale reconstruction in image analysis: applications and efficient algorithms", *Image Processing, IEEE Transactions on,* vol. 2, no. 2, pp. 176-201.

Zwarts, M.J. & Stegeman, D.F. 2003, "Multichannel surface EMG: Basic aspects and clinical utility", *Muscle & nerve,* vol. 28, no. 1, pp. 1-17.

8

Conclusions and Future Extensions

8.1 Summary

This thesis was directed to the analysis of muscular pattern through sEMG and its relation to fatigue and pathology. Different experimental protocols were designed and implemented, all of them based on multichannel EMG. Multichannel signal analysis allowed the assessment of muscles with multiple innervation zones by the identification of the regions within the muscles where consecutive signals presented similar shapes (i.e. high cross-correlation coefficients) and where it was possible to observe the propagation of motor unit action potentials along sarcomeres. Information extracted from this kind of signals is not biased by the position of the electrodes and can be reliable interpreted in the assessment of upper-limb disorders (Saitou et al. 2000). Besides, the use of spatial filters allowed crosstalk reduction and the estimation of conduction velocity of motor unit action potentials which has a direct relation to fatigue and pathology (De Luca 1984).

On the other hand, two dimensional sEMG allows the assessment of surface' potential distribution when analyzing the signal as an image, either as sample by sample or averaged in short time intervals (Merletti et al. 2010). This technique has gain particular attention in recent years, allowing researchers to analyze phenomena such as muscle compartmentalization and motor units' distribution heterogeneity, which is associated to regional variations in neuromuscular activity due to pain or fatigue, among others (Tucker et al. 2009, Madeleine et al. 2006). It has also been associated to changes in force level (Holtermann, Roeleveld & Karlsson 2005). Based on this evidence, a new set of features related to the spatial distribution of HDEMG maps was defined and tested for the identification of tasks at the elbow joint. When combined with features extracted from the local intensity of activation maps, not only a high accuracy was achieved but also high precision and sensitivity.

Therefore, techniques described and indices proposed in this thesis have been able to characterize and provide new information on the interaction between different muscles of the upper-limb, either to analyze muscular pattern associated to pathology or to identify the contribution of different muscles to given tasks.

The research developed and compiled in the body of this thesis opens a new research line for the group of Biomedical Signals and Systems of the Biomedical Engineering Research Centre (CREB) at the Technical University of Catalonia (UPC): analysis of multichannel surface EMG.

Conclusions of the different studies in this thesis have already been introduced at the end of the chapters composing the present work. They are summarized in the following:

8.2 Conclusions

8.2.1 Muscular imbalances in Lateral Epicondylalgia following recovery

Muscular imbalances in patients diagnosed and treated for Lateral Epicondylalgia were evaluated during experimental protocols described in Chapter 3 and following the methodology described in detail in Chapter 4. Results were fully discussed in Section 4.4.1 of Chapter 4.

Findings on patients with lateral epicondylalgia after recovery and reinstatement to daily-life work activities indicate a differentiated activation pattern in voluntary contractions of forearm muscles during wrist extension ($p<0.05$ for a t-test) and hand grip ($p<0.03$ for MANOVA). Moreover, a significantly increased fatigability has been found in recovered patients in both tasks ($p<0.04$).

Such differentiation was analyzed based on different co-activation and fatigue indices extracted from EMG variables commonly analyzed in clinical environments: Average Rectified Value (ARV), Root Mean Square (RMS), Mean and Median Frequency (MNF and MDF) and Conduction Velocity (CV). The main advantage of the focus adopted in this work is that all of these variables were extracted from signals recorded in an optimal region of the muscle that can only be assessed with multichannel EMG since other methods (namely bipolar on intramuscular recording) will fail to identify the location of innervation zone and tendons when such information is not common to the general population as in the case of forearm muscles (Saitou et al. 2000, Signorino, Mandrile & Rainoldi 2006, Mananas et al. 2005). Other advantages are related to the spatial selectivity of the double differential signals, as for example, the reduction of crosstalk components (Mesin et al.

2009) which are expected to be high in signals from the forearm (Mogk, Keir 2003) given the large amount of muscles in this area.

Regarding fiber type composition, MNF and MDF estimates showed higher values for the extensor carpi ulnaris, both in patients and healthy subjects, pointing to a higher composition of type II fibers in this muscle and thus a higher predisposition to myoelectric fatigue ($p<0.05$). It is therefore not surprising that this muscle did not showed differences concerning fatigue index between healthy subjects and patients (p.n.s.).

Differences in co-activation patterns may reflect muscular imbalances caused by the predominance of a group of muscles which can be overactive during a kind of movement. Several studies have related such imbalances with biomechanical deficits in different pathologies involving hamstring (Yeung, Suen & Yeung 2009), rotator cuff (Wang, Cochrane 2001)and low back muscles (Nadler et al. 2002).

Muscular imbalances in this work were analyzed with two indices: Co-activation index (CI) and orientation angles in the contraction level space (θ and φ). All of them indicated differences in the participation of the extensor carpi ulnaris and flexor carpi radialis in patients after rehabilitation, and thus the use of compensation mechanisms to complete the task ($p<0.05$ in all cases). Coordination between flexors and extensors was also assessed by the orientation angles θ and φ for the set of vectors v (Eq. 4-10) and also showed a different behavior in patients, pointing to flexor-extensor imbalances associated to ECU-FCR and ECR-FCR ($p<0.03$). Finally, the orientation approach avoids normalizations of the power of submaximal signals with respect to the value observed at maximal levels of contraction which is commonly used but could be biased because of methodological considerations, (Buchanan et al. 2004), especially when considering that the relationship between EMG amplitude and force is not linear (Staudenmann et al. 2010).

On the other hand, myoelectric fatigue was assessed from the rate of change of EMG variables during a sustained contraction. In both groups, healthy and former LE patients, significant rates of change (i.e. slopes) were found. However, slopes were significant steeper (in absolute value) for patients than for healthy subjects, especially when analyzed from conduction velocity and for the muscles extensor carpi radialis, extensor digitorum communis and flexor carpi radialis ($p<0.04$). Conduction velocity is directly related to physiological determinants of localized fatigue (De Luca 1984) and may be associated to changes in fiber-type composition in patients (Kupa et al. 1995). This can be explained in terms of muscular adaptation to overload of upper extremity as required by work activities in patients.

Finally, obtained results were consistent independently from the task analyzed: wrist extension or hand grip. Recalling that different populations were analyzed in different tasks (Table 3-3 in Chapter 3), it is possible to infer that the methodology employed lead to results that are reproducible and repeatable.

In conclusion, findings indicate differentiated activation patterns during isometric contractions of wrist extensor muscles between normal subjects and those with history of lateral epicondylalgia. Moreover, a significantly increased fatigability has been found in recovered patients. Such findings might be helpful in designing new therapeutic (i.e. rehabilitation) and prevention approaches. On the other hand, subjects at risk might be detected by the systematic evaluation of muscular imbalances in workers exposed to repetitive tasks.

8.2.2 Assessment of muscular pattern in contractions related to Repetitive Strain Injury

The protocol designed for assessing the muscular pattern during contraction associated to Repetitive Strain Injuries was tested and validated. It was based on short time-duration isometric contractions that were repeated several times for each finger and considered different deviation angles of the wrist. With this respect, it was found that the activation pattern of the analyzed muscles was not significantly affected by the wrist rotation angle given that similar co-activation indices were obtained for each muscle and finger. However, it was found that the load-sharing between muscles depended on which finger was exerting the force ($p<0.02$) and that the activation of muscles was higher when pressing with the opposite finger, that is, the finger that is located at the other side of the limb, as for example in the case of a high activation of the Extensor Carpi Ulnaris in the lateral side of the forearm when pressing with the thumb, which is located in the medial side ($p<0.001$). It was also possible to assess myoelectric fatigue in the muscles as analyzed from the repetitive-short duration contractions of fingers.

Finally, considering similar activation patterns were found when pressing with every finger with or without rotation of the wrist, it is possible to infer that both, the protocol and the proposed indices are repetitive. Such results are encouraging and motivate the use of techniques based on multichannel sEMG for the study of repetitive strain injuries in experienced musicians. This kind of analysis will be useful in establishing possible mechanisms underlying this syndrome as well as its possible prevention and treatment.

8.2.3 HD-EMG maps of the Upper limb

High- Density EMG maps of the Upper limb were obtained for a population of 12 healthy subjects in Chapter 6. The experimental protocol was based on the acquisition and processing of sEMG signals with 2D electrode arrays as described in Chapter 5.

The main objective of the study was to extract information from HD-EMG maps that could be associated with four tasks at the elbow joint (forearm pronation and supination, and elbow flexion and extension) at different effort levels. Variability of individual maps with respect to average maps for each muscle maintained low values (mean variability < 23%). Consequently, average maps can be considered as globally associated with the general muscular pattern of the 12 subjects in the database. Additionally, it was shown that information extracted from the amplitude of signals recorded in high-dimensional configuration has more power to differentiate between tasks and effort levels than single bipolar signals ($p<0.001$). Conclusions from Chapter 6 supported the claim that, compared to bipolar signals, features extracted from HD-EMG recordings are more robust because of the contact redundancy implied by the recording of a number of signals over a large surface of the muscle, as well as to error introduced by the relative location of the electrodes with respect to the origin of the potentials.

Two steps were involved in achieving the main goal of Chapter 6: detection of low quality signals or artifacts and segmentation of the active zones within each electrode array.

A supervised algorithm for the automatic detection of low quality signals based on temporal and frequency features was developed. The algorithm is easy to implement and has low computational complexity, making it suitable for online or offline detection of low-quality signals. The detection accuracy is very high (>99.4%) and more important, both the precision and the sensitivity to detect artifacts are also very high (>90%). Additionally, a sensitivity analysis showed that variations in fixed parameters of the algorithm do not affect its general detection performance which makes it robust. Finally, by increasing the precision of the algorithm it was possible to limit false positive detections, making it very useful for offline applications where it is necessary to replace artifact channels from information contained in the neighbor channels, provided that such information is sufficient and available and that those channels are not labeled as artifacts when they are not. When compared to other previous methods available in the literature, its main advantages are: 1). no distribution of the amplitude of the signals is assumed (Gronlund et al. 2005), thus it can be applied to signal sets comprising quite different levels of muscle

activation and 2). It takes into account information provided by neighboring channels in the close proximity, decreasing the possibility of false positive detections.

On the other hand, image analysis techniques were used for the automatic segmentation of active regions of the maps generated from HD-EGM signals. This segmentation allowed the calculation of average HD-EMG maps for the population of 12 subjects, by determining the ranges of active zones in the *x* and *y* axes relative to upper-limb perimeter and muscle length respectively and referred to the electrode location recommended by SENIAM for sEMG.

Other methods have been previously proposed for the segmentation of activation maps. For example Vieira et al. in (Vieira, Merletti & Mesin 2010) proposed a method based on watershed that segmented regions associated to local variations in the level of neuromuscular activity within the same muscle. However, in the present work, we were interested in the isolation of the whole-individual muscle activity from background. Therefore, it was necessary to avoid the segmentation of regions associated to local maxima or minima (i.e. peaks or valleys in the topographical map). Watershed in this case is not feasible because by definition, it is highly sensitive to inhomogeneities in the map and if not properly applied, it can lead to oversegmentation (Serra 1982). Consequently, the segmentation used in this work was achieved by applying an h-dome transformation based on the morphological reconstruction of the map and was especially useful for the segmentation of active areas in the electrode array located around the forearm, where at least three disjointed areas of activation were expected.

Finally, it was possible to infer changes in the spatial distribution of the energy of average maps ($p<0.001$ in the analyzed muscles) as well as in its absolute values of intensity. Such changes were associated to voluntary level of effort and even to the type of task: flexion or extension of the elbow or pronation or supination of the forearm. Changes in intensity levels were not always proportional to effort level and were different for different muscles. Consequently, HD-EMG maps obtained from 2D arrays, instead of traditional single bipolar channels, and variables related to both their maximum intensity and spatial distribution should be considered in the identification of different kind of tasks at elbow level as well as in the identification of the intended force. It can also be used in the analysis of load sharing among the muscles involved on the execution of a given task.

8.2.4 Identification of Isometric Contractions based on HD-EMG Maps

The main objective of the analysis presented in Chapter 7 was the identification of tasks based solely on features extracted from HD-EMG maps. Such tasks consisted in the

extension and flexion of the elbow and in the pronation and supination of the forearm. Different levels of effort related to MVC for each task were also considered (see protocol definition on Chapter 5).

The focus adopted in this work for the classification in different tasks was on the field of pattern recognition which is commonly used for the control of powered prostheses (Parker, Englehart & Hudgins 2006). It consists in mapping the activation (i.e. the levels of intensity of the signals) of a given set of muscles into types of task by relying in distinct co-activation patterns corresponding to different tasks. Although pattern recognition from sEMG signals has been extensively investigated for the past 50 years, there are still some challenges to overcome before its translation to clinical applications. One of them is the robustness of the classification to changes in the force exerted by the individual when manipulating the prosthesis (Scheme, Englehart 2011). As pattern-recognition control relies on clustering repeatable patterns of EMG activity into discernible classes, it can led to high classification errors because such patterns may be different for different levels of force because of changes in the load-sharing of synergistic muscles or even because of differences in their motor unit recruitment thresholds, especially if low levels of contraction are required (Merletti, Parker 2004). Recent studies have demonstrated that classification accuracy decreases when considering various levels of effort for training the classifier (Scheme, Englehart 2011, Tkach, Huang & Kuiken 2010). Thus, the correct identification of the level of activation for proportional control is still an open subject that needs to be resolved before translating pattern- recognition approaches to clinical environment (Parker, Englehart & Hudgins 2006, Scheme, Englehart 2011, Englehart, Hudgins 2003), especially when considering its application to other devices that are not necessarily prostheses. The approach presented in Chapter 7 was directed to solve this problem based on the hypothesis that contractions exerted at different levels of force may reflect changes in the spatial distribution of the potentials in the surface of the muscle (Holtermann, Roeleveld & Karlsson 2005). Such changes imply that muscle fiber types are not randomly distributed, but organized in regions with different histochemical muscle fiber composition. In addition, findings in Chapter 6 pointed to a differentiated spatial distribution not only as product of effort level but also as product of type of task. Thus two sets of features were extracted from each muscle:

- Intensity-based features: Mean and Maximum values of intensity
- Spatial-based features: Center of gravity of the maps and Coordinates of the maximum intensity.

Regarding spatial-based features, the regions corresponding to isolated areas of maximal intensity (i.e. local peaks) were segmented from the image in order to calculate the center of gravity of the map in a way analogous to a system of masses instead of calculating it as a distributed mass. It was found that that the isolated masses method was better in discriminating between types of task than the method of distributed mass.

Four different tasks were successfully identified from HD- EMG maps. The classifier used intensity features or combinations of intensity features and spatial features, obtaining higher accuracies in the second case. In any case, the classifier was always trained with features extracted from signals recorded at three levels of effort and the error rate (ER) for any task was always less than 8% (ER= 100% -Acc) (Scheme, Englehart 2011). This result represents a major accomplishment when compared to recent studies that considered the use of combinations of levels of effort to train and validate the classifier and that achieved error rates higher than 15% (Scheme, Englehart 2011, Tkach, Huang & Kuiken 2010).

Finally, classification showed high performance indices when considering not only the discrimination between tasks (average Acc=97%, S=93%, P=93%, SP=97% for 4 groups) but also when discriminating between contractions performed at different levels of effort (average Acc= 96%, S=77%, P=78%, SP=98% for 12 groups). Such results show the potential of spatial-based + intensity-based features in time domain to simultaneously discriminate between tasks and effort levels, and thus to help in the estimation of motion intention during robotic-aided rehabilitation. These features can only be extracted from HD-EMG maps and overcome most of the drawbacks of single bipolar channels in each muscle, mainly the lack of contact-redundancy and possible shifts between the points of origin of the potentials and the recording electrodes due to movement. The first is implied in the use of multiple electrode arrays and the second could be a relative measure reflecting the "movement" of the innervation zones in the recorded maps.

8.3 Main contributions

The main contributions of this thesis are related to both experimental protocols based on multichannel sEMG signals, and new algorithms and indices for their analysis. In summary, the most relevant contributions are:

- The definition of experimental protocols intended to find optimal regions for the recording of sEMG signals. The protocols were especially proposed for muscles of the forearm that present multiple innervation zones distributed in a wide surface area in the general population. To the best knowledge of the

author, this thesis is the first study in which the conduction velocity of Motor Unit Action Potentials as obtained from multichannel sEMG signals of forearm muscles was used to assess differences in myoelectric fatigue between patients and controls during voluntary contractions. Besides, because of the problematic associated to sEMG recording in forearm muscles, the use of multichannel sEMG in addition to the estimation of CV within physiological expected ranges allowed the determination of the best channels to estimate the EMG associated variables, avoiding possible bias leading to erroneous conclusions.

- A sensor system intended for HD-EMG recording in 2D, using multiple electrodes inserted on semi-elastic and hydrophobic fabric allowing the sensor to adapt to muscle geometry and to remain placed for long periods of time. These sensors were used in an experimental protocol where more than 330 sEMG channels were simultaneously recorded from forearm and upper-arm muscles for the first time.
- New indices associated to the co- activation of different muscles and based on the amplitude observed in signals that were recorded in an optimal region of the muscle. Normalizations involving the amplitude of the signal during high levels of contraction were avoided and the defined indices measured the load-sharing between individual muscles on a given task or their orientation angles in a vector space.
- An algorithm for the detection of low-quality signals in multichannel sEMG recordings with high number of channels, either online or offline with precision and sensitivity higher than other methods previously published.
- The segmentation of active regions in HD-EMG maps and associated with the global distribution area of the potentials or to localized regions where the levels of intensity where higher than the surrounding regions. The use of morphological operators avoided the segmentation of isolated peaks of intensity that can appear as consequence of inhomogeneities in the contact impedance between the skin and the recording electrodes.
- An original procedure based on 2-steps LDC which uses a new set of features from the HD-EMG maps in order to identify tasks associated to the degrees of freedom at the elbow joint and to the intended level of force with much higher accuracy than those obtained in similar studies so far.

8.4 Future Extensions

Work developed in the present thesis open new possibilities for research in the area of analysis of multichannel sEMG at the Department of Automatic Control (ESAII) at Technical University of Catalonia.

Indices obtained in this thesis were useful to identify muscular imbalances, biomechanical deficits and, in general, muscular pattern of different muscles for completing a given task during isomeric contractions. It will be of interest to analyze such pattern during dynamic contractions which are the most common during daily-life activities. However, sEMG signals cannot be considered wide-sense stationary in this condition so it is necessary to apply other signal processing techniques, perhaps non-linear, and evaluate if muscular pattern can be related to indices similar to those proposed in this work. Additionally, an automatic identification of shifts of innervation zones under the skin and with respect to the recording electrodes can be used in the reduction of the effects of muscle-fiber lengthening on the recorded signal. Other processing also includes the detection and filtering of movement artifacts in dynamic conditions.

Regarding repetitive strain injuries, the experimental protocol and the necessary hardware and software are ready to be applied to professional musicians and to be extended to a bigger population of control subjects. The assessment of myoelectric fatigue in instrumentalists is of particular interest because other studies have found that changes in the oxidative capacity of the muscular fibers are correlated with the manifestation of RSI. Given that this condition has not been completely understood and that there is not an agreement regarding its diagnosis and treatment in the rehabilitation community, it will be of interest to obtain quantitative indices that help improving the condition of subjects affected with this syndrome and to prevent it in professional musicians which is one of the most affected populations.

On the subject of activation maps, the techniques developed and the signals recorded will permit the study of temporal characteristics of the maps at a sample by sample scale, allowing the estimation of variables such as global conduction velocity in the two dimensions of the space. It could also be possible to analyze fiber-type distribution from spectral characteristics of the signals in the different channels and to relate it to intensity inhomogeneities already inferred from research in this subject. In addition, available HD-EMG signals will also be useful in the identification of spatial and temporal changes

induced by myoelectric fatigue in sustained contractions. It will be interesting to analyze if myoelectric fatigue induce shifts in the distribution of active potentials and if those shifts can be correlated to information extracted from the distribution of amplitude and spectral characteristics of the signals in the space domain. Finally, HDEMG signals recorded during sustained contractions will permit the analysis of the robustness of features proposed in this study in the identification of tasks during long-term contractions.

On the other hand, additional databases were recorded as product of the different experimental protocols conducted during the development of this thesis. These databases are ready to be analyzed and will be useful in some of the studies described above:

- Multichannel sEMG in 1D during isokinetic exercises and involving eccentric and concentric contractions of the extrinsic muscles of the forearm. The signals were recorded in the set of muscles described for hand-grip in Chapter 3 in controls (10 subjects) and patients diagnosed with Lateral Epicondylalgia after recovery (10 subjects).
- HD-EMG signals in 2D in patients with reduced mobility of the upper the upper-limb (12 subjects) after cerebral-accident or incomplete spinal cord injury. The signals were recorded following the protocol described in Chapter 5.

Finally, experience acquired in the design of electrode arrays has motivated the development of a new wireless electrode-system based on smart-textile technology. Such development is part of a project that has recently received funding from the Spanish Government (Ministerio de Economía y Competitividad).

8.5 Publications derived from this thesis

8.5.1 Journal papers

- Rojas- Martínez M, Mañanas MA, Alonso JF. High-Density Surface EMG Maps from Upper-arm and Forearm Muscles (2012). Accepted October 9th 2012. *Journal of NeuroEngineering and Rehabilitation*. Impact factor in JCR 3.264, first quartile in the categories *Biomedical Engineering* and *Rehabilitation*.
- Rojas M, Mañanas MA, Alonso JF, Merletti R (2012). Identification of Isometric Contractions Based on High Density EMG Maps. Accepted June 26th 2012. *Journal of Electromyography and Kynesiology*. Impact factor in JCR 1.969, first quartile in the category *Rehabilitation*.
- Unyo C, Chaler J, Rojas M, Pujol E, Muller B, Mañanas M. Forearm muscle strength in lateral epicondylitis patients (2012). Accepted July 16th 2012. *European Journal of Physical*

and Rehabilitation Medicine. Impact factor in JCR 1.402, second quartile in the category *Rehabilitation.*

- Rojas M, García M, Alonso JF, Mañanas MA, Marin J (2011). Evaluación de la Función Neuromuscular del Antebrazo Durante Contracciones Isométricas Mediante Electromiografía de Superficie Multicanal. *RIAII*, 8(2):35-44. Impact factor in JCR 0.231, fourth quartile in the category *Automatic & Control Sytems.*

Other papers

Additionally, the EMG signals registered with the experimental protocols described in this thesis have been used in other applications:

- Marateb H, Rojas M, Mansourian M, Merletti R, Mañanas Villanueva M (2011). Outlier detection in high-density surface electromyographic signals. *Medical and Biological Engineering and Computing*, 50(1):79-89. Impact factor in JCR 1.878, second quartile in the category *Biomedical Engineering.*

8.5.2 Book chapters

- M.A. Mañanas, M. Rojas, (2007) Análisis de señales EMG de superficie mediante matrices lineales de electrodos, Fundació Institut Guttmann, Tecnologías Aplicadas al Proceso Neurorehabilitador: Estrategias para valorar su eficacia, pp. 335-348, Badalona, España, Depósito Legal B-34509-08. Fundació Institut Guttmann.

8.5.3 International Congresses

- M. Rojas, M.A. Mañanas (2009). "Evaluation of Neuromuscular Function by Mutichannel Surface Electromyography during Motor Rehabilitation". *III Congreso Internacional sobre Domótica, Robótica y Teleasistencia DRT4ALL 2009*. pp. 195-200. ISBN: 978-84-88934-39-0
- Unyó C, Chaler J, Pujol E, Müller B, Rojas M, Mañanas MA, Garreta R (2008). "Forearm muscle strength in lateral epicondylitis patients", *7th Mediterranean Congress of Physical and Rehabilitation Medicine*, Portoroz, Slovenia.
- M. Rojas, M. A. Mañanas, B. Müller, and J. Chaler (2007). "Activation of Forearm Muscles for Wrist Extension in Patients Affected by Lateral Epicondylitis," *Proceedings of IEEE International Conference of the Engineering in Medicine and Biology Society 2007*, pp 4858-61

- M. Rojas, M.A. Mañanas, J. Chaler (2006). "Analysis of forearm muscles during gripping exercise by means of linear electrode arrays at different levels of effort", *XVI Congress of the International Society of Electrophysiology and Kinesiology*, 2006
- M. A. Mañanas, M. Rojas, F. Mandrile, J. Chaler (2005), "Evaluation of muscle activity and fatigue in extensor forearm muscles during isometric contractions". *Proceedings of the IEEE Engineering in Medicine and Biology 27th Annual Conference 2005*, pp. 5824-7.

Other articles

The EMG signals registered with the experimental protocols described in this thesis have been used in other applications:

- H. R. Marateb, M. Rojas- Martínez, M. A. Mañanas Villanueva, R. Merletti (2010). "Robust Outlier Detection in High-Density Surface Electromyographic Signals", Proceedings of the 2010 IEEE Engineering in Medicine and Biology, Buenos Aires, Argentina, pp 4850-4853.

8.5.4 National Congresses

- M. Rojas, M.A. Mañanas, C. Unyó, E. Pujol, J. Chaler (2007). "Activación de los músculos del Antebrazo para la Extensión de Muñeca en pacientes con Epicondilitis Lateral", XXV Congreso Anual de la Sociedad Española de Ingeniería Biomédica, CASEIB 2007, ISBN 84-612-0368-0
- M. Rojas, M. A. Mañanas, F. Vassallo, J. Chaler, R. Garreta, B. Müller (2005), "Utilización de matrices lineales de electrodos para el Análisis de la Actividad de Músculos del Antebrazo y Patologías Asociadas". Actas del Simposio de Ingeniería de Sistemas y Automática en Bioingeniería, I Congreso Español de Informática, pp. 33-38. ISBN: 84-609-6891-X

8.6 References

Buchanan, T.S., Lloyd, D.G., Manal, K. & Besier, T.F. 2004, "Neuromusculoskeletal modeling: estimation of muscle forces and joint moments and movements from measurements of neural command.", *Journal of Applied Biomechanics,* vol. 20, no. 4, pp. 367-95}.

De Luca, C.J. 1984, "Myoelectrical manifestations of localized muscular fatigue in humans.", *Critical Reviews in Biomedical Engineering,* vol. 11, no. 4, pp. 251.

Englehart, K. & Hudgins, B. 2003, "A robust, real-time control scheme for multifunction myoelectric control", *IEEE Transactions on Biomedical Engineering,* vol. 50, no. 7, pp. 848-854.

Gronlund, C., Roeleveld, K., Holtermann, A. & Karlsson, J.S. 2005, "On-line signal quality estimation of multichannel surface electromyograms", *Medical & biological engineering & computing,* vol. 43, no. 3, pp. 357-364.

Holtermann, A., Roeleveld, K. & Karlsson, J.S. 2005, "Inhomogeneities in muscle activation reveal motor unit recruitment", *Journal of Electromyography and Kinesiology,* vol. 15, no. 2, pp. 131-137.

Kupa, E.J., Roy, S.H., Kandarian, S.C. & De Luca, C.J. 1995, "Effects of Muscle-Fiber Type and Size on Emg Median Frequency and Conduction-Velocity", *Journal of applied physiology,* vol. 79, no. 1, pp. 23-32.

Madeleine, P., Leclerc, F., Arendt-Nielsen, L., Ravier, P. & Farina, D. 2006, "Experimental muscle pain changes the spatial distribution of upper trapezius muscle activity during sustained contraction", *Clinical Neurophysiology,* vol. 117, no. 11, pp. 2436-2445.

Mananas, M.A., Rojas, M., Mandrile, F. & Chaler, J. 2005, "Evaluation of muscle activity and fatigue in extensor forearm muscles during isometric contractions", *Proc. 27th Annual International Conference of the Engineering in Medicine and Biology Society 2005*, pp. 5824.

Merletti, R. & Parker, P. 2004, *Electromyography: Physiology, Engineering, and Non-Invasive Applications*, IEEE Press and J. Wiley, Series in Biomedical Engineering.

Merletti, R., Aventaggiato, M., Botter, A., Holobar, A., Marateb, H. & Vieira, T.M.M. 2010, "Advances in surface EMG: recent progress in detection and processing techniques.", *Critical Reviews in Biomedical Engineering,* vol. 38, no. 4, pp. 305-45.

Mesin, L., Smith, S., Hugo, S., Viljoen, S. & Hanekom, T. 2009, "Effect of spatial filtering on crosstalk reduction in surface EMG recordings", *Medical engineering & physics,* vol. 31, no. 3, pp. 374-383.

Mogk, J.P.M. & Keir, P.J. 2003, "Crosstalk in surface electromyography of the proximal forearm during gripping tasks", *Journal of Electromyography and Kinesiology,* vol. 13, no. 1, pp. 63-71.

Nadler, S.F., Malanga, G.A., Bartoli, L.A., Feinberg, J.H., Prybicien, M. & Deprince, M. 2002, "Hip muscle imbalance and low back pain in athletes: influence of core strengthening", *Medicine and science in sports and exercise,* vol. 34, no. 1, pp. 9-16.

Parker, P., Englehart, K. & Hudgins, B. 2006, "Myoelectric signal processing for control of powered limb prostheses", *Journal of Electromyography and Kinesiology,* vol. 16, no. 6, pp. 541-548.

Saitou, K., Masuda, T., Michikami, D., Kojima, R. & Okada, M. 2000, "Innervation zones of the upper and lower limb muscles estimated by using multichannel surface EMG.", *Journal of human ergology,* vol. 29, no. 1-2, pp. 35-52.

Scheme, E. & Englehart, K. 2011, "Electromyogram pattern recognition for control of powered upper-limb prostheses: State of the art and challenges for clinical use", *Journal of Rehabilitation Research and Development,* vol. 48, no. 6, pp. 643-659.

Serra, J. 1982, *Image Analysis and Mathematical Morphology,* Academic Press, London.

Signorino, M., Mandrile, F. & Rainoldi, A. 2006, "Localization of innervation zones in forearm extensor muscles. A methodological study", *Proc. of the XVI International conference of the International Society of Electrophysiology and Kinesiology*, pp. 220.

Staudenmann, D., Roeleveld, K., Stegeman, D.F. & van Dieen, J.H. 2010, "Methodological aspects of SEMG recordings for force estimation - A tutorial and review", *Journal of Electromyography and Kinesiology,* vol. 20, no. 3, pp. 375-387.

Tkach, D., Huang, H. & Kuiken, T.A. 2010, "Study of stability of time-domain features for electromyographic pattern recognition", *Journal of Neuroengineering and Rehabilitation,* vol. 7, pp. 21.

Tucker, K., Falla, D., Graven-Nielsen, T. & Farina, D. 2009, "Electromyographic mapping of the erector spinae muscle with varying load and during sustained contraction", *Journal of Electromyography and Kinesiology,* vol. 19, no. 3, pp. 373-379.

Vieira, T.M.M., Merletti, R. & Mesin, L. 2010, "Automatic segmentation of surface EMG images: Improving the estimation of neuromuscular activity", *Journal of Biomechanics,* vol. 43, no. 11, pp. 2149-2158.

Wang, H.K. & Cochrane, T. 2001, "Mobility impairment, muscle imbalance, muscle weakness, scapular asymmetry and shoulder injury in elite volleyball athletes", *Journal of Sports Medicine and Physical Fitness,* vol. 41, no. 3, pp. 403-410.

Yeung, S.S., Suen, A.M. & Yeung, E.W. 2009, "A prospective cohort study of hamstring injuries in competitive sprinters: preseason muscle imbalance as a possible risk factor", *British journal of sports medicine,* vol. 43, no. 8.